Hadronic Interactions

Ralph Engel

Karlsruhe Institute of Technology (KIT)

Additional material for reading

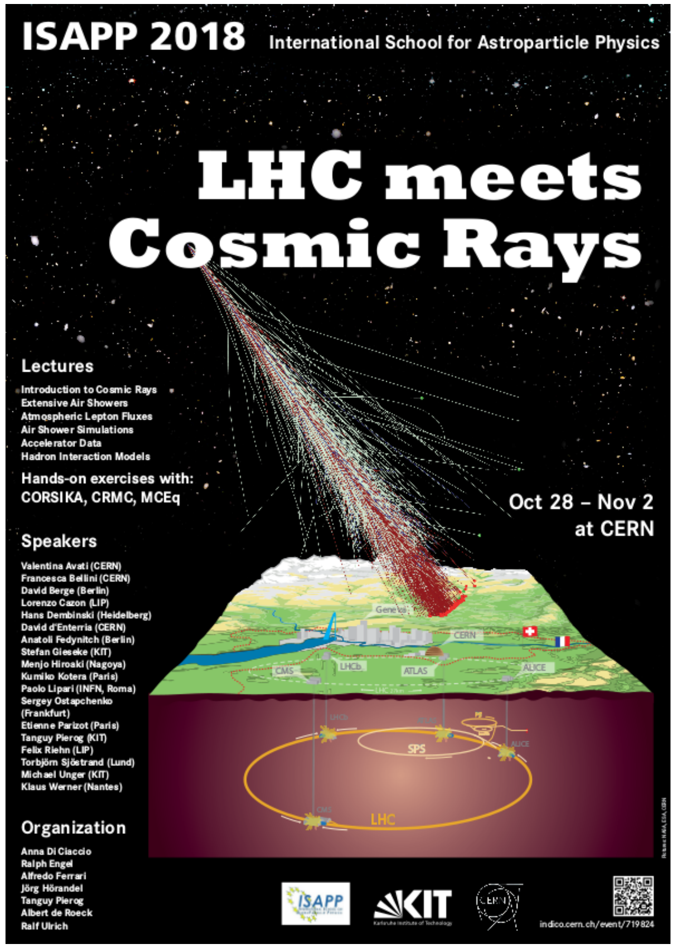

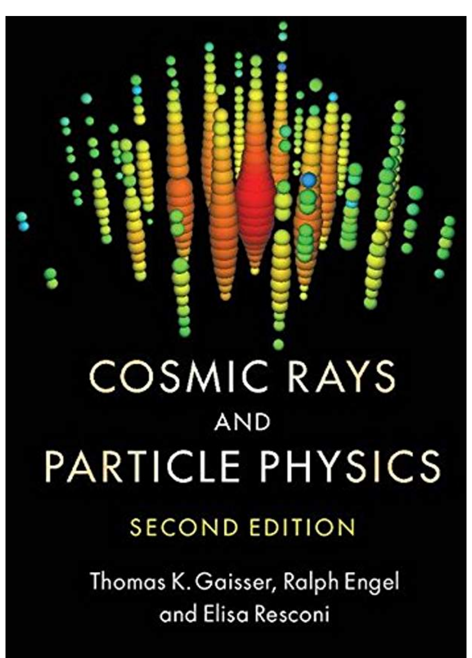

https://indico.cern.ch/event/719824/

Cosmic ray flux and interaction energies

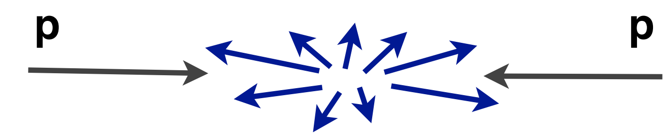

Center-of-mass energy

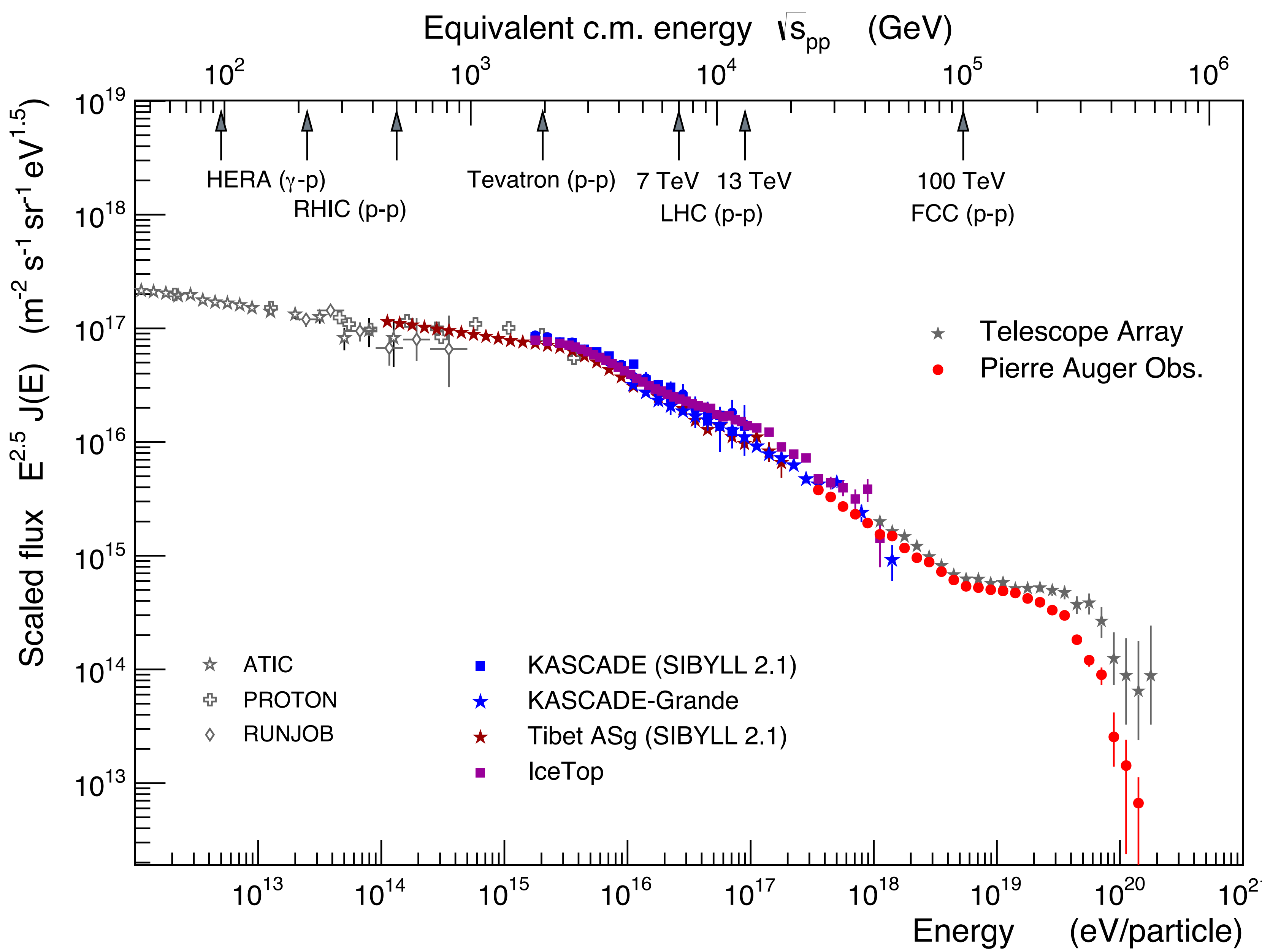

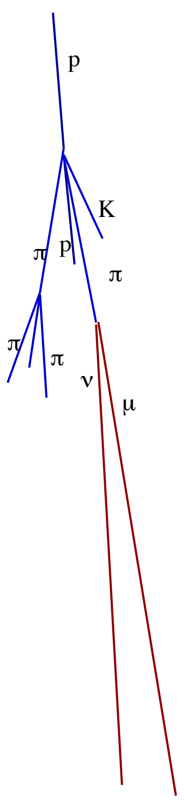

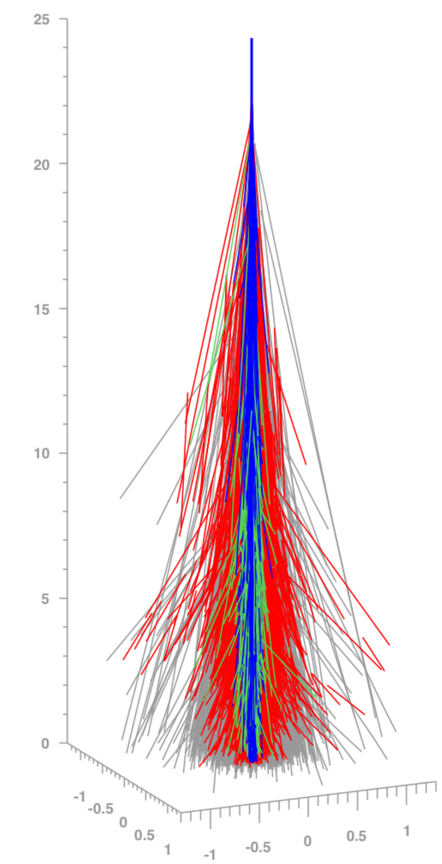

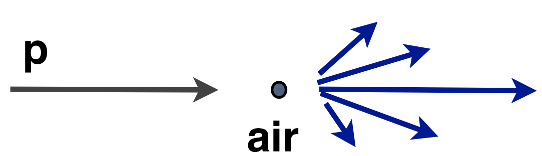

Laboratory energy

Mandelstam variable $s = (p_1 + p_2)^2 = (E_1^\star + E_2^\star)^2$

Modeling of hadronic interactions

NA61 experiment in CERN SPS beam

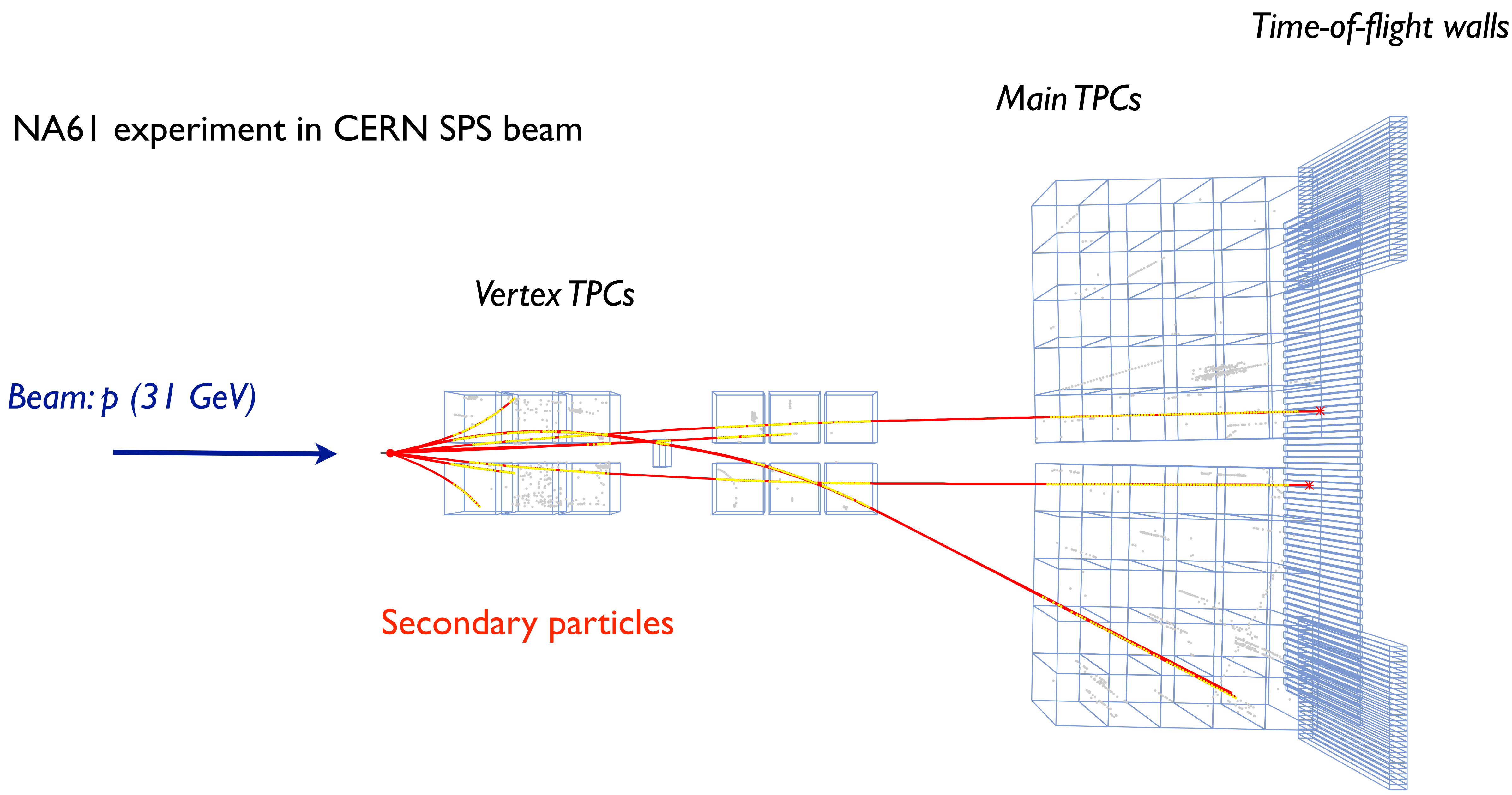

Typical particle multiplicities: 5 to 15 secondaries

Cross section and interaction rate

Definition

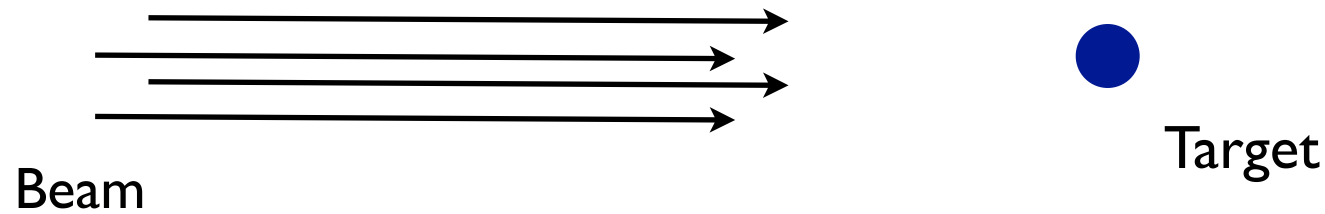

$$\sigma = \frac{1}{\Phi}\frac{\mathrm{d}N_{\mathrm{int}}}{\mathrm{d}t}$$

(Units: 1 barn = 10^{-28} m^2
1 mb = 10^{-27} cm^2)

Interaction rate

Flux of particles
on single target

$$\Phi = \frac{\mathrm{d}N_{\mathrm{beam}}}{\mathrm{d}A\,\mathrm{d}t}$$

Total cross section: count number of interaction types (elastic, inelastic)

Inclusive cross section: count number of particles of certain type in final state

Cross section and interaction rate

Definition

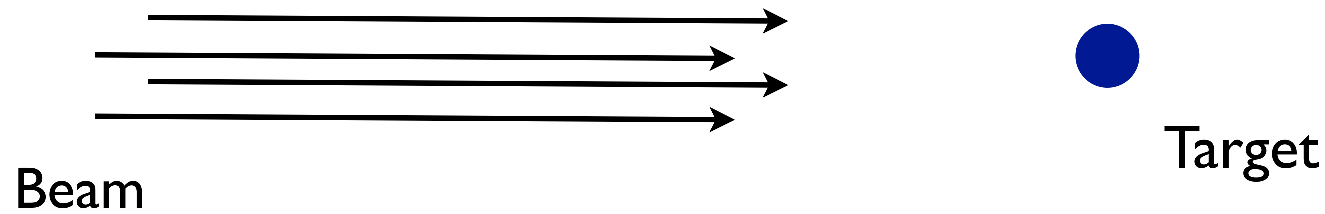

$$\sigma = \frac{1}{\Phi}\frac{dN_{\rm int}}{dt}$$

(Units: 1 barn = 10^{-28} m^2
1 mb = 10^{-27} cm^2)

Interaction rate

Flux of particles on single target

$$\Phi = \frac{dN_{\rm beam}}{dA\; dt}$$

$$dX = \rho_{\rm target}\, dl$$

$$\frac{dN_{\rm int}}{dt\,dV} = \frac{\rho_{\rm target}}{\langle m_{\rm target}\rangle}\,\sigma\,\Phi$$

$$\frac{dN_{\rm int}}{dt\,dV} = \frac{dN_{\rm int}}{dl\,dt\,dA} = -\rho_{\rm target}\frac{d\Phi}{dX}$$

$$\frac{d\Phi}{dX} = -\frac{\sigma}{\langle m_{\rm target}\rangle}\,\Phi$$

$$\langle m_{\rm air}\rangle \approx 14.51\, m_p = 24160\,{\rm mb\,g\,cm^{-2}}$$

The Earth's atmosphere in numbers

altitude (km)	vertical depth (g/cm^2)	local density ($10^{-3}\,g/cm^3$)	Molière unit (m)	Cherenkov threshold (MeV)	Cherenkov angle ($^\circ$)
40	3	3.8×10^{-3}	2.4×10^{4}	386	0.076
30	11.8	1.8×10^{-2}	5.1×10^{3}	176	0.17
20	55.8	8.8×10^{-2}	1.0×10^{3}	80	0.36
15	123	0.19	478	54	0.54
10	269	0.42	223	37	0.79
5	550	0.74	126	28	1.05
3	715	0.91	102	25	1.17
1.5	862	1.06	88	23	1.26
0.5	974	1.17	79	22	1.33
0	1032	1.23	76	21	1.36

$$X_v = X_0 e^{-h/h_0}$$

In reality the temperature and hence the scale height decrease with increasing altitude until the tropopause (12-16 km). At sea level $h_0 \cong 8.4$ km, and for $40 < X_v < 200\,\mathrm{g/cm^2}$, where production of secondary particles peaks, $h_0 \cong 6.4$ km.

Particle	Constituent quarks	Mass (MeV)	Mean life ($c\tau$)	Decay channels	branching ratio (%)
p	uud	938.3	∞	–	–
n	udd	939.6	2.64×10^8 km	$p\ e^-\ \overline{\nu}_e$	100
$N^+(1444)$	uud	1440	≈ 300 MeV	$p\ \pi^0$	
				$n\ \pi^+$	
				$p\ \pi^+\ \pi^-$	
				$n\ \pi^+\ \pi^0$	
				$p\ \gamma$	$0.35 - 0.48$
$\Delta^+(1230)$	uud	1232	117 MeV	$p\ \pi^0$	66.7
				$n\ \pi^+$	33.3
Λ^0	uds	1115.7	7.89 cm	$p\ \pi^-$	63.9
				$n\ \pi^+$	35.8
				$p\ e^-\ \overline{\nu}_e$	8.3×10^{-2}
				$p\ \mu^-\ \overline{\nu}_\mu$	16.3×10^{-2}
Σ^+	uus	1189.4	2.40 cm	$p\ \pi^0$	51.6
				$n\ \pi^+$	48.3
Ξ^-	dss	1321.7	4.91 cm	$\Lambda\ \pi^-$	99.9
Ω^-	sss	1672.5	2.46 cm	$\Lambda\ K^-$	67.8
				$\Xi^0\ \pi^-$	23.6
				$\Xi^-\ \pi^0$	8.6
Λ_c^+	udc	2286	59.9 μm	$\Lambda/p/n\ \ldots$	73
				$\Lambda\ e^+\ \nu_e$	2.1
				$\Lambda\ \mu^+\ \nu_\mu$	2.0

Particle	Constituent quarks	Mass (MeV)	Mean life ($c\tau$)	Decay channels	branching ratio (%)
π^+	$u\bar{d}$	139.6	7.80 m	$\mu^+ \nu_\mu$	99.99
				$\mu^+ \nu_\mu \gamma$	2.0×10^{-2}
				$e^+ \nu_e$	1.2×10^{-2}
π^0	$\frac{1}{\sqrt{2}}\left(d\bar{d} - u\bar{u}\right)$	135.0	25.5 nm	$\gamma \gamma$	98.8
				$e^+ e^- \gamma$	1.17
K^+	$u\bar{s}$	493.7	3.71 m	$\mu^+ \nu_\mu$	63.6
				$\pi^+ \pi^0$	20.7
				$\pi^+ \pi^- \pi^+$	5.59
				$\pi^0 e^+ \nu_e$	5.07
				$\pi^0 \mu^+ \nu_\mu$	3.35
				$\pi^+ \pi^0 \pi^0$	1.76
K^0	$d\bar{s}$	497.6	–	–	–
K^0_L	$\frac{1}{\sqrt{2}}\left(d\bar{s} - s\bar{d}\right)$	497.6	15.34 m	$\pi^\pm e^\mp \nu_e$	40.5
				$\pi^\pm \mu^\mp \nu_\mu$	27.0
				$\pi^0 \pi^0 \pi^0$	19.5
				$\pi^+ \pi^- \pi^0$	12.5
				$\pi^+ \pi^-$	0.19
K^0_S	$\frac{1}{\sqrt{2}}\left(d\bar{s} + s\bar{d}\right)$	497.6	2.68 cm	$\pi^+ \pi^-$	69.2
				$\pi^0 \pi^0$	30.7
				$\pi^+ \pi^- \gamma$	0.18

Some useful relations (units)

- Speed of light: $c = 2.9979 \times 10^{10}\,\mathrm{cm\,s^{-1}}$
- Gravitational constant: $G = 6.6738 \times 10^{-8}\,\mathrm{cm^3\,g^{-1}\,s^{-2}}$
- Planck constant: $h = 6.626 \times 10^{-27}\,\mathrm{erg\,s} = 4.136 \times 10^{-15}\,\mathrm{eV\,s}$,
  $\hbar = h/(2\pi) = 1.0546 \times 10^{-27}\,\mathrm{erg\,s}$
- Boltzmann constant: $k_B = 8.6173 \times 10^{-5}\,\mathrm{eV\,K^{-1}} = 1.3806 \times 10^{-16}\,\mathrm{erg\,K^{-1}}$
- Avogadro constant: $N_A = 6.0221 \times 10^{23}$. By definition, N_A atoms of carbon $^{12}\mathrm{C}$ have a mass of $12\,\mathrm{g}$. Therefore, the mean mass of a nucleon can be written as $m_N = (m_p + m_n)/2 \approx (1/N_A)\,\mathrm{g} = 1.6605 \times 10^{-24}\,\mathrm{g}$.
- Energy units: $1\,\mathrm{erg} = 10^{-7}\,\mathrm{J}$, $1\,\mathrm{eV} = 1.6022 \times 10^{-12}\,\mathrm{erg}$,
  $1\,\mathrm{cm^{-1}} = 0.000123986\,\mathrm{eV}$, $1\,\mathrm{fm} = 5.06773\,\mathrm{GeV^{-1}}$
- A photon of $E_\gamma = 1\,\mathrm{keV}$ has a frequency of $\nu = 2.4 \times 10^{17}\,\mathrm{Hz}$. This statement is based on $E_\gamma = h\nu$. Direct conversion of units using $\hbar = h/(2\pi) = 6.582 \times 10^{-22}\,\mathrm{MeV\,s}$ would give a result that differs by 2π.
- Distances: $1\,\mathrm{pc} = 3.0857 \times 10^{18}\,\mathrm{cm}$, $1\,\mathrm{AU} = 1.496 \times 10^{13}\,\mathrm{cm}$
- Cross sections: $1\,\mathrm{mb} = 10^{-27}\,\mathrm{cm^2}$, $(1\,\mathrm{fm})^2 = 10\,\mathrm{mb}$,
  $(1\,\mathrm{GeV})^{-2} = 0.389365\,\mathrm{mb}$
- Thomson cross section: $\sigma_\mathrm{T} = 8\pi r_e^2/3 = 665.25\,\mathrm{mb} = 6.652 \times 10^{-25}\,\mathrm{cm^2}$, where r_e is the classical electron radius $r_e = e^2/(m_e c^2) = 2.818 \times 10^{-13}\,\mathrm{cm}$
- Solar mass and luminosity: $M_\odot = 1.9885 \times 10^{33}\,\mathrm{g}$, $L_\odot = 3.828 \times 10^{33}\,\mathrm{erg\,s^{-1}}$
- Flux density used in radio astronomy (Jansky): $1\,\mathrm{Jy} = 10^{-26}\mathrm{W\,m^{-2}\,Hz^{-1}} = 10^{-23}\,\mathrm{erg\,s^{-1}\,cm^{-2}\,Hz^{-1}}$
- Magnetic field strength: $1\,\mathrm{G} = 10^{-4}\,\mathrm{T}$

Total and elastic cross sections

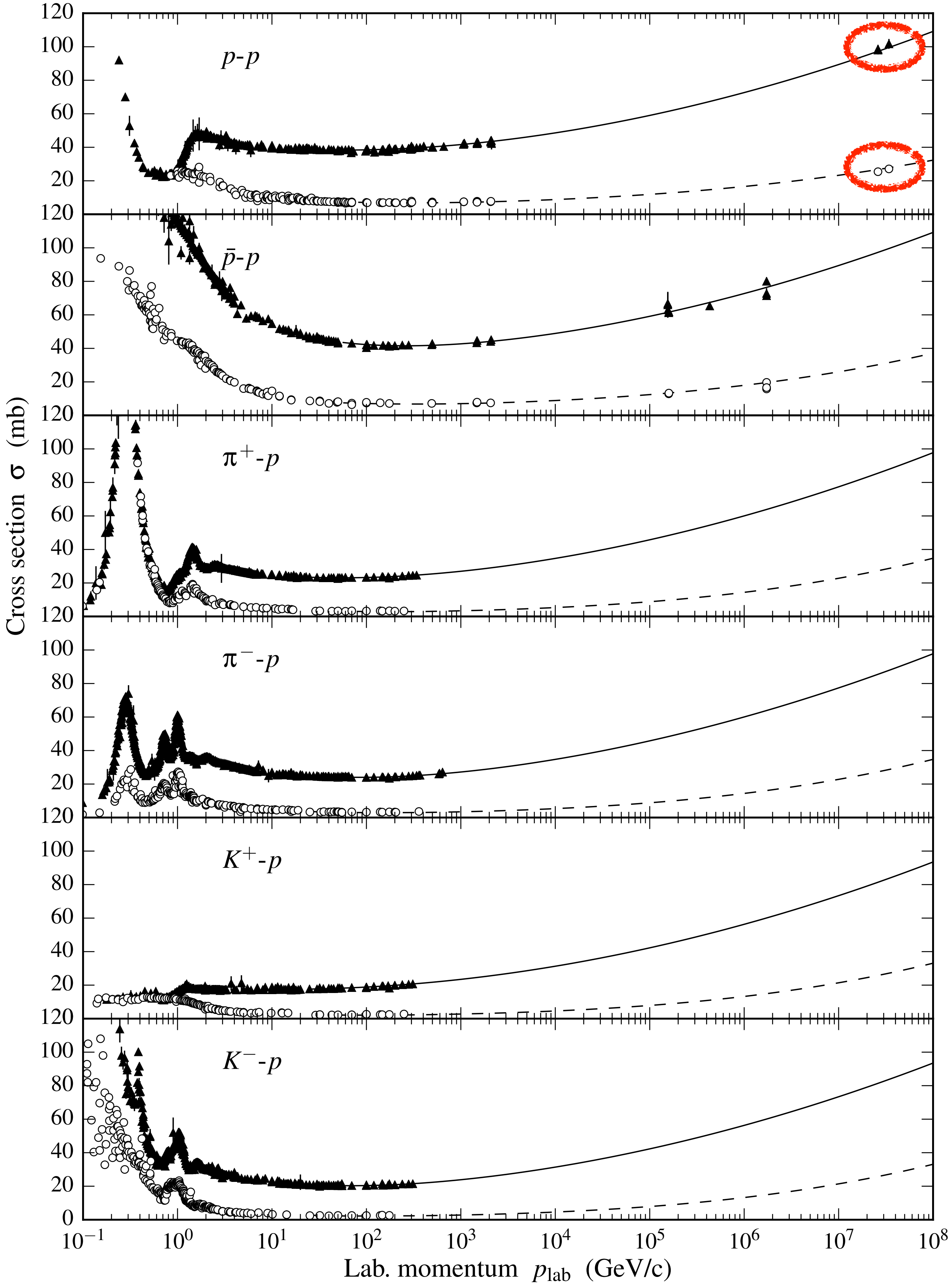

LHC results

1. Low energy interactions:
resonance formation,
spin-dependent angular decay,
up to ~3 GeV

2. Intermediate energy:
approximate scaling, up to 1000 GeV

3. High energy interactions:
scaling violation, multiple interactions
and minijet production

(Gaisser, Engel, Resconi 2016)

Compilation of total cross sections

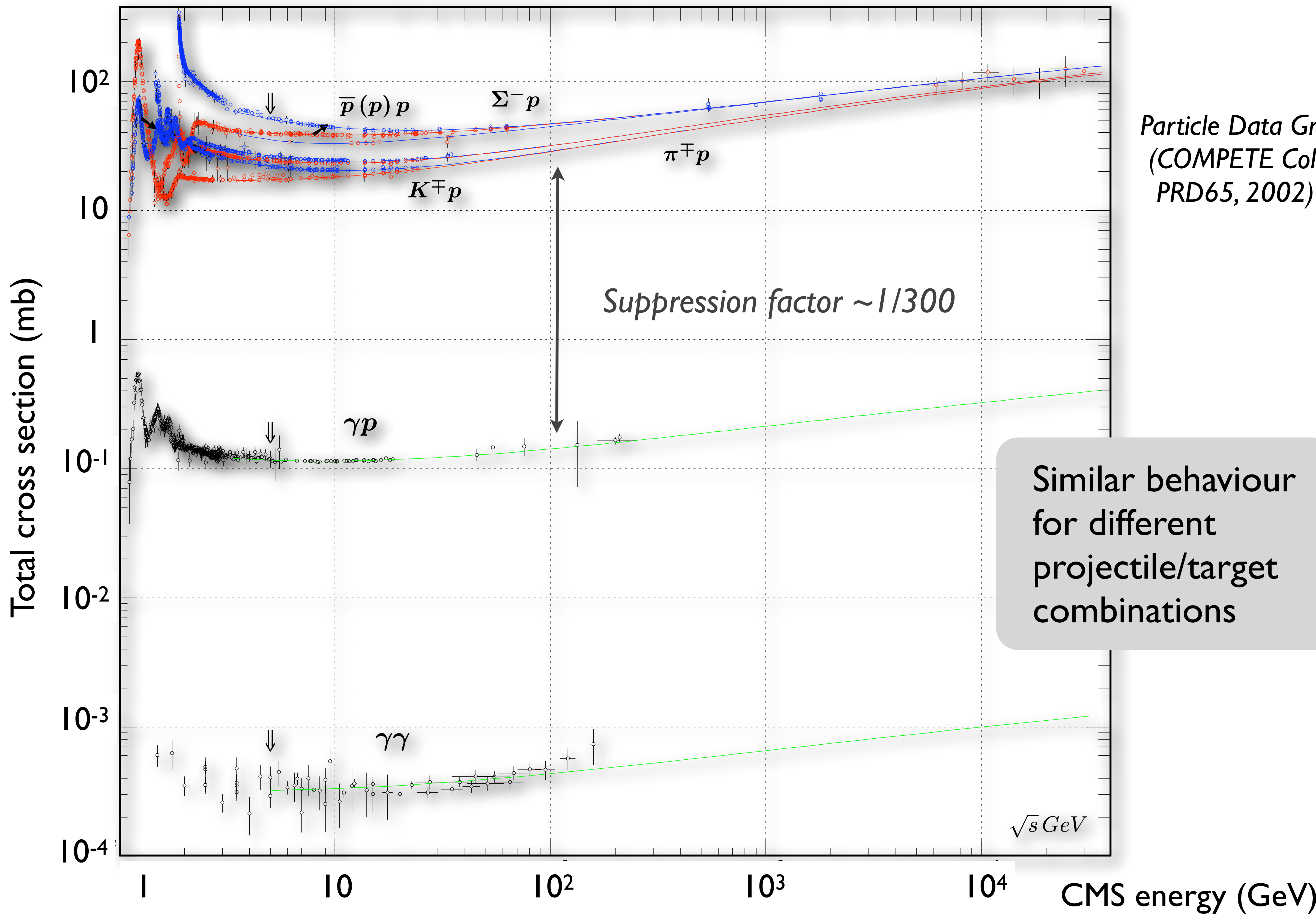

Particle Data Group (COMPETE Collab. PRD65, 2002)

Similar behaviour for different projectile/target combinations

1. Low energy region

Hadronic interaction of photons

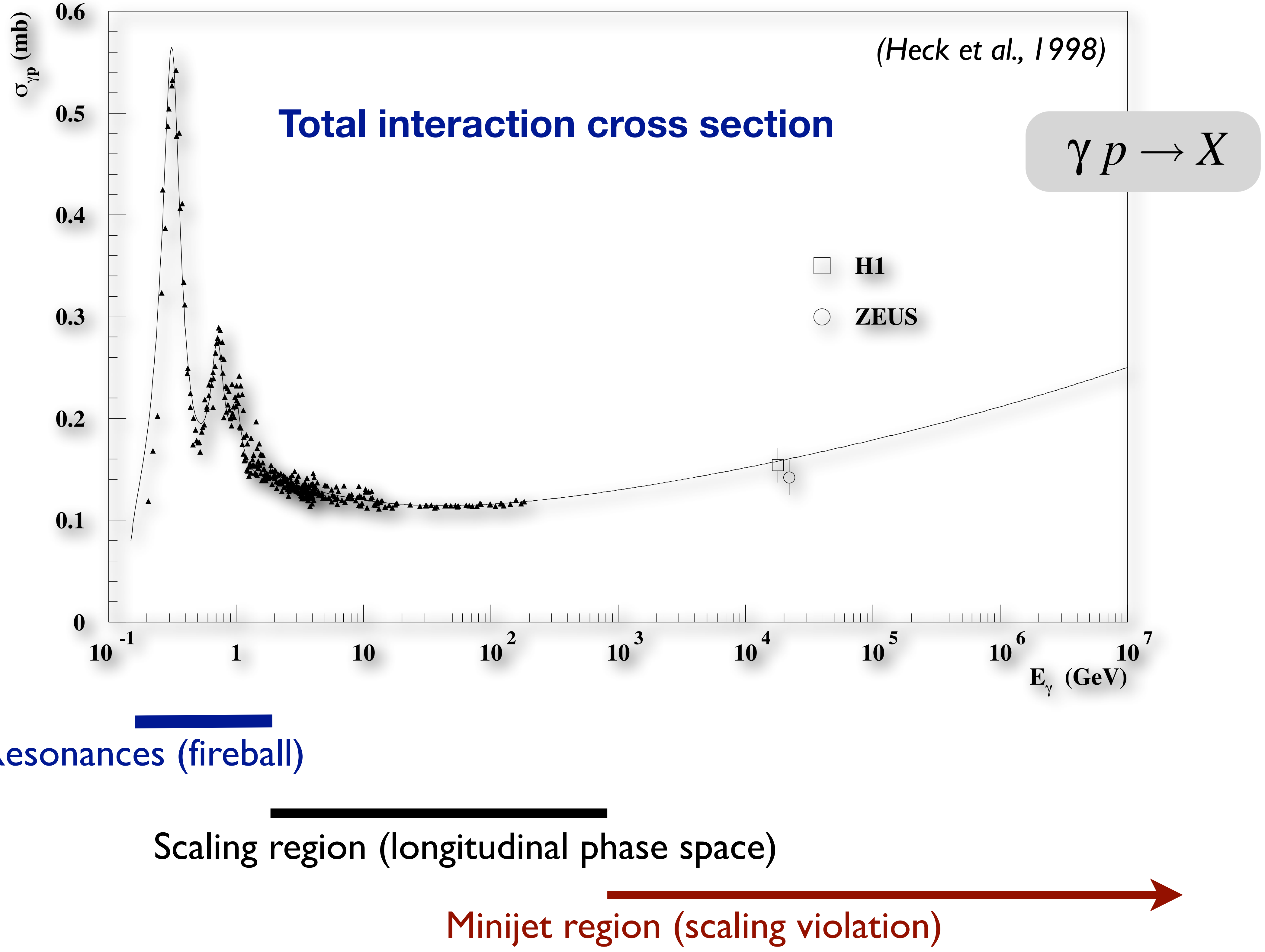

Photoproduction of resonances

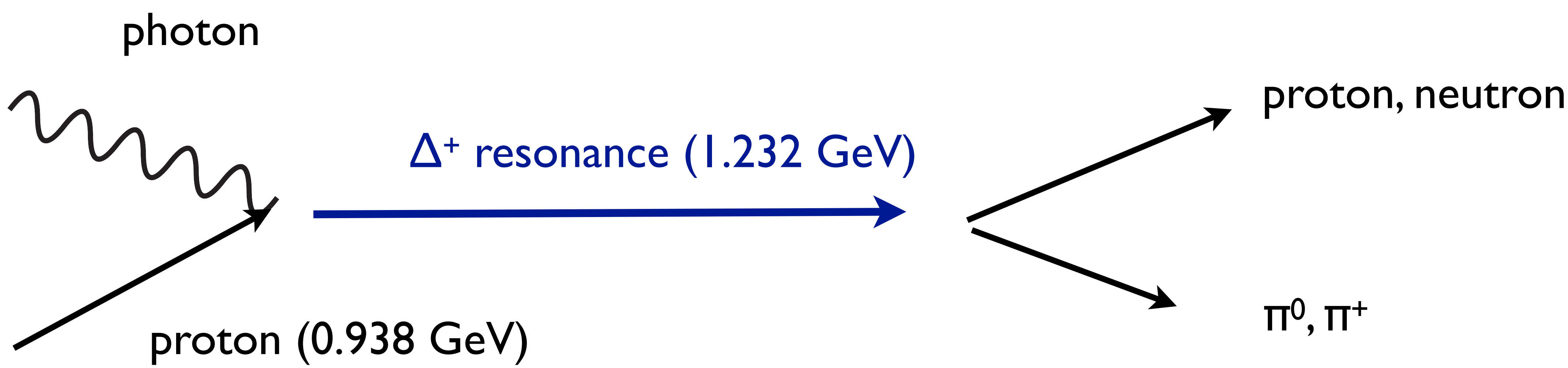

CMB: Energy threshold not sharp $\quad E_{\gamma,\mathrm{max}} \approx 10^{-3}\mathrm{eV}$

$$E_{p,\Delta} = \frac{m_\Delta^2 - m_p^2}{2E_{\gamma,\mathrm{max}}(1-\cos\theta)} \approx 10^{20}\mathrm{eV}$$

In proton rest frame:

$$E_{\gamma,\mathrm{lab}} \approx 300\ \mathrm{MeV}$$

Decay branching ratio proton:neutron = 2:1

Mean proton energy loss 20%

Decay isotropic up to spin effects

Well-established resonances in photoproduction

Baryon resonances and their physical parameters implemented in SOPHIA (see text). Superscripts $^+$ and ^{0} in the parameters refer to $p\gamma$ and $n\gamma$ excitations, respectively. The maximum cross section, $\sigma_{\max} = 4m_{\mathrm{N}}^2 M^2 \sigma_0/(M^2 - m_{\mathrm{N}}^2)^2$, is also given for reference

Resonance	M	Γ	$10^3 b_\gamma^+$	σ_0^+	$\sigma_{\max}^+$	$10^3 b_\gamma^0$	σ_0^0	$\sigma_{\max}^0$
$\Delta(1232)$	1.231	0.11	5.6	31.125	411.988	6.1	33.809	452.226
$N(1440)$	1.440	0.35	0.5	1.389	7.124	0.3	0.831	4.292
$N(1520)$	1.515	0.11	4.6	25.567	103.240	4.0	22.170	90.082
$N(1535)$	1.525	0.10	2.5	6.948	27.244	2.5	6.928	27.334
$N(1650)$	1.675	0.16	1.0	2.779	7.408	0.0	0.000	0.000
$N(1675)$	1.675	0.15	0.0	0.000	0.000	0.2	1.663	4.457
$N(1680)$	1.680	0.125	2.1	17.508	46.143	0.0	0.000	0.000
$\Delta(1700)$	1.690	0.29	2.0	11.116	28.644	2.0	11.085	28.714
$\Delta(1905)$	1.895	0.35	0.2	1.667	2.869	0.2	1.663	2.875
$\Delta(1950)$	1.950	0.30	1.0	11.116	17.433	1.0	11.085	17.462

Breit-Wigner resonance cross section

$$\sigma_{\mathrm{bw}}(s; M, \Gamma, J) = \frac{s}{(s - m_{\mathrm{N}}^2)^2} \frac{4\pi b_\gamma (2J+1) s \Gamma^2}{(s - M^2)^2 + s\Gamma^2}$$

Direct pion production

Possible interpretation: p fluctuates from time to time to n and π^+

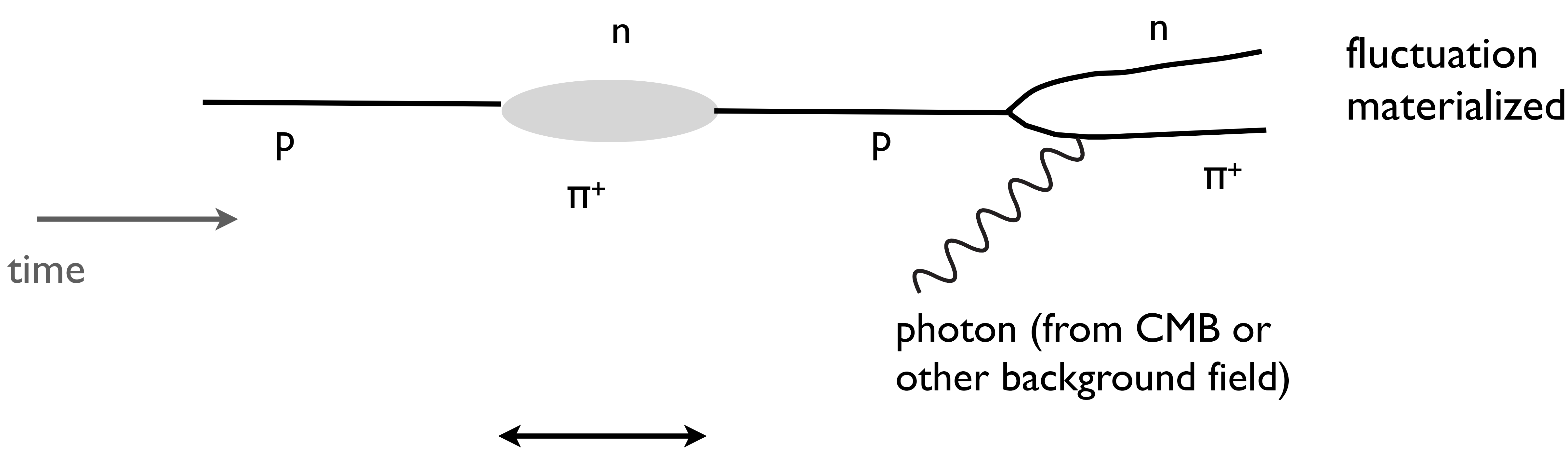

Heisenberg uncertainty relation $\Delta E \Delta t \approx 1$

Energy threshold very low: $$E_{\mathrm{cm,min}} = m_\pi + m_p \approx 1.07\ \mathrm{GeV}$$

(Δ^+ resonance: 1.232 GeV)

Lifetime of fluctuations

Consider photon with momentum k

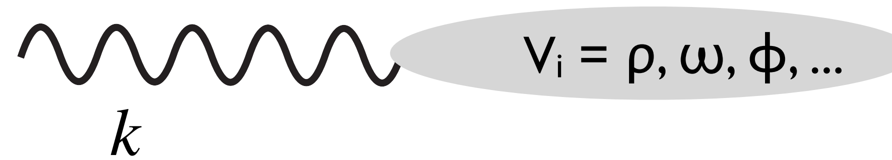

Heisenberg uncertainty relation $\Delta E\, \Delta t \approx 1$

Length scale (duration) of hadronic interaction $\Delta t_{\text{int}} < 1\text{fm} \approx 5\text{GeV}^{-1}$

$$\Delta t \approx \frac{1}{\Delta E} = \frac{1}{\sqrt{k^2 + m_V^2} - k} = \frac{1}{k(\sqrt{1 + m_V^2/k^2} - 1)} \approx \frac{2k}{m_V^2}$$

Fluctuation long-lived for k > 3 GeV

$$\boxed{\Delta t \approx \frac{2k}{m_V^2} > \Delta t_{\text{int}}}$$

Multiparticle production: vector meson dominance

Photon is considered as superposition of ``bare´´ photon and hadronic fluctuation

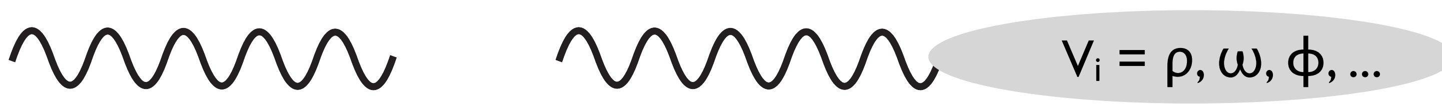

$$|\gamma\rangle = |\gamma_{\rm bare}\rangle + P_{\rm had} \sum_i |V_i\rangle$$

$$P_{\rm had} \approx \frac{1}{300} \ldots \frac{1}{250}$$

Cross section for hadronic interaction ~1/300 smaller than for pi-p interactions

Multiparticle production

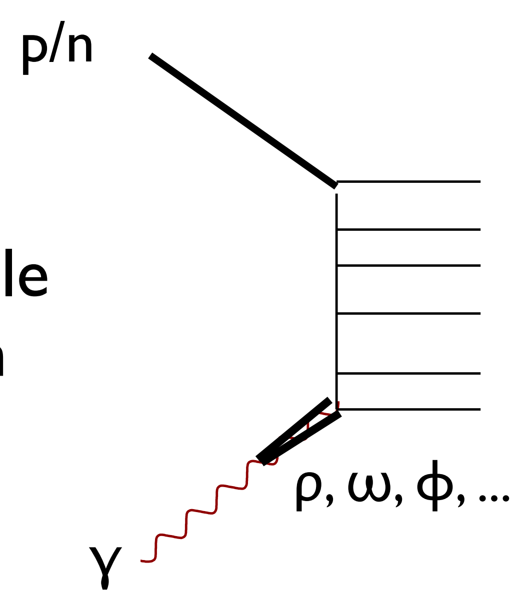

Elastic scattering

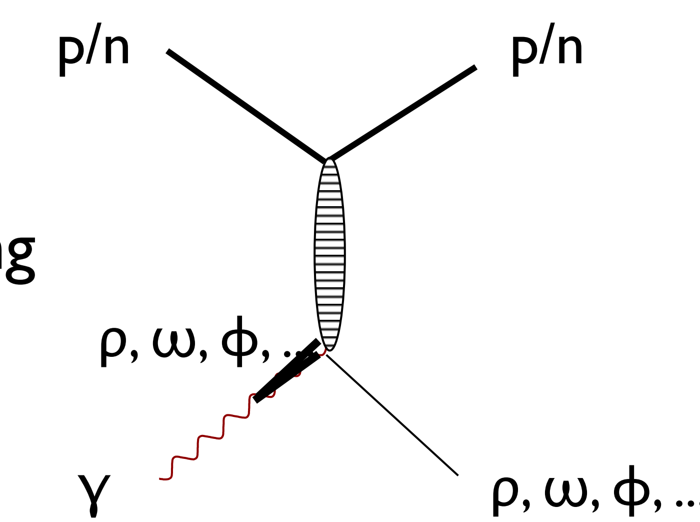

Putting all together: description of total cross section

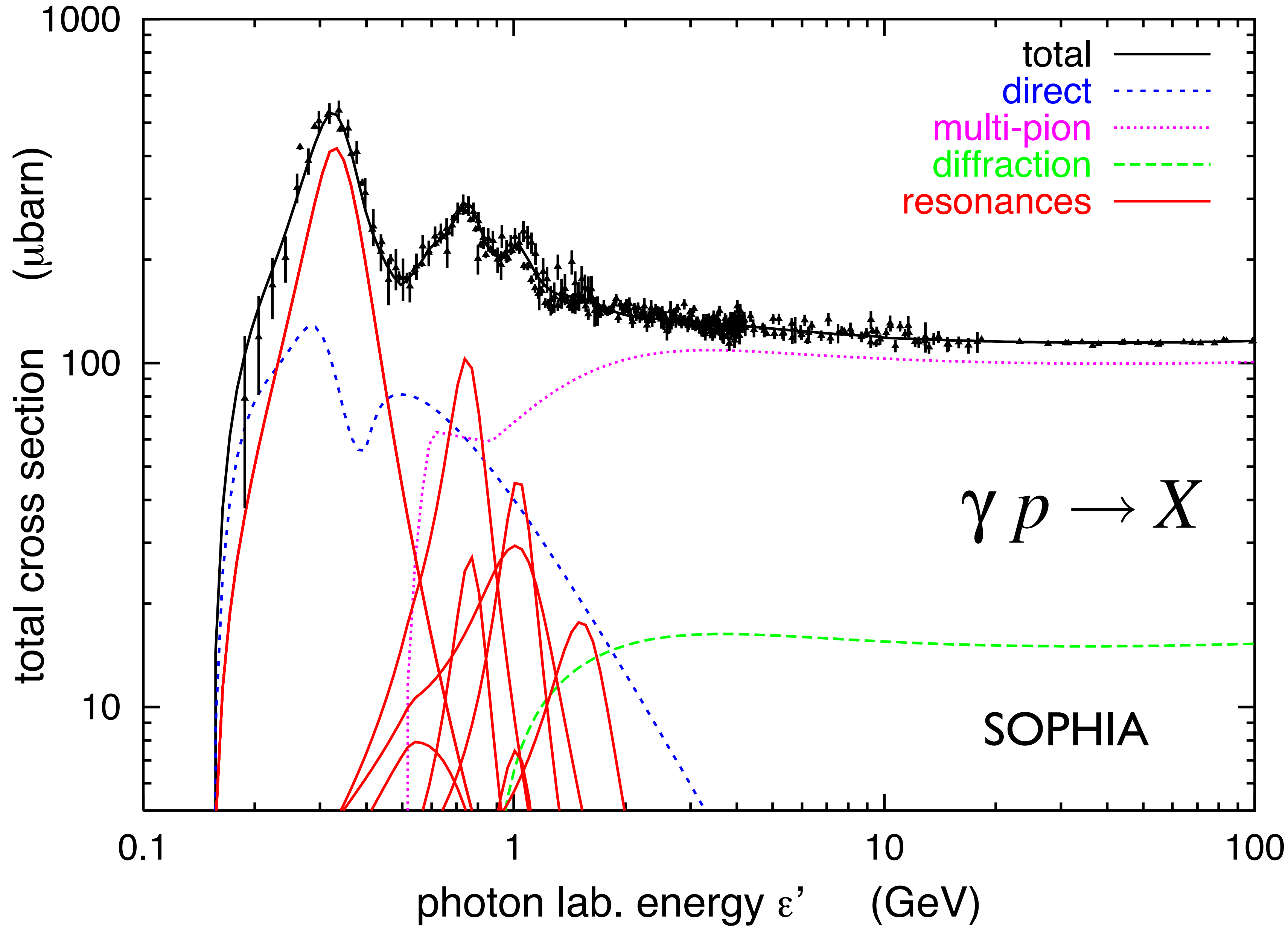

- PDG: 9 resonances, decay channels, angular distributions
- Regge parametrization at higher energy
- Direct contribution: fit to difference to data

Many measurements available, still approximations necessary

SOPHIA (Mücke et al. CPC124, 2000)

Comparison with measured partial cross sections

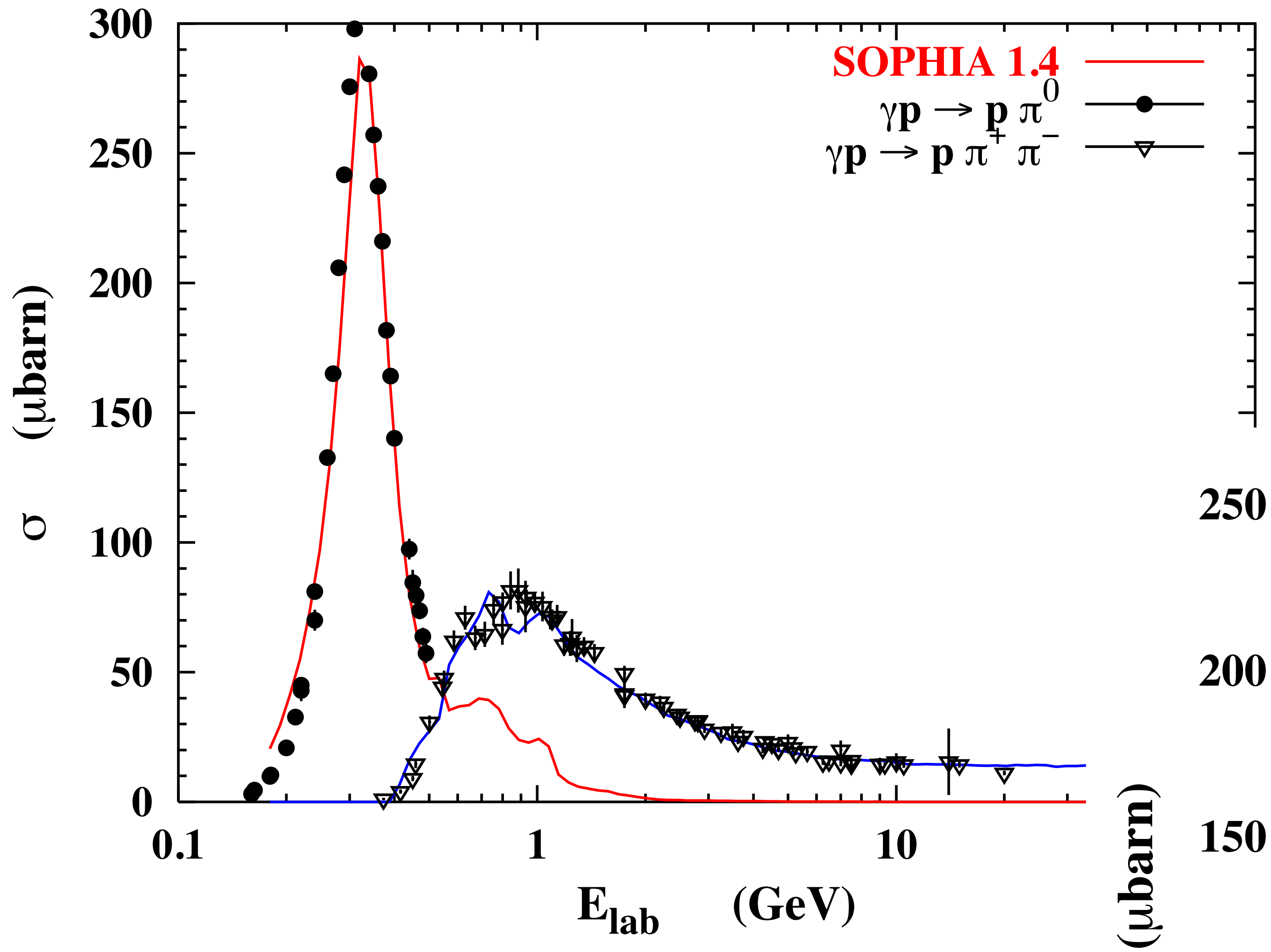

Data from fixed-target experiments

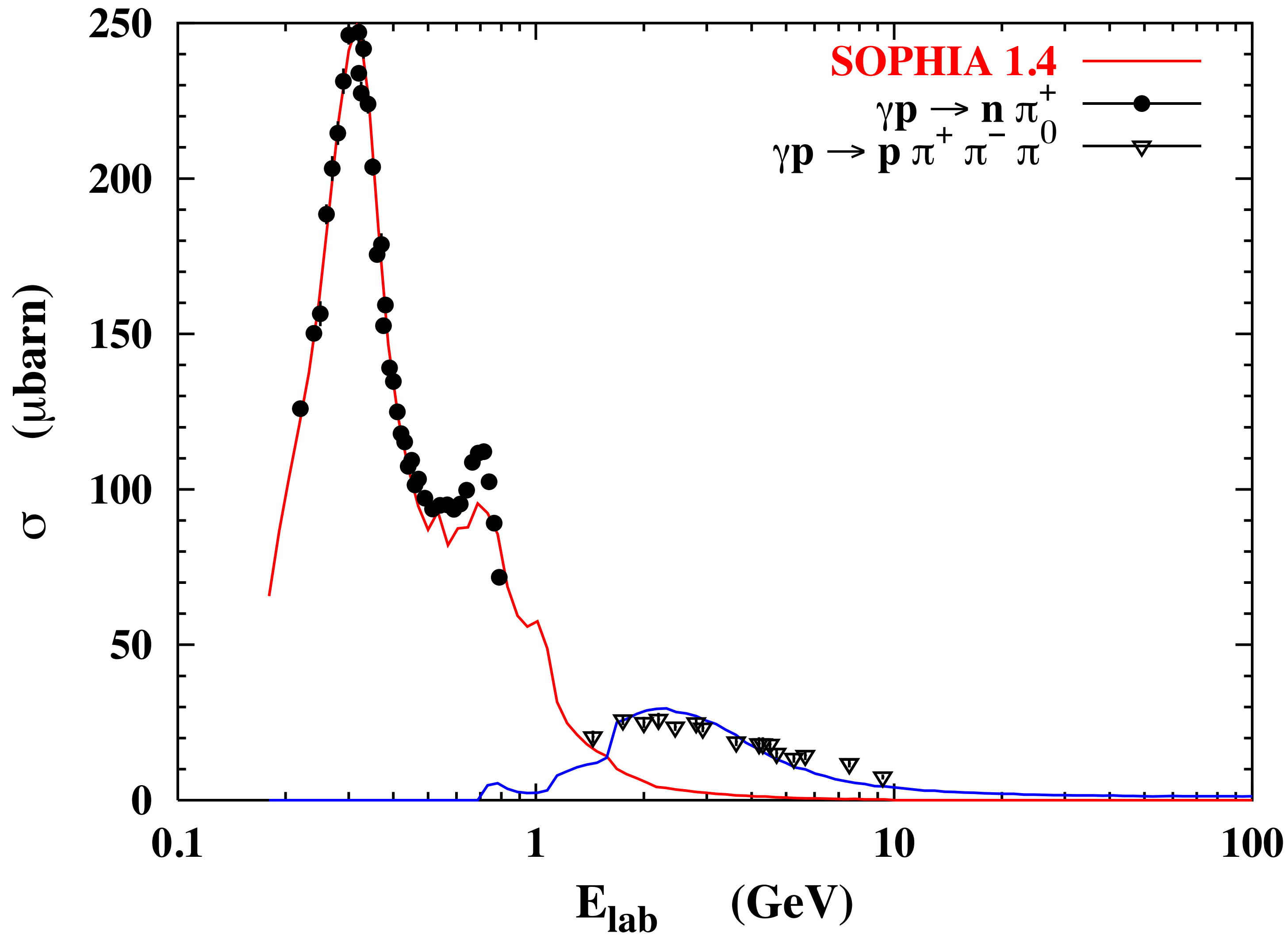

SOPHIA (Mücke et al. CPC124, 2000)

Comparison with measured partial cross sections

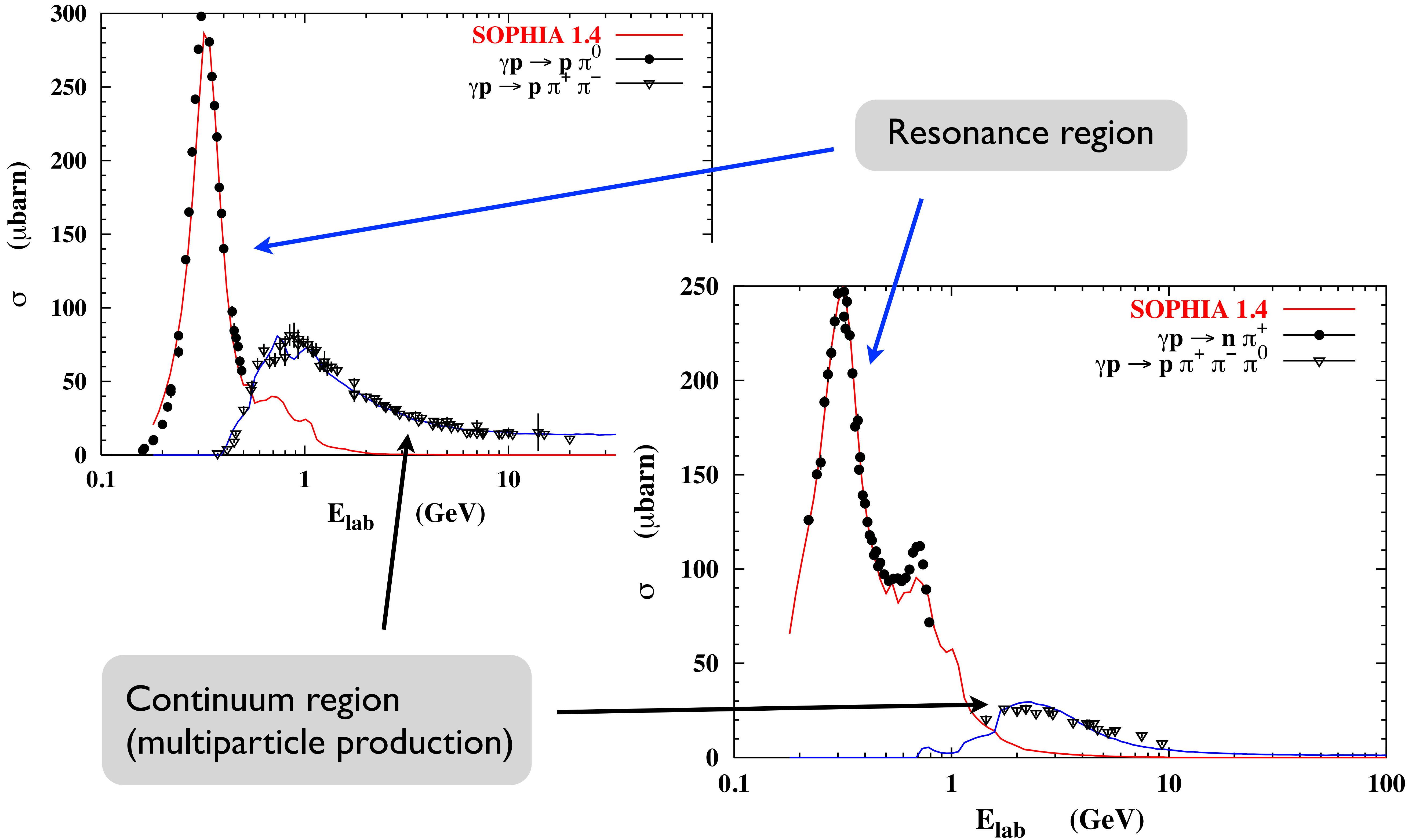

Measurement of nucleus disintegration

Photoproduction

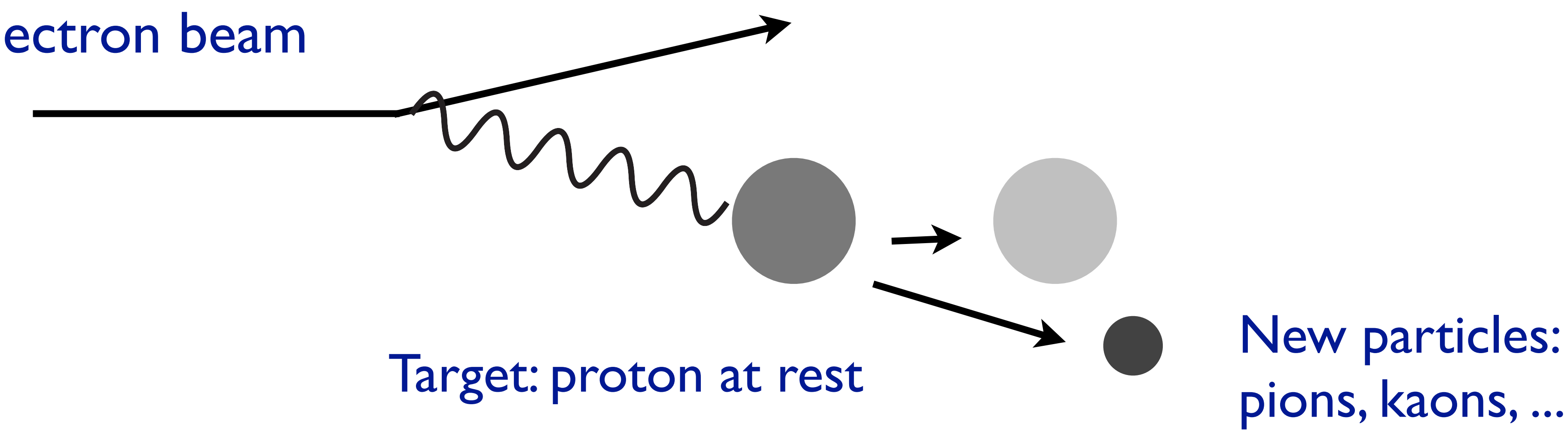

Photodissociation

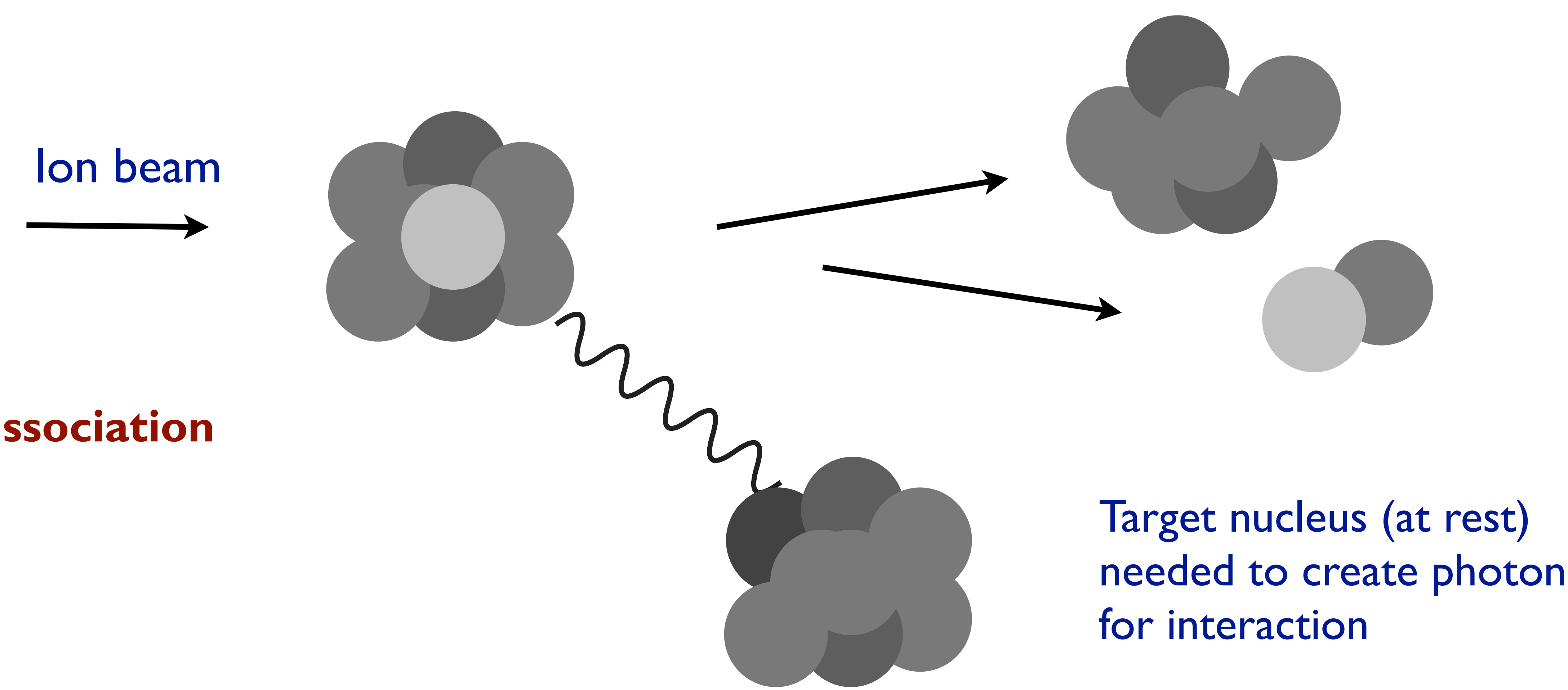

Effective em. dissociation cross section

Main contribution:
giant dipole resonance

Dominant emission processes:

- single nucleon
- quasi-deuteron
- alpha particle

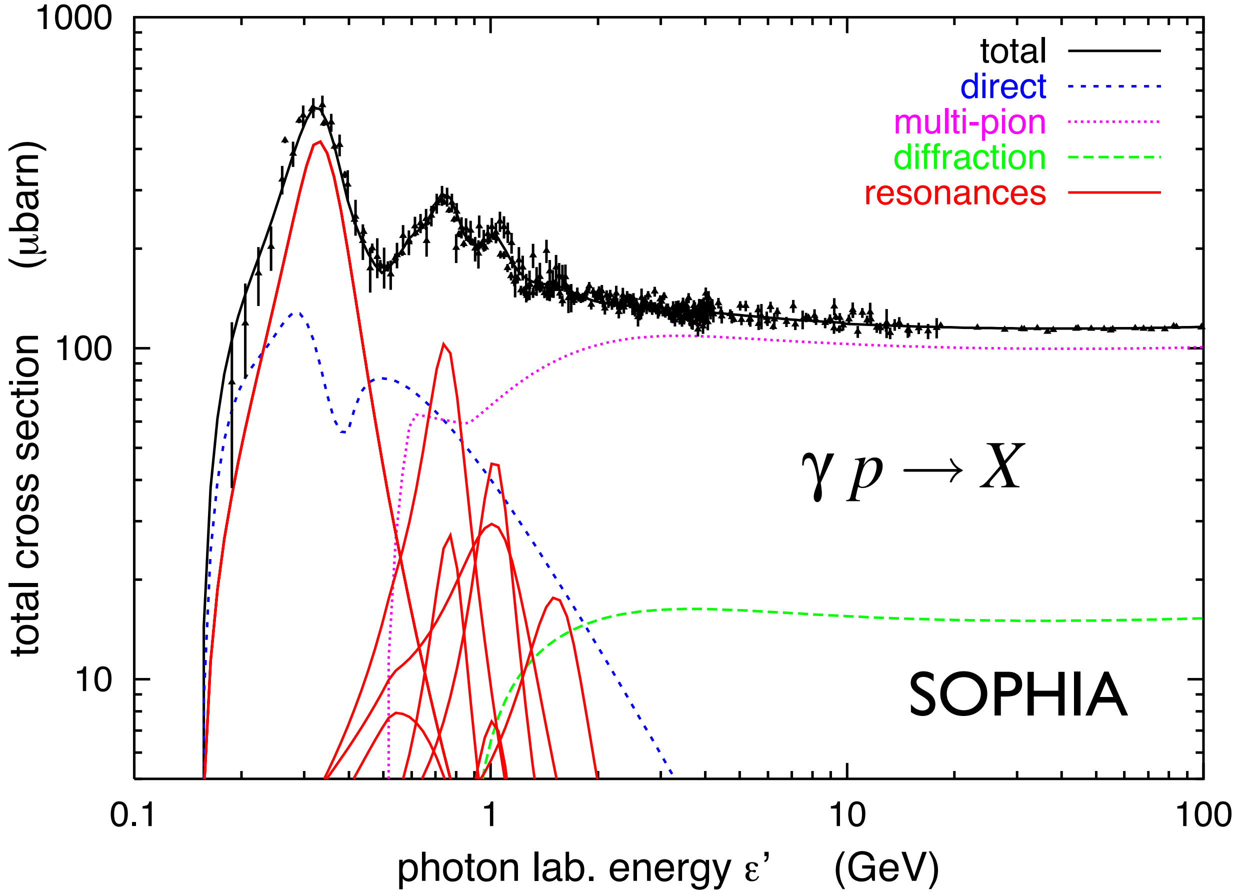

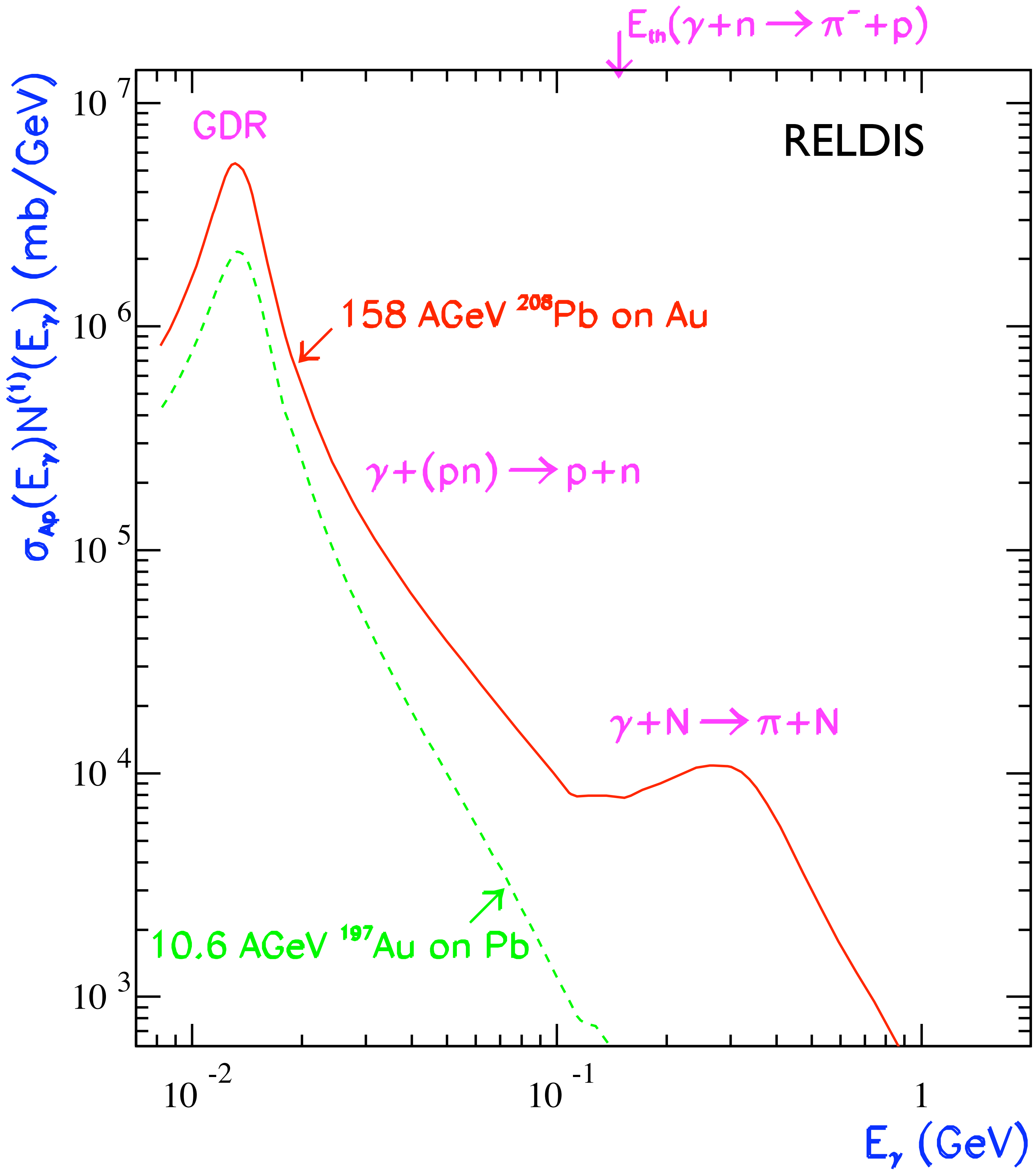

(Pshenichnov 2002)

Example: photo-dissociation of nuclei

Saclay & Livermore data

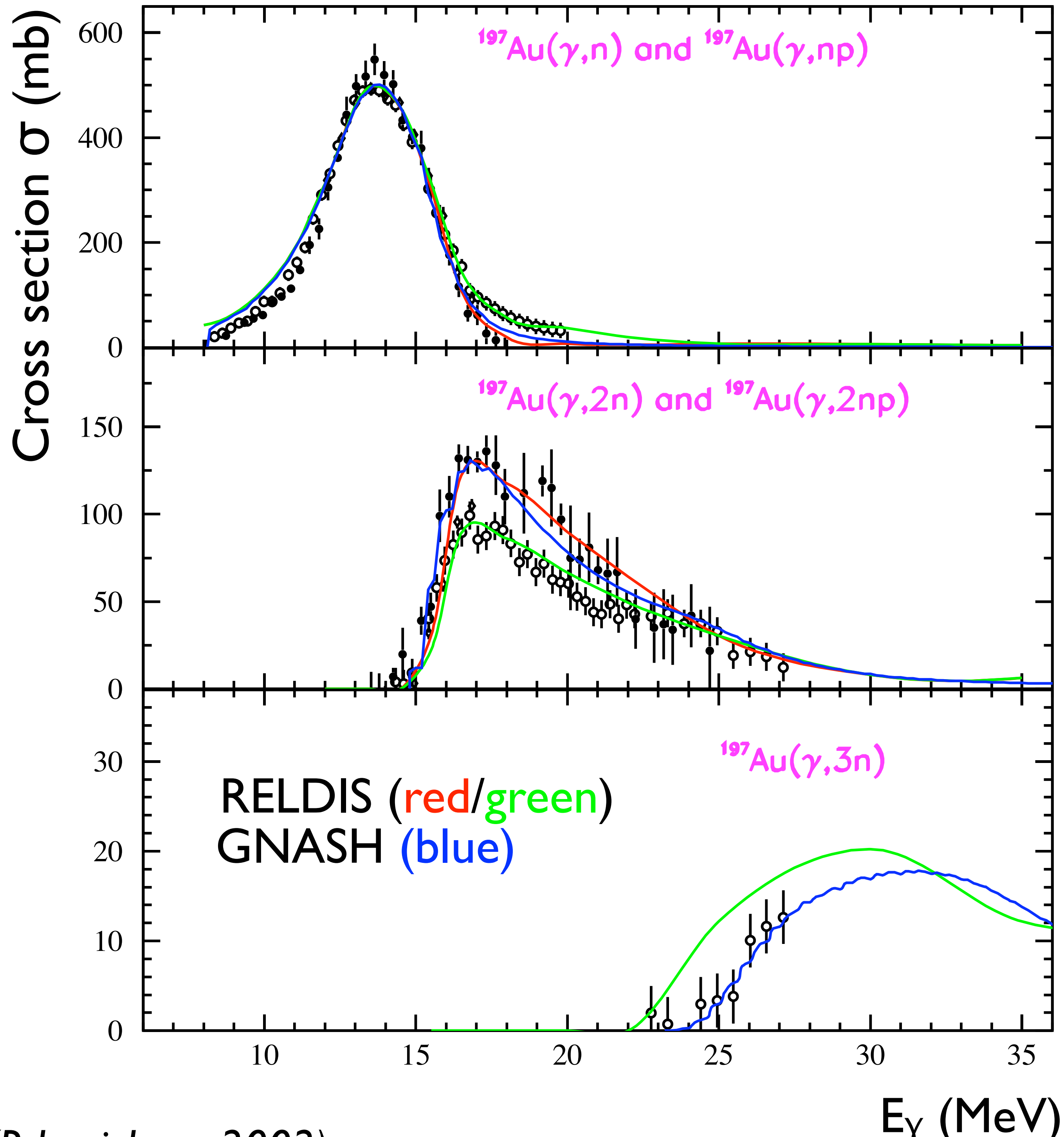

(Pshenichnov 2002)

Projectile: 30 AGeV Pb, different targets

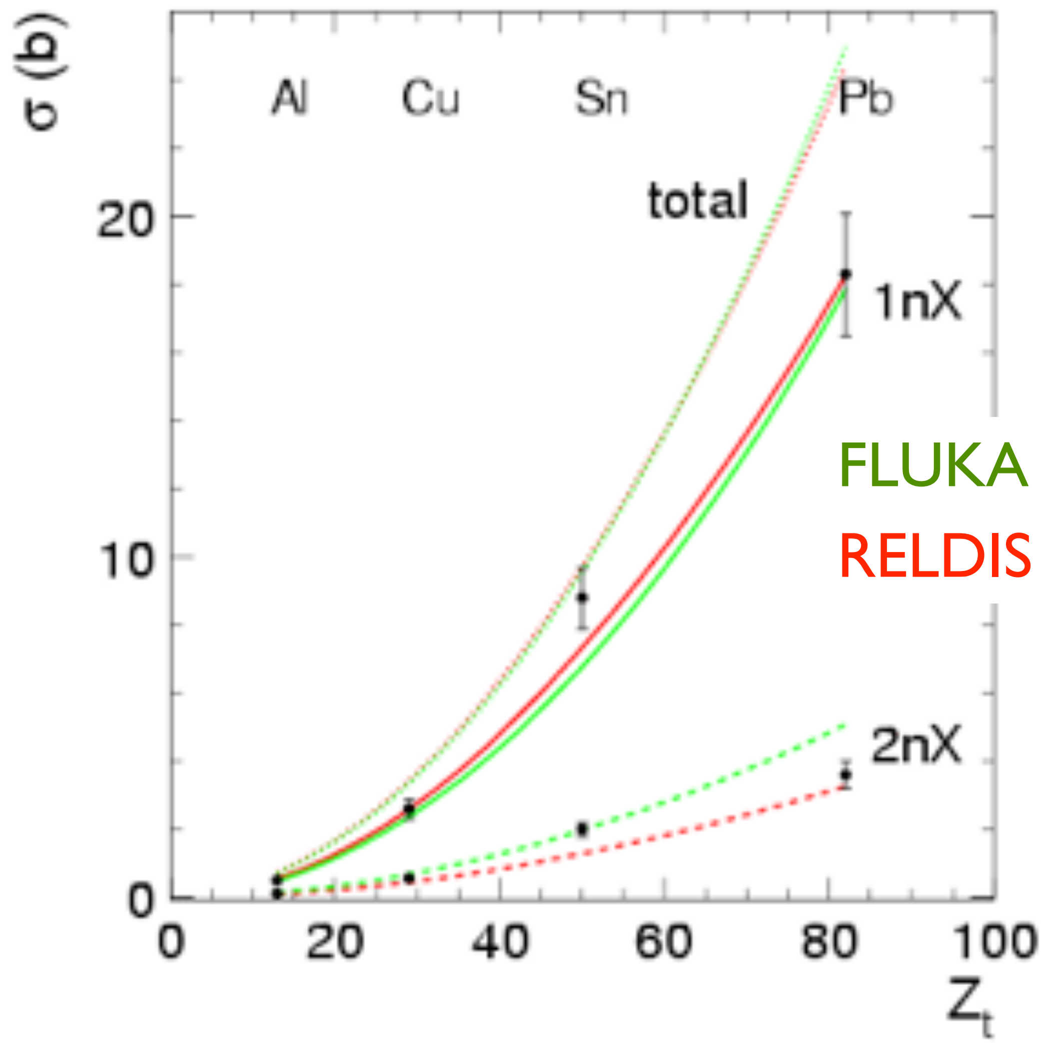

(Smirnov, 2005)

Energy considerations for nuclei

Energy of nucleus needed for formation of giant dipole resonance in CMB

Nucleus at rest

$$\begin{aligned} s &= (\overbrace{p_\gamma}^{13\ \text{MeV}} + p_A)^2 \\ &= p_\gamma^2 + p_A^2 + 2(p_\gamma \cdot p_A) \\ &= (Am_p)^2 + 2Am_pE_\gamma \end{aligned}$$

Iron: $E_A \sim 3\ 10^{20}$ eV
Helium: $E_A \sim 2\ 10^{19}$ eV

Nucleus with E_A in CMB field

$$s = (Am_p)^2 + 2E_\gamma^{\text{CMB}} E_A (1 - \cos\theta)$$

Photo-disintegration for energies

$$\boxed{E_A \geq A \frac{m_p E_\gamma}{(1 - \cos\theta) E_\gamma^{\text{CMB}}}}$$

Light nuclei disintegrate very fast while traveling through CMB

Radiation fields as possible target

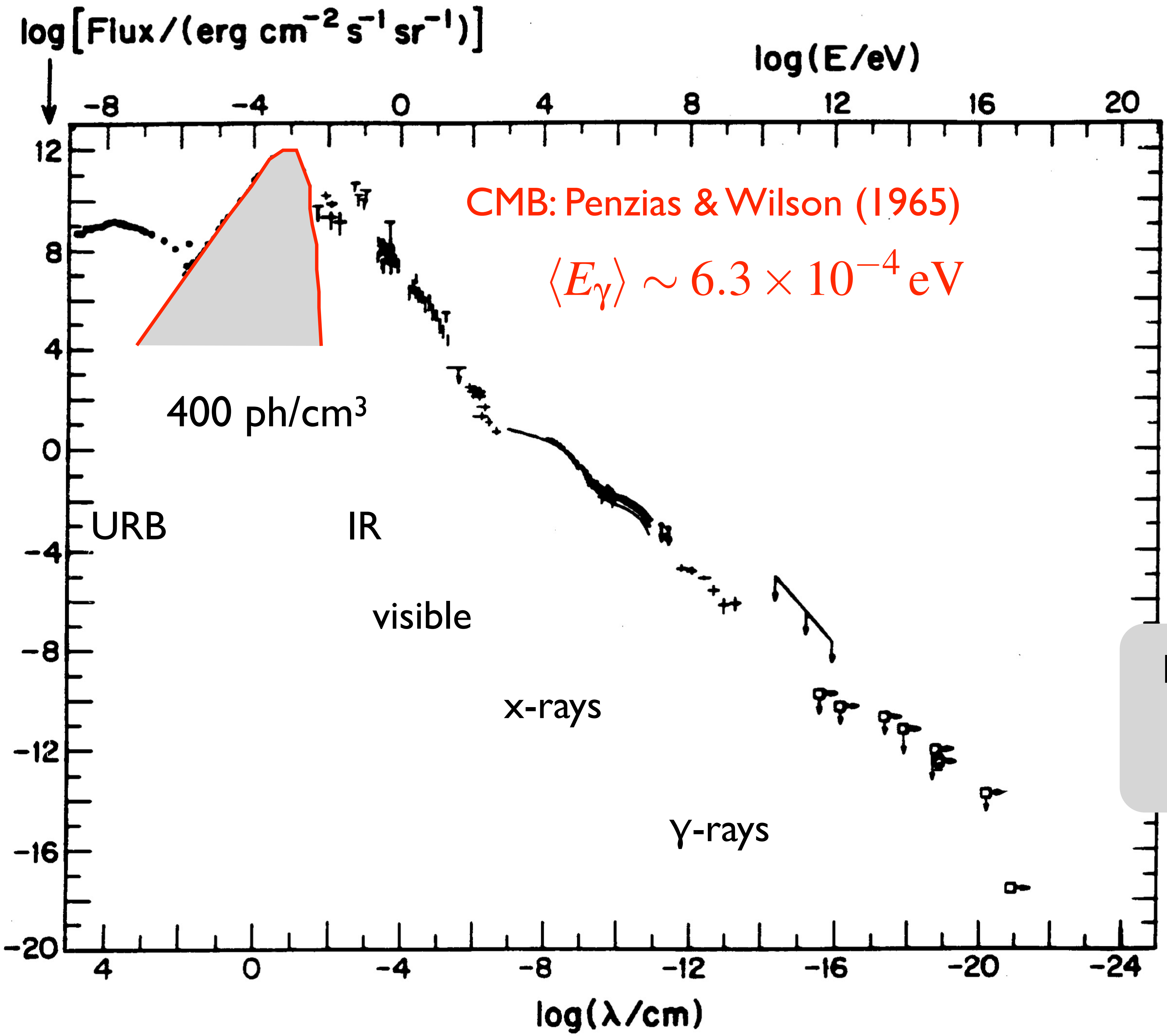

Small interaction probability compensated by large density

In source regions:

- much higher densities
- power-law spectra

Comparison of energy loss lengths

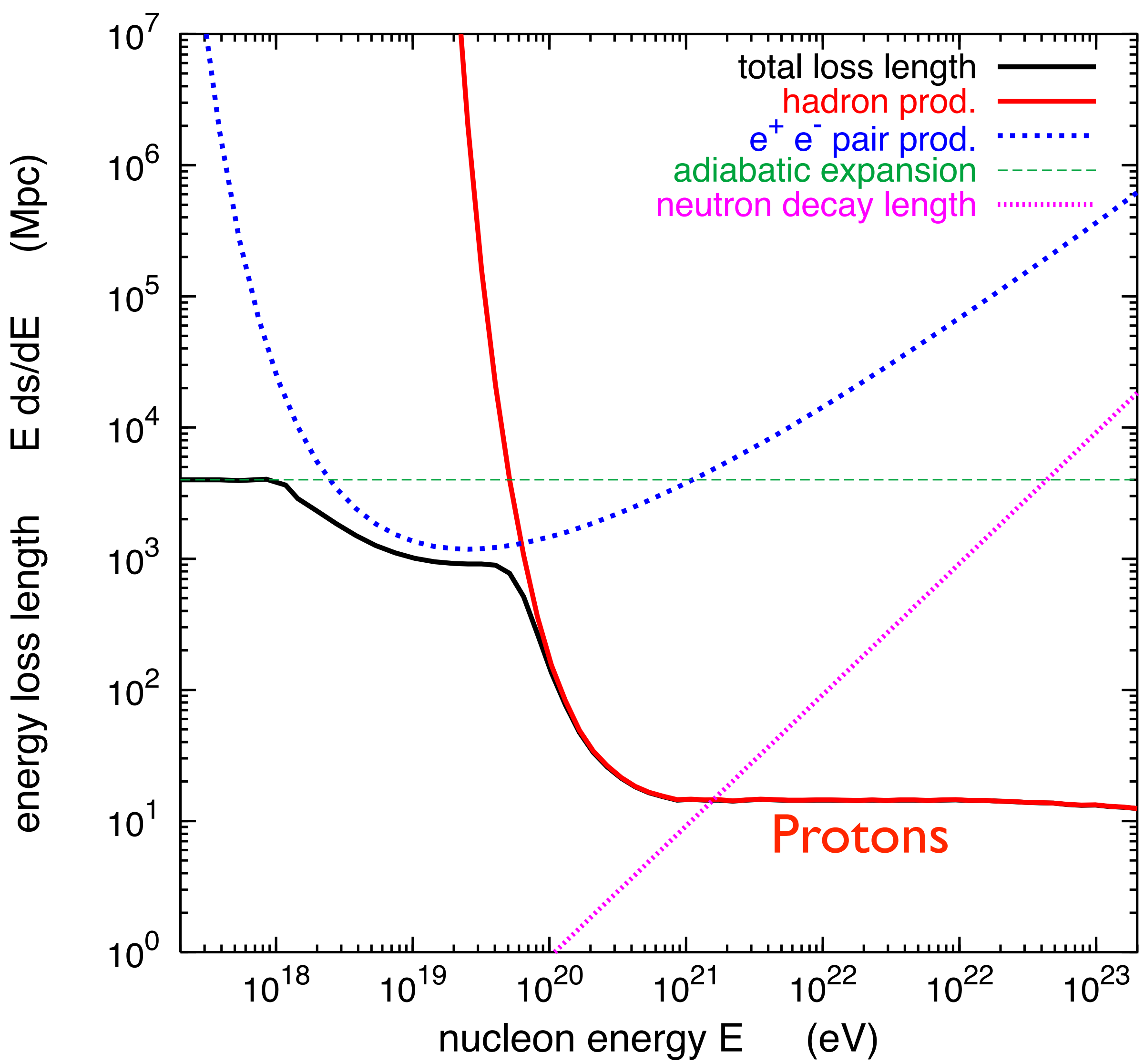

Energy loss length

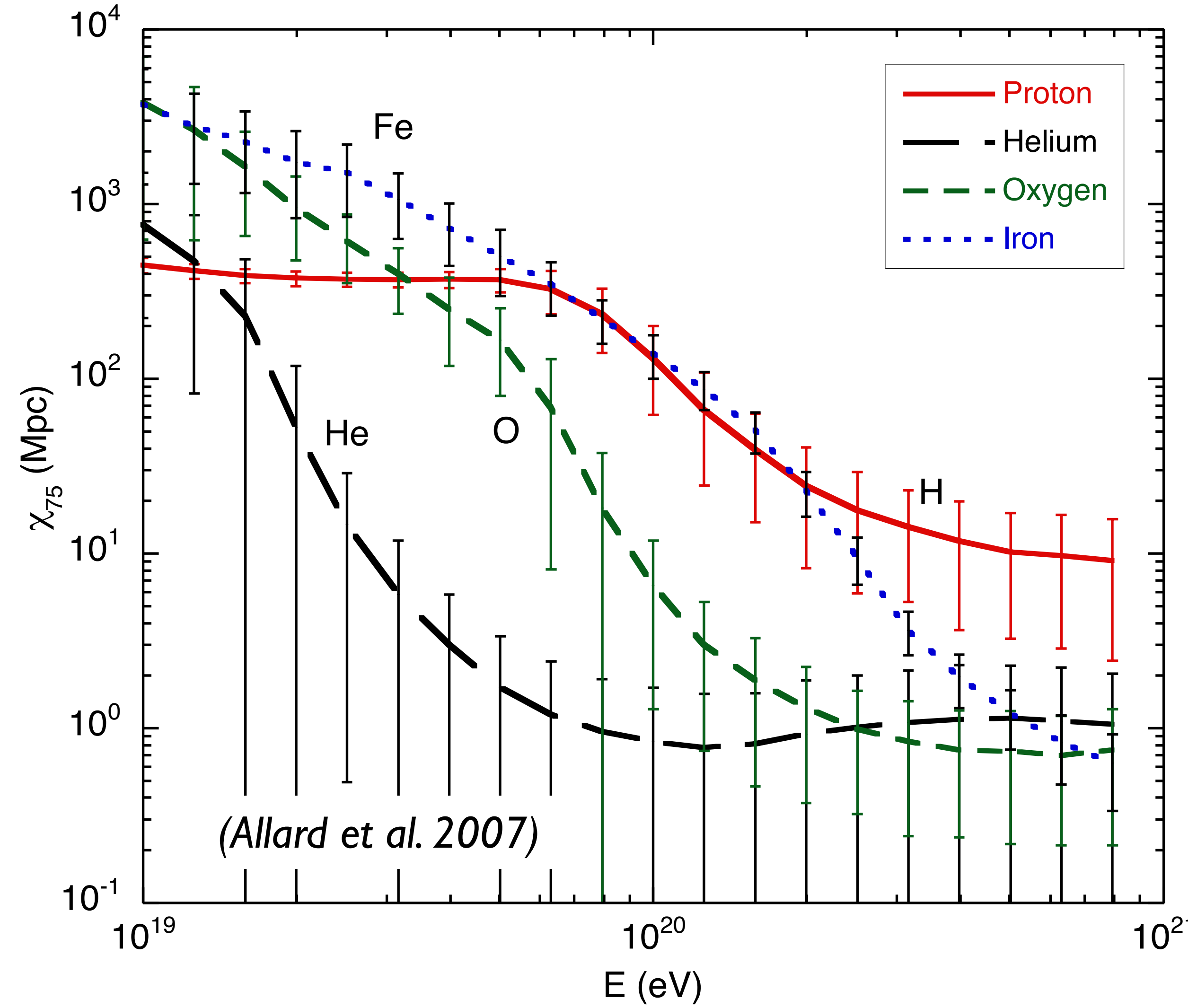

Photo-pion production

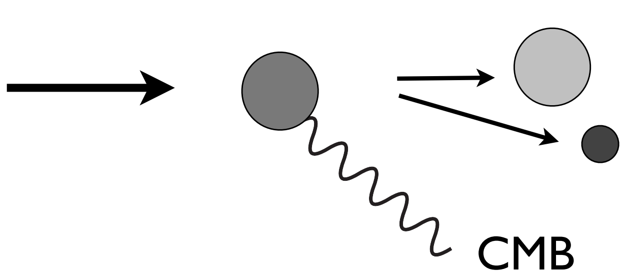

Photo-dissociation (giant dipole resonance)

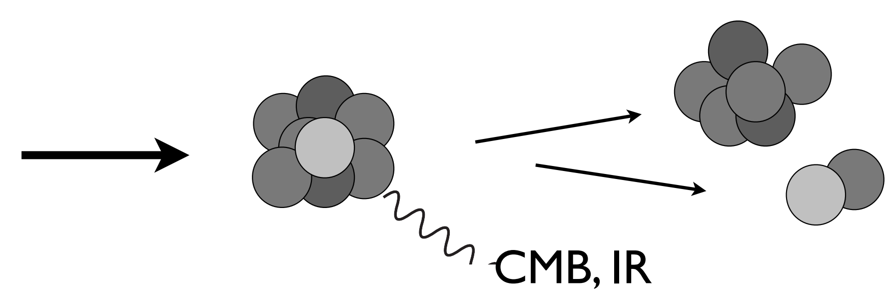

Parametrization of cross sections

Examples of used parametrizations

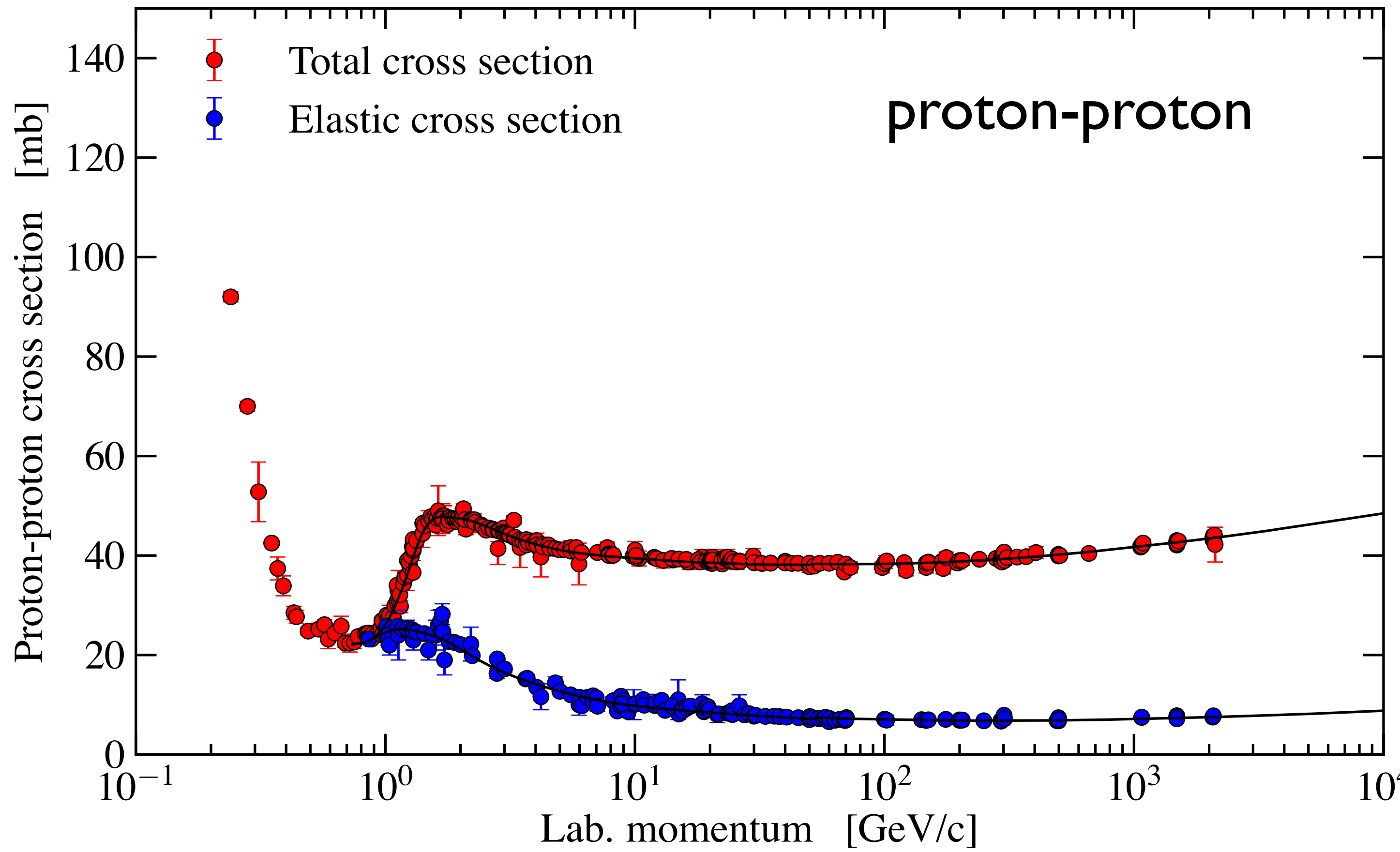

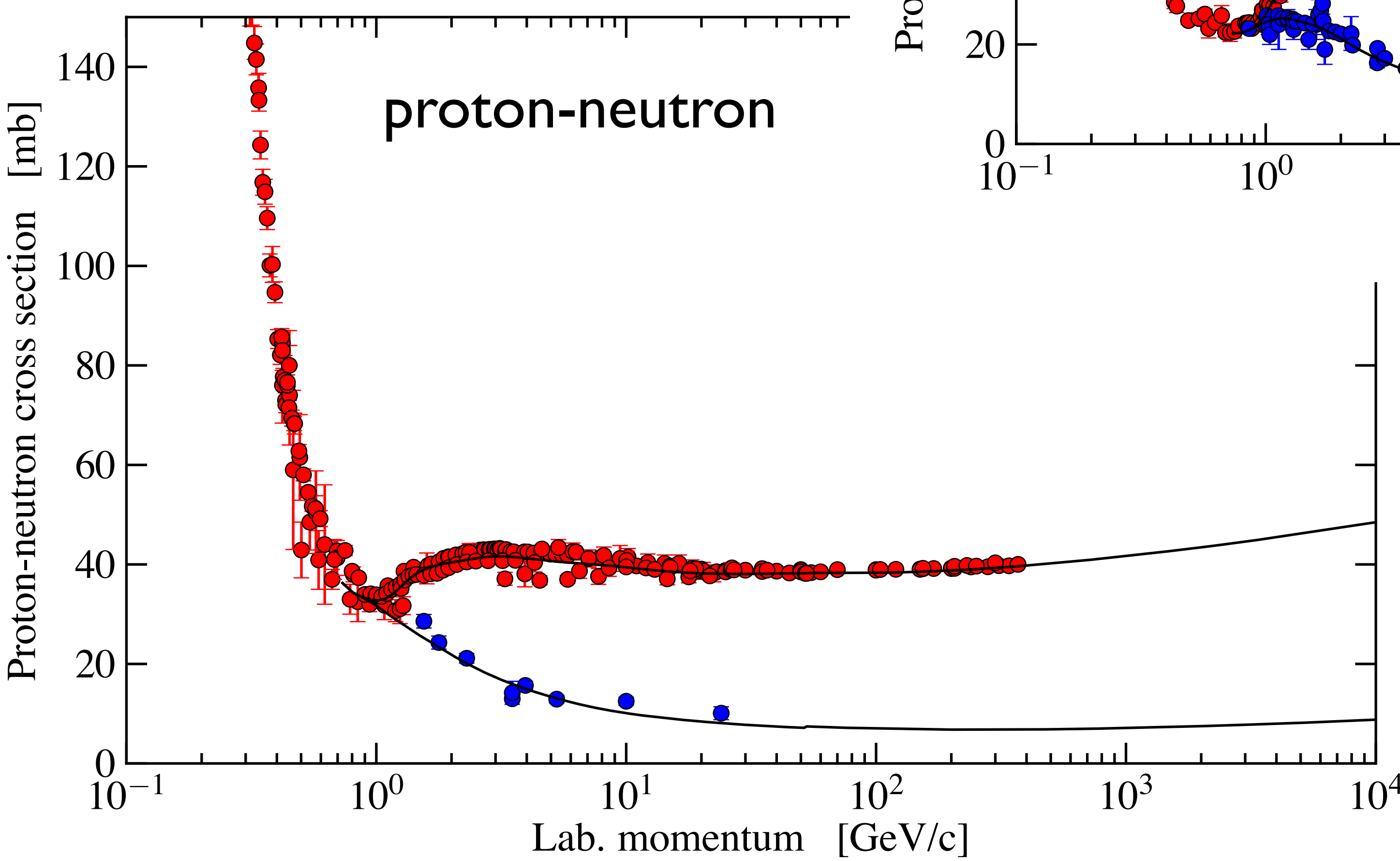

All relevant total cross sections measured at low energy

Example: resonances in hadron-hadron interactions

Large number of resonances

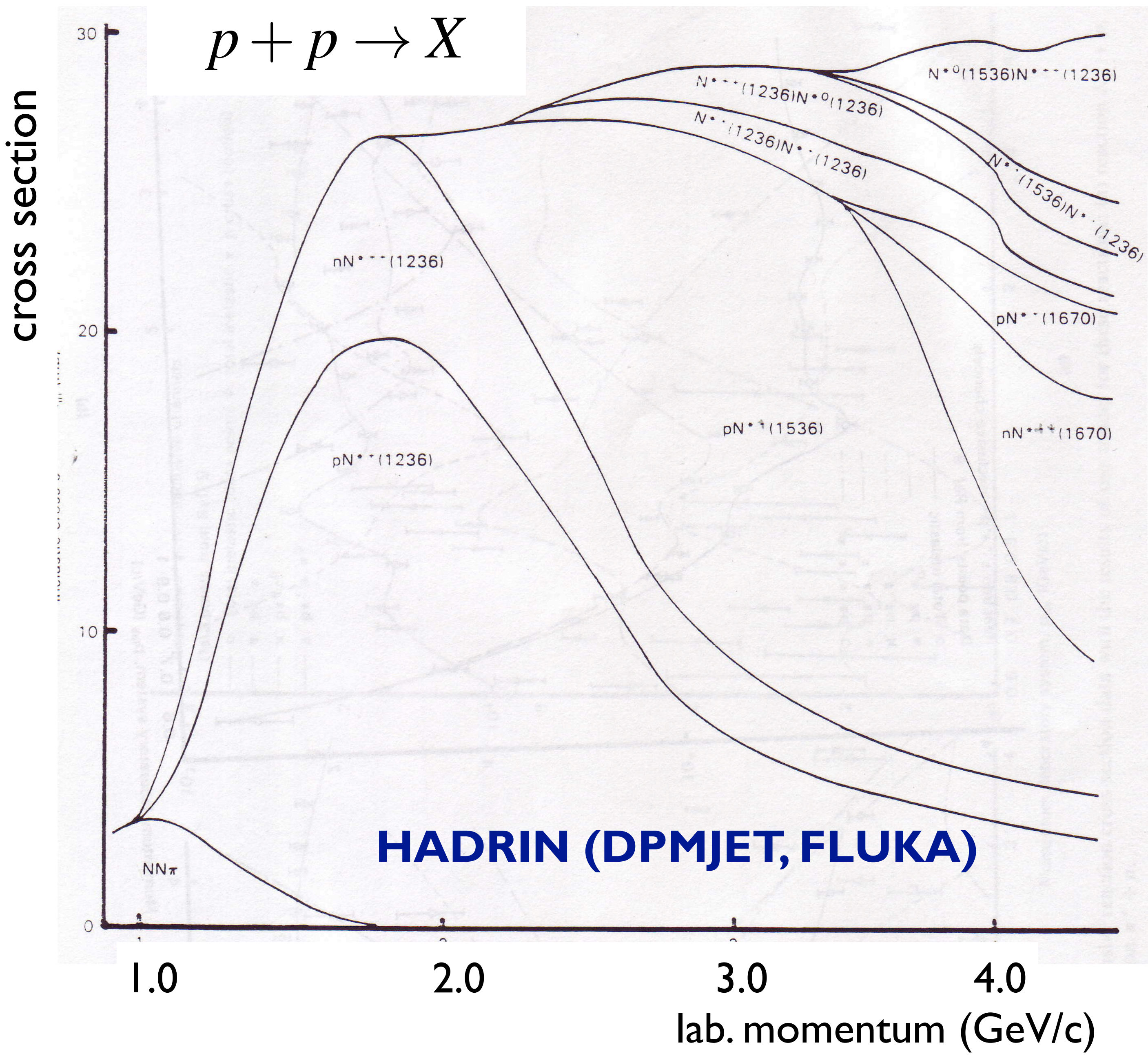

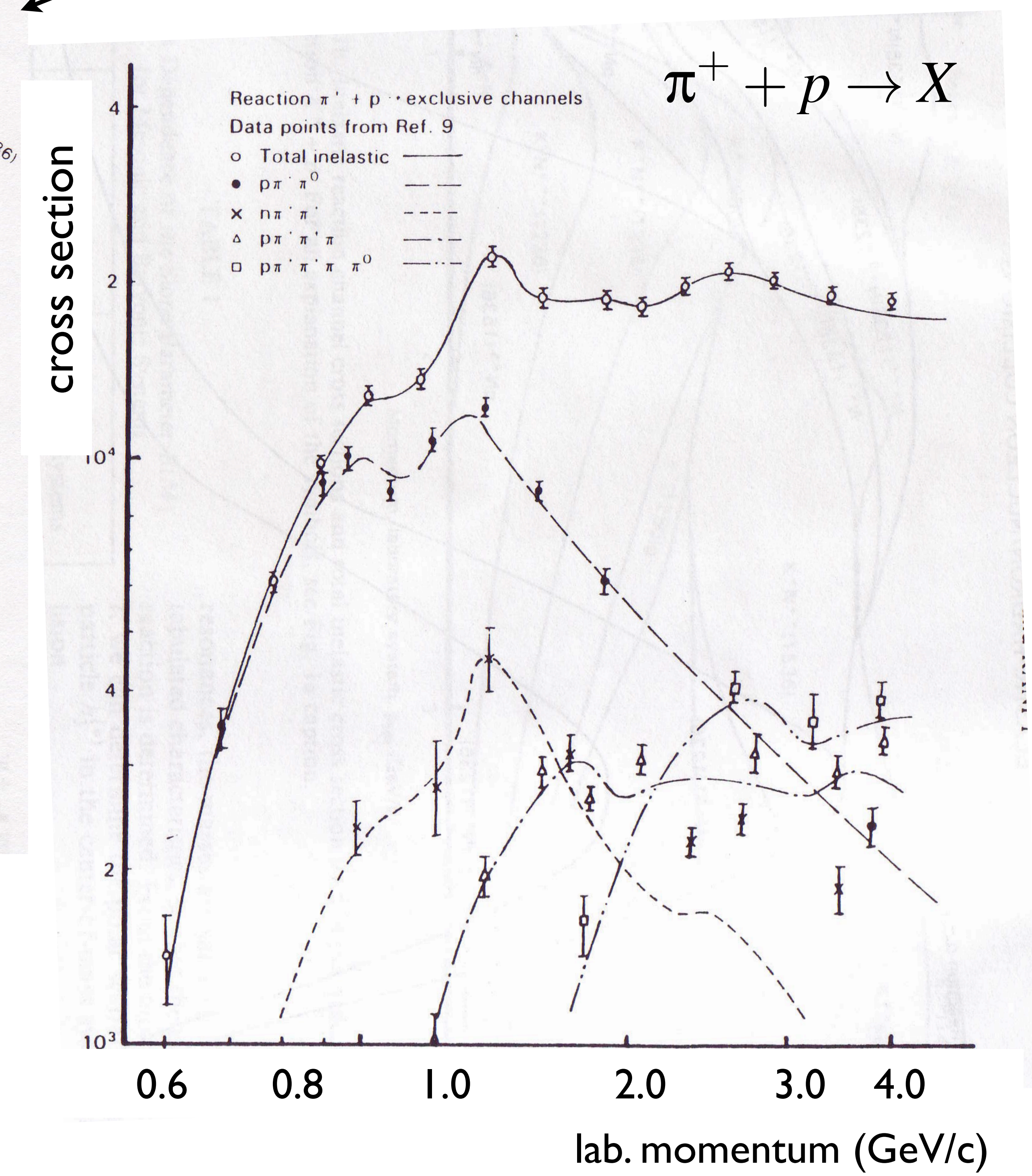

(Hänßgen, Ranft, Comp. Phys. Commun. 39, 1984)

2. Intermediate energy region

Expectations from uncertainty relation

Assumptions:

- hadrons built up of partons
- partons deflected/liberated in collision process, small momentum
- partons fragment into hadrons (pions, kaons,...) after interaction
- interaction viewed in c.m. system (other systems equally possible)

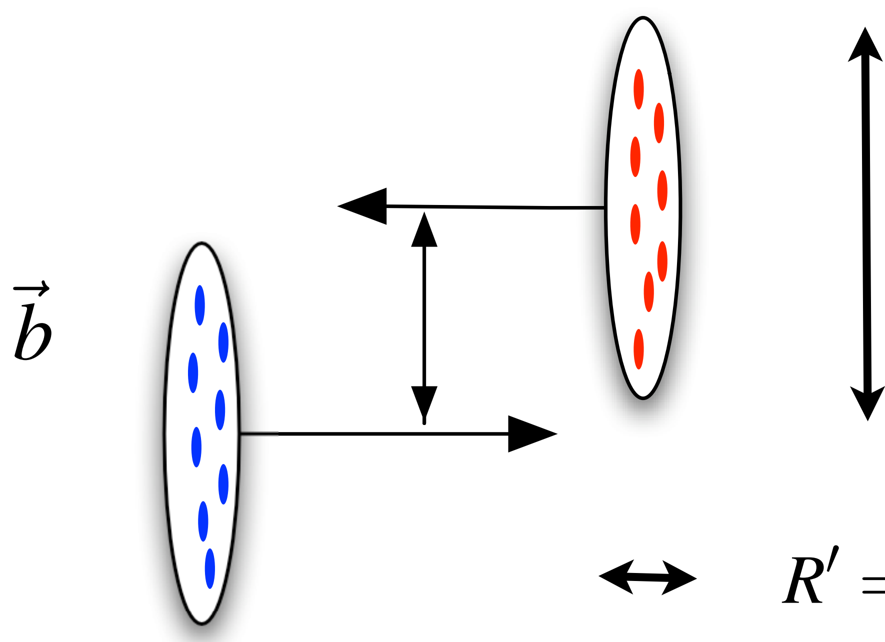

$R \approx 1\mathrm{fm} \approx 5\mathrm{GeV}^{-1}$

$$R' = R/\Gamma = R\,\frac{m_p}{E_p}$$

Heisenberg uncertainty relation

$$\Delta x\, \Delta p_x \simeq 1$$

$$\Gamma = E_p/m_p$$

Longitudinal momenta of secondaries

$$\langle p_\parallel \rangle \sim \Delta p_\parallel \approx \frac{1}{R'} \approx \frac{1}{5} E_p$$

Transverse momenta of secondaries

$$\langle p_\perp \rangle \sim \Delta p_\perp \sim \frac{1}{R} \approx 200\,\mathrm{MeV}$$

QCD-inspired interpretation: color flow model

Partonic view:

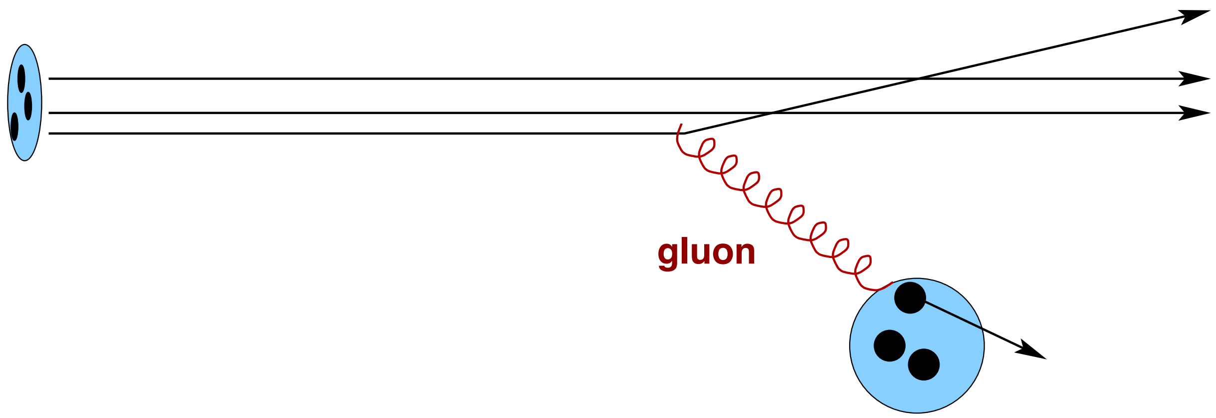

(Note: small momentum transfer, no asymptotic freedom of partons)

Color flow:

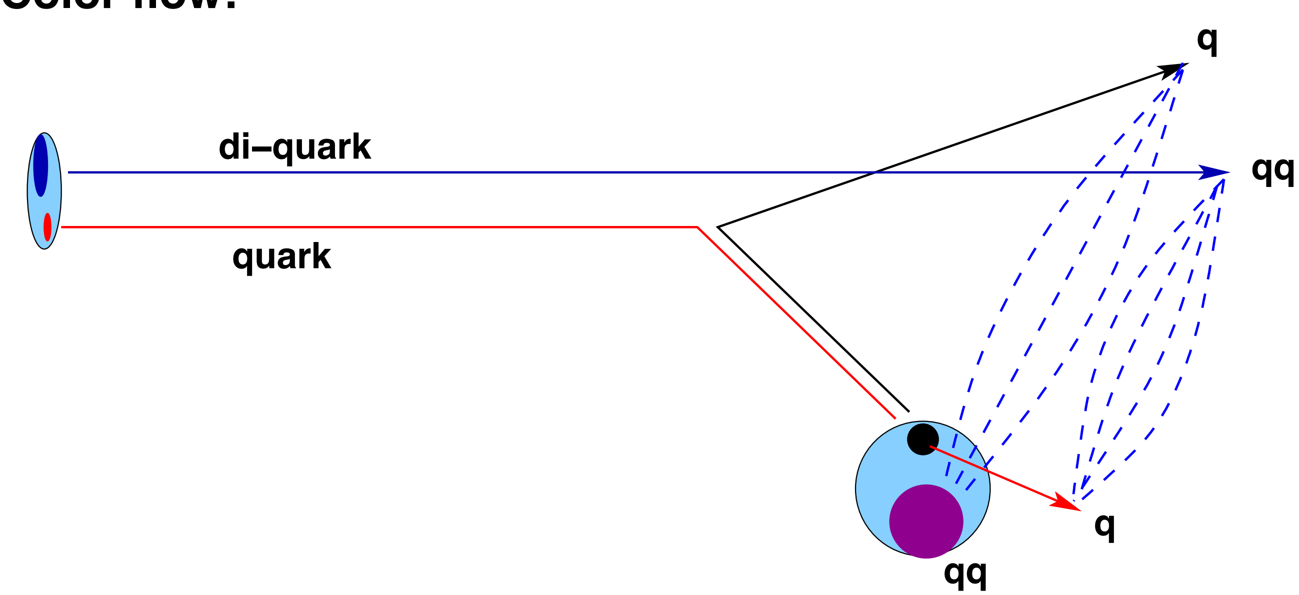

’t Hooft: large-N_c limit of QCD

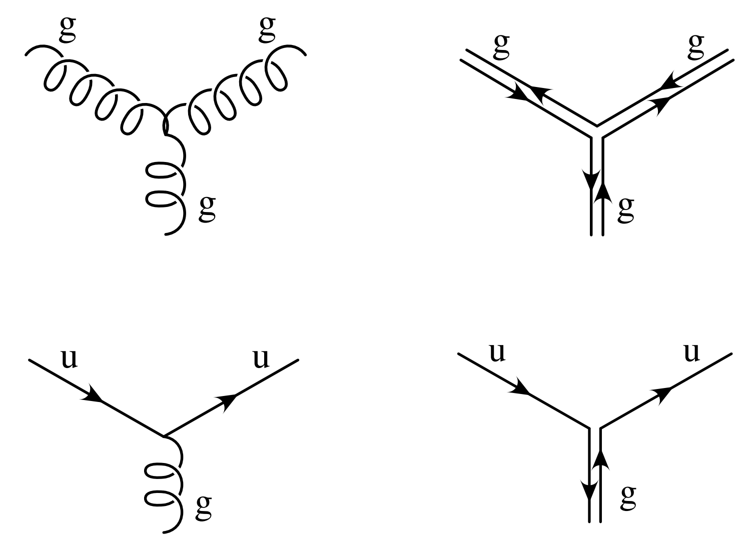

One-gluon exchange:
two color fields (strings)

Comparison to e^+e^- annihilation into quarks

Annihilation at high energy

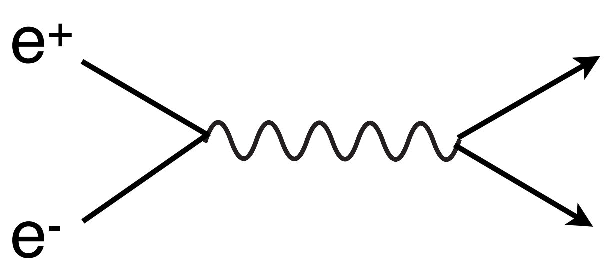

Quarks together are
color-neutral system

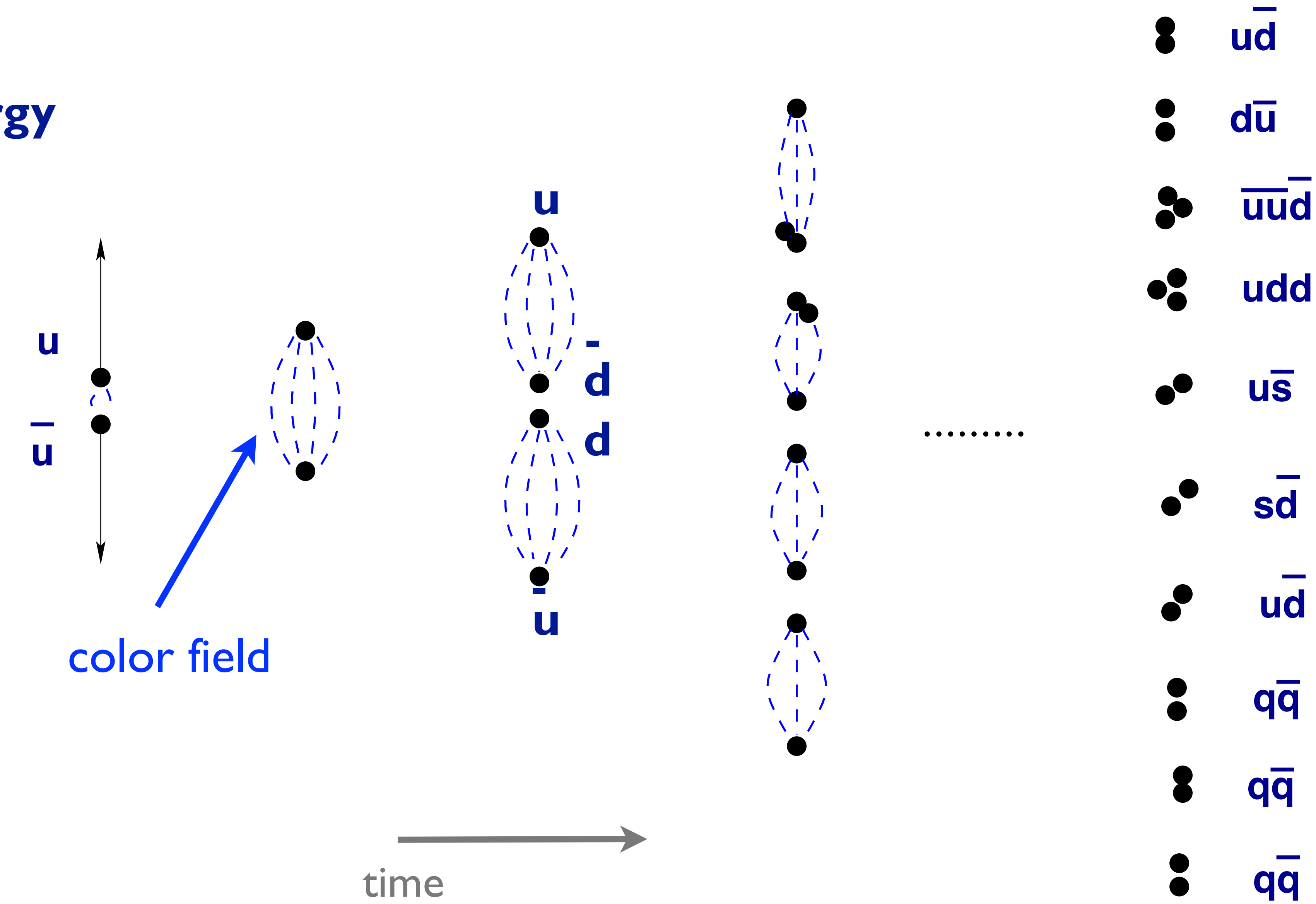

Confinement in QCD

$$V(r) = -\frac{4}{3}\frac{\alpha_s}{r} + \lambda\, r$$

String fragmentation

Kinematic distribution of secondary particles

Ansatz

- Lorentz-invariant under transformations along string direction
- Transverse momenta result of vacuum fluctuations

Lorentz invariant function

$$\mathrm{d}N = f(p)\,\delta(p^2 - m^2)\,\mathrm{d}^4 p$$

$$p = (E, \vec{p})$$

$$= f(p)\,\frac{\mathrm{d}^3 p}{2E}$$

Separation of long. and transverse degrees of freedom

$$= \frac{1}{2} f(p)\,\mathrm{d}^2 p_\perp\,\frac{\mathrm{d}p_\parallel}{E}$$

New variable $\frac{\mathrm{d}p_\parallel}{E} = \mathrm{d}y$

$$= \frac{1}{2}\,f_\perp(p_\perp)\,\mathrm{d}^2 p_\perp\,f_\parallel(y)\,\mathrm{d}y$$

$\beta^{-1} \ldots$ effective temperature

$$\sim\ \exp(-\beta p_\perp^2)\,\mathrm{d}^2 p_\perp\quad f_\parallel(y)\,\mathrm{d}y$$

Rapidity and pseudorapidity

$$
\begin{aligned}
\mathrm{d}N &= f(p)\,\delta(p^2-m^2)\,\mathrm{d}^4p \\
&= f(p)\,\frac{\mathrm{d}^3p}{2E} \\
&= \frac{1}{2}f(p)\,\mathrm{d}^2p_\perp\,\frac{\mathrm{d}p_\parallel}{E} \\
&= \frac{1}{2}\,f_\perp(p_\perp)\,\mathrm{d}^2p_\perp\,f_\parallel(y)\,\mathrm{d}y
\end{aligned}
$$

$$\frac{\mathrm{d}p_\parallel}{E} = \mathrm{d}y$$

Polar angle relative to beam axis

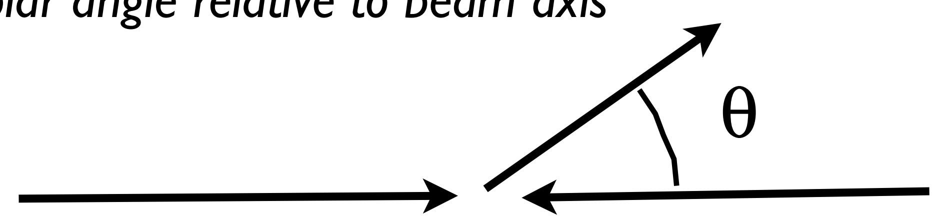

Experiments without particle identification: **pseudorapidity**

Rapidity

$$y = \frac{1}{2}\ln\frac{E+p_\parallel}{E-p_\parallel} = \ln\frac{E+p_\parallel}{m_\perp}$$

Transverse mass $\quad m_\perp = \sqrt{m^2+p_\perp^2}$

Rapidity of massless particles

$$y = \frac{1}{2}\ln\frac{1+\cos\theta}{1-\cos\theta} = -\ln\tan\frac{\theta}{2}$$

$$\eta = -\ln\tan\frac{\theta}{2}$$

Pseudorapidity and polar angle

η	deg.	mrad.
3	5.7	99
5	0.77	13
8	0.04	0.7
10	0,005	0.09

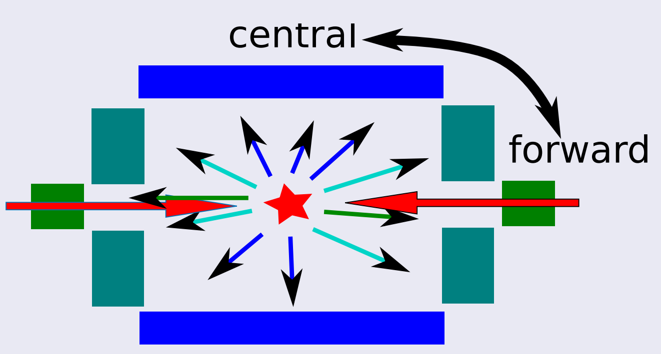

- Central ($|\eta| < 1$)
- Endcap ($1 < |\eta| < 3.5$)
- Forward ($3 < |\eta| < 5$), HF
- CASTOR+T2 ($5 < |\eta| < 6.6$)
- FSC ($6.6 < |\eta| < 8$)
- ZDC ($|\eta| > 8$), LHCf

Rapidity of massless particles

Polar angle relative to beam axis

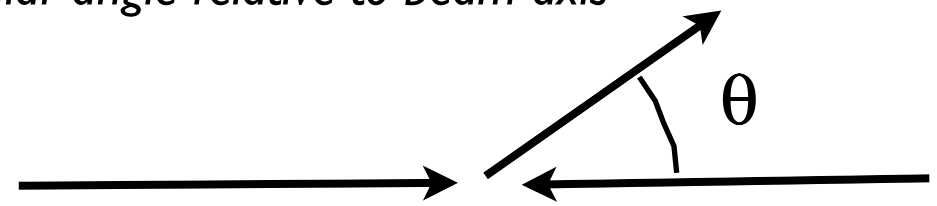

$$y = \frac{1}{2}\ln\frac{1+\cos\theta}{1-\cos\theta} = -\ln\tan\frac{\theta}{2}$$

Experiments without particle identification: **pseudorapidity**

$$\eta = -\ln\tan\frac{\theta}{2}$$

String fragmentation and rapidity

Lorentz invariance of splittings in strings:

Transformation of rapidity

$$y' = y + \text{const.}$$

$$f_{\|}(y') = f_{\|}(y) = \rho$$

Particle density independent of rapidity

Total width energy-dependent

$$y_{\max} - y_{\min} \sim \log(s/m^2)$$

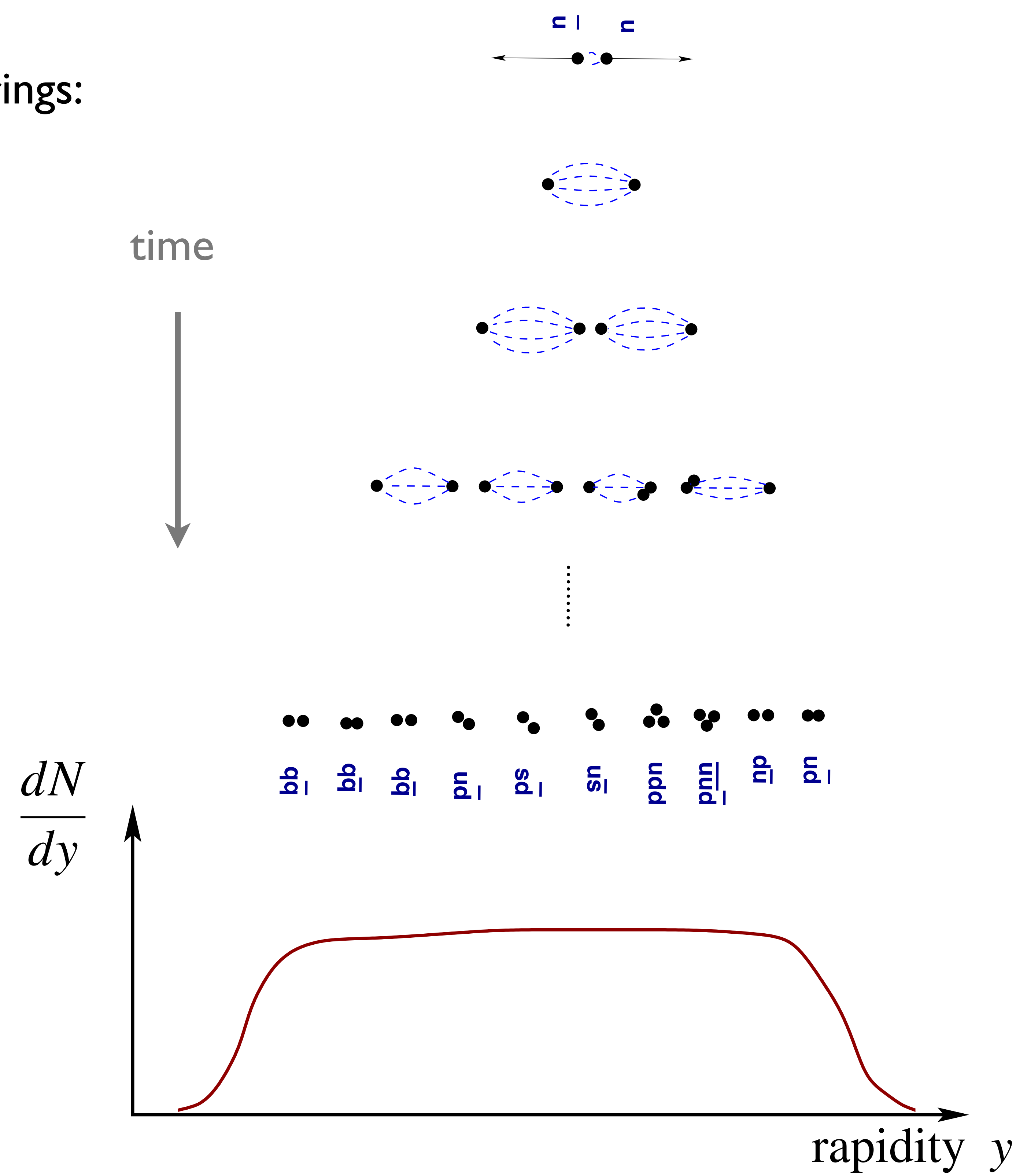

Final state particles: two-string model

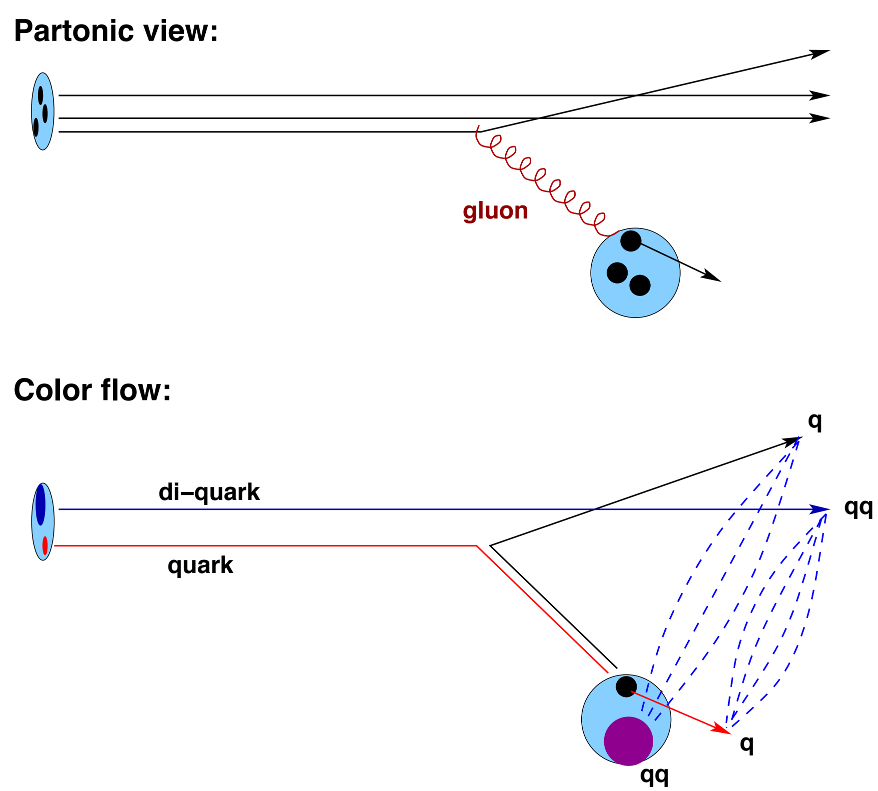

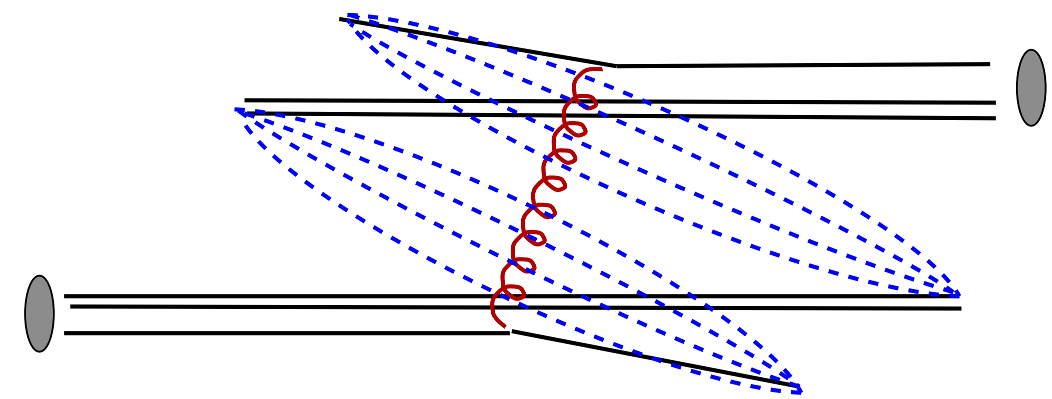

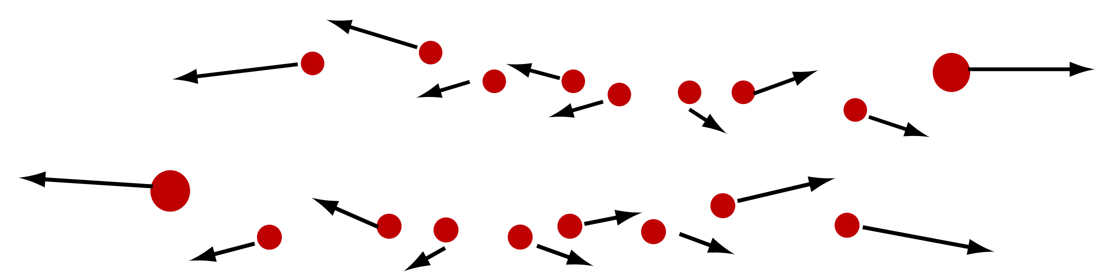

Lab. system ⟶ **CM system**

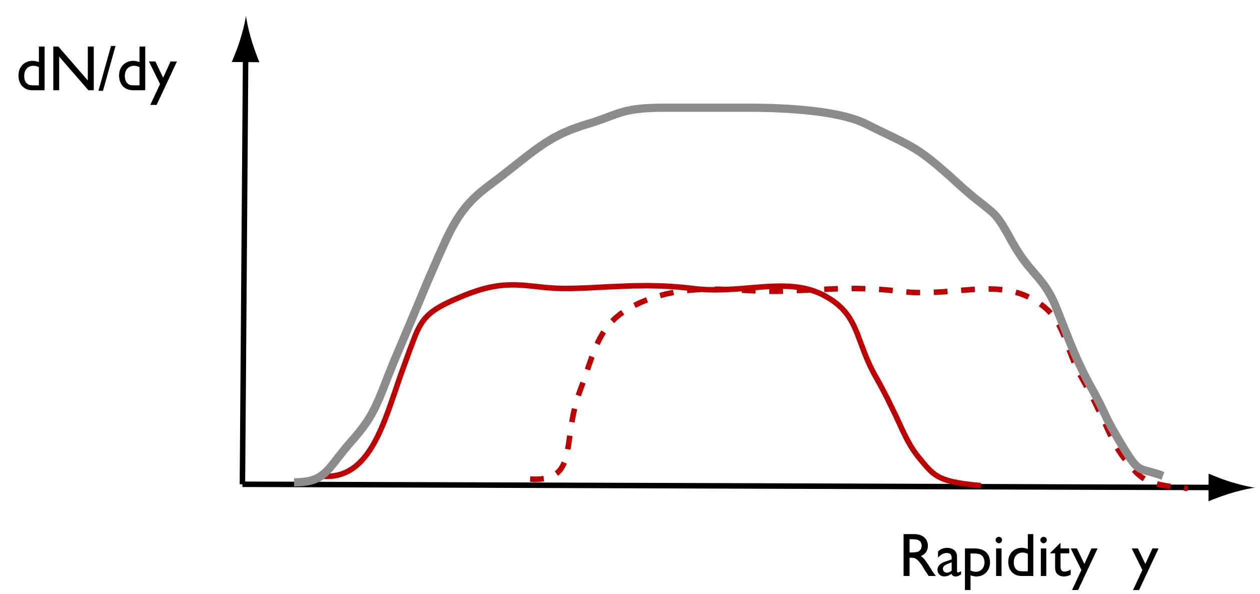

Final state particles: two-string model

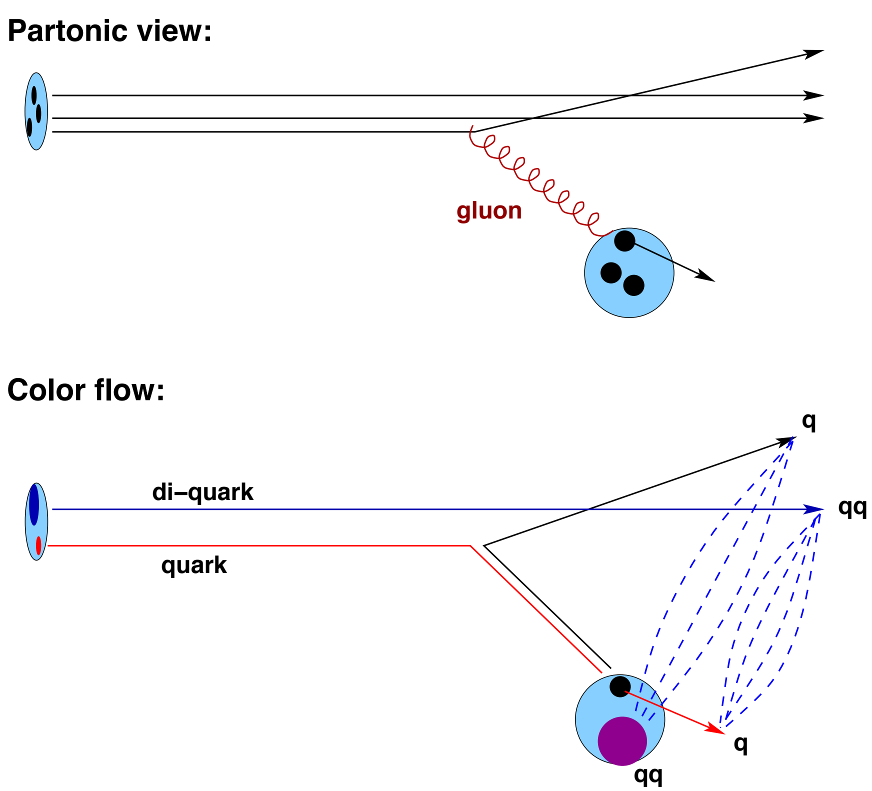

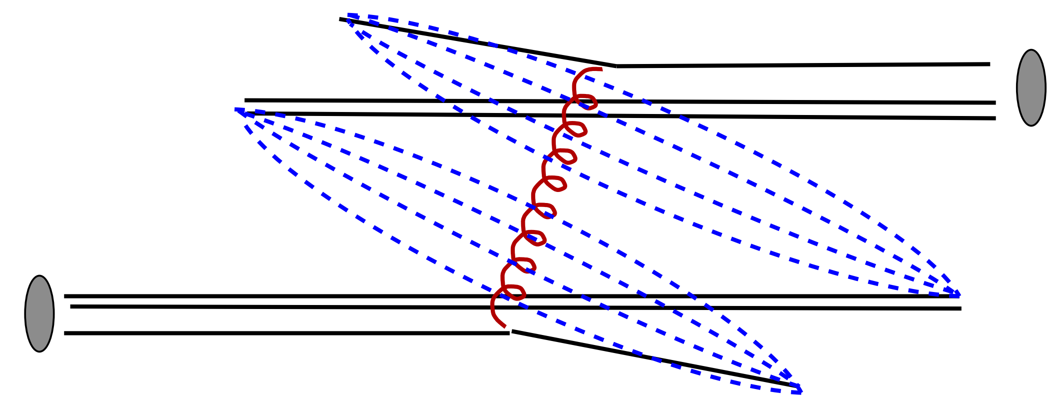

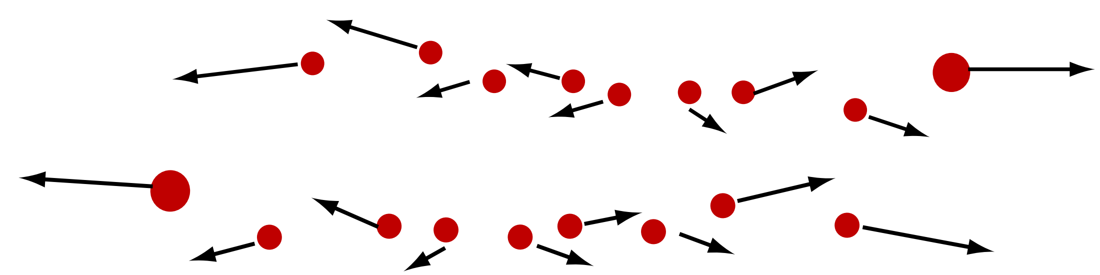

Lab. system → **CM system**

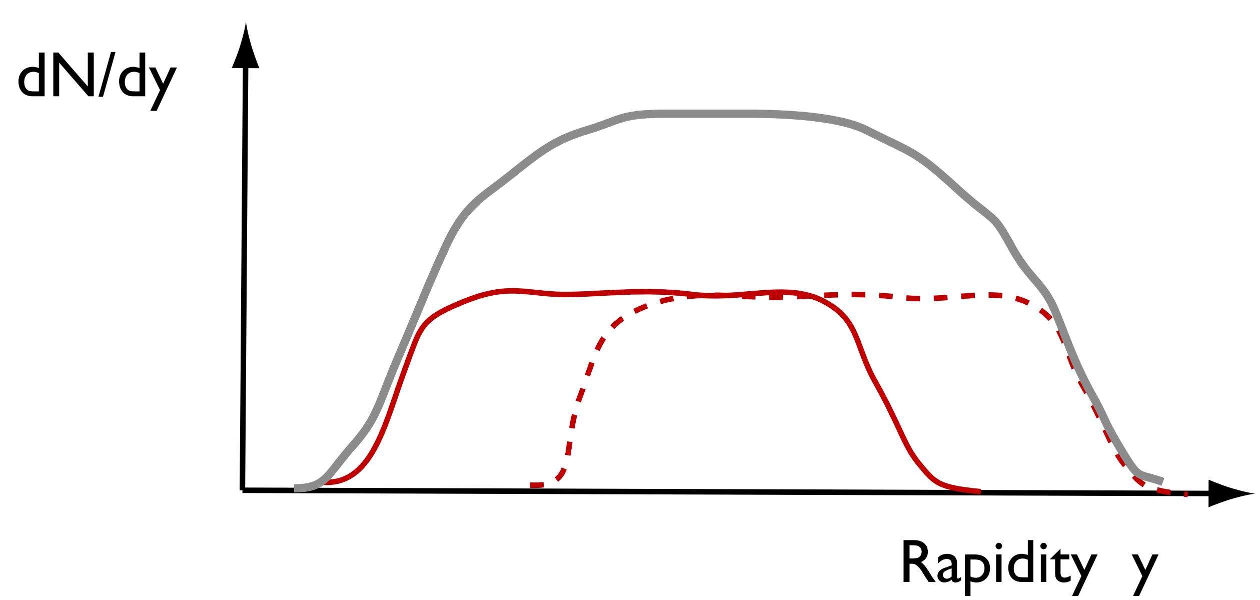

Color flow and final state particles (ii)

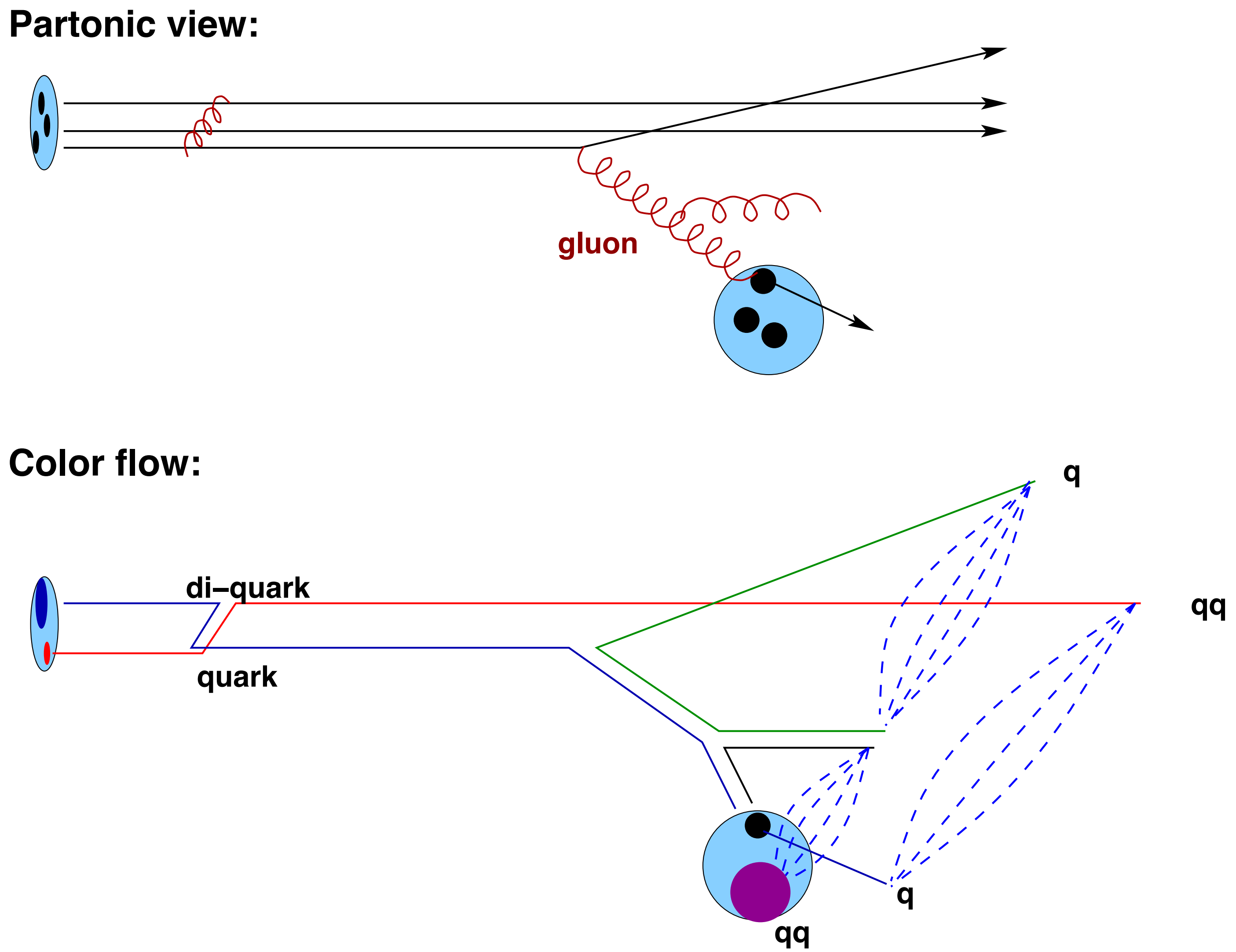

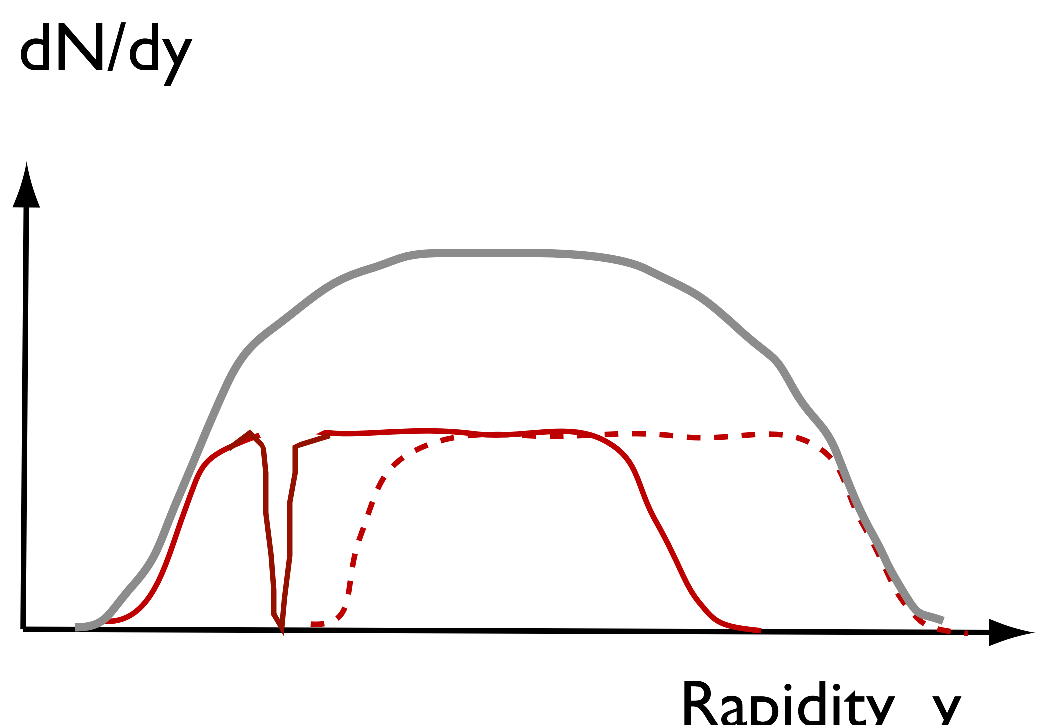

Initial and final state radiation
does not change topology

Other predicted color flow configurations

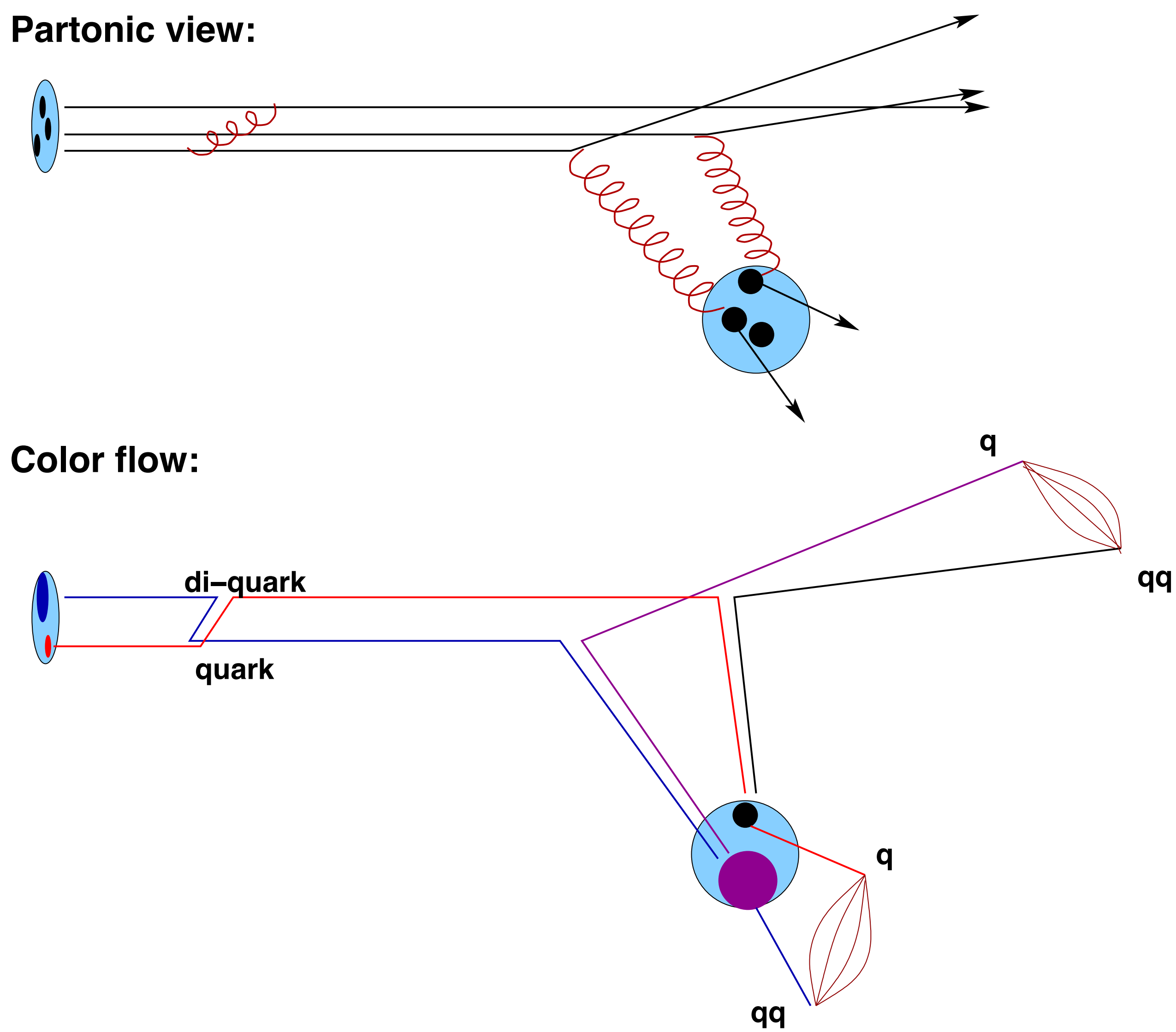

Two-gluon exchange:
diffraction dissociation

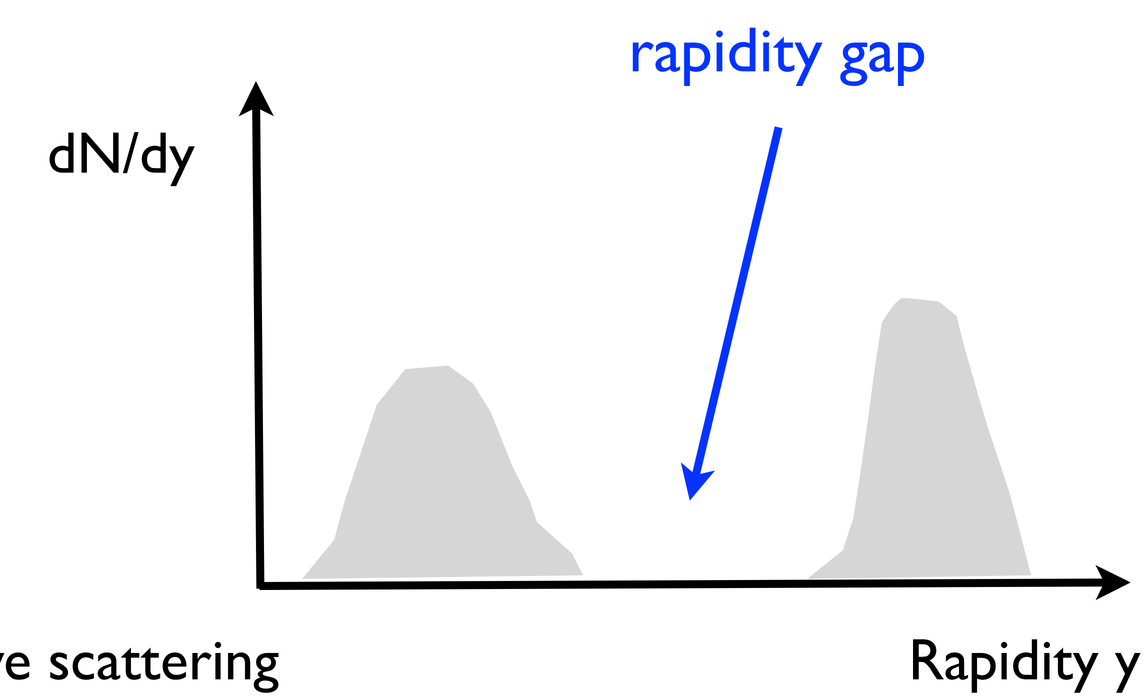

At very high energy (multi-gluon exchange):
Almost 50% of all events are elastic or inelastic diffractive scattering

Momentum fractions of string ends

Asymmetric momentum sharing of valence quarks: most energy given to di-quark

Quark in nucleon
(example: SIBYLL)

$$f_{\mathrm{q|nuc}}(x) \sim \frac{(1-x)^3}{(x^2+\mu^2)^{\frac{1}{4}}}$$

Many other parametrizations work well in describing data (example: DPMJET, FLUKA)

$$f_{\mathrm{q|nuc}}(x) \sim \frac{(1-x)^{\frac{3}{2}}}{\sqrt{x}} \qquad f_{\mathrm{q|mes}}(x) \sim \frac{1}{\sqrt{x(1-x)}}$$

Sea quark momentum fractions

$$f_{\mathrm{q_{sea}}}(x) \sim \frac{1}{x}$$

or

$$f_{\mathrm{q_{sea}}}(x) \sim \frac{1}{\sqrt{x}}$$

Particle production spectra (i)

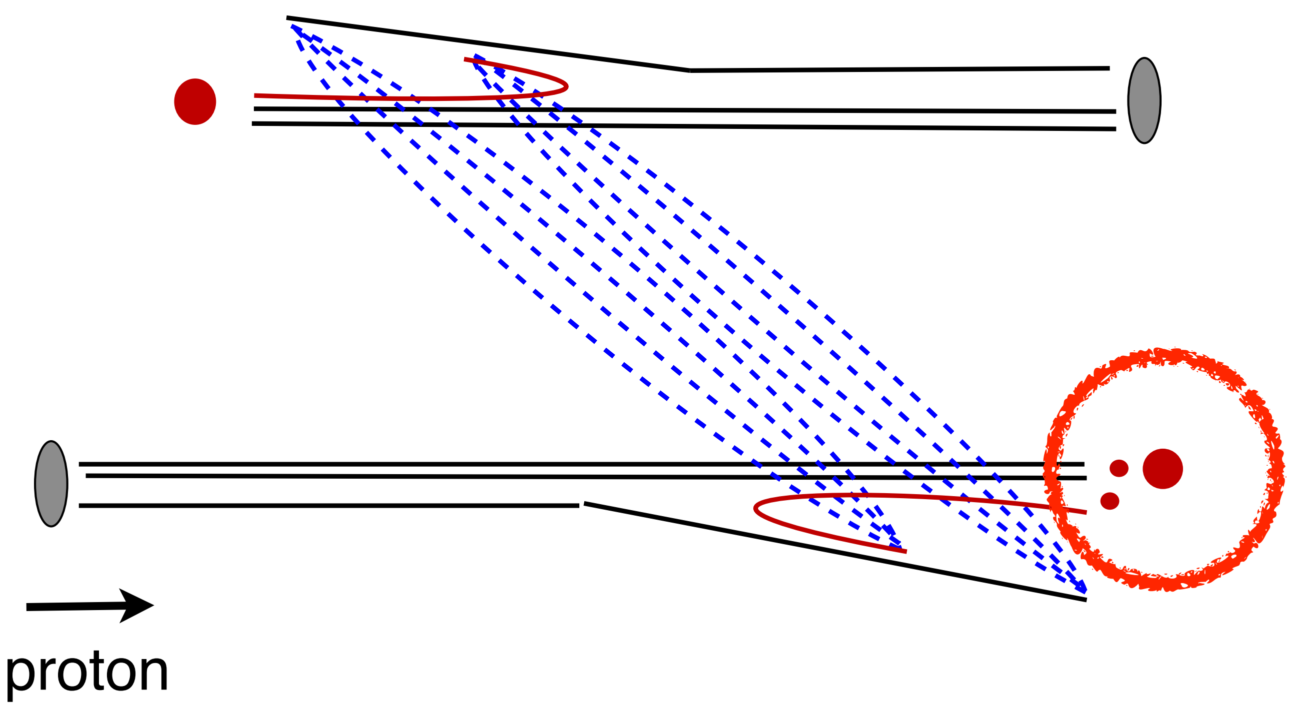

Fluctuations: generation of sea quark anti-quark pair and leading/excited hadron

Leading particle effect:

approx. 40–50% of energy of primary particle given to leading particle

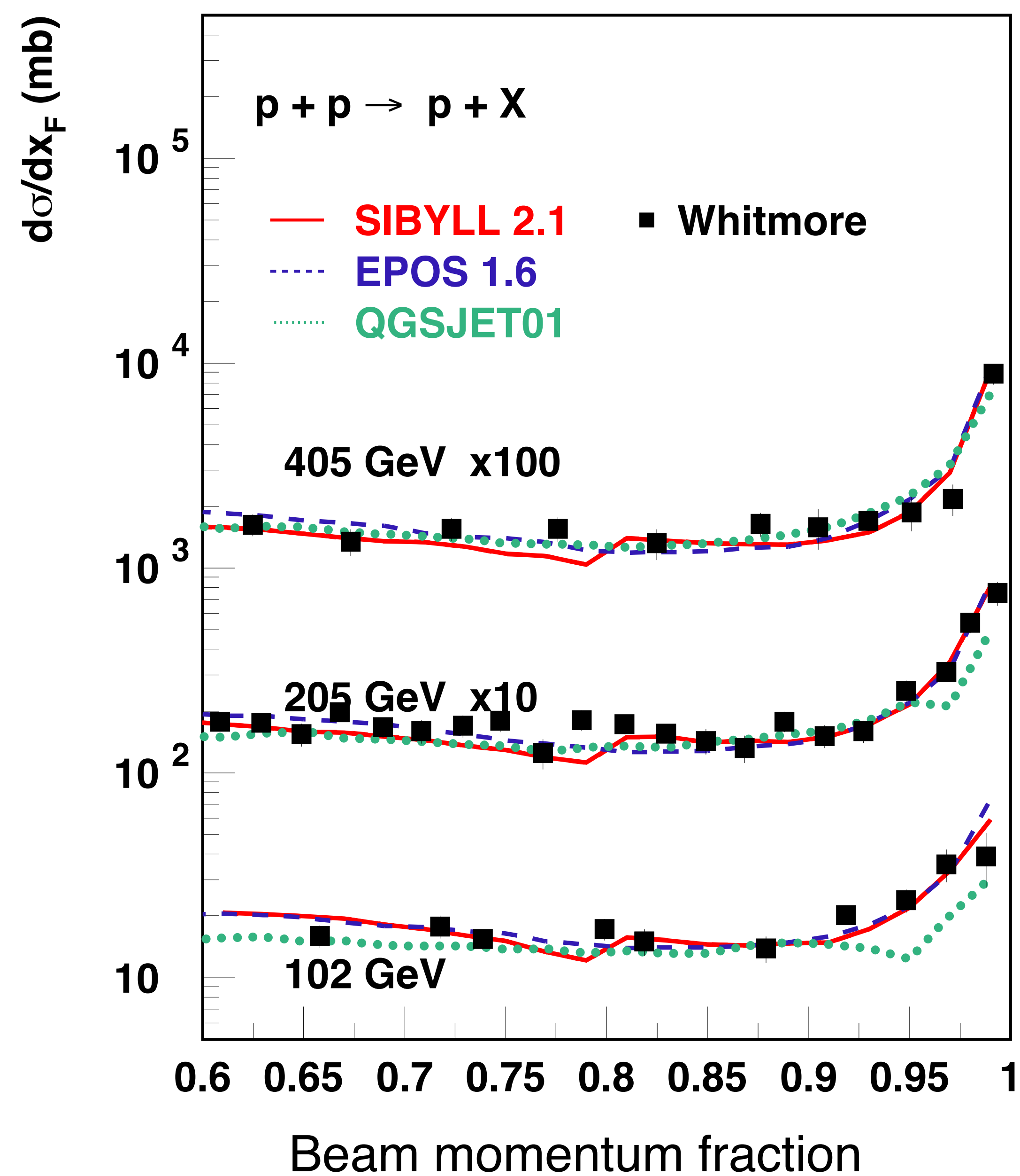

Particle production spectra (ii)

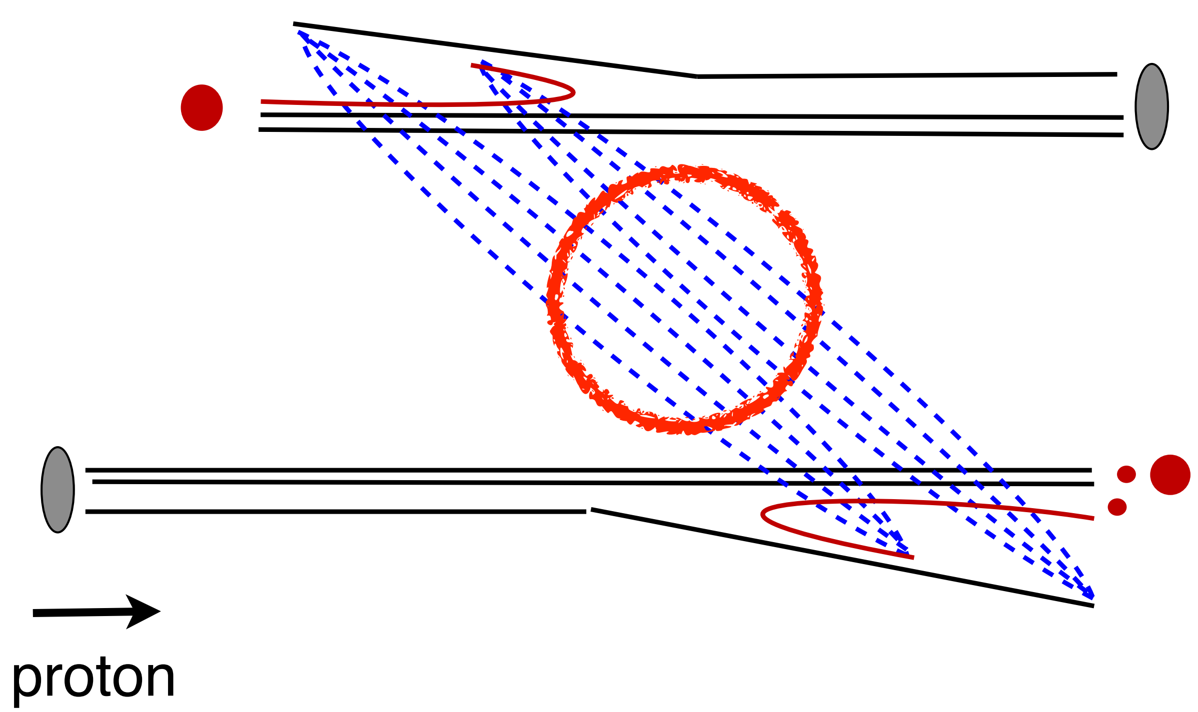

Fluctuations: generation of sea quark anti-quark pair and leading/excited hadron

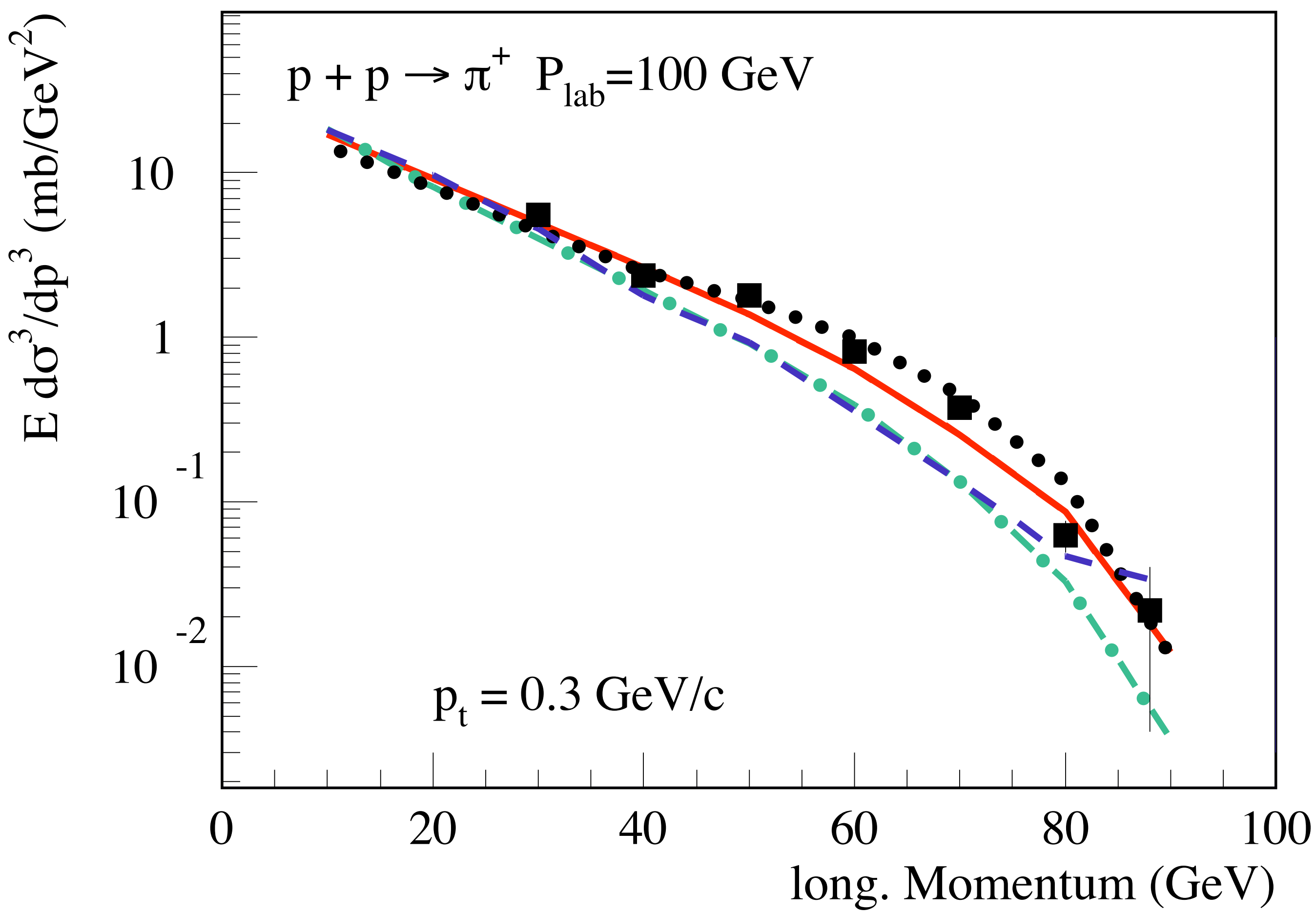

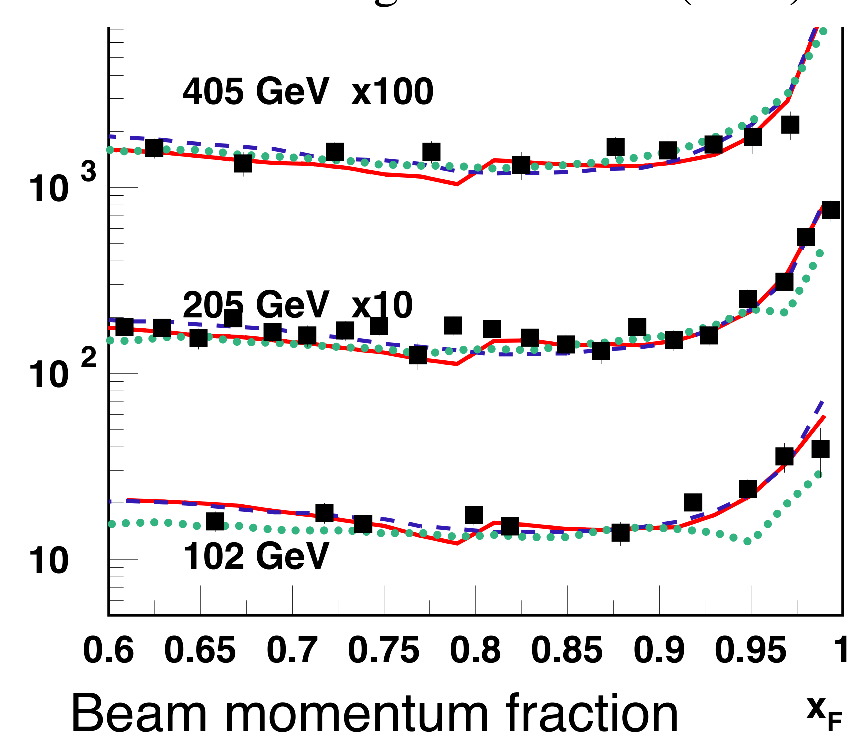

Kinematic variables: Feynman x_F

Example: 100 GeV p-p collisions, charged secondaries

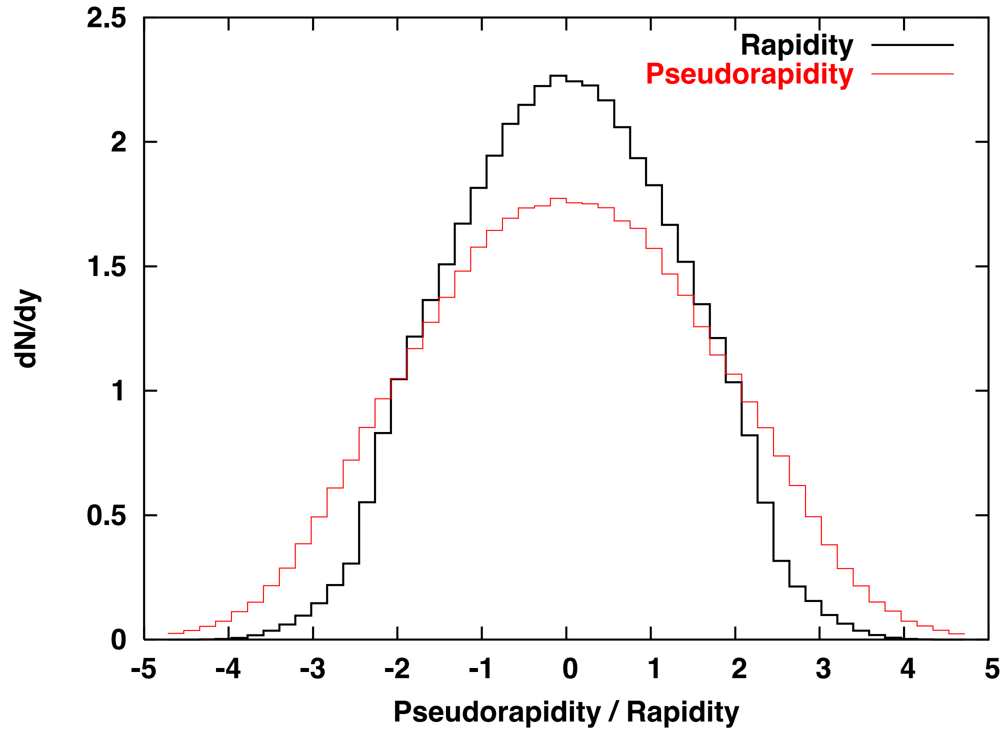

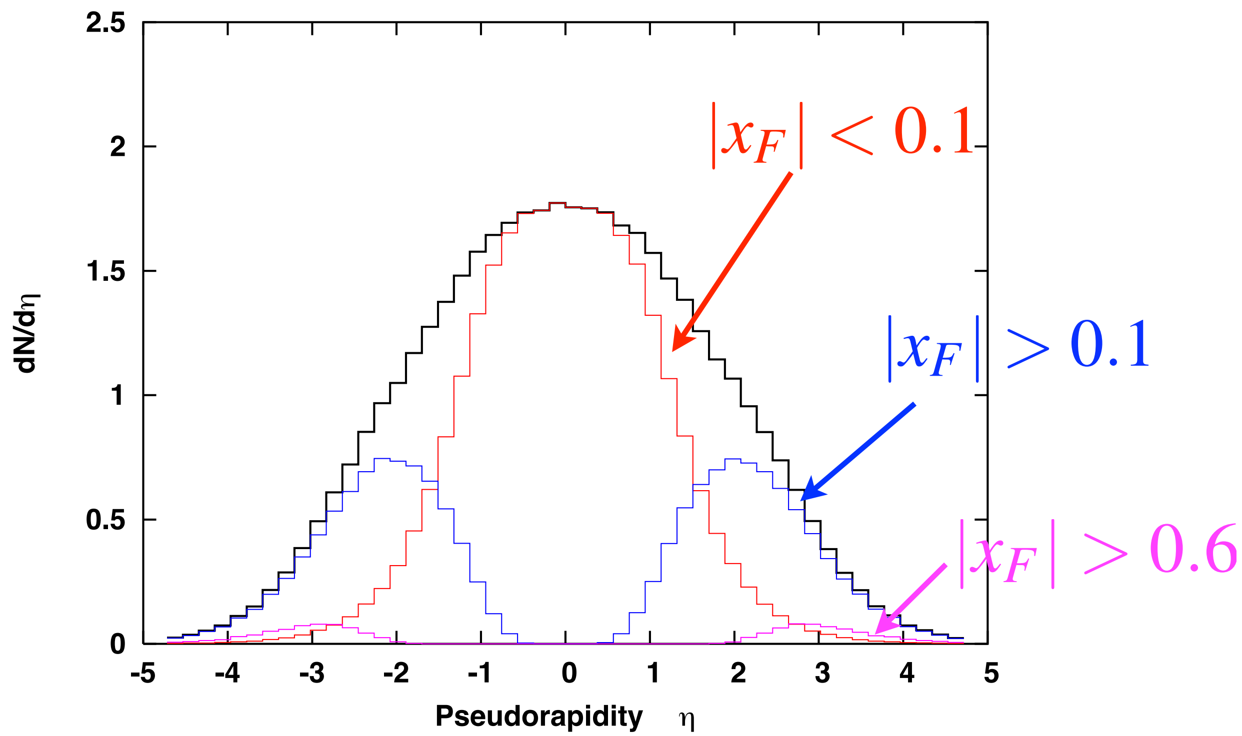

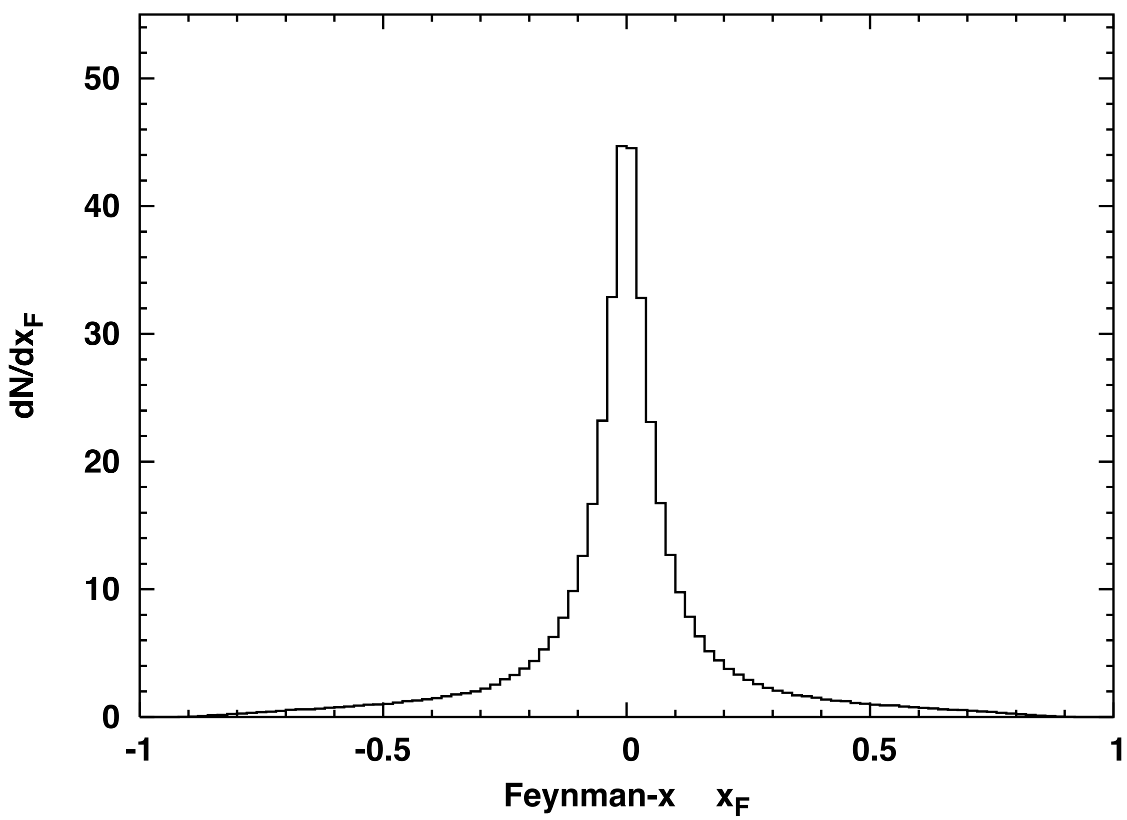

$$x_F = \frac{p_\parallel}{p_{\max}} \approx \frac{2p_\parallel}{\sqrt{s}}$$

Transverse momentum ~350 MeV:

small $|x_F|$ corresponds to small pseudorapidity (large angles)

Feynman scaling

Feynman (1972)

$$2E\frac{dN}{d^3p} \to \frac{dN}{dx_F\, d^2p_\perp} \to f(x_F, p_\perp)$$

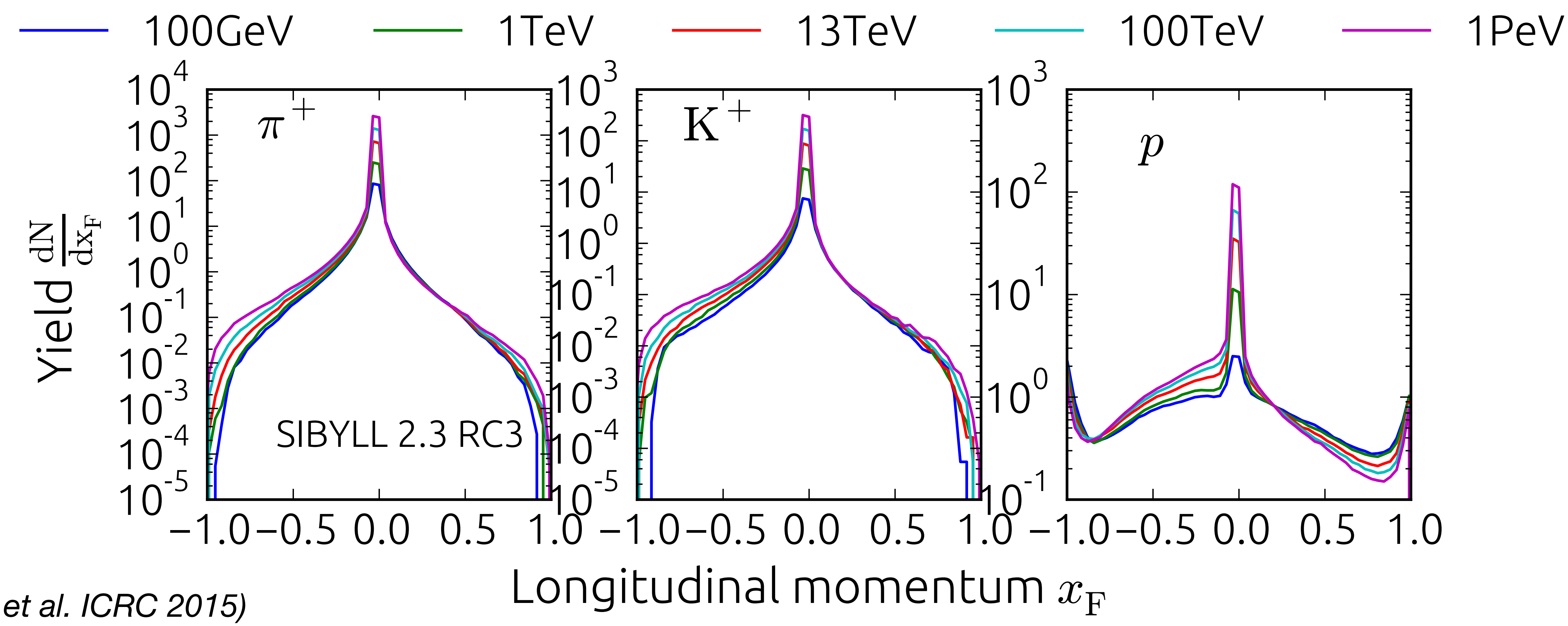

(Riehn et al. ICRC 2015)

Implication: distribution at high-energy approximately independent of energy

$$\frac{dN}{dx} \approx \tilde{f}(x) \qquad x = E/E_{\text{prim}}$$

NA22 European Hybrid Spectrometer data

(Roesler, 2006)

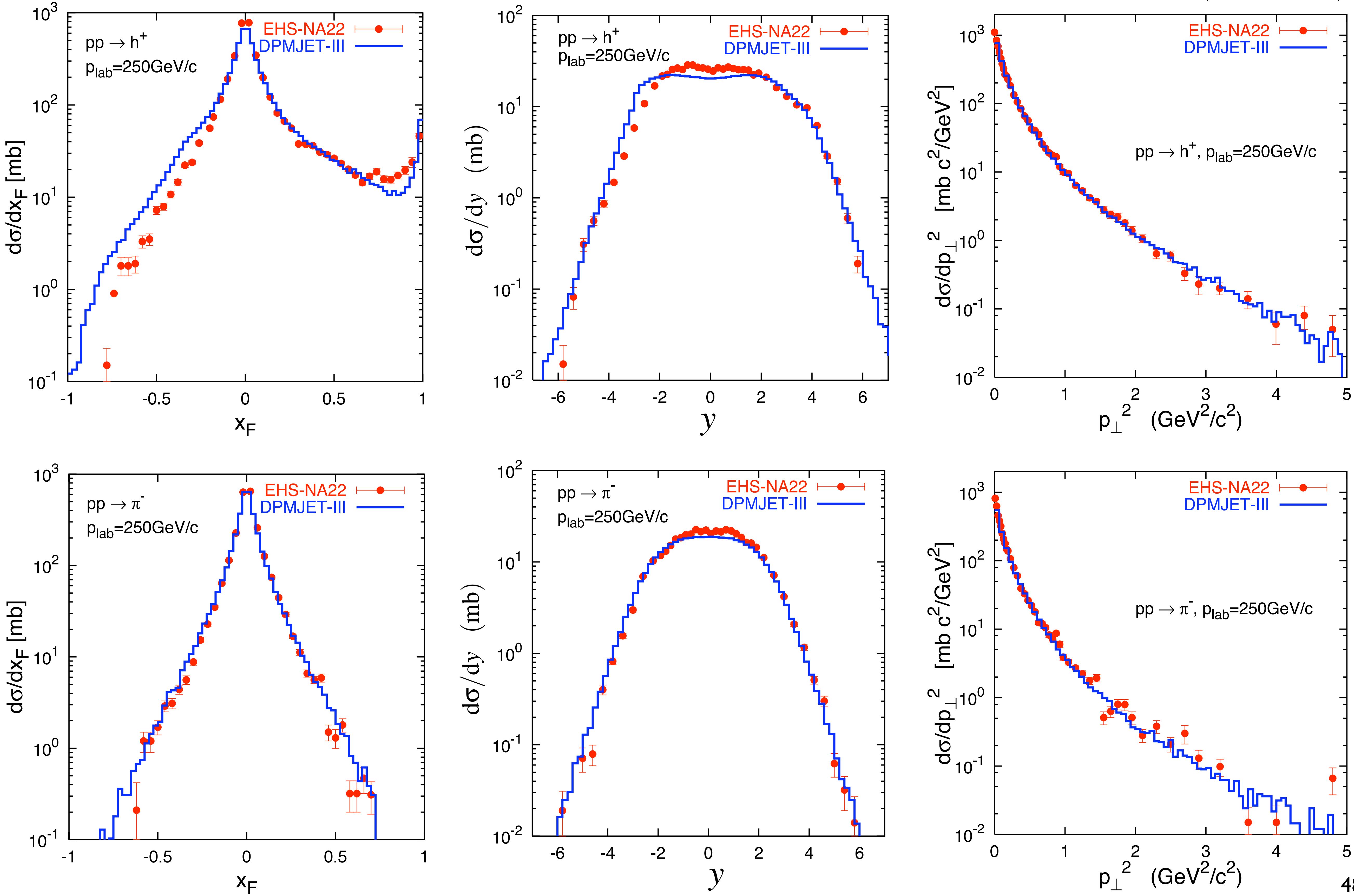

Secondary particle multiplicities

proton - proton, $E_{lab} = 200GeV$

	Exp.	DPMJET-III
charged	7.69 ± 0.06	7.64
neg.	2.85 ± 0.03	2.82
p	1.34 ± 0.15	1.26
n	0.61 ± 0.30	0.66
π^+	3.22 ± 0.12	3.20
π^-	2.62 ± 0.06	2.55
K^+	0.28 ± 0.06	0.30
K^-	0.18 ± 0.05	0.20
Λ	0.096 ± 0.01	0.10
$\bar{\Lambda}$	0.0136 ± 0.004	0.0105

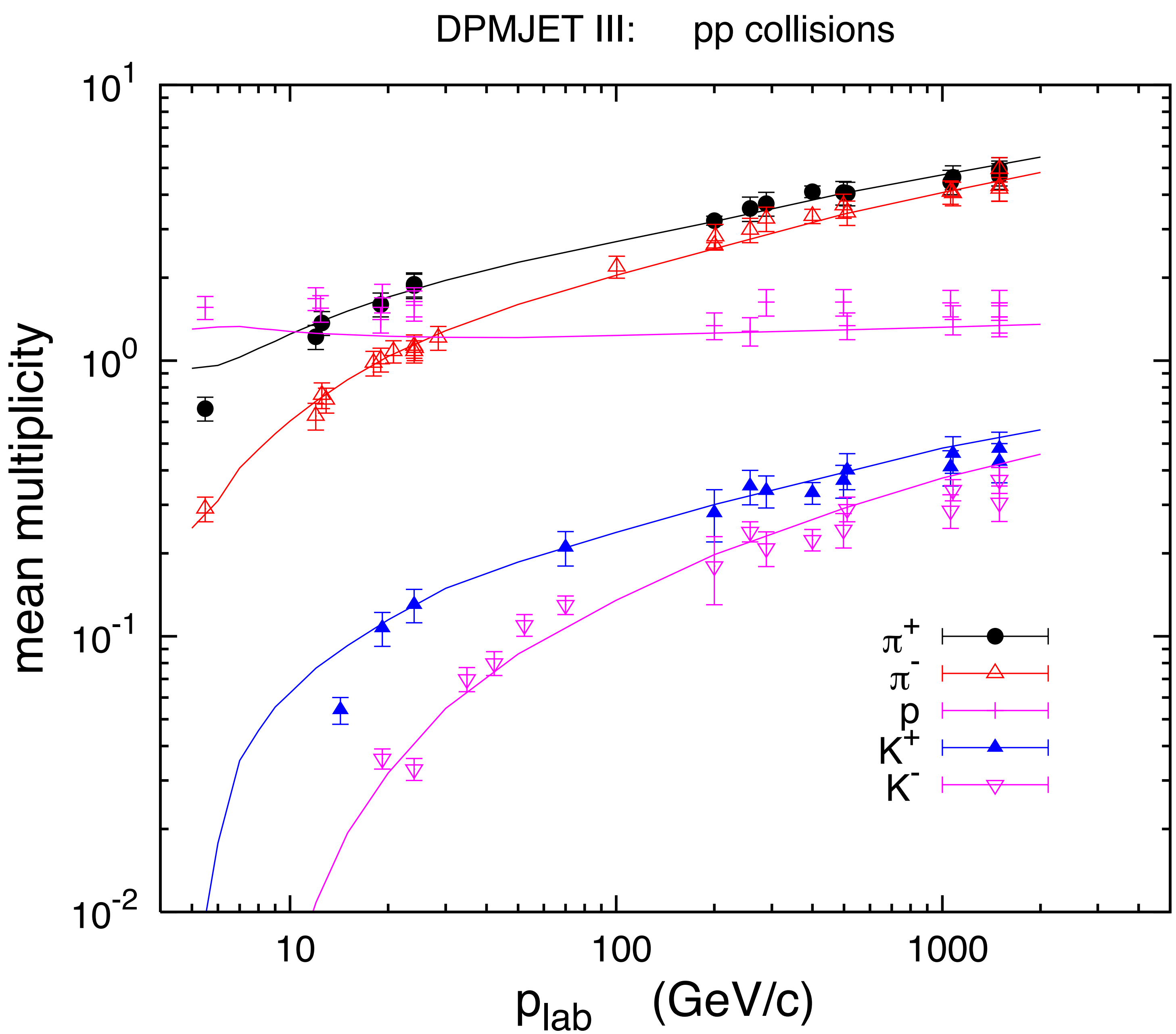

Secondary particle multiplicities

Power-law increase of number of secondary particles

$$n_{\rm ch} \sim s^{0.1}$$

Leading particles

proton - proton, $E_{lab} = 200$GeV

	Exp.	DPMJET-III
charged	7.69 ± 0.06	7.64
neg.	2.85 ± 0.03	2.82
p	1.34 ± 0.15	1.26
n	0.61 ± 0.30	0.66
π^+	3.22 ± 0.12	3.20
π^-	2.62 ± 0.06	2.55
K^+	0.28 ± 0.06	0.30
K^-	0.18 ± 0.05	0.20
Λ	0.096 ± 0.01	0.10
$\bar{\Lambda}$	0.0136 ± 0.004	0.0105

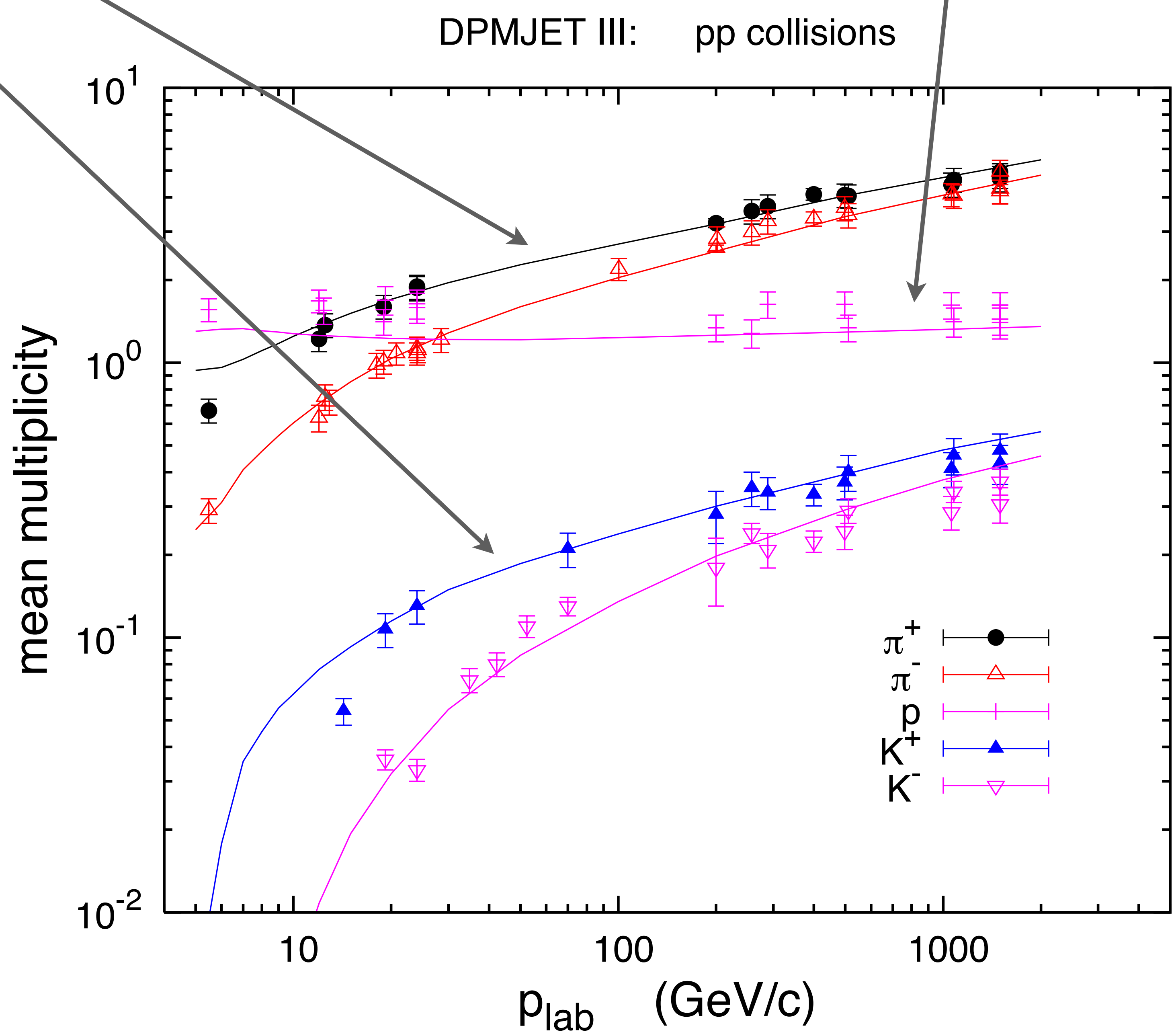

Interaction of hadrons with nuclei

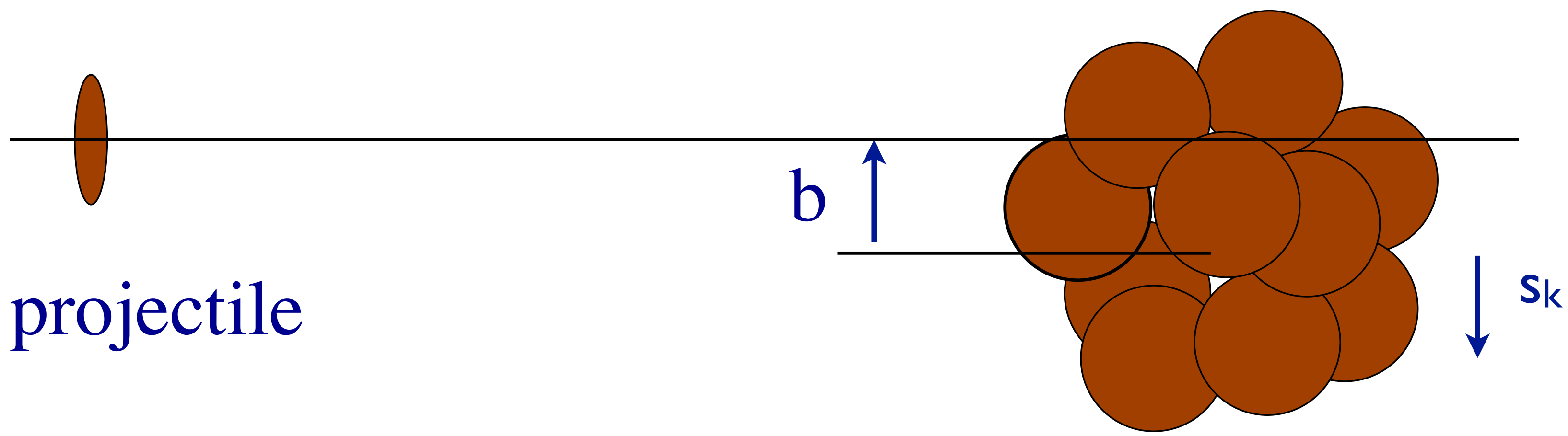

Glauber approximation:

$$\sigma_{\text{inel}} = \int d^2\vec{b} \left[1 - \prod_{k=1}^{A} \left(1 - \sigma_{\text{tot}}^{NN} T_N(\vec{b} - \vec{s}_k) \right) \right] \approx \int d^2\vec{b} \left[1 - \exp\left\{ -\sigma_{\text{tot}}^{NN} T_A(\vec{b}) \right\} \right]$$

$$\sigma_{\text{prod}} \approx \int d^2\vec{b} \left[1 - \exp\left\{ -\sigma_{\text{ine}}^{NN} T_A(\vec{b}) \right\} \right]$$

Coherent superposition of elementary nucleon-nucleon interactions

Example: proton-carbon cross section

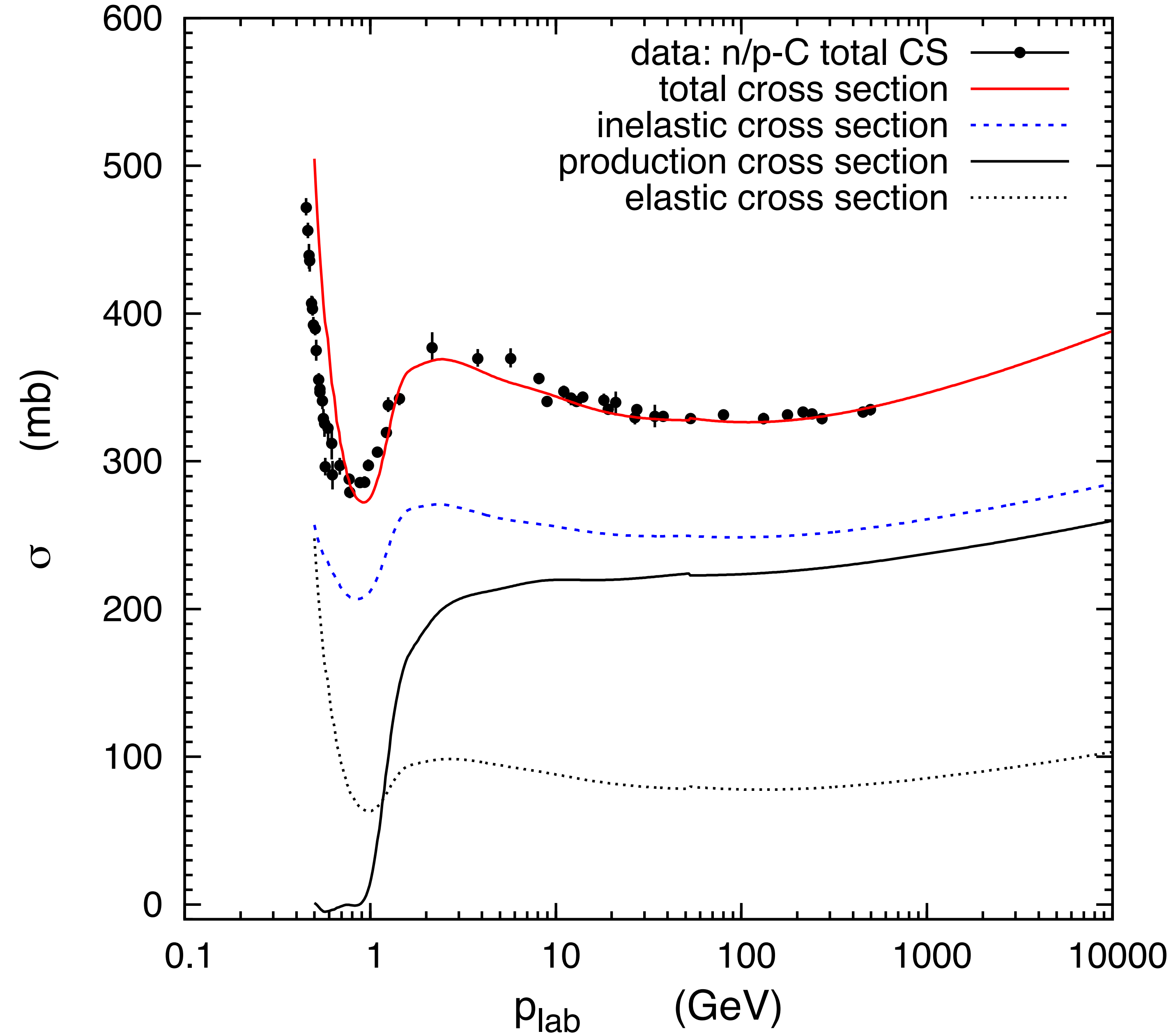

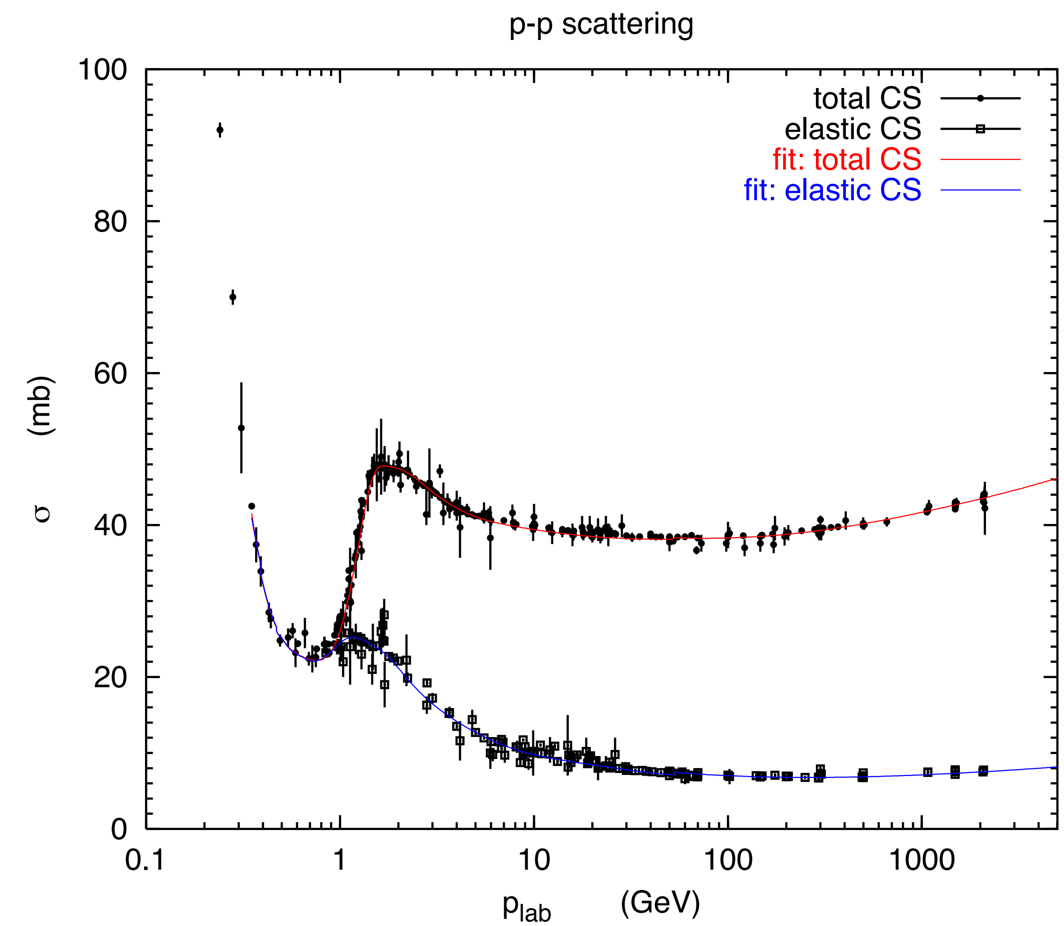

$$\sigma_{\text{prod}}^{\text{pC}} = \frac{A\sigma_{\text{ine}}^{\text{pp}}}{\langle n_{\text{part}} \rangle}$$

Number of participating target nucleons (1.8 at 100 GeV)

String configuration for nucleus as target

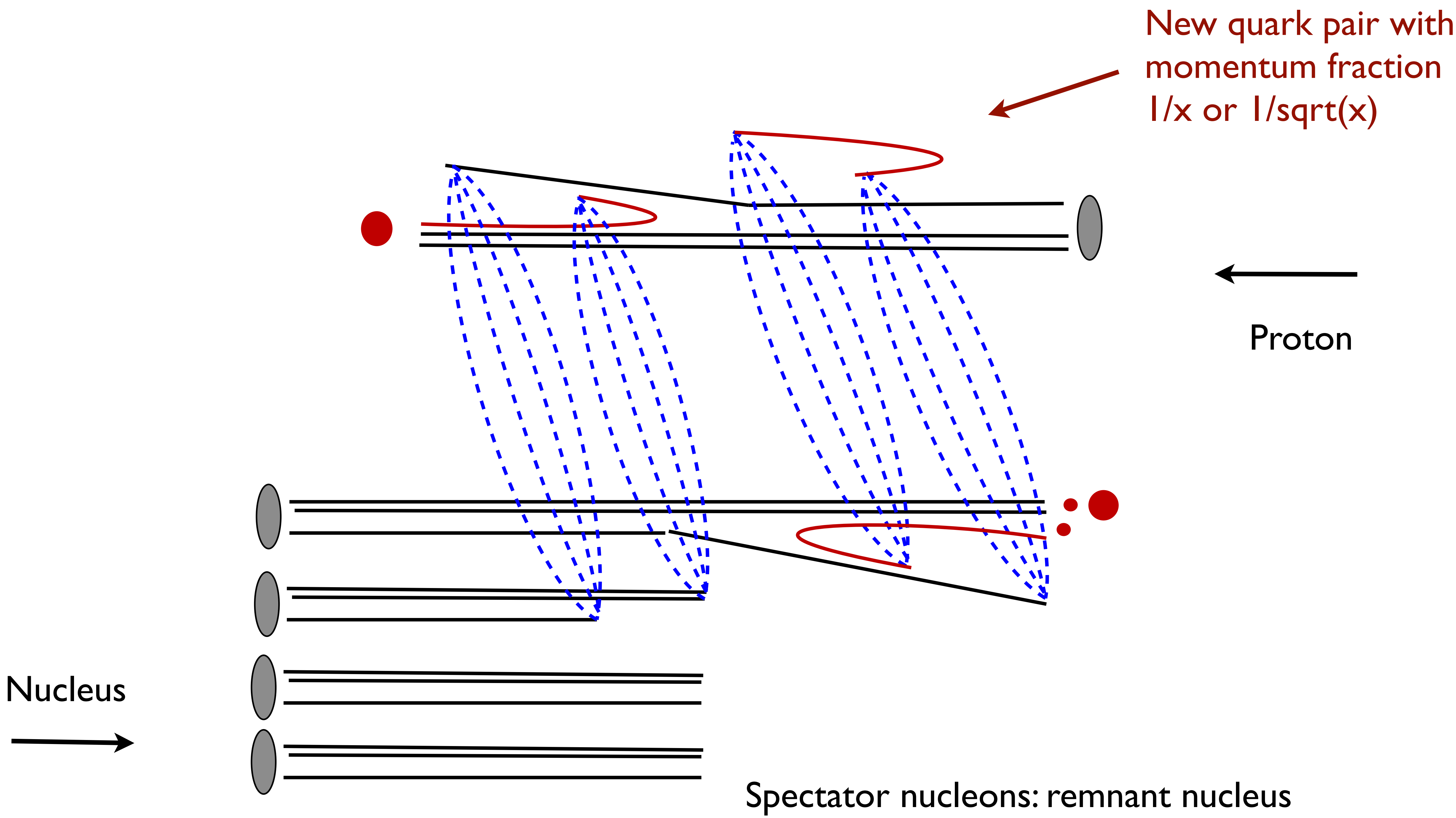

SIBYLL: central & leading particle production

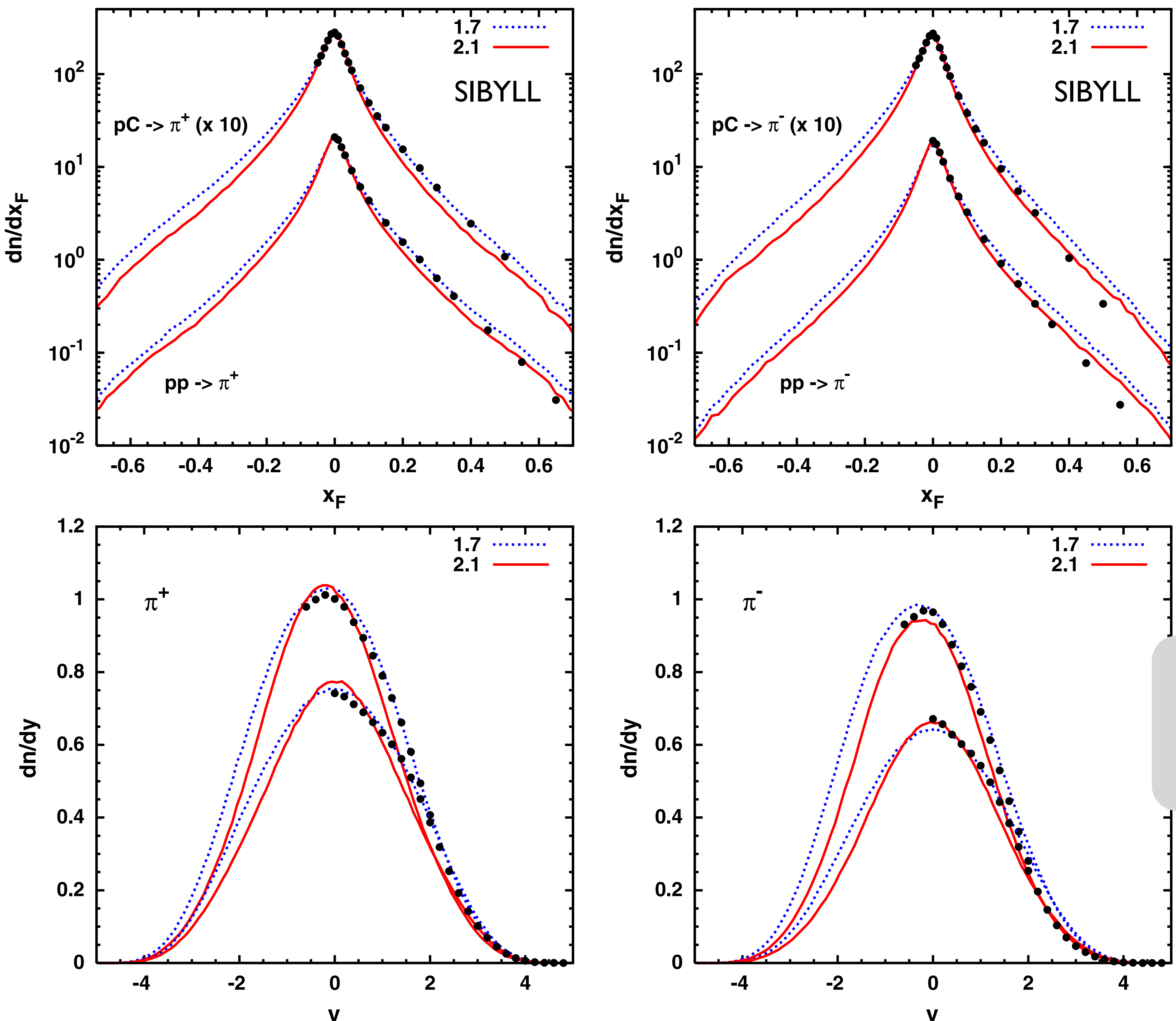

NA49 p-p and p-C at 158 GeV

Proton-proton and proton-nucleus distributions very similar

(Ahn et al., PRD80 (2009) 094003)

SIBYLL: central & leading particle production

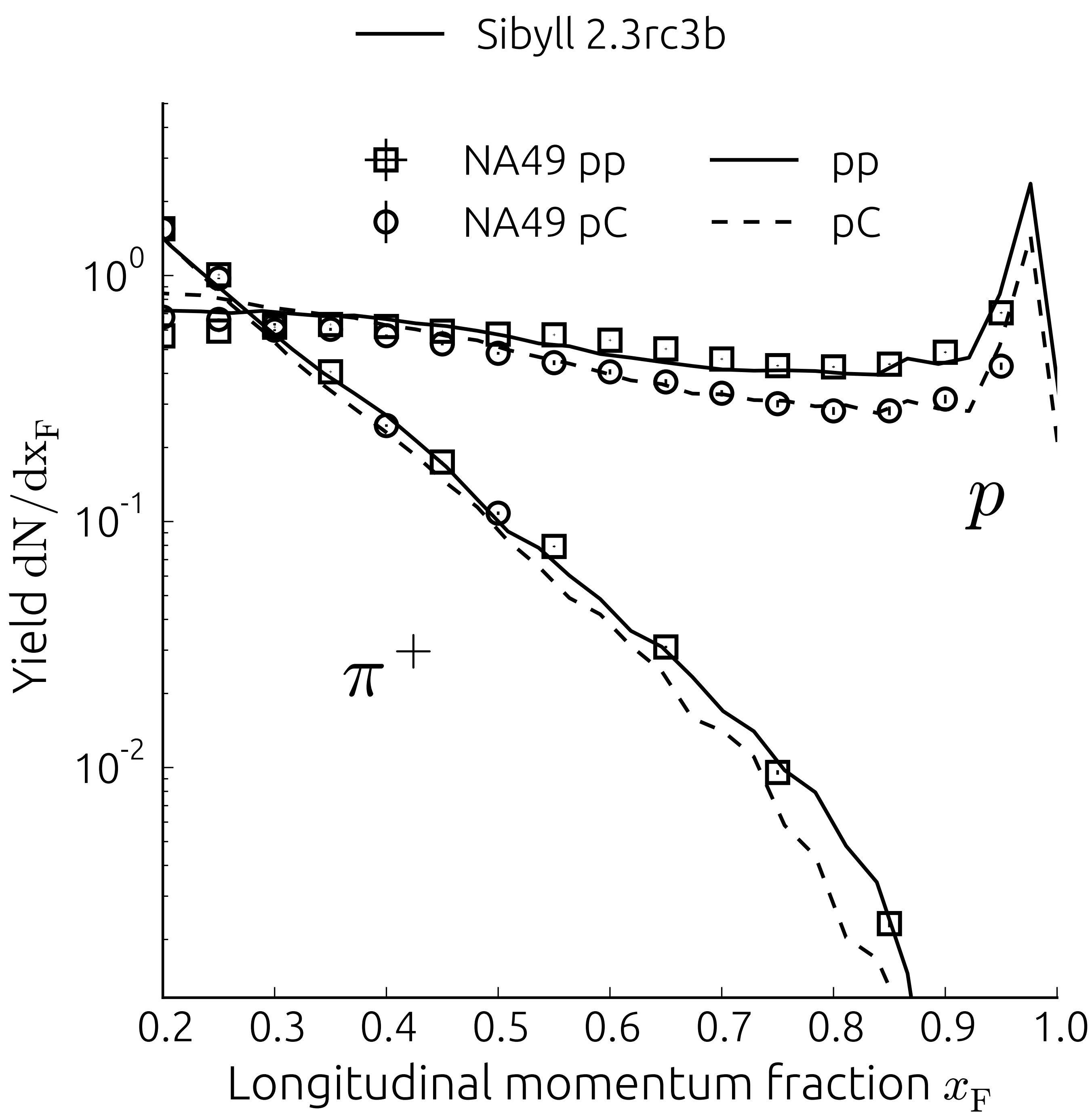

NA49 p-p and p-C at 158 GeV

Leading particle effect less pronounced due to additional interactions with nucleons in target nucleus

(Riehn et al. ICRC 2017)

Leading particle effect and nuclei

Projectile component of net proton spectrum

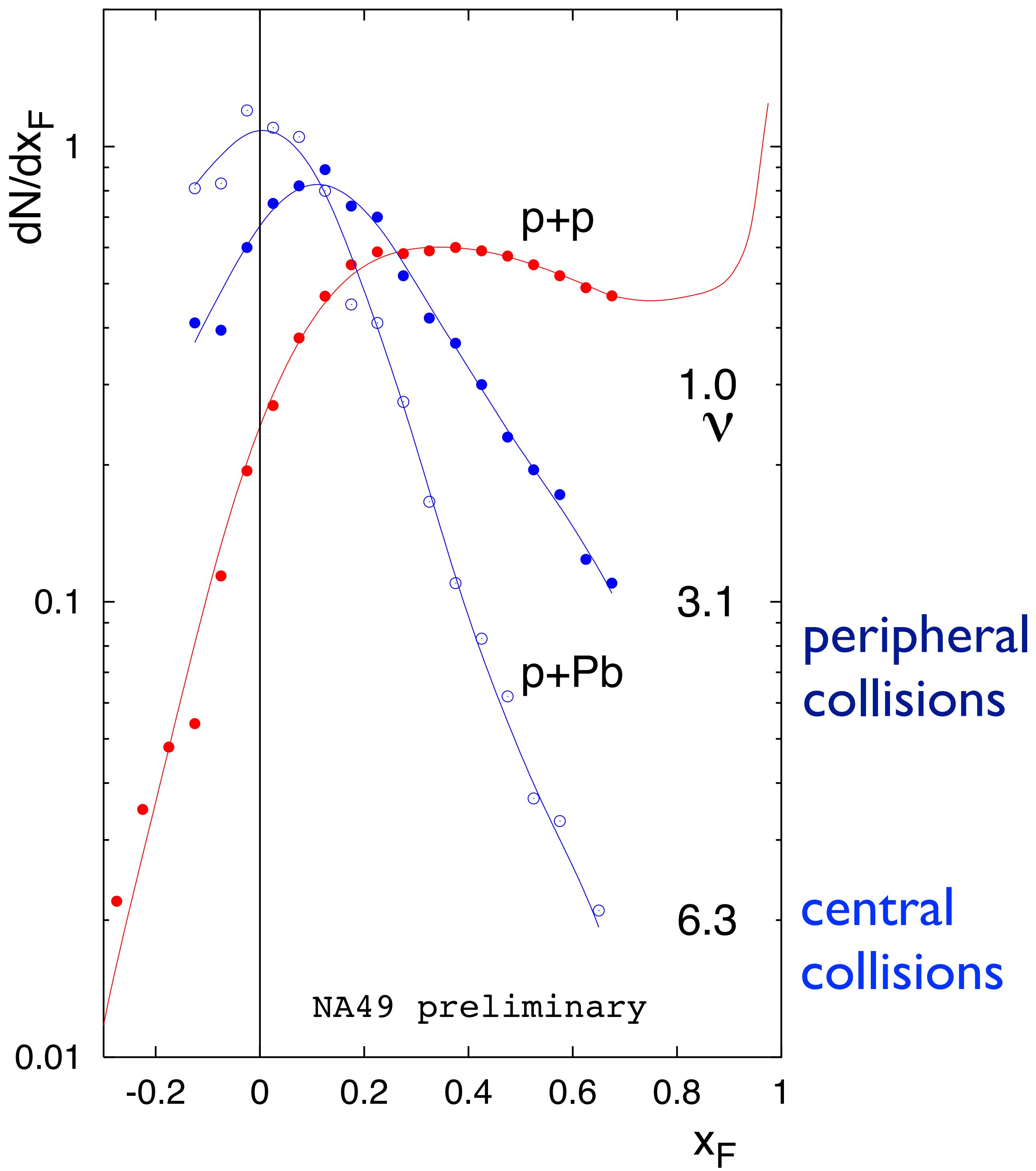

E_{lab} = 149 GeV

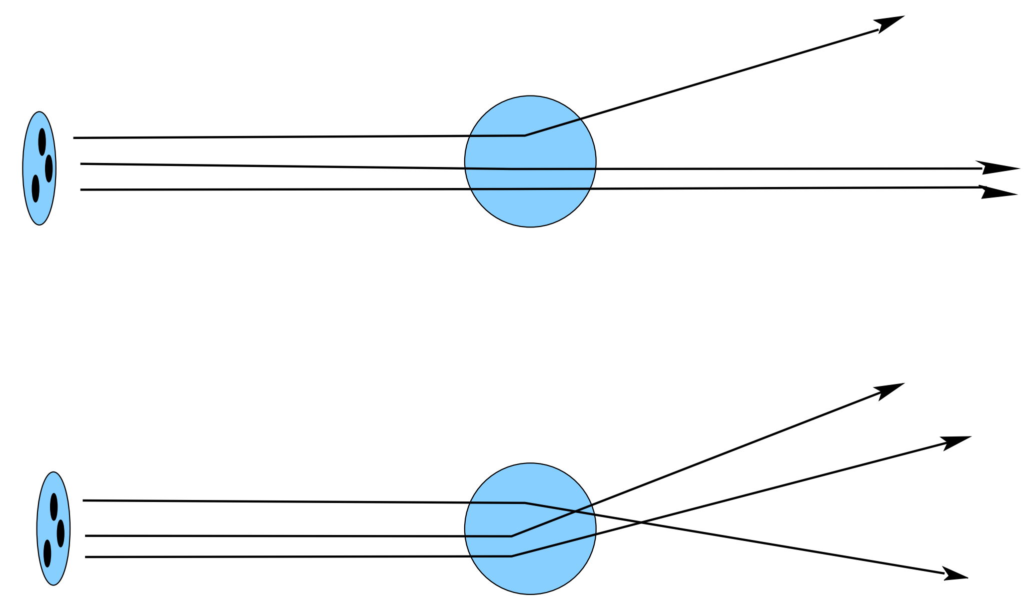

Central collisions:

- no leading particle effect,
- secondaries of highest energy are mesons

Basic features of multiparticle production

- Leading particle effect
  - ~50% of energy carried by leading nucleon
  - incoming proton: p:n ~ 2:1 (approximately)

- Secondary particles
  - power-law increase of multiplicity
  - quark counting: ~ 33% π^0, 66% $\pi^\pm$
  - transverse momentum energy-independent
  - scaling of secondary particle distributions
  - baryons are pair-produced, delayed threshold

- Total cross sections
  - no good microscopic model (Regge theory)
  - often parametrization of data used
  - Glauber model for nuclei

- Diffraction (rapidity gaps)
  - elastic scattering & low-mass diffraction dissociation
  - large multiplicity fluctuations

Comparison of low/intermediate energy models

DPMJET II & III *(Ranft / Roesler, RE, Fedynitch, Ranft, Bopp)*	• microscopic (universal) model • resonances for low energy hadron projectiles (HADRIN, NUCRIN) • two- and multi-string model
FLUKA *(Ferrari, Sala, Ranft, Roesler)*	• microscopic (universal) model • resonances (PEANUT), photodissociation • two-string model, DPMJET at high energy
GHEISHA *(Fesefeld)*	• parametrization of data (GEANT 3) • wide range of projectiles/targets • limited to E_{lab} < 500 GeV
UrQMD (Bleicher et al.)	• combination of microscopic model with data parametrization (no Glauber calc.) • optimized for interactions of nuclei
SOPHIA *(Mücke, RE, et al.)*	• dedicated photon-nucleon model • resonances, two-strings, E_{lab} < 500 GeV
RELDIS *(Pshenichnov)*	• dedicated photodissociation model for nuclei, wide range of nuclei

Example: Waxman-Bahcall neutrino limit (i)

Maximum ``reasonable´´neutrino flux due to interaction of cosmic rays in sources

Assumptions:

- sources accelerate only protons (other particles yield fewer neutrinos)
- injection spectrum at sources known (power law index -2)
- each proton interacts once on its way to Earth (optically thin sources)

Proton flux at sources

$$\Phi_p(E_p) = \frac{dN_p}{dE_p dA dt d\Omega} = A\, E_p^{-\alpha}$$

Master equation

$$\boxed{\Phi_\nu(E_\nu) = \int \frac{dN_\nu}{dE_\nu}(E_p)\, \Phi_p(E_p)\, dE_p}$$

Number of neutrinos produced in interval $E_\nu \ldots E_\nu + dE_\nu$, per proton interaction

Spectrum weighted moments (i)

$$\Phi_\nu(E_\nu) = \int \frac{dN_\nu}{dE_\nu}(E_p)\,\Phi_p(E_p)\,dE_p$$

Aim: re-writing of equation for scaling of yield function

Scaling of neutrino yield

$$x = \frac{E_\nu}{E_p}$$

fraction of proton energy given to neutrino

$$\boxed{\frac{dN_\nu}{dE_\nu}(E_p) = \frac{1}{E_p}\frac{dN_\nu}{dx}} \quad (1)$$

energy-independent yield function

Elementary math

$$dE_p = \frac{E_\nu}{x^2}\,dx \quad (2)$$

$$\Phi_p(E_p) = A\,E_p^{-\alpha} = A\left(\frac{E_\nu}{x}\right)^{-\alpha} = x^\alpha\,A\,E_\nu^{-\alpha} \quad (3)$$

Spectrum weighted moments (ii)

$$\Phi_\nu(E_\nu) = \int \frac{dN_\nu}{dE_\nu}(E_p)\, \Phi_p(E_p)\, dE_p$$

substitutions (1) - (3)

$$\Phi_\nu(E_\nu) \;=\; \int_0^1 x^{\alpha-1}\, \frac{dN_\nu}{dx}\, A\, E_\nu^{-\alpha}\, dx$$

$$\Phi_\nu(E_\nu) \;=\; \left[\int_0^1 x^{\alpha-1}\, \frac{dN_\nu}{dx}\, dx\right] A\, E_\nu^{-\alpha}$$

Spectrum weighted moment
(just a number that depends
only on particle physics)

Proton flux
(but with neutrino energy
instead of proton energy)

Example: Waxman-Bahcall neutrino limit (ii)

Proton spectrum
with $\alpha = 2$

$$\Phi_\nu(E_\nu) = \left[\int_0^1 x \frac{dN_\nu}{dx} dx\right] A\, E_\nu^{-2}$$

Spectrum weighted moment for α=2:
mean energy fraction of proton given to neutrino
times number of neutrinos per interaction

Relevant interaction & decay chain (33% of all interactions with small E_{cm})

$$p + \gamma \longrightarrow n\, \pi^+ \longrightarrow n\, \mu^+\, \nu_\mu \longrightarrow n\, \underbrace{e^+\, \nu_e\, \bar{\nu}_\mu\, \nu_\mu}$$

20% of p
energy

each particle has 25% of the
energy of the π^+

$$\Phi_{\nu_\mu}(E_{\nu_\mu}) = 0.33 \times 0.2 \times 0.25\;\; A E_{\nu_\mu}^{-2}$$

Atmospheric muons and neutrinos

Atmosphere is dense target, secondary particles can interact or decay

Spectrum weighted moment

Example: pion flux in atmosphere at depth X

$$\frac{d\Phi_\pi(E,X)}{dX} = -\left(\frac{1}{\Lambda_\pi} + \frac{\varepsilon_\pi}{E\,X\cos\theta}\right)\Phi_\pi(E,X) \quad + \quad \frac{Z_{N\pi}}{\lambda_N}\Phi_N(E)e^{-X/\Lambda_N}$$

Regeneration of particle flux through interaction

$$\Lambda_N = \lambda_N/(1-Z_{NN})$$

Loss of pions due to decay

$$\varepsilon_\pi = \frac{m_\pi h_0}{\tau_\pi\ \cos\theta}$$

$$X_v = X_0 E^{-h/h_0}$$

Generation of pions by primary nucleons

Muon and neutrino fluxes: pion and kaon flux have to be folded with decay distributions

(*Gaisser, Cosmic Rays and Particle Physics, 1990*)

Spectrum weighted moments for α = 2.7

Detailed simulation of interactions for air target with DPMJET

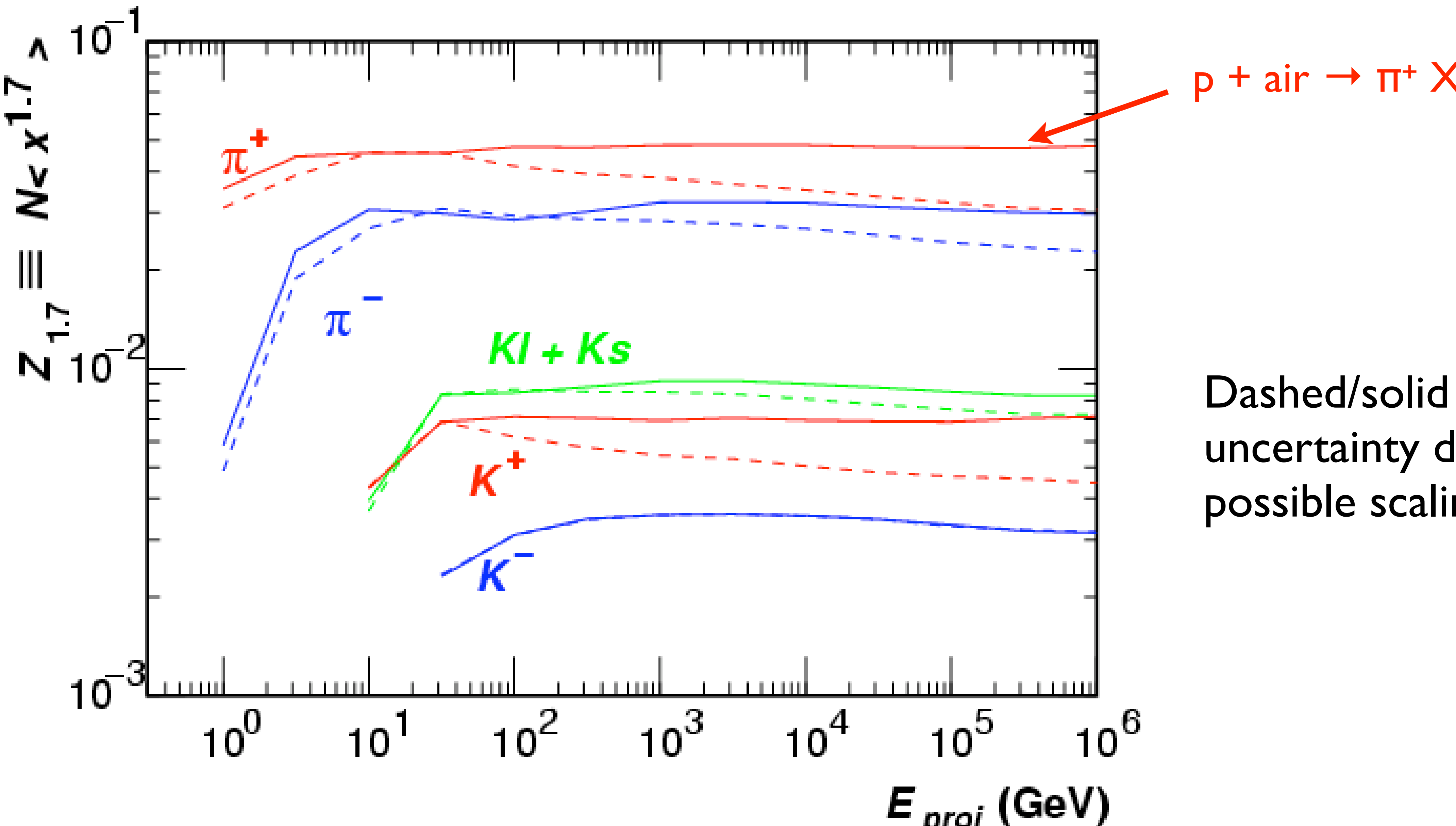

Dashed/solid lines: uncertainty due to possible scaling violation

(Honda et al., C2CR 2005)

3. High energy region

Transition from intermediate to high energy

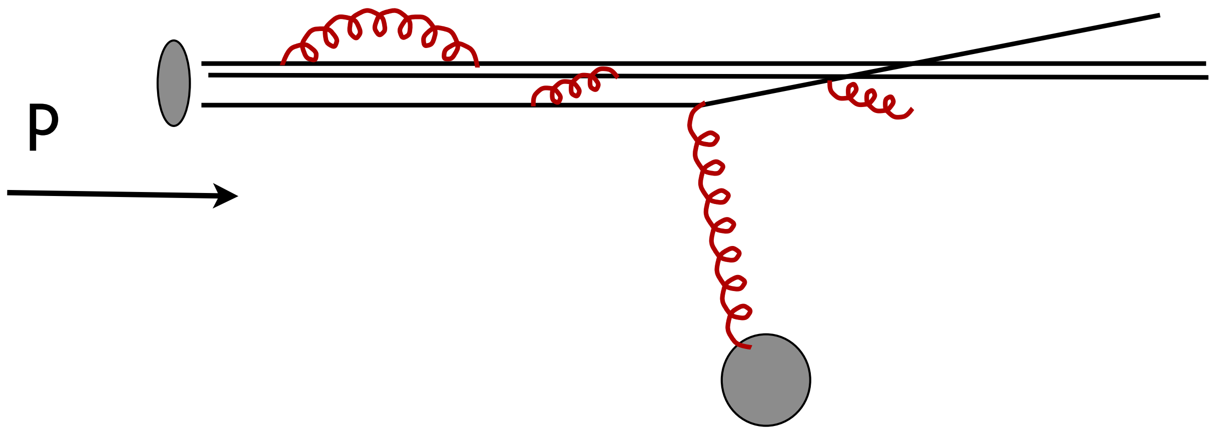

Intermediate energy:

- E_{lab} < 1,500 GeV
- E_{cm} < 50 GeV
- dominated by valence quarks

Lifetime of fluctuations
$$\Delta t \approx \frac{1}{\Delta E} = \frac{1}{\sqrt{p^2+m^2}-p} = \frac{1}{p(\sqrt{1+m^2/p^2}-1)} \approx \frac{2p}{m^2}$$

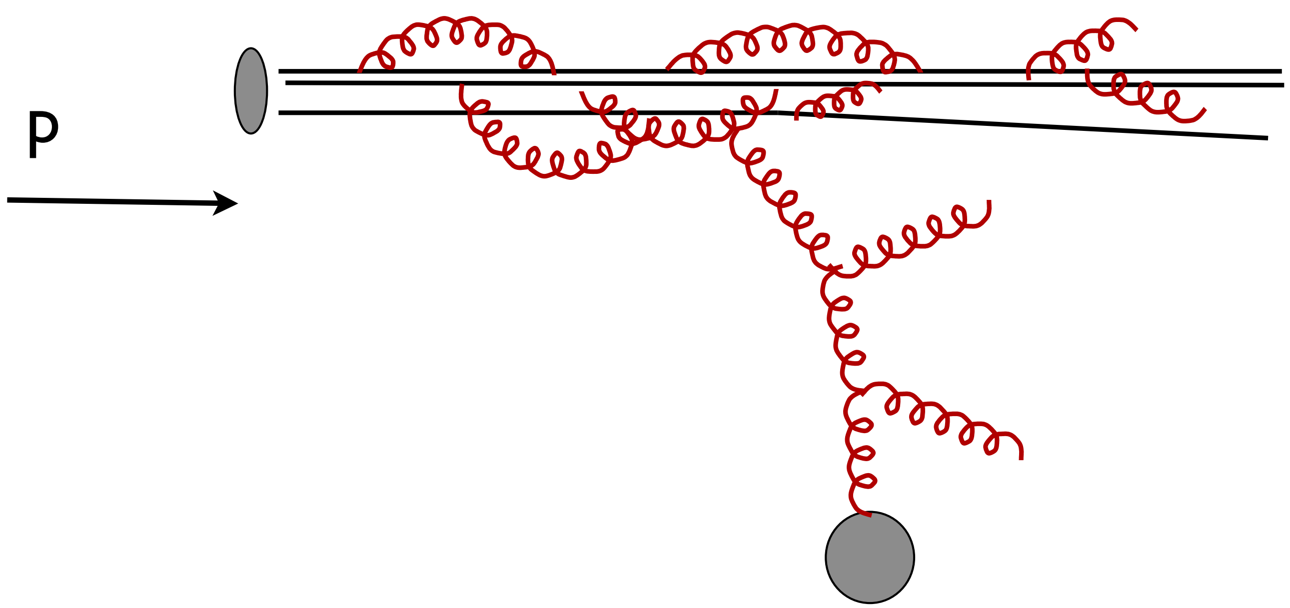

High energy regime:

- E_{lab} > 21,000 GeV
- E_{cm} > 200 GeV
- dominated by gluons and sea quarks

Transition from intermediate to high energy

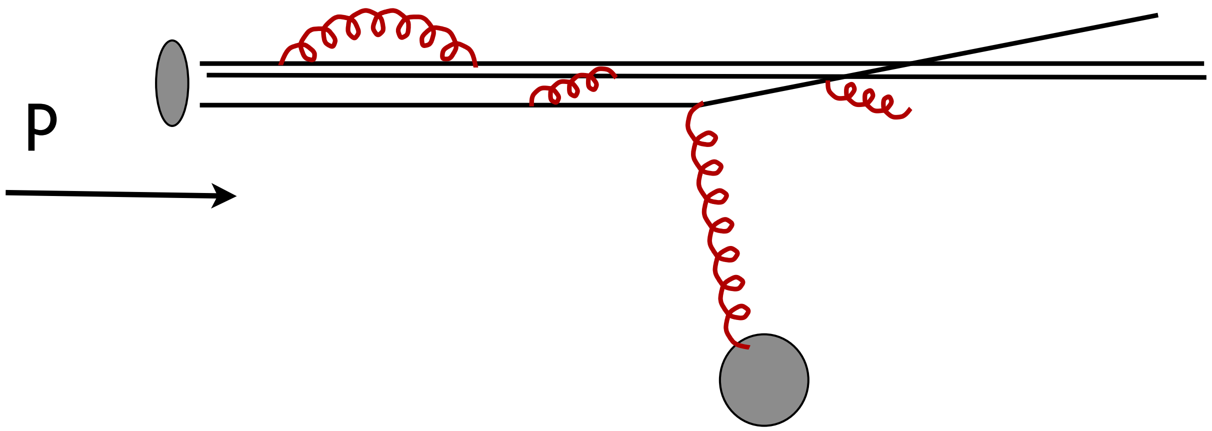

Intermediate energy:

- E_{lab} < 1,500 GeV
- E_{cm} < 50 GeV
- dominated by valence quarks

Lifetime of fluctuations

$$\Delta t \approx \frac{1}{\Delta E} = \frac{1}{\sqrt{p^2+m^2}-p} = \frac{1}{p(\sqrt{1+m^2/p^2}-1)} \approx \frac{2p}{m^2}$$

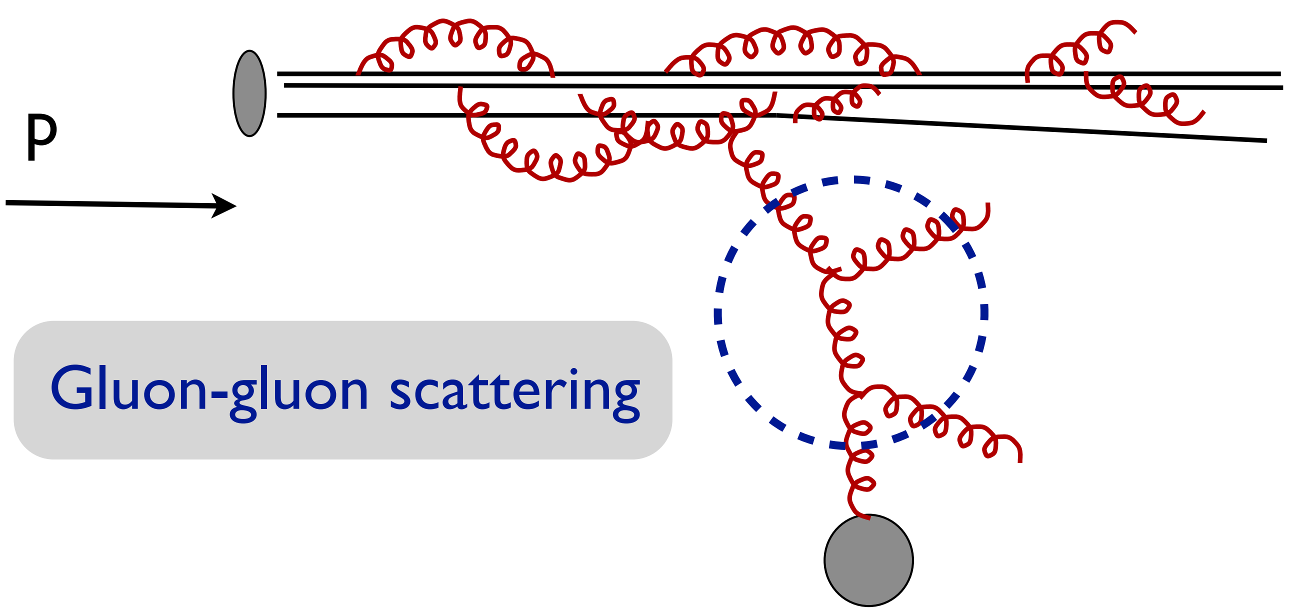

High energy regime:

- E_{lab} > 21,000 GeV
- E_{cm} > 200 GeV
- dominated by gluons and sea quarks

Scattering of quarks and gluons: jet production

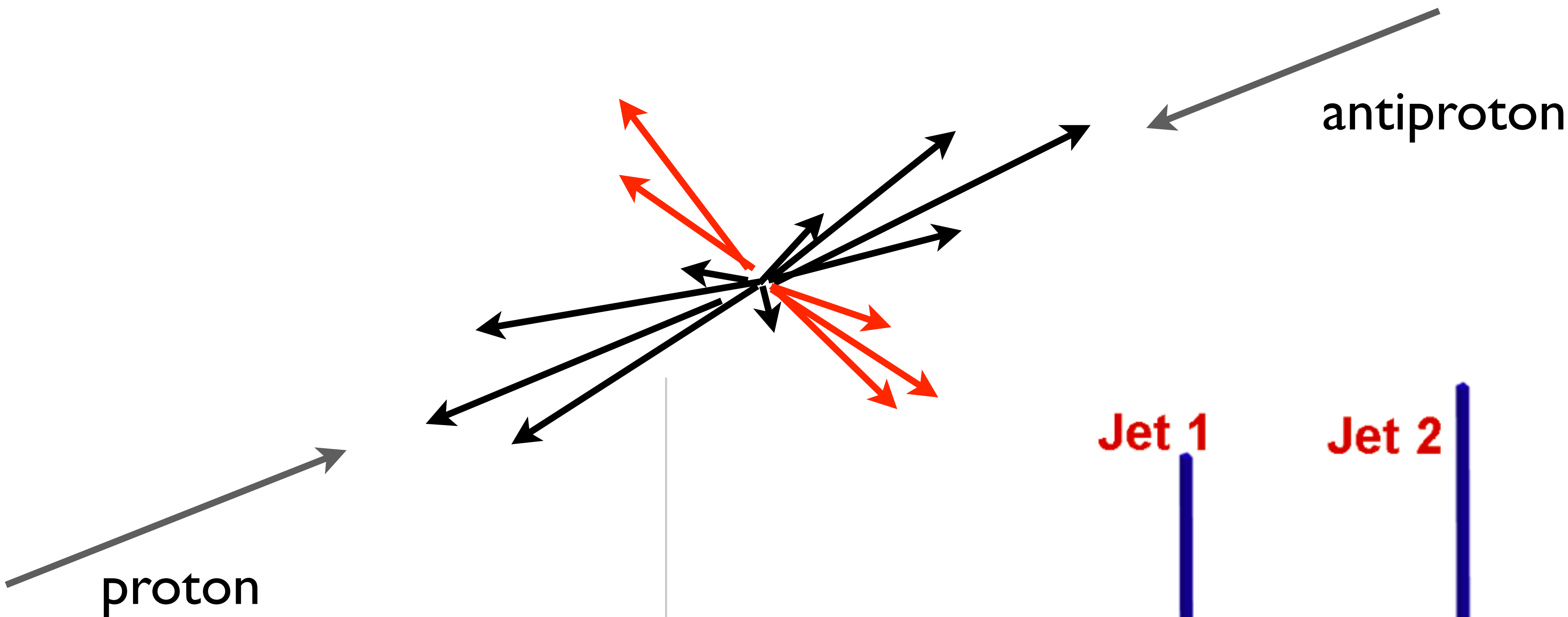

Proton-antiproton collision at Tevatron

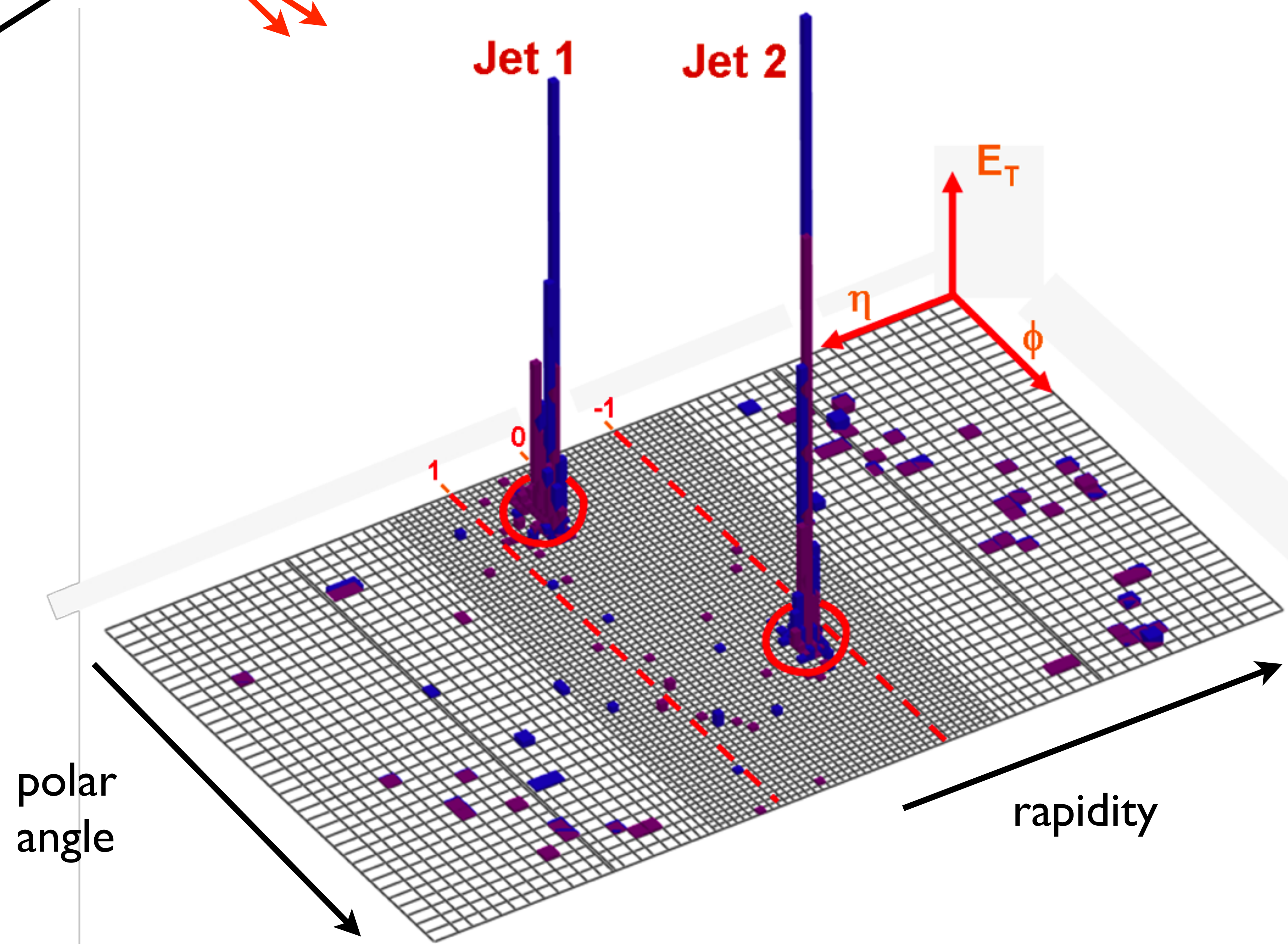

Interpretation within perturbative QCD

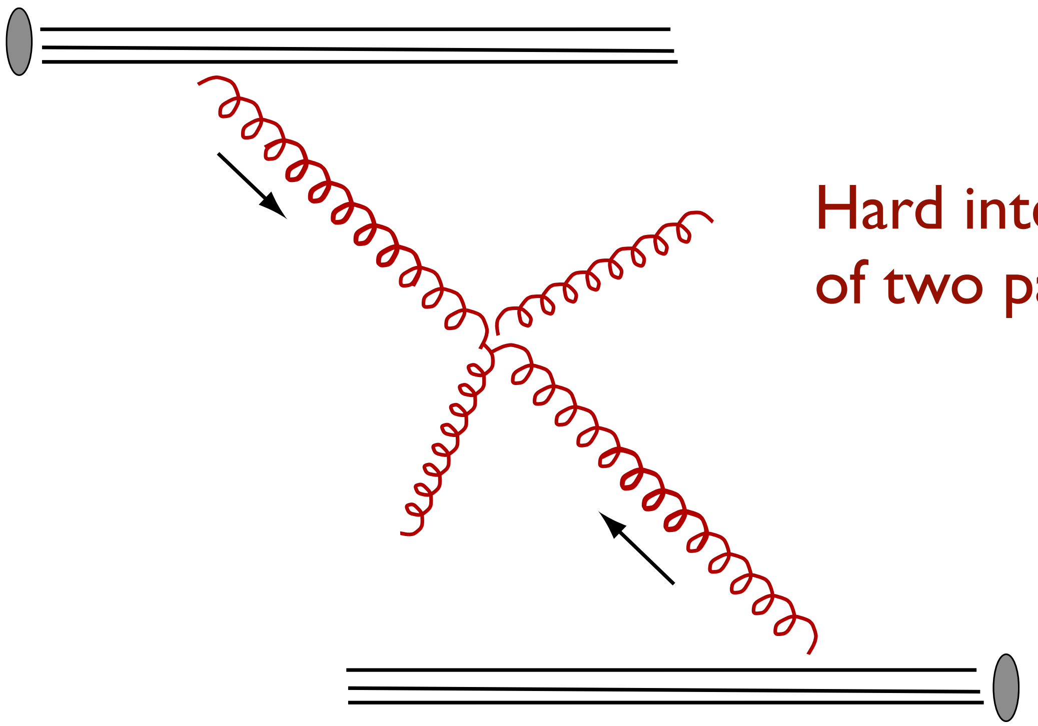

Hard interaction
of two partons

QCD predictions known
for parton-parton cross sections

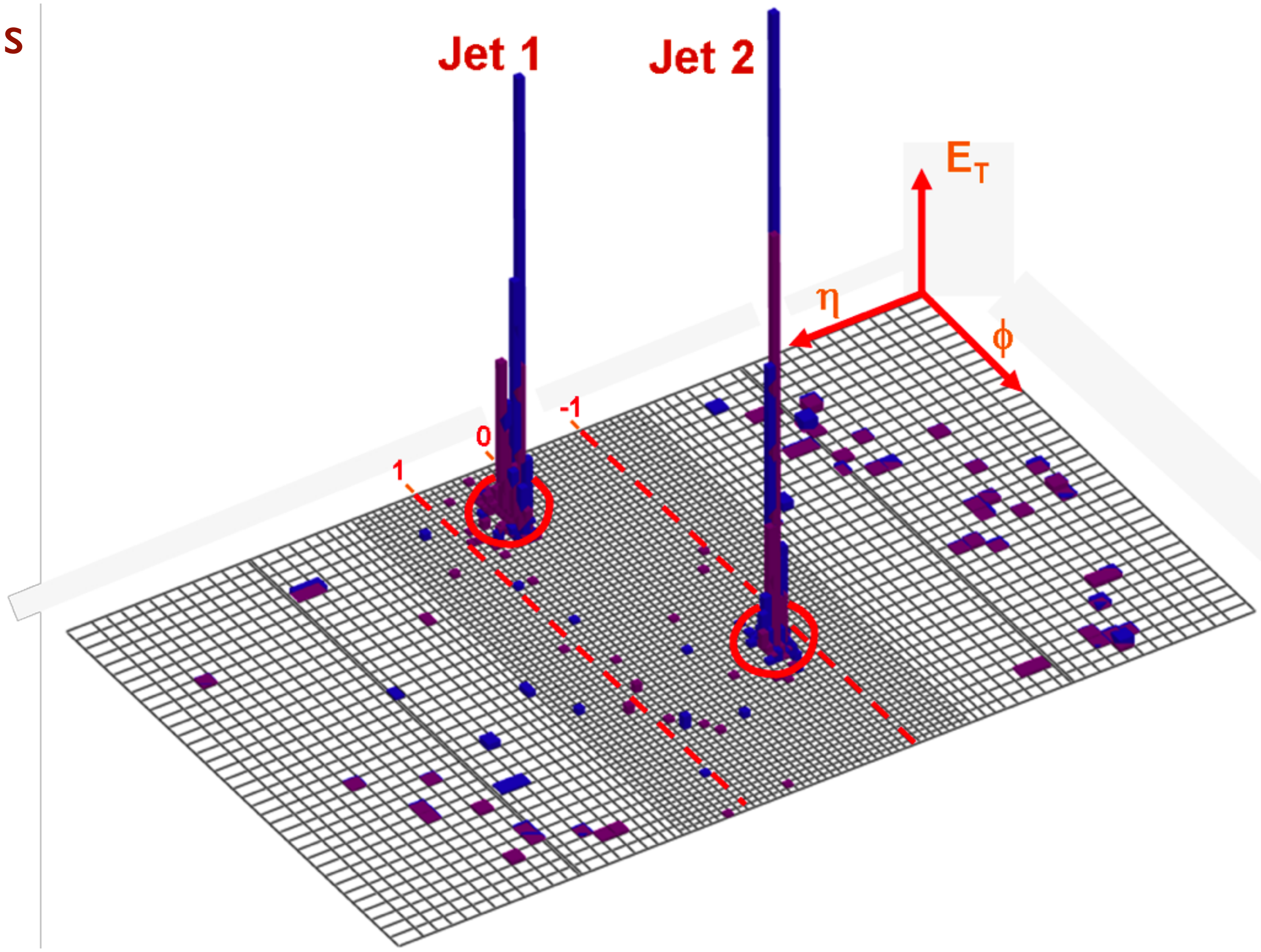

Terminology

Soft interaction: no large momentum transfer

Hard interaction: large momentum transfer ($|t| > 2\ \mathrm{GeV}^2$)

QCD parton model: inclusive minijet cross section

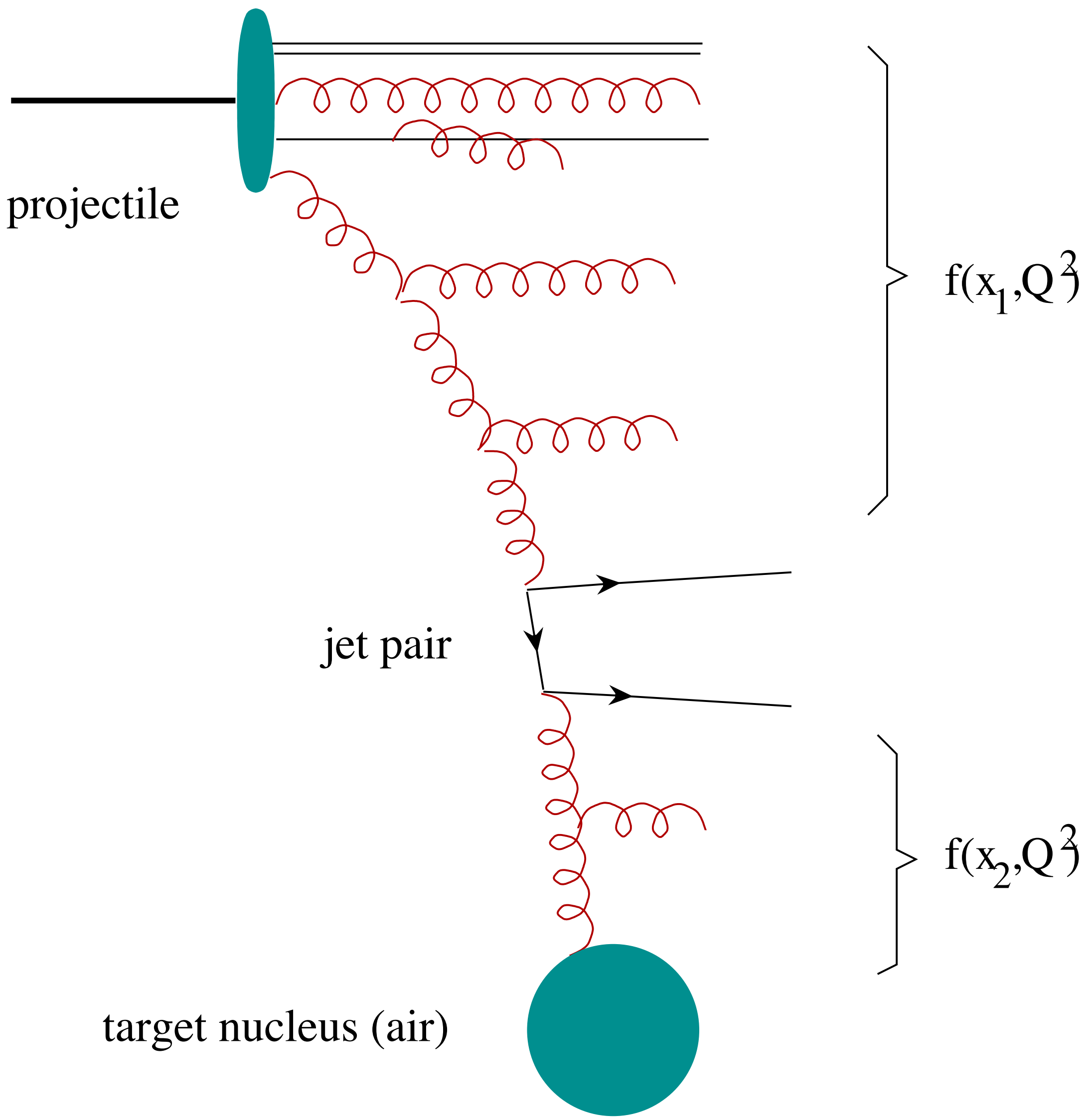

Proton-proton cross section

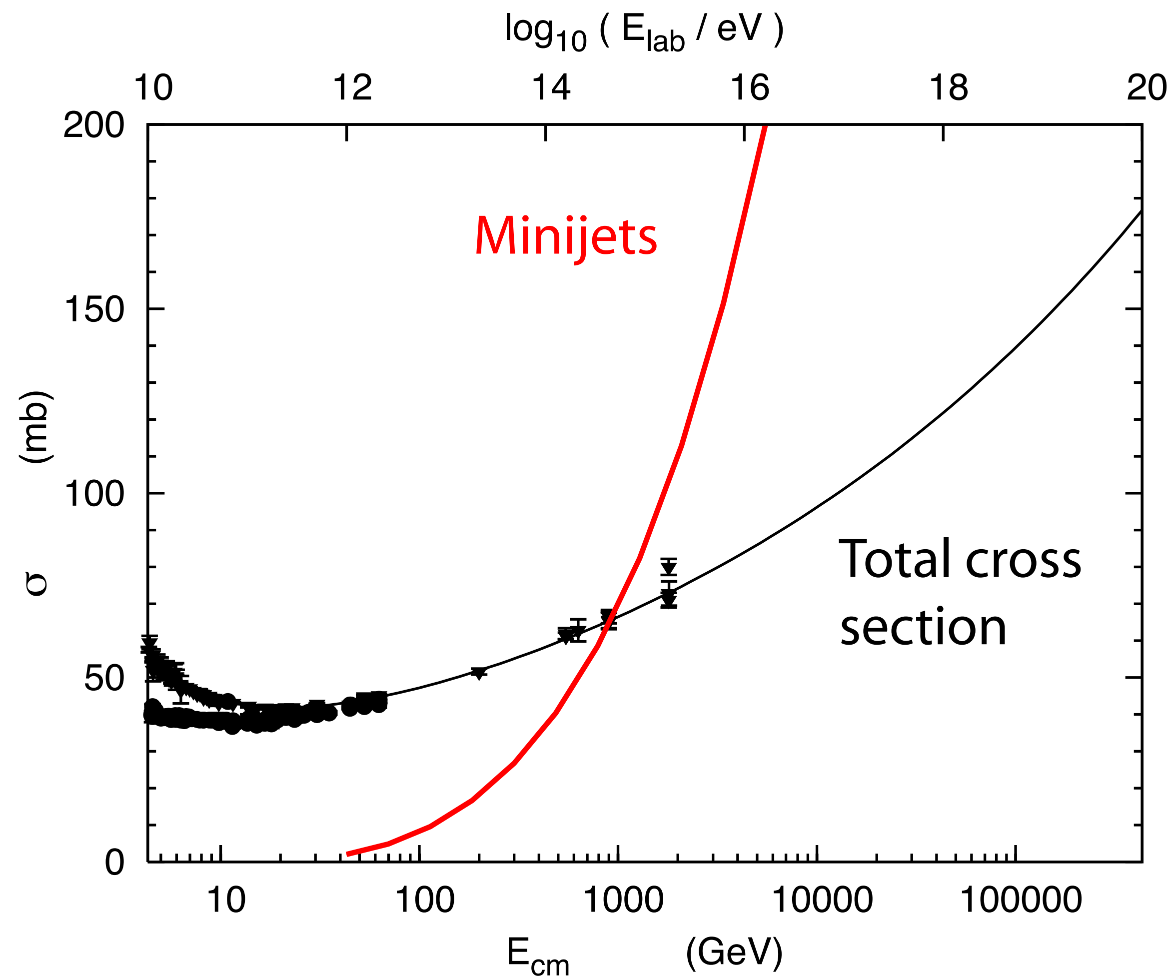

$$\sigma_{QCD} = \sum_{i,j,k,l} \frac{1}{1+\delta_{kl}} \int dx_1\, dx_2 \int_{p_\perp^{\mathrm{cutoff}}} dp_\perp^2\, f_i(x_1,Q^2)\, f_j(x_2,Q^2)\, \frac{d\sigma_{i,j\to k,l}}{dp_\perp}$$

Perturbative QCD predictions for parton densities

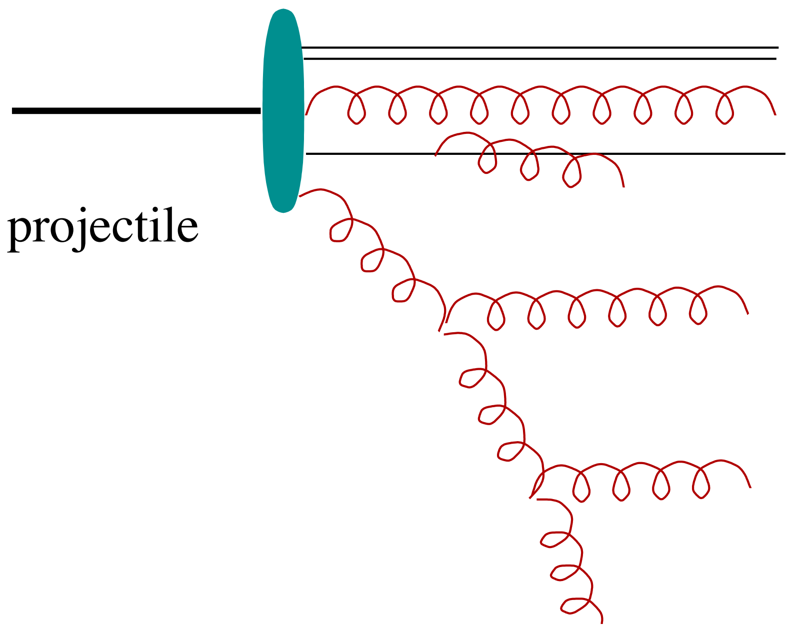

Evolution of parton number
given by DGLAP equation
(and non-linear versions of it)

HERA data

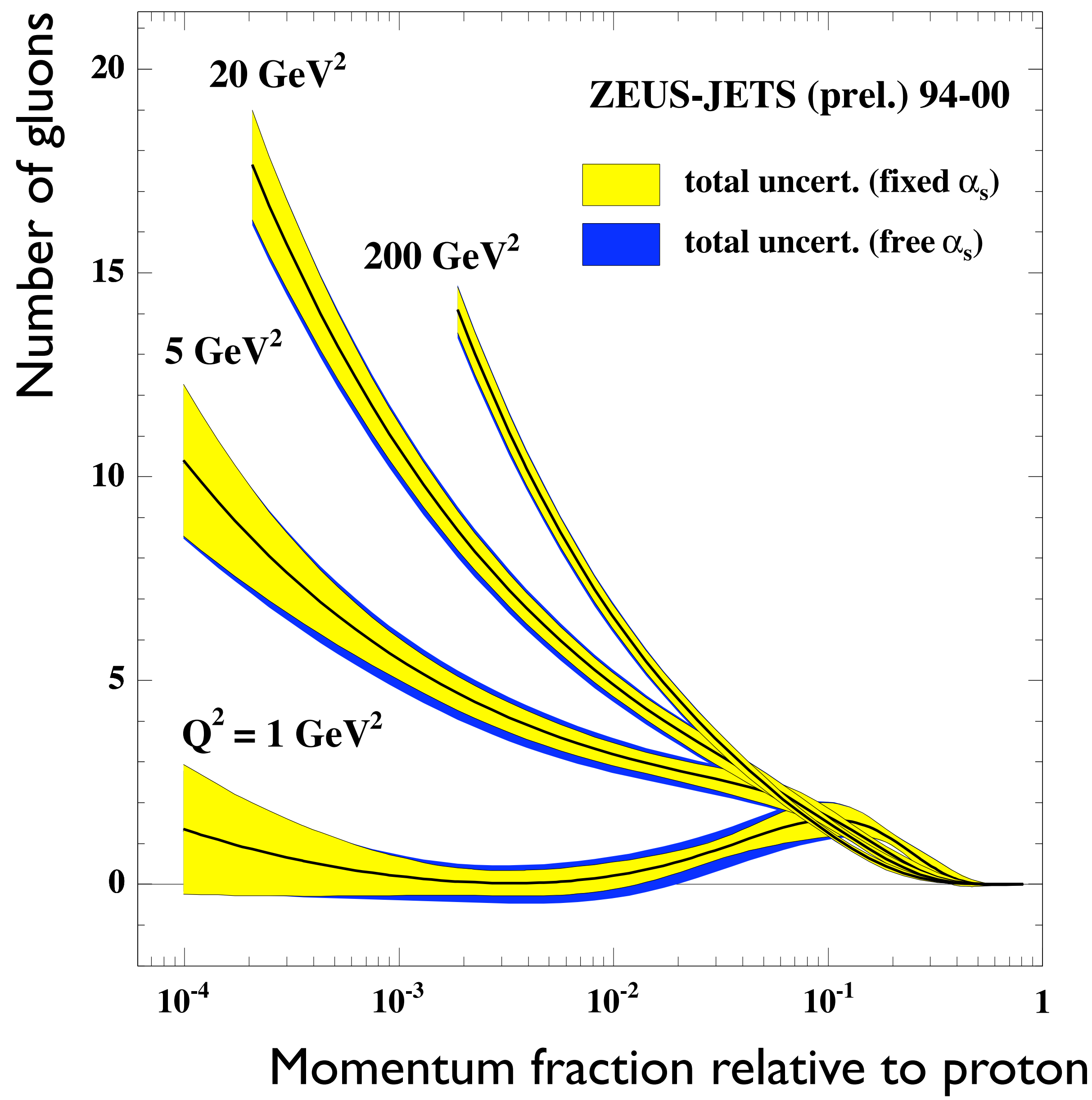

$$\frac{d f_i(x,Q^2)}{d\log Q^2} = \frac{\alpha_s(Q^2)}{2\pi} \int_x^1 \frac{dy}{y} \sum_j f_j(y,Q^2)\, P_{j\to i}\left(\frac{x}{y}\right)$$

Prediction of
perturbative QCD

Parton densities not really known at very low x

Range of x values (momentum fractions) needed in calculation

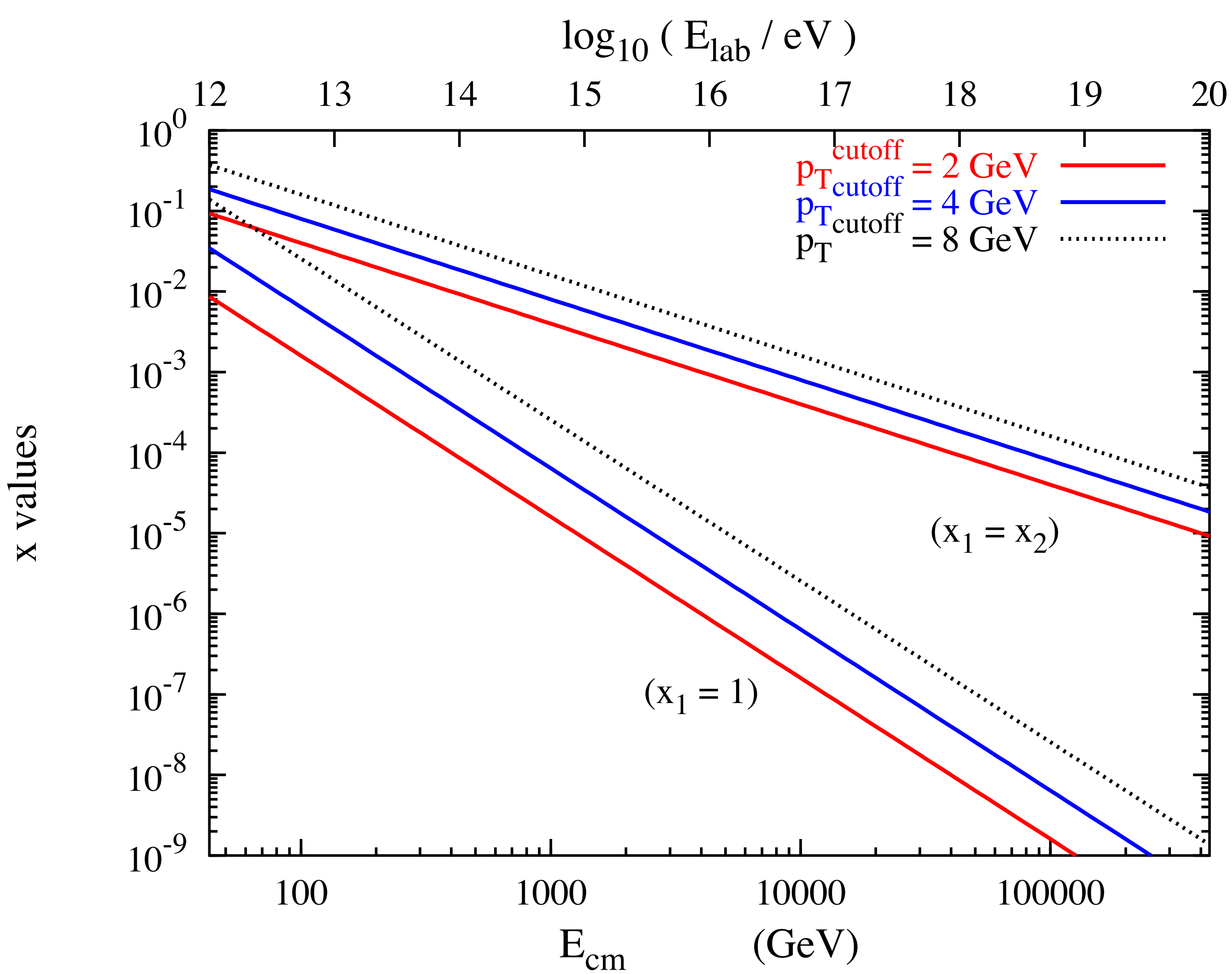

HERA measurement range

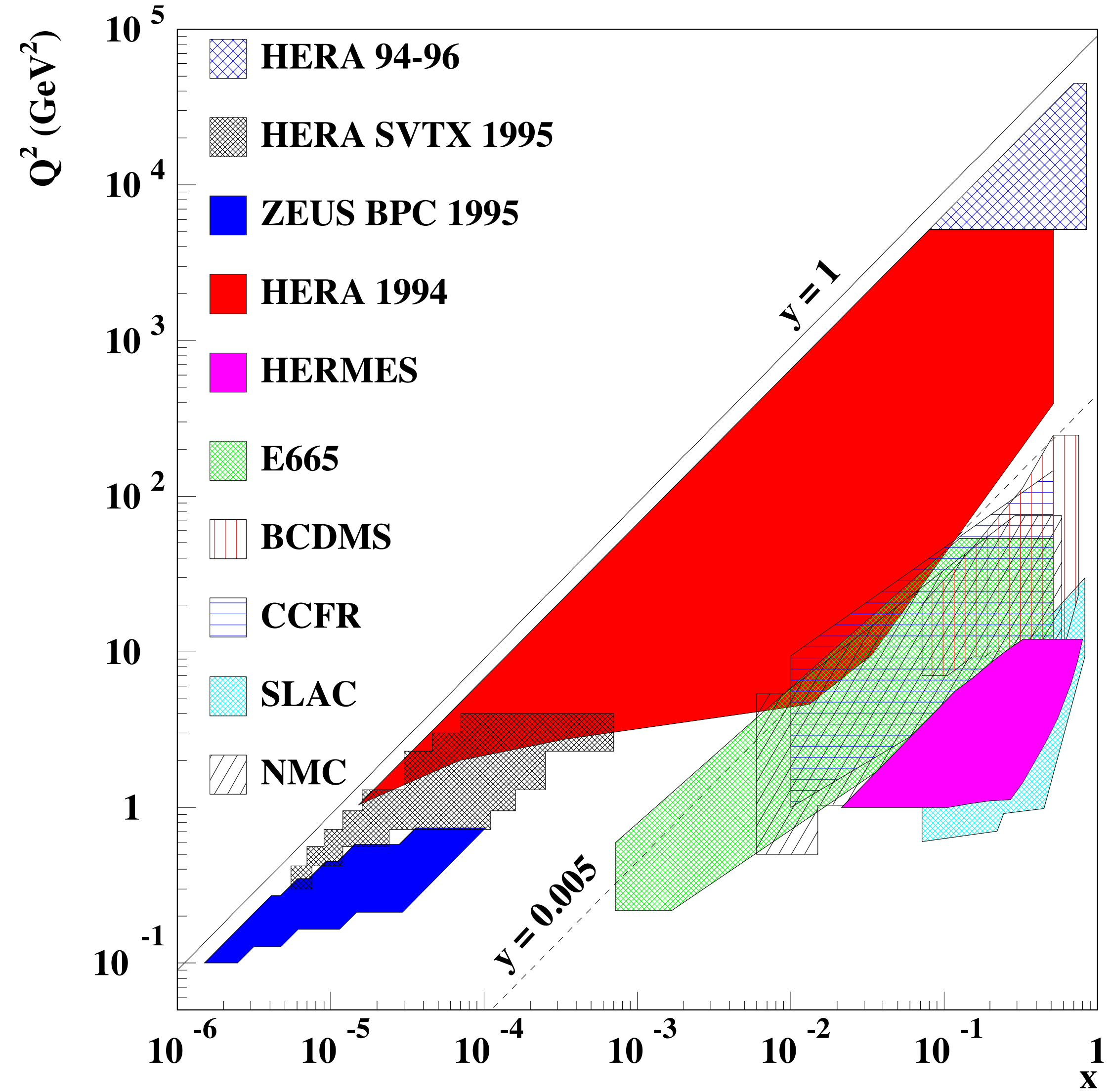

$$\hat{s} = x_1 x_2 s \geq 4p_\perp^2$$

Strong dependence on cutoff parameter

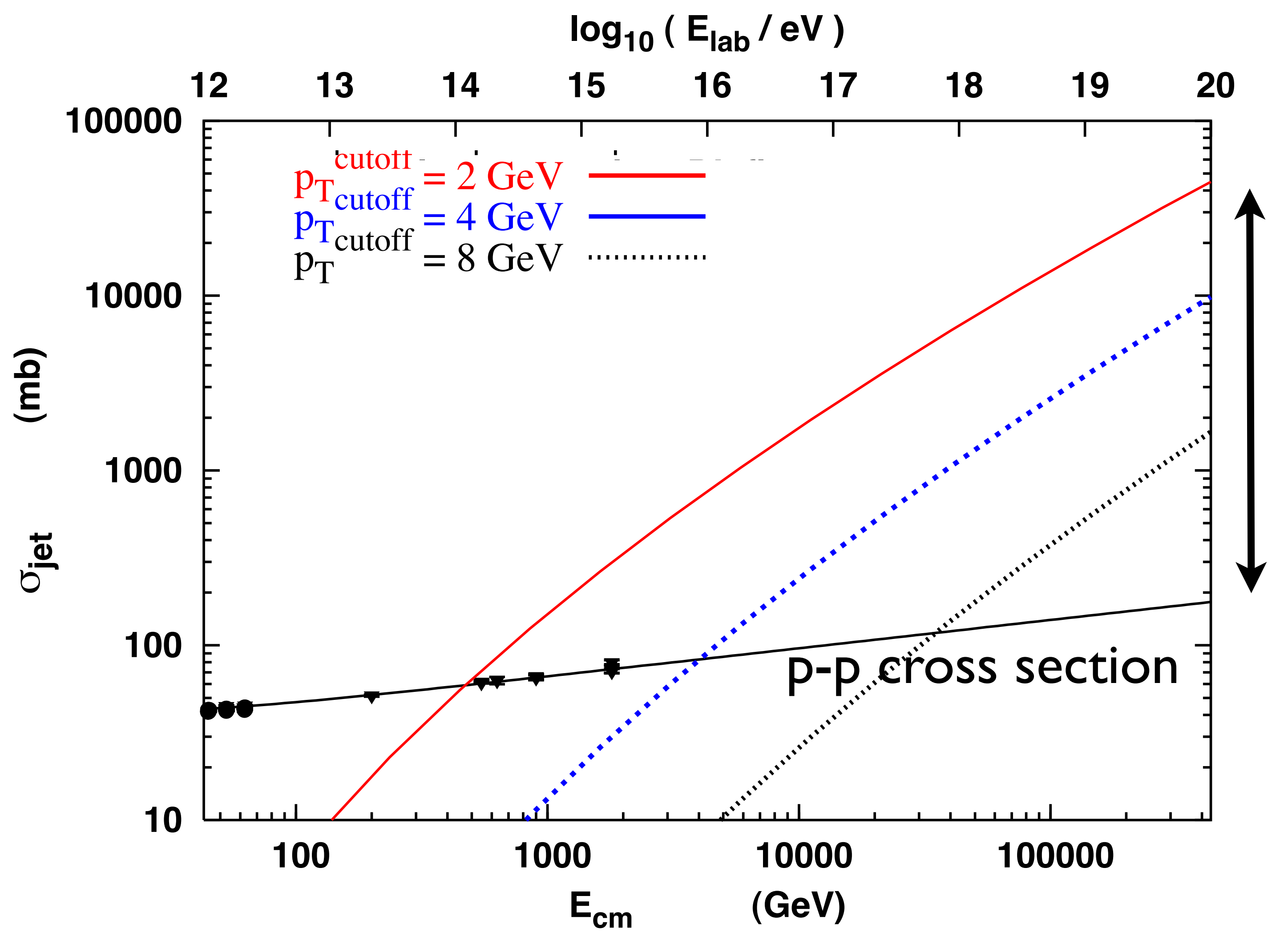

Numerical values depend on chosen parton density parametrization

Limited predictive power due to dependence on transverse momentum cutoff

$$\sigma_{QCD} = \sum_{i,j,k,l} \frac{1}{1+\delta_{kl}} \int dx_1\, dx_2 \int_{p_\perp^{\rm cutoff}} dp_\perp^2\, f_i(x_1,Q^2)\, f_j(x_2,Q^2)\, \frac{d\sigma_{i,j\to k,l}}{dp_\perp}$$

Multiple parton-parton interactions

Proton-proton cross section

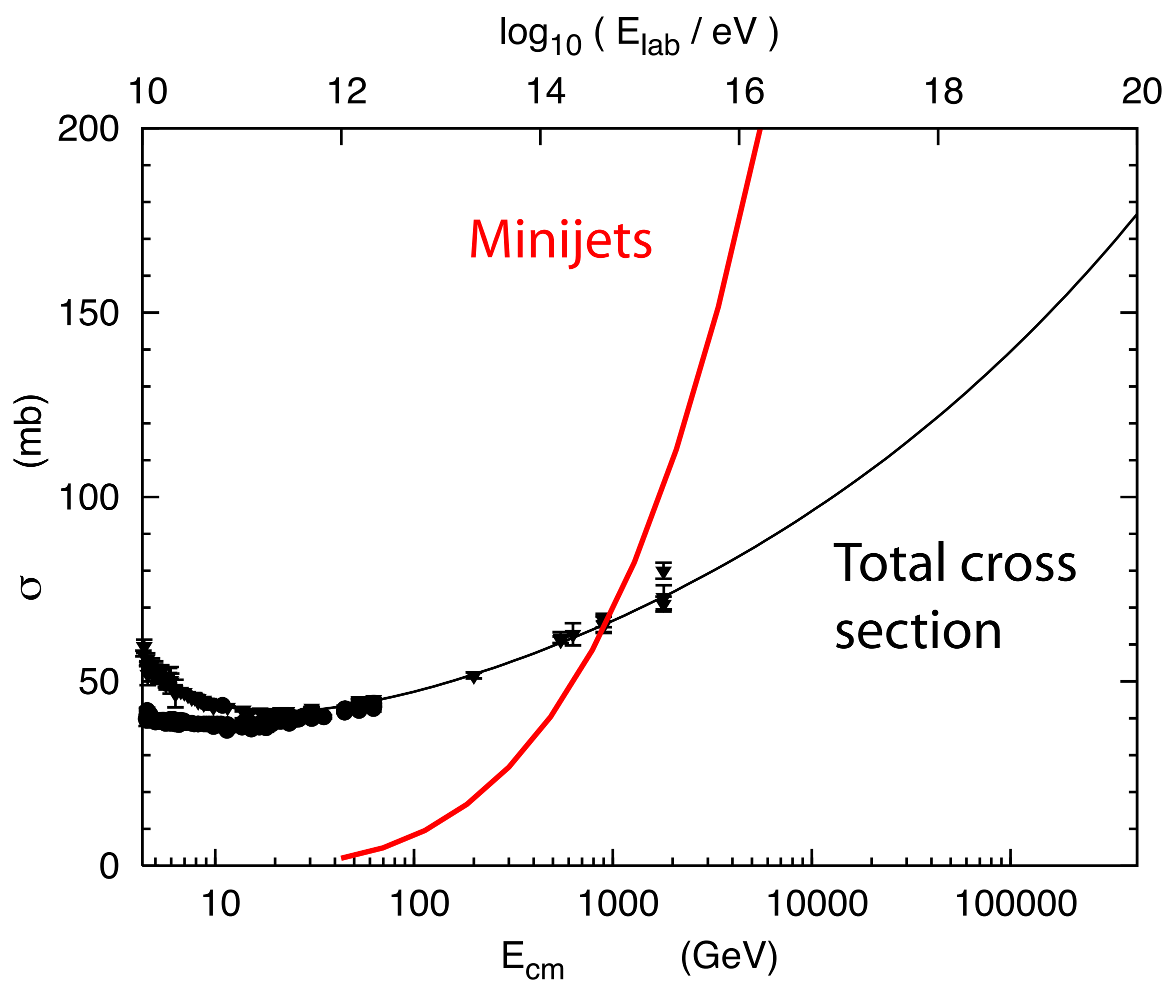

QCD prediction:
inclusive cross section

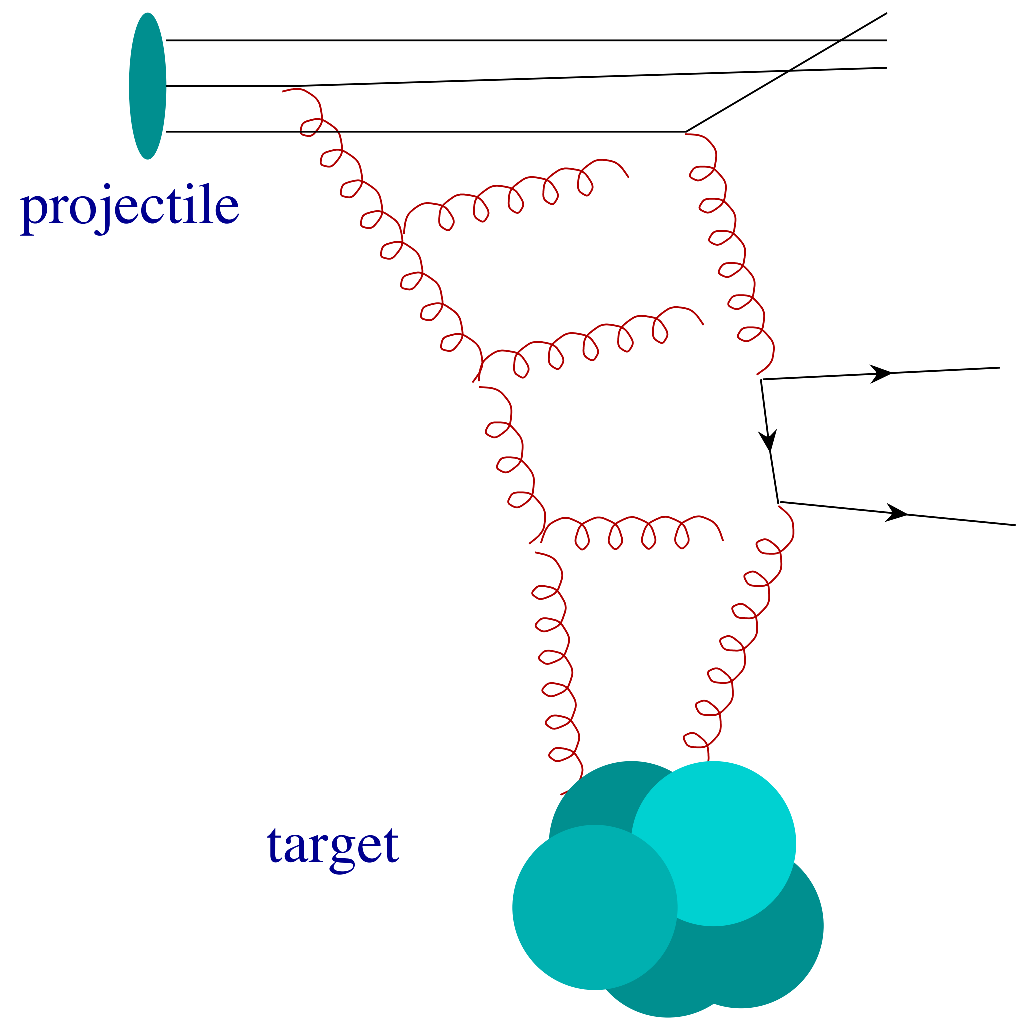

Average number of minijet pairs

$$\langle n_{\text{jet}} \rangle = \frac{\sigma_{\text{QCD}}}{\sigma_{\text{ine}}}$$

Geometric view: Poissonian probability distribution

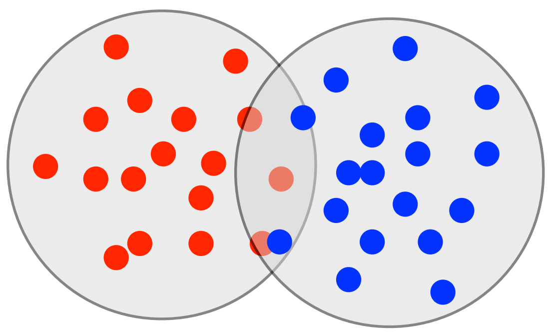

Peripheral collision:
only very few parton-pairs interacting

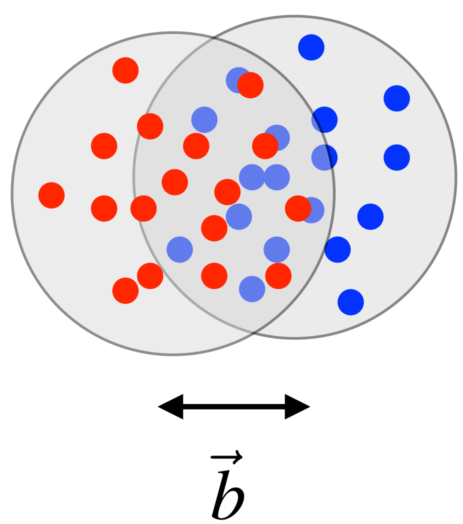

Central collision:
many parton-pairs interacting

$$P_n = \frac{\langle n_{\mathrm{hard}}(\vec{b})\rangle^n}{n!} \exp\left(-\langle n_{\mathrm{hard}}(\vec{b})\rangle\right)$$

mean number of interactions for given impact parameter of collision

Need to know mean number of interactions as function of impact parameter

Multiple soft and hard interactions

$$\sigma_{n_s,n_h} = \int d^2b\, \frac{[n_{\rm soft}(b,s)]^{n_s}}{n_s!}\, \frac{[n_{\rm hard}(b,s)]^{n_h}}{n_h!}\, e^{-n_{\rm hard}(b,s)-n_{\rm soft}(b,s)}$$

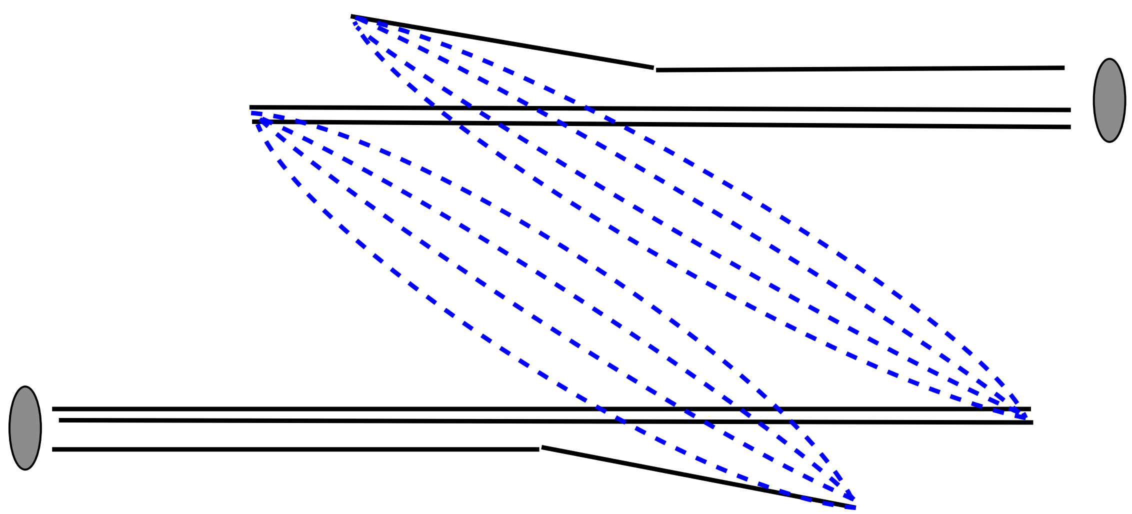

$n_s=1$, $n_h=0$

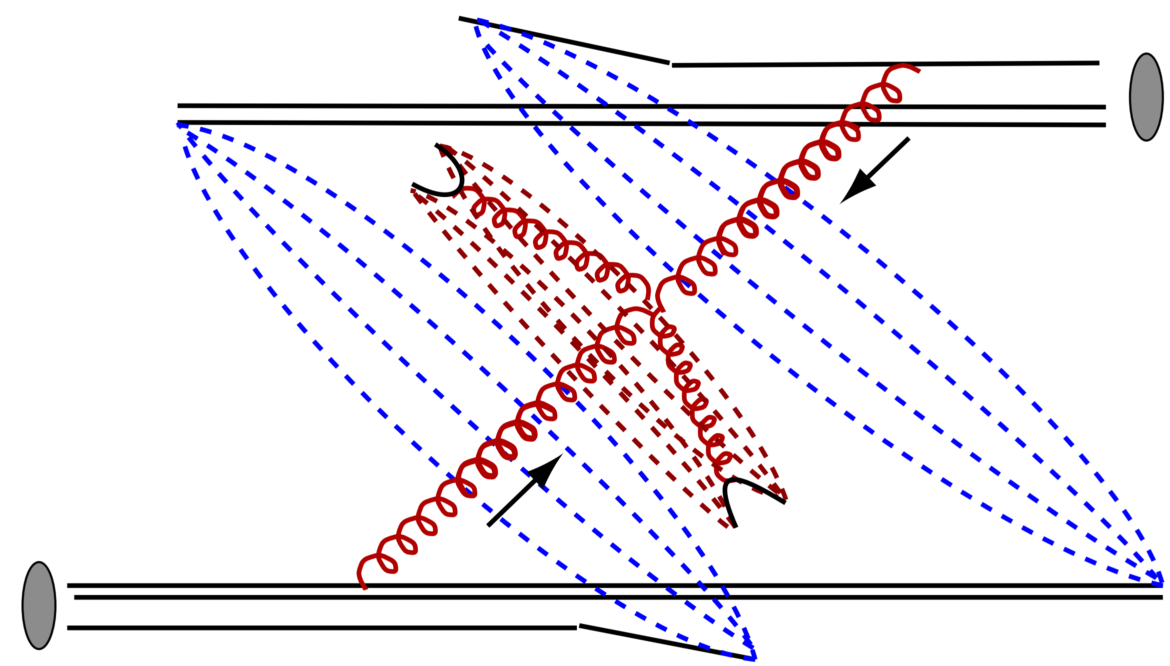

$n_s=1$, $n_h=1$

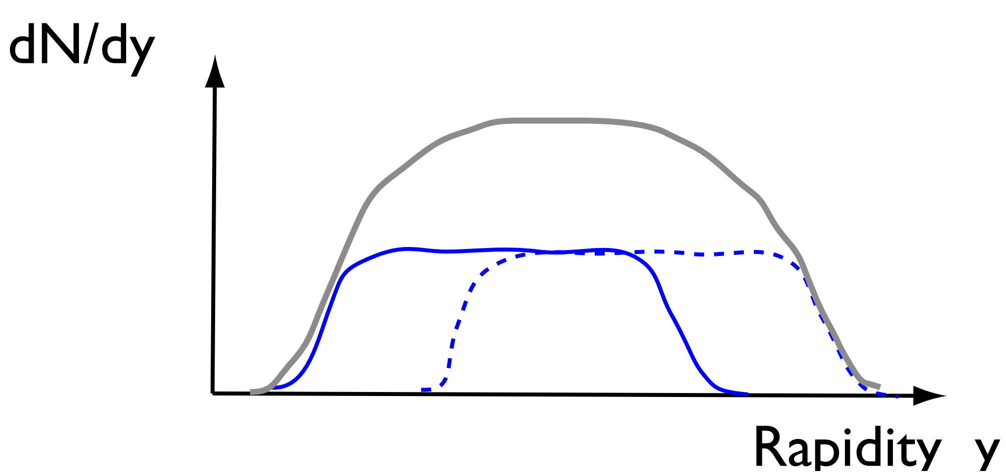

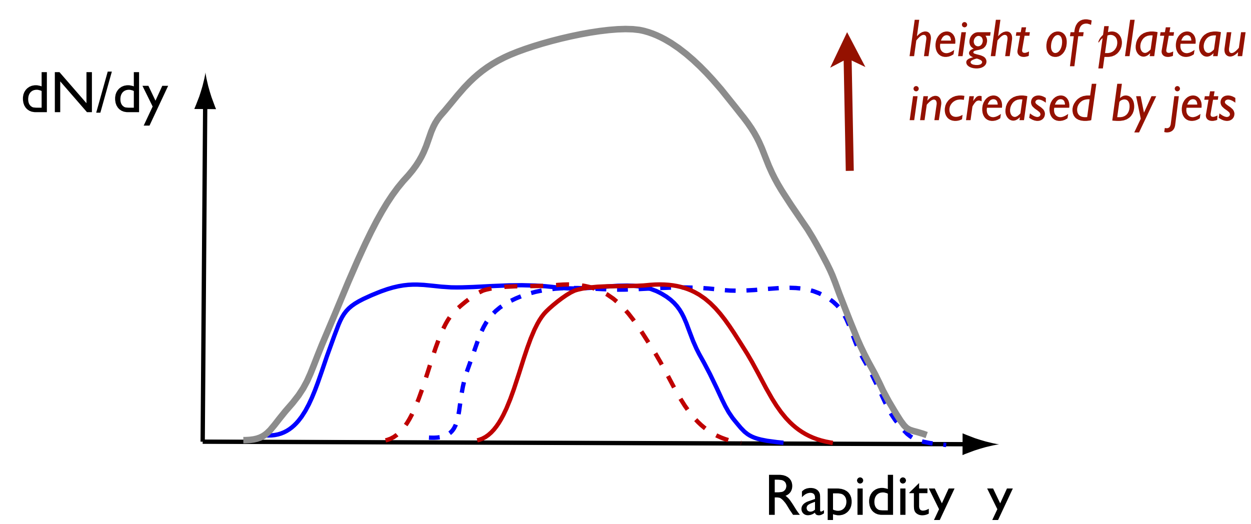

Interaction of two (soft) parton pairs

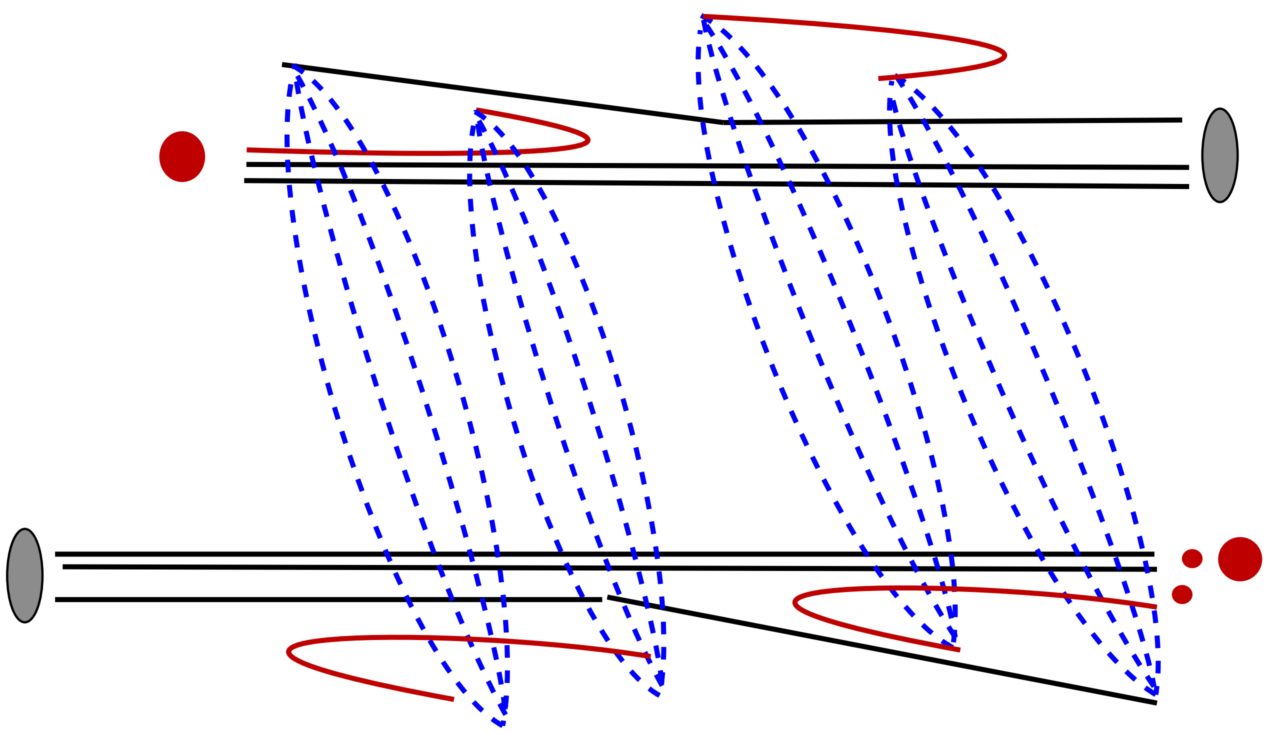

Two soft interactions

Generic diagram of interaction of two parton pairs

- gluon exchange between each pair produces two strings
- sea quarks needed for string ends (different combinations possible)
- each string fragments into hadrons with small transverse momenta

Comparison with collider data

Note: one cut pomeron means
one soft or hard interaction

Charged particle multiplicity distribution at 200 GeV cms.

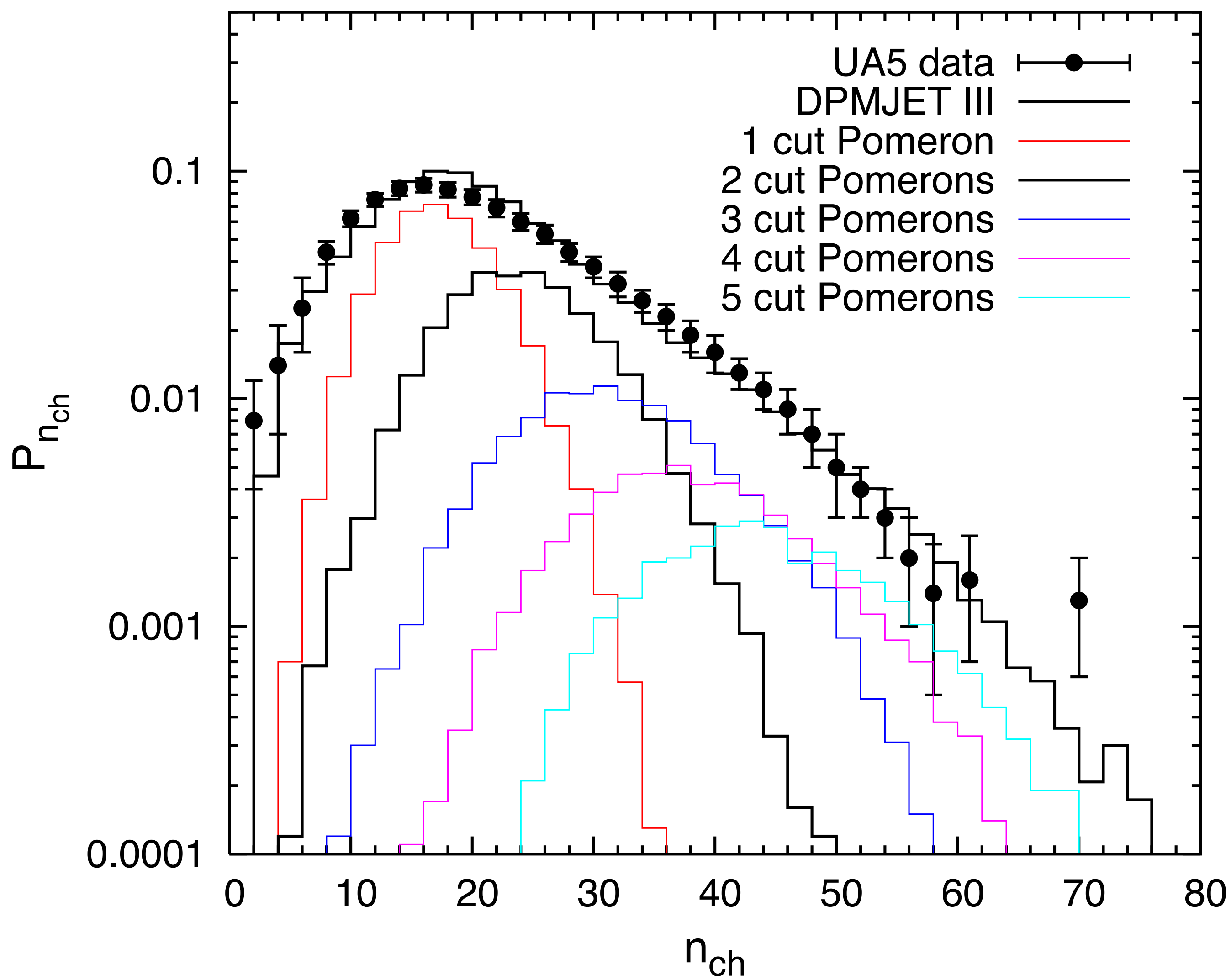

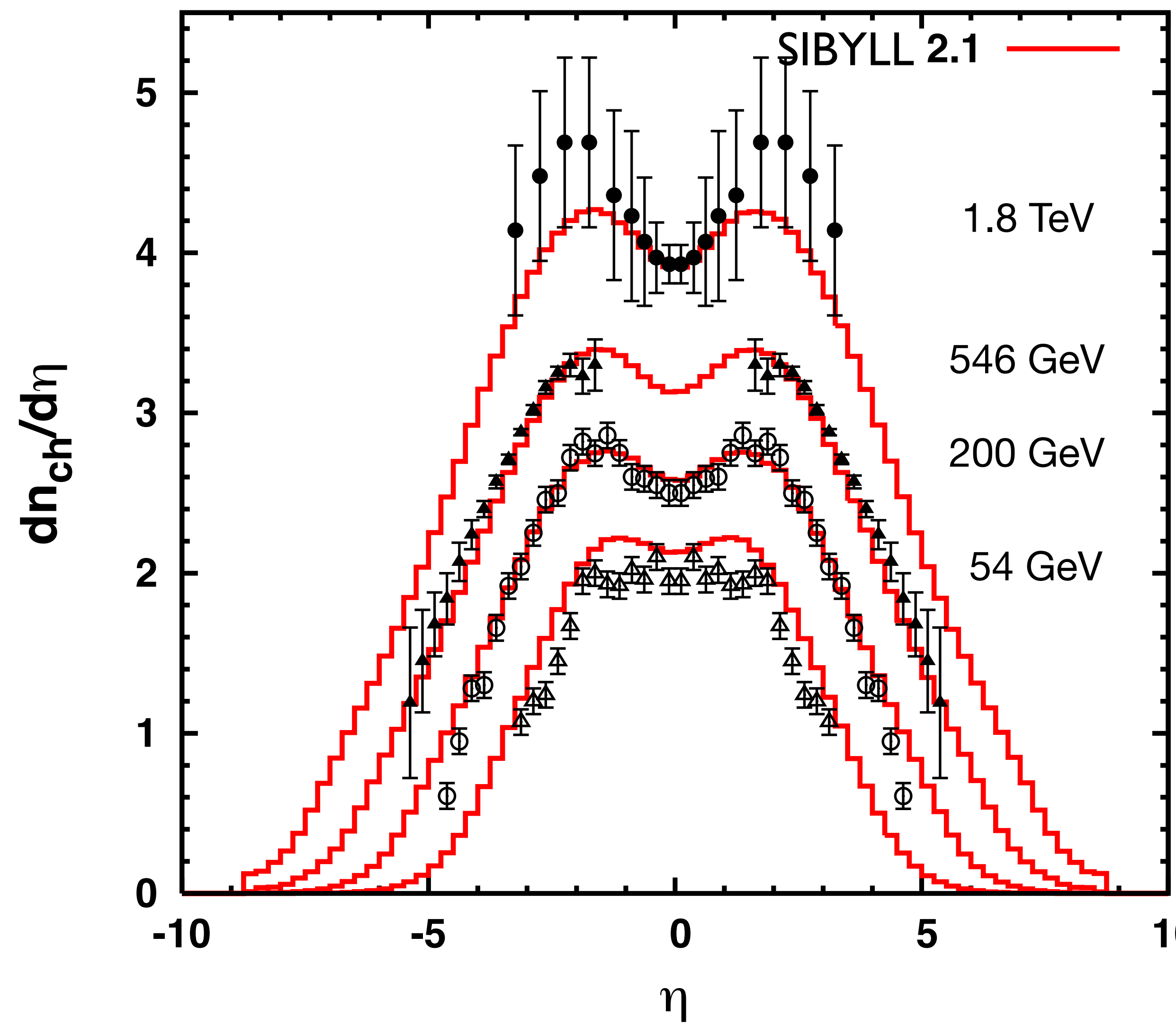

Charged particle pseudorapidity distributions

Status of Feynman scaling

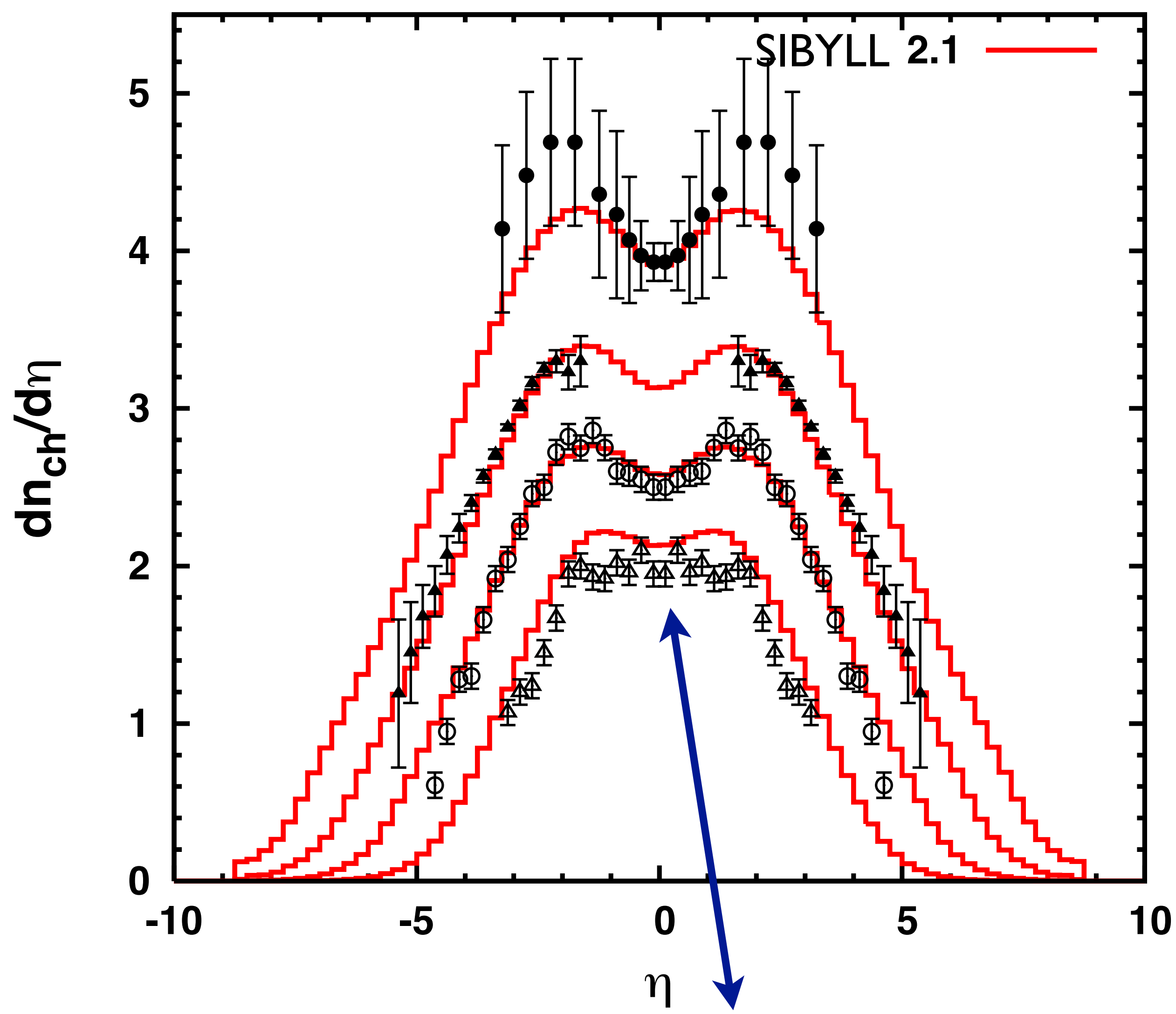

Feynman scaling violated for small $|x_F|$

$$\frac{dN}{dy\, d^2 p_\perp} \approx \frac{dN}{dy}\, g(p_\perp^2)$$

Feynman scaling

$$2E\frac{dN}{d^3p} = \frac{dN}{dy\, d^2 p_\perp} \longrightarrow f(x_F, p_\perp)$$

Feynman scaling might approximately hold in forward direction

X_F spectra : 900GeV data vs. 7TeV data

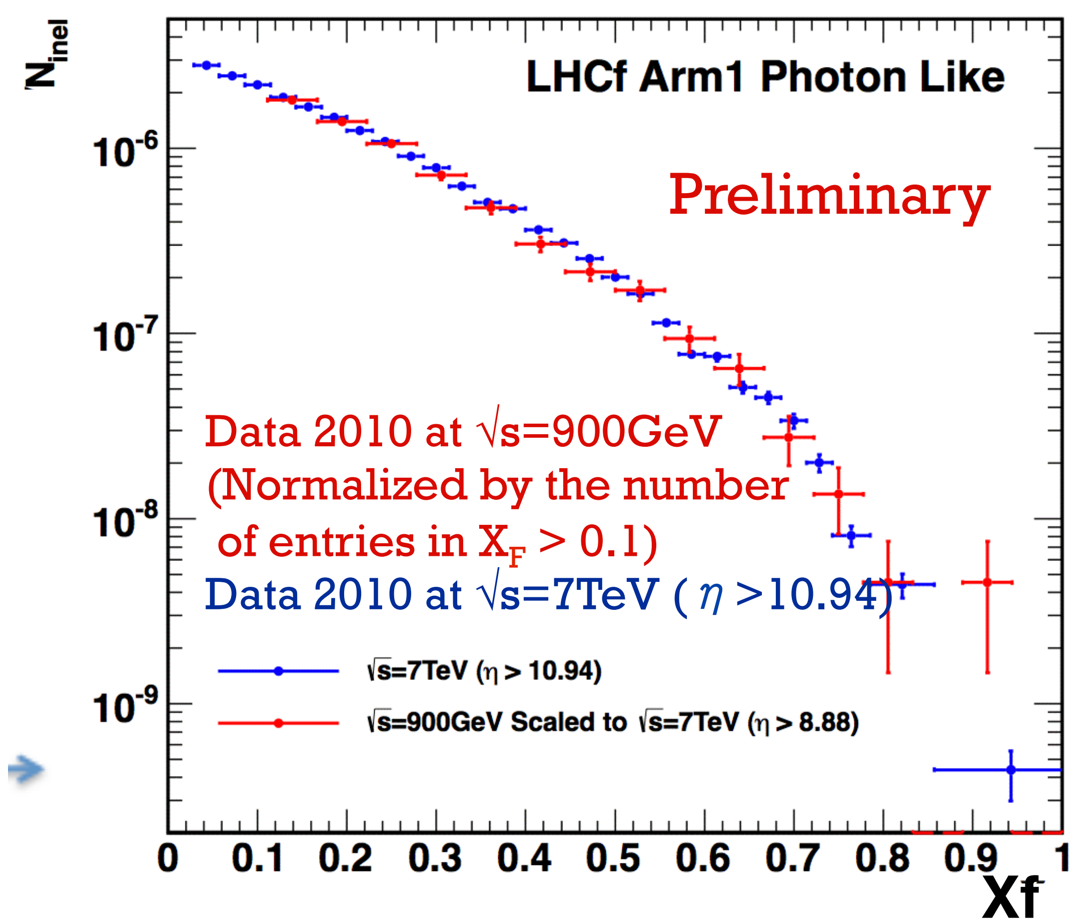

Problem: high parton densities

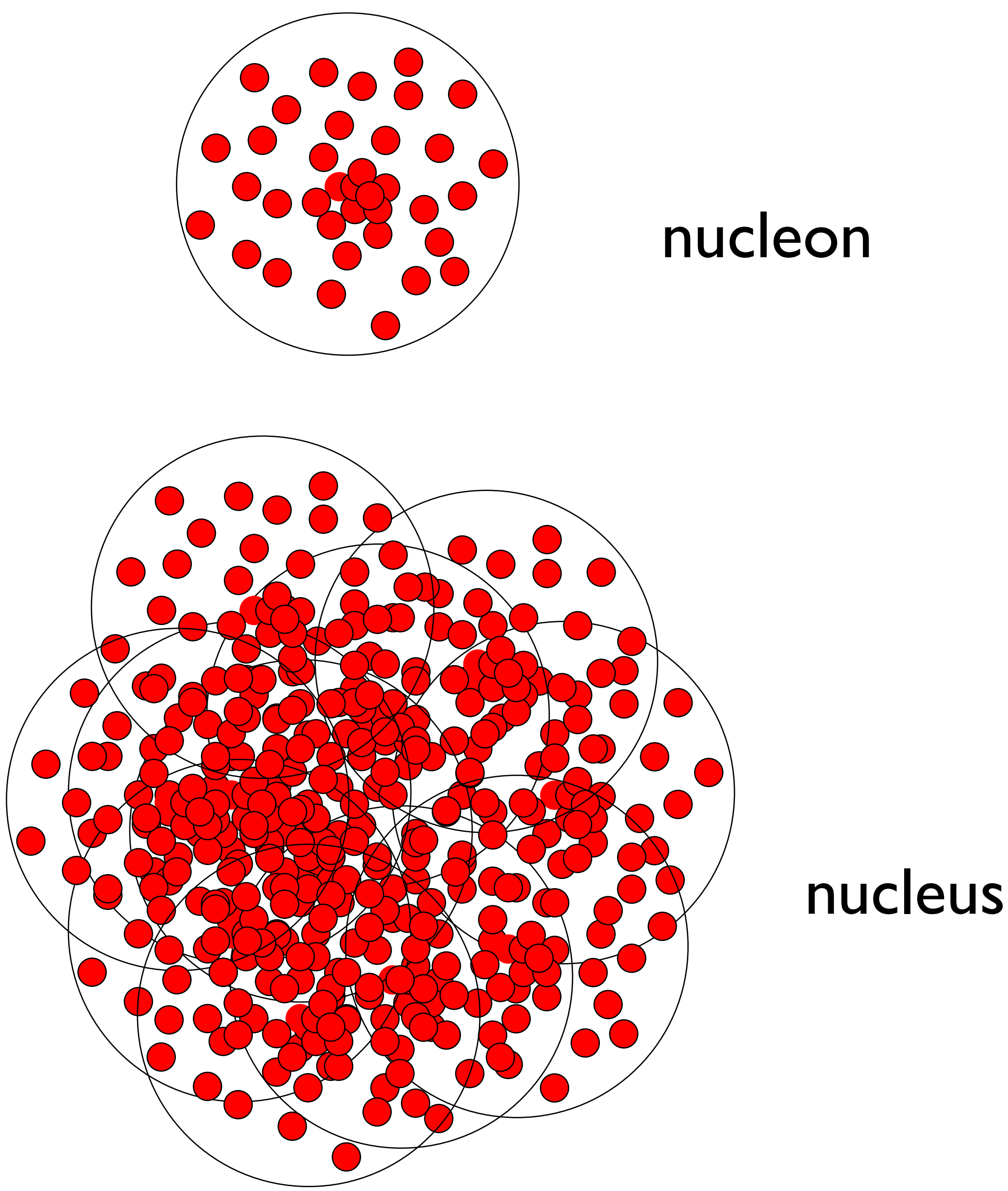

Non-linear effects / Saturation:

- parton wave functions overlap
- number of partons does not increase anymore at low x
- extrapolation to very high energy unclear

Simple geometric criterion

$$\pi R_0^2 \simeq \frac{\alpha_s(Q_s^2)}{Q_s^2} \cdot xg(x, Q_s^2)$$

size of proton

Size of one gluon

number of gluons

Comparison of high energy interaction models

DPMJET II.5 and III *(Fedynitch, Ranft / Roesler, RE, Ranft, Bopp)*	• universal model • saturation for hard partons via geometry criterion • HERA parton densities
EPOS *(Pierog, Werner et al.)*	• universal model • saturation by RHIC data parametriztions • custom-developed parton densities
QGSJET 01 *(Kalmykov, Ostapchenko)*	• no saturation corrections • old pre-HERA parton densities • replaced by QGSJET II
QGSJET II.0x *(Ostapchenko)*	• saturation correction for soft partons via pomeron-resummation • custom-developed parton densities
SIBYLL 2.1, 2.3 *(Riehn, Engel, RE, Fletcher, Gaisser, Lipari, Stanev)*	• saturation for hard partons via geometry criterion • HERA parton densities

High parton densities: modification of minijet threshold

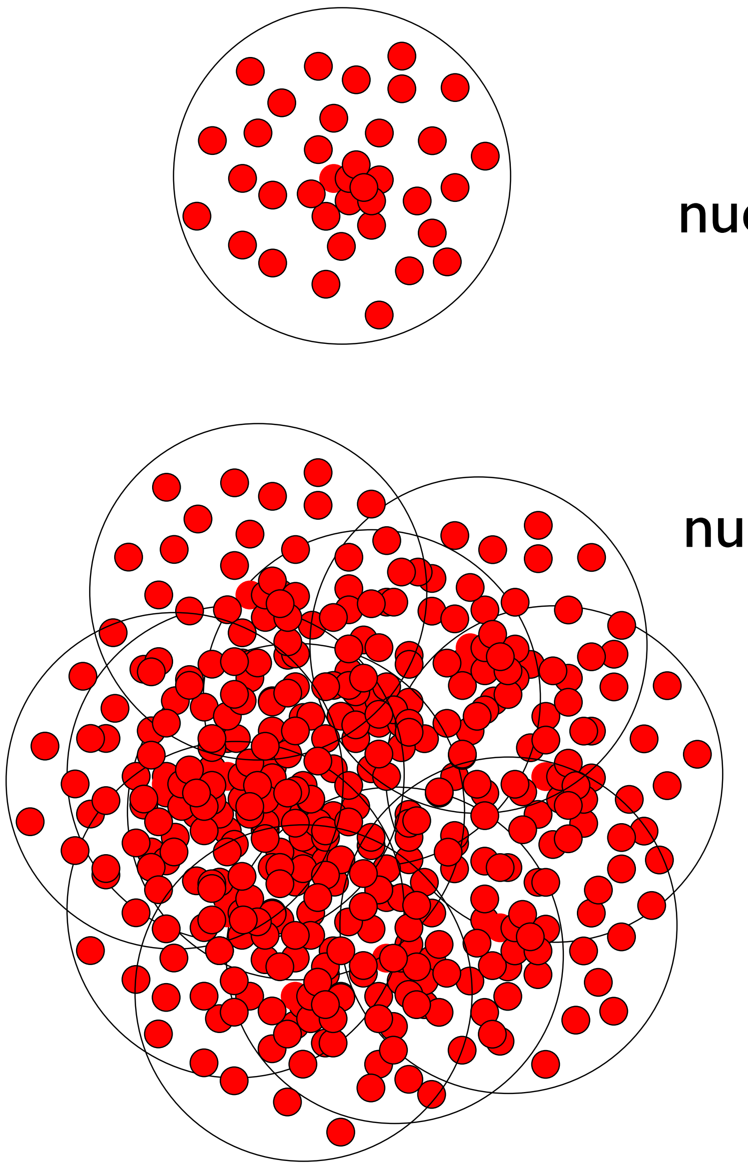

SIBYLL: simple geometric criterion

$$\pi R_0^2 \simeq \frac{\alpha_s(Q_s^2)}{Q_s^2} \cdot xg(x, Q_s^2)$$

$$xg(x, Q^2) \sim \exp\left[\frac{48}{11-\frac{2}{3}n_f} \ln \frac{\ln \frac{Q^2}{\Lambda^2}}{\ln \frac{Q_0^2}{\Lambda^2}} \ln \frac{1}{x}\right]^{\frac{1}{2}}$$

No dependence on impact parameter !

SIBYLL: $$p_\perp(s) = p_\perp^0 + 0.065\mathrm{GeV} \exp\left\{0.9\sqrt{\ln s}\right\}$$

DPMJET: $$p_\perp(s) = p_\perp^0 + 0.12\mathrm{GeV} \left(\log_{10} \frac{\sqrt{s}}{50\mathrm{GeV}}\right)^3$$

QGSJET II: high parton density effects

Re-summation of enhanced pomeron graphs

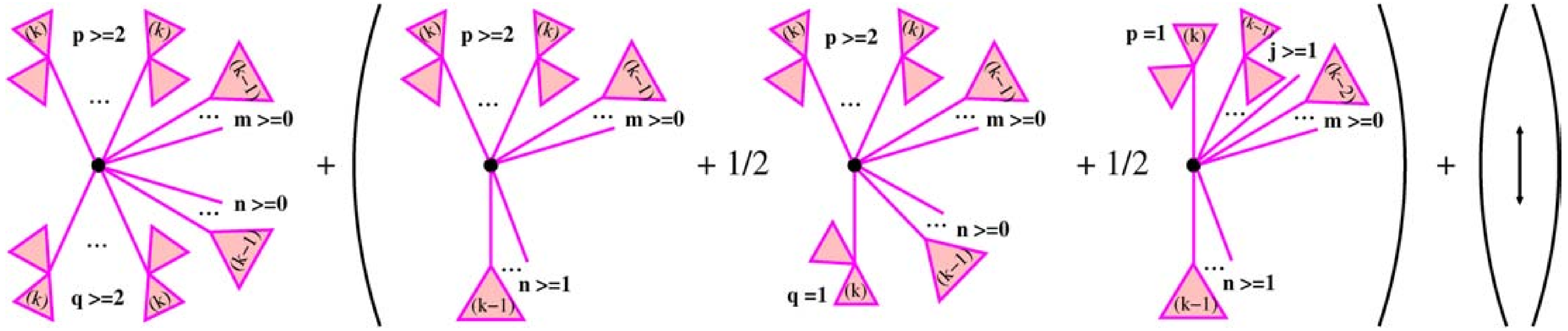

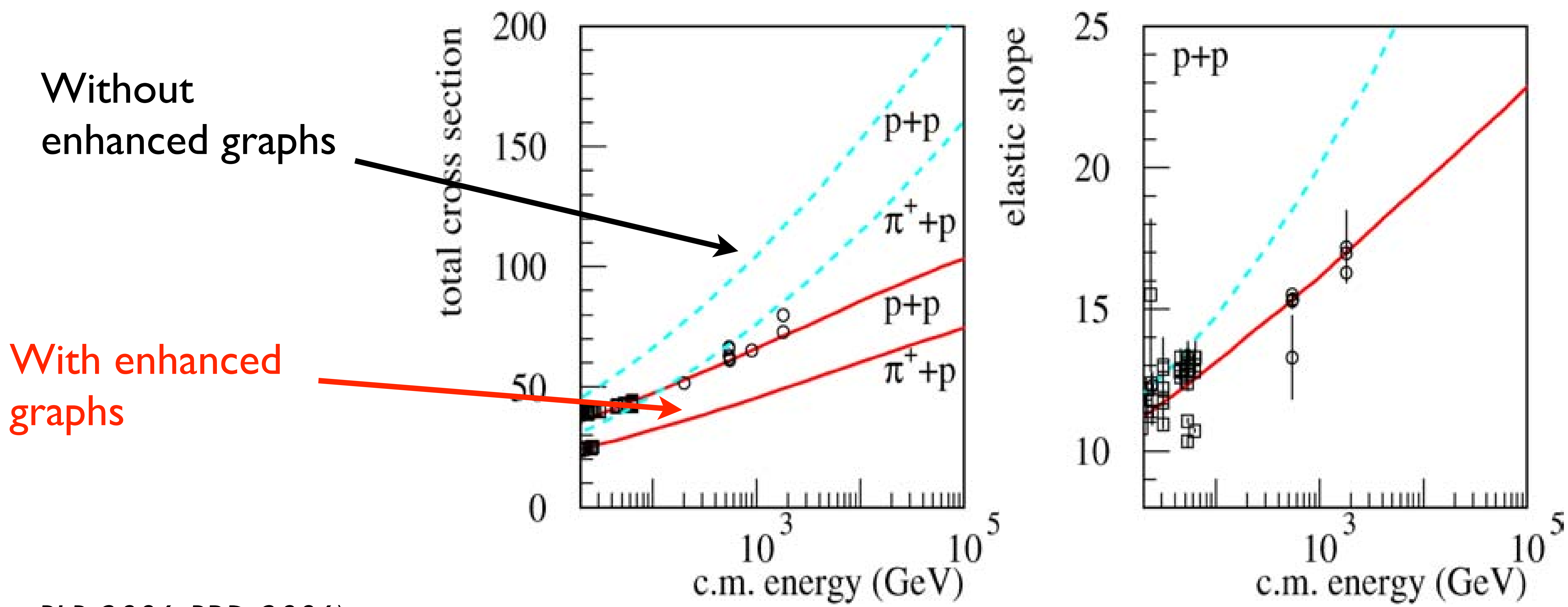

(Ostapchenko, PLB 2006, PRD 2006)

EPOS – high parton density effects (i)

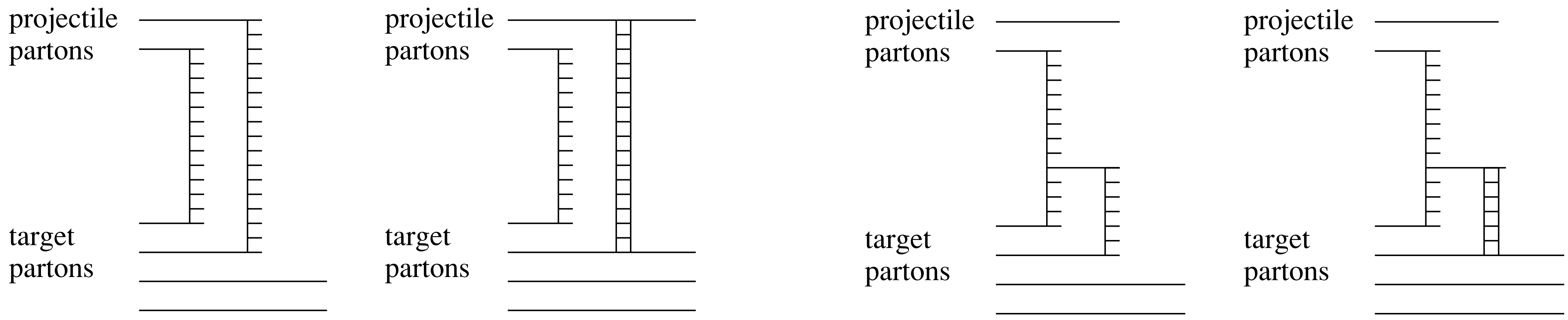

No effective coupling

$$A_{\mathrm{pom}} \sim (x_1 x_2)^{\beta}$$

With effective coupling

$$A_{\mathrm{pom}} \sim x_1^{\beta} x_2^{\beta-\varepsilon}$$

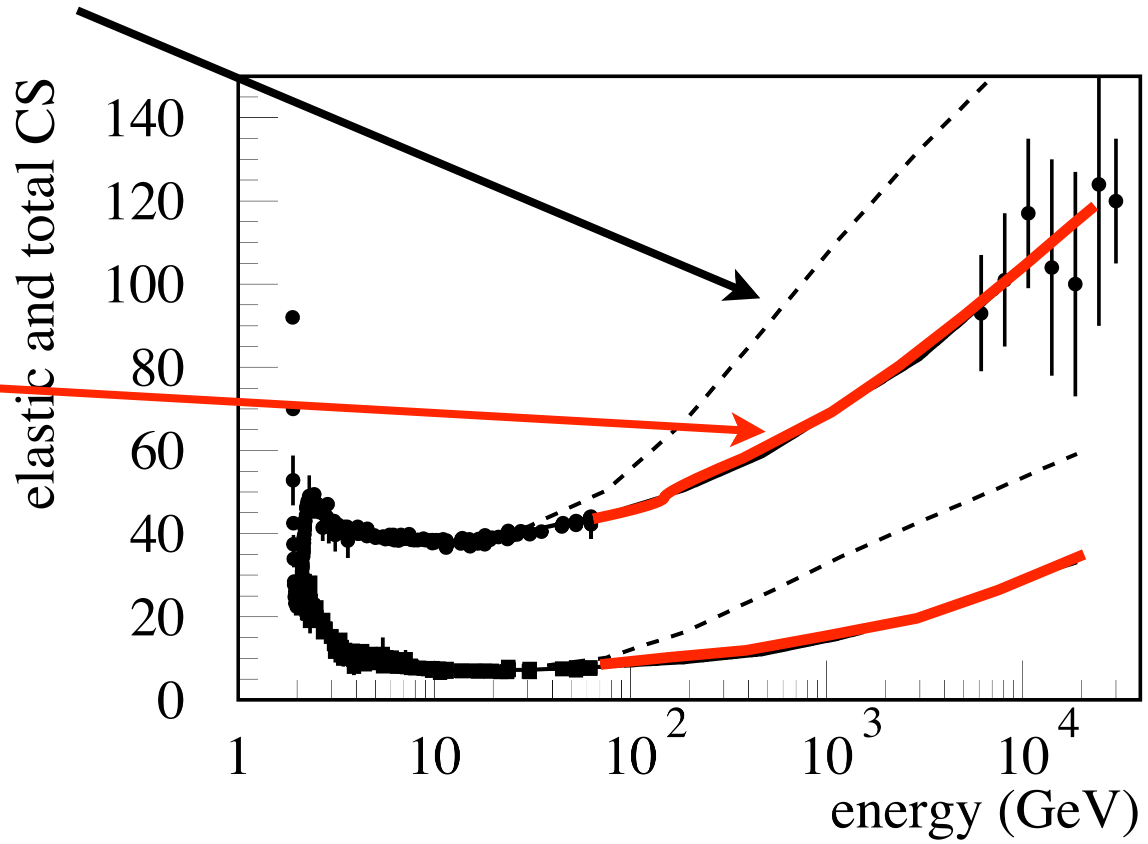

Parametrization

$$\varepsilon_S = a_S\, \beta_S Z,$$
$$\varepsilon_H = a_H\, \beta_H Z,$$

(Werner et al., PRC 2006)

EPOS – high parton density effects (ii)

(Werner et al., PRC 2006)

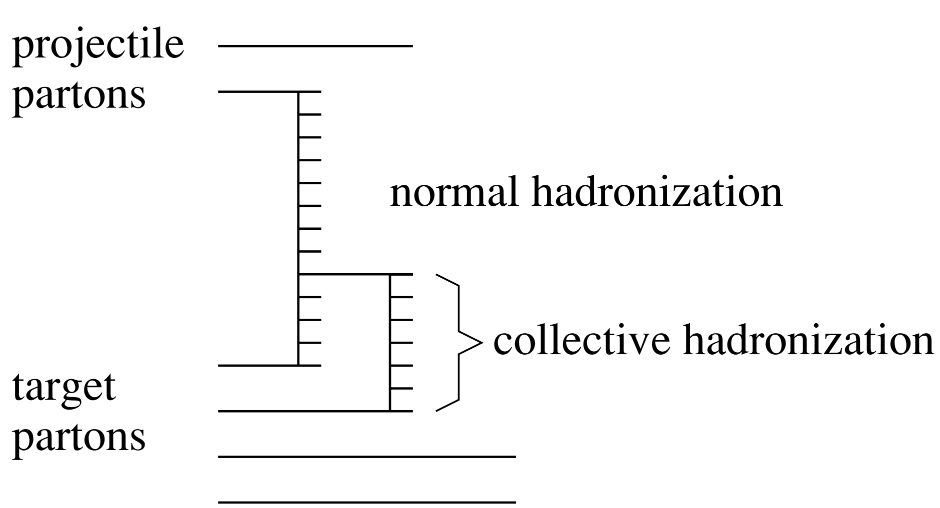

Coefficient	Corresponding variable	Value
s_M	Minimum squared screening energy	$(25\ \mathrm{GeV})^2$
w_M	Defines minimum for z_0'	6.000
w_Z	Global Z coefficient	0.080
w_B	Impact parameter width coefficient	1.160
a_S	Soft screening exponent	2.000
a_H	Hard screening exponent	1.000
a_T	Transverse momentum transport	0.025
a_B	Break parameter	0.070
a_D	Diquark break probability	0.110
a_S	Strange break probability	0.140
a_P	Average break transverse momentum	0.150

Uncertainty in energy extrapolation !

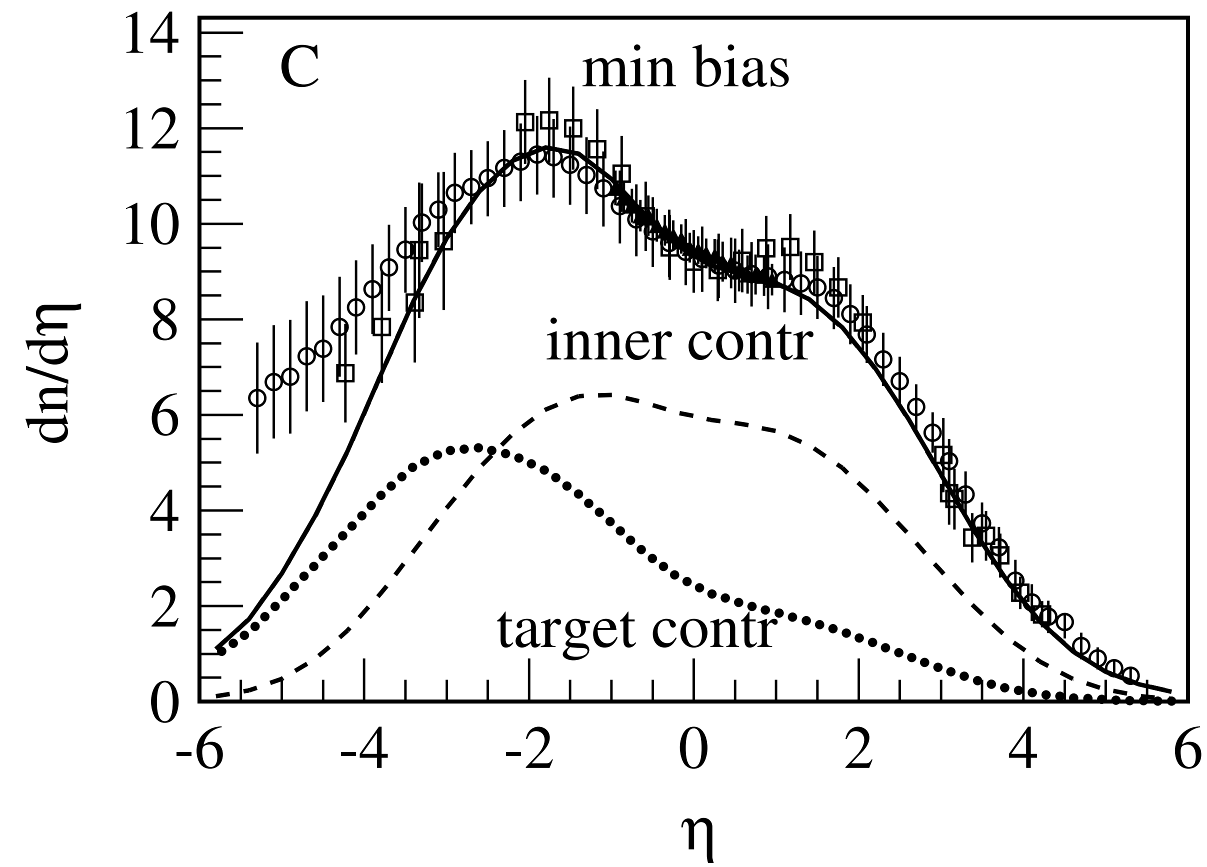

$$Z_T(i,\,j) = z_0\,\exp\!\left(-\,b_{ij}^2/2b_0^2\right) + \sum_{\substack{\text{target nucleons}\\ j'\neq j}} z_0'\,\exp\!\left(-\,b_{ij'}^2/2b_0^2\right),$$

$$b_0 = w_B\,\sqrt{\sigma_{\mathrm{inel}\,pp}/\pi}$$

$$z_0 = w_Z\,\log s/s_M,$$

$$z_0' = w_Z\,\sqrt{(\log s/s_M)^2 + w_M{}^2},$$

Different implementations of soft interactions

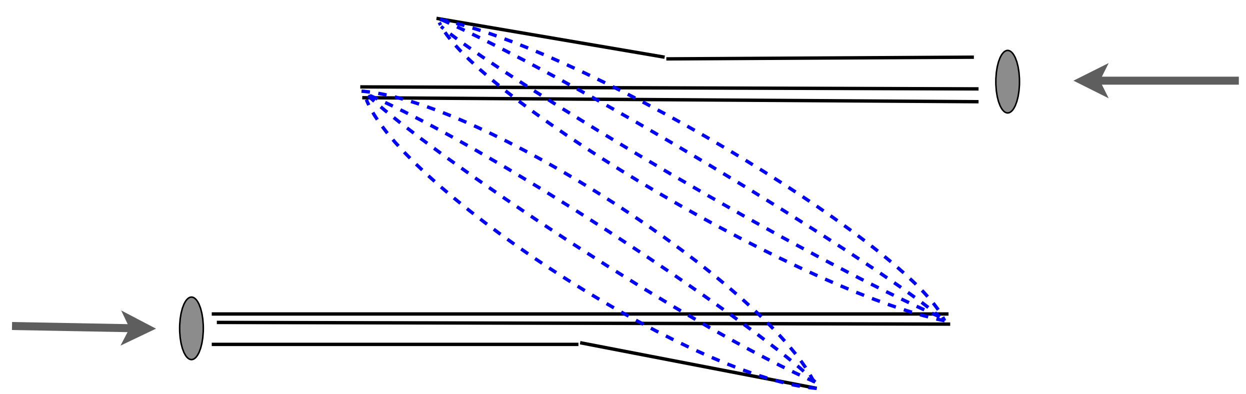

SIBYLL 2.1:
strings connected to valence quarks;
first fragmentation step with harder fragmentation function

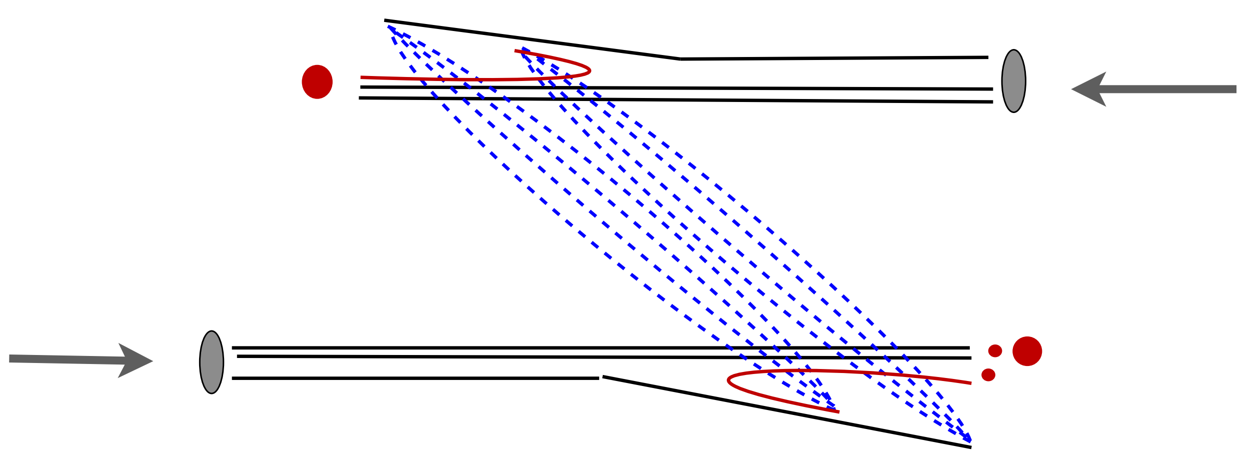

QGSJET & SIBYLL 2.3:
fixed probability of strings connected to valence quarks or sea quarks;
explicit construction of remnant hadron

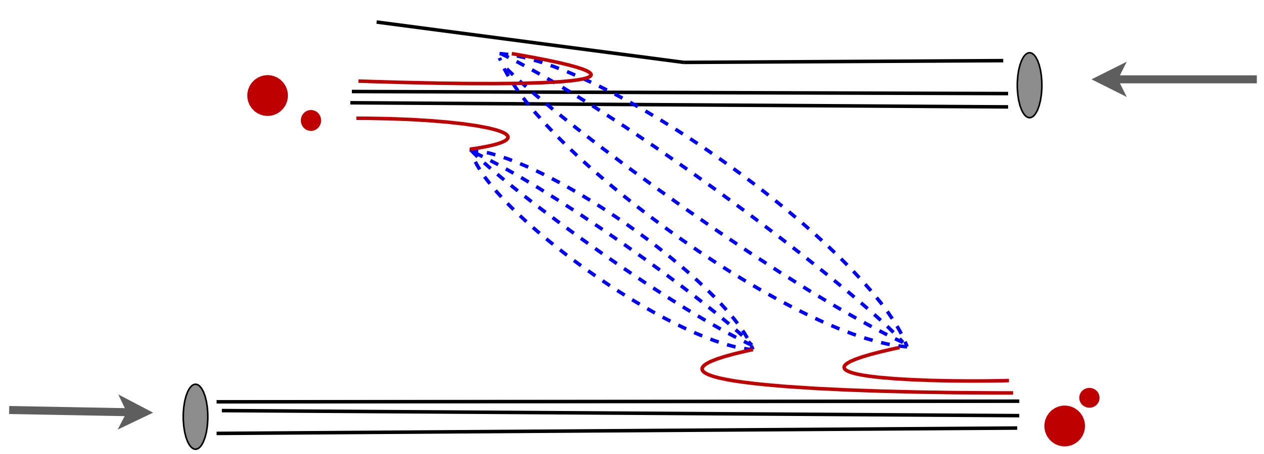

EPOS:
strings always connected to sea quarks;
bags of sea and valence quarks fragmented statistically

EPOS: remant vs. string contributions

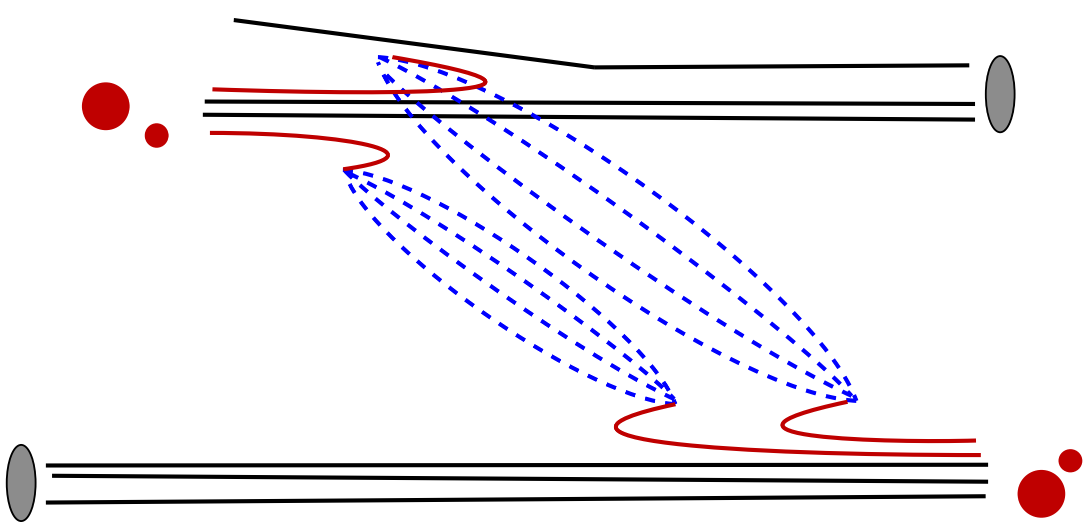

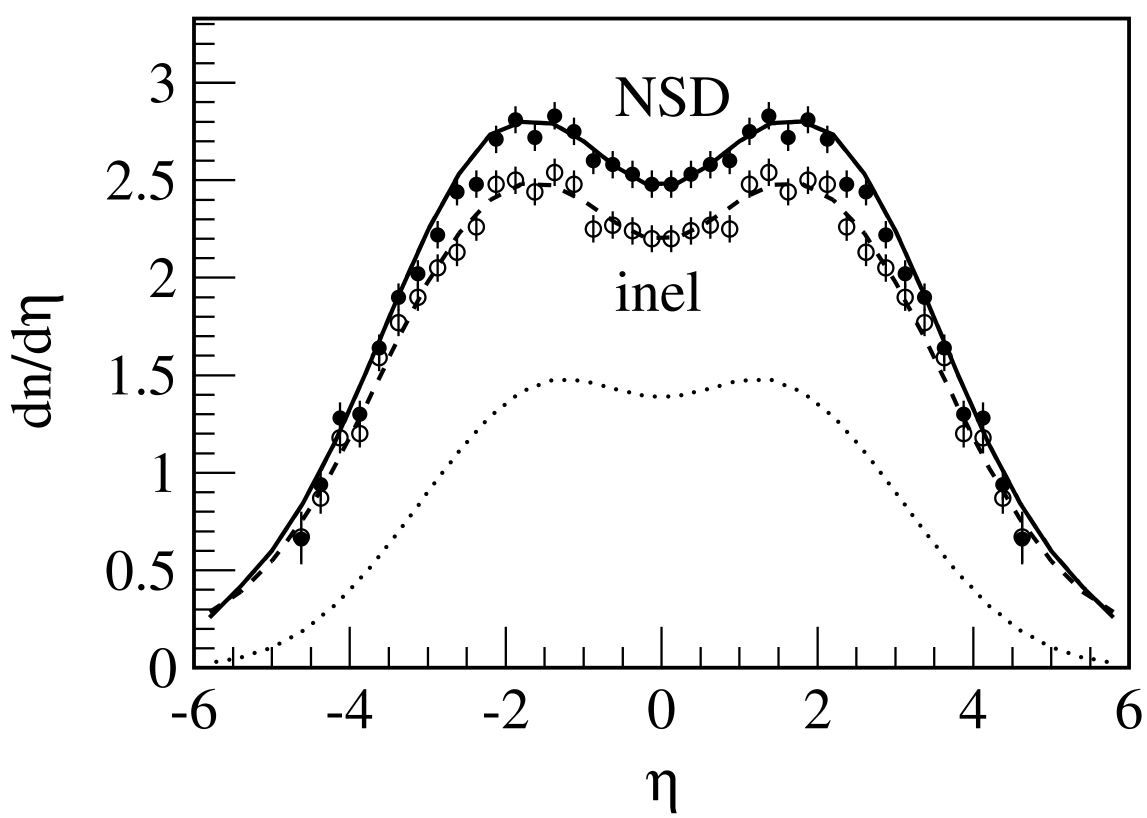

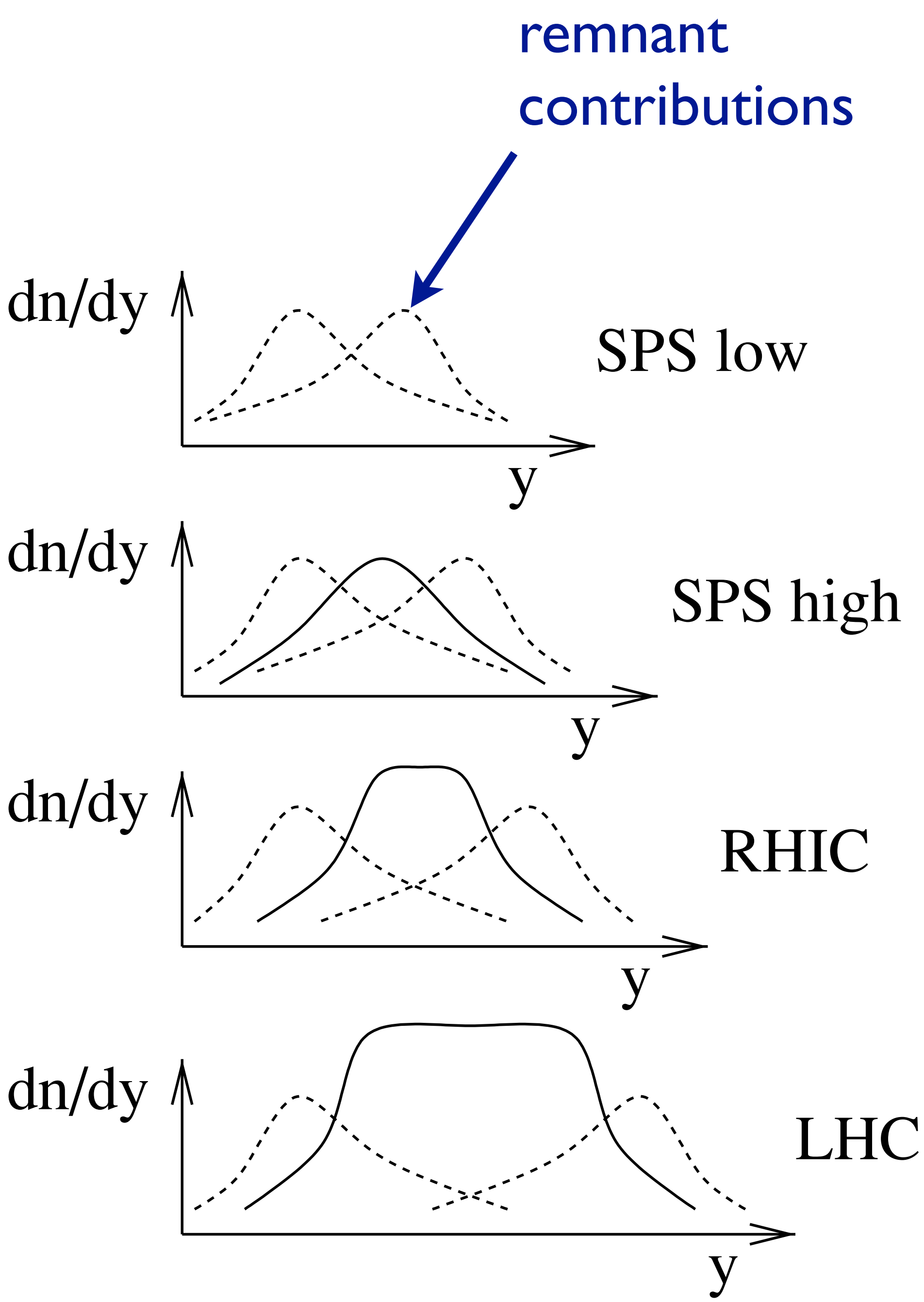

EPOS: change from remnant-dominated to string-dominated particle production

Different implementations of two-gluon scattering

SIBYLL

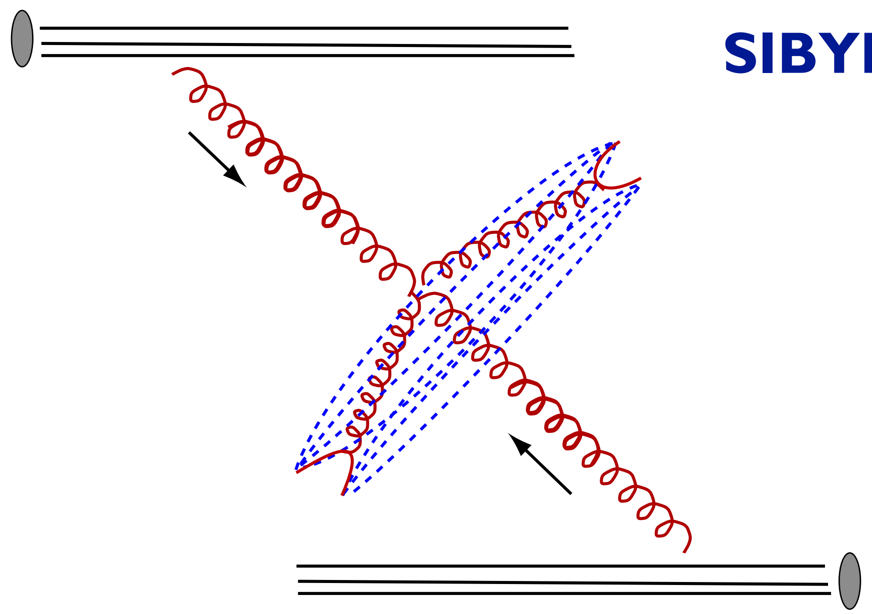

Kinematics etc. given by parton densities and perturbative QCD

Two strings stretched between quark pairs from gluon fragmentation

QGSJET

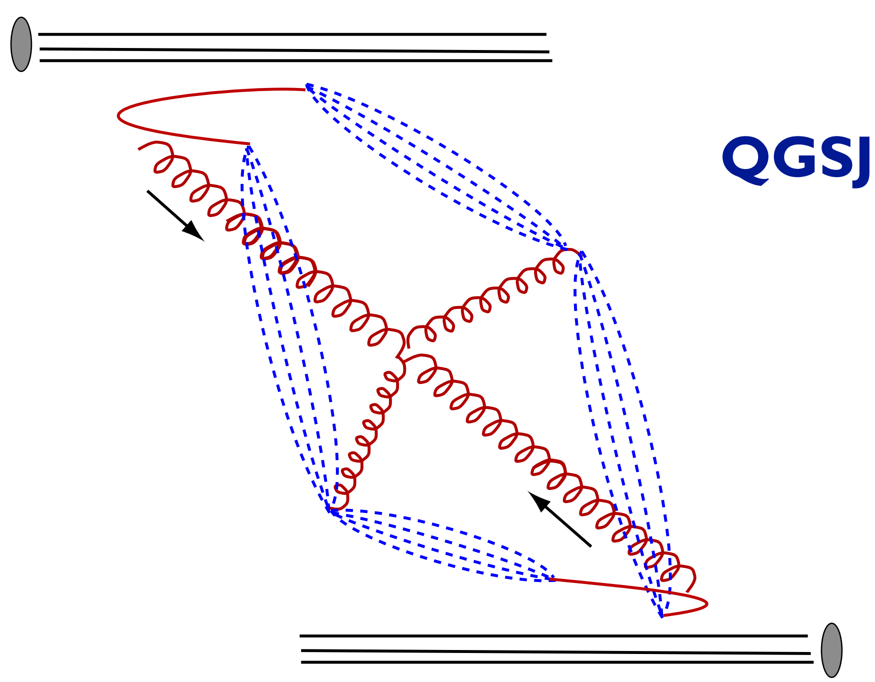

EPOS

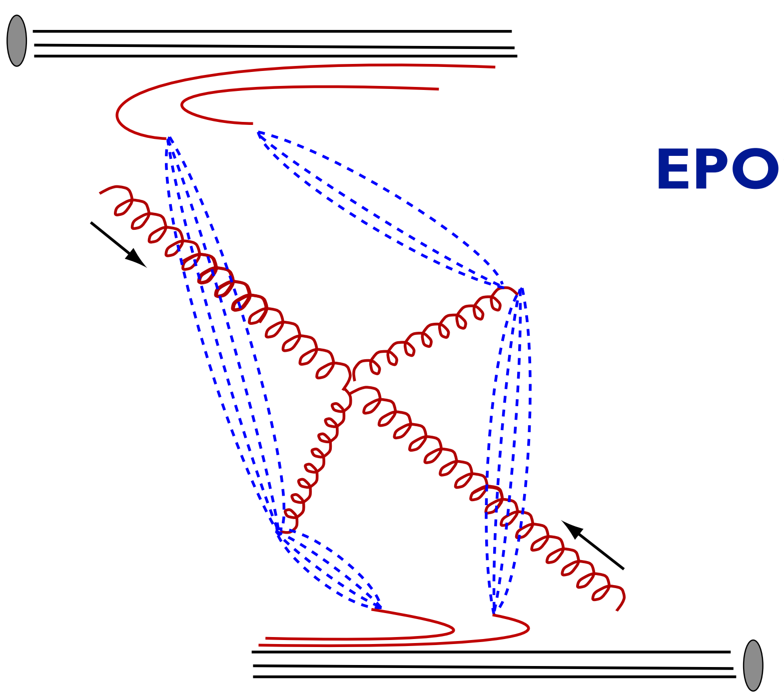

Charged particle distribution in pseudorapidity

Detailed LHC comparison

(D'Enterria et al., APP 35, 2011)

Protons: E_{lab} = 3 x 10^{16} eV

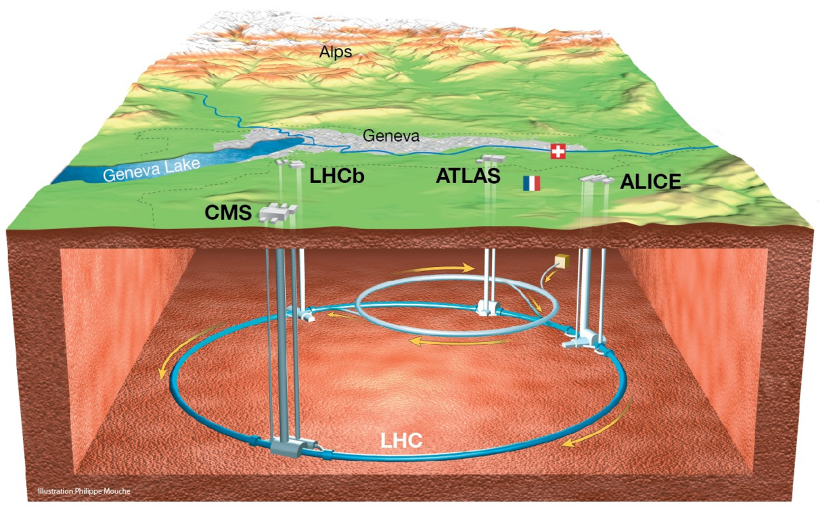

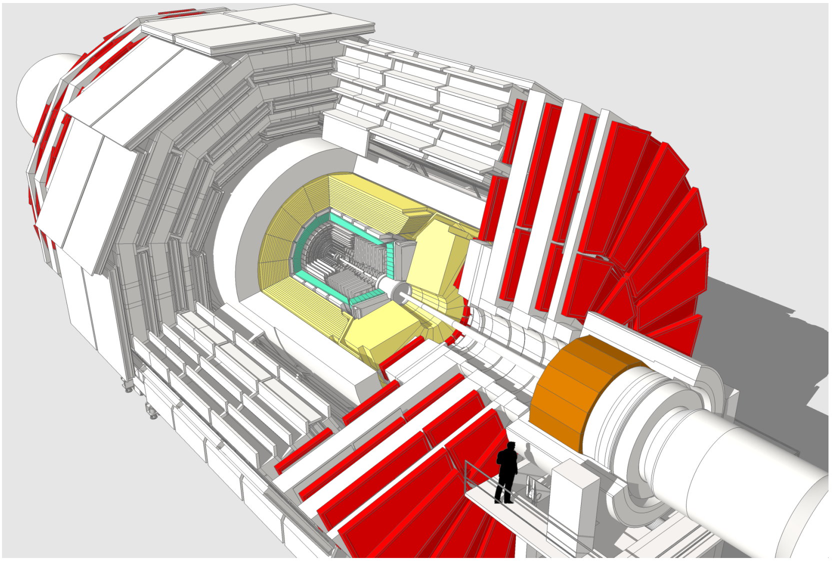

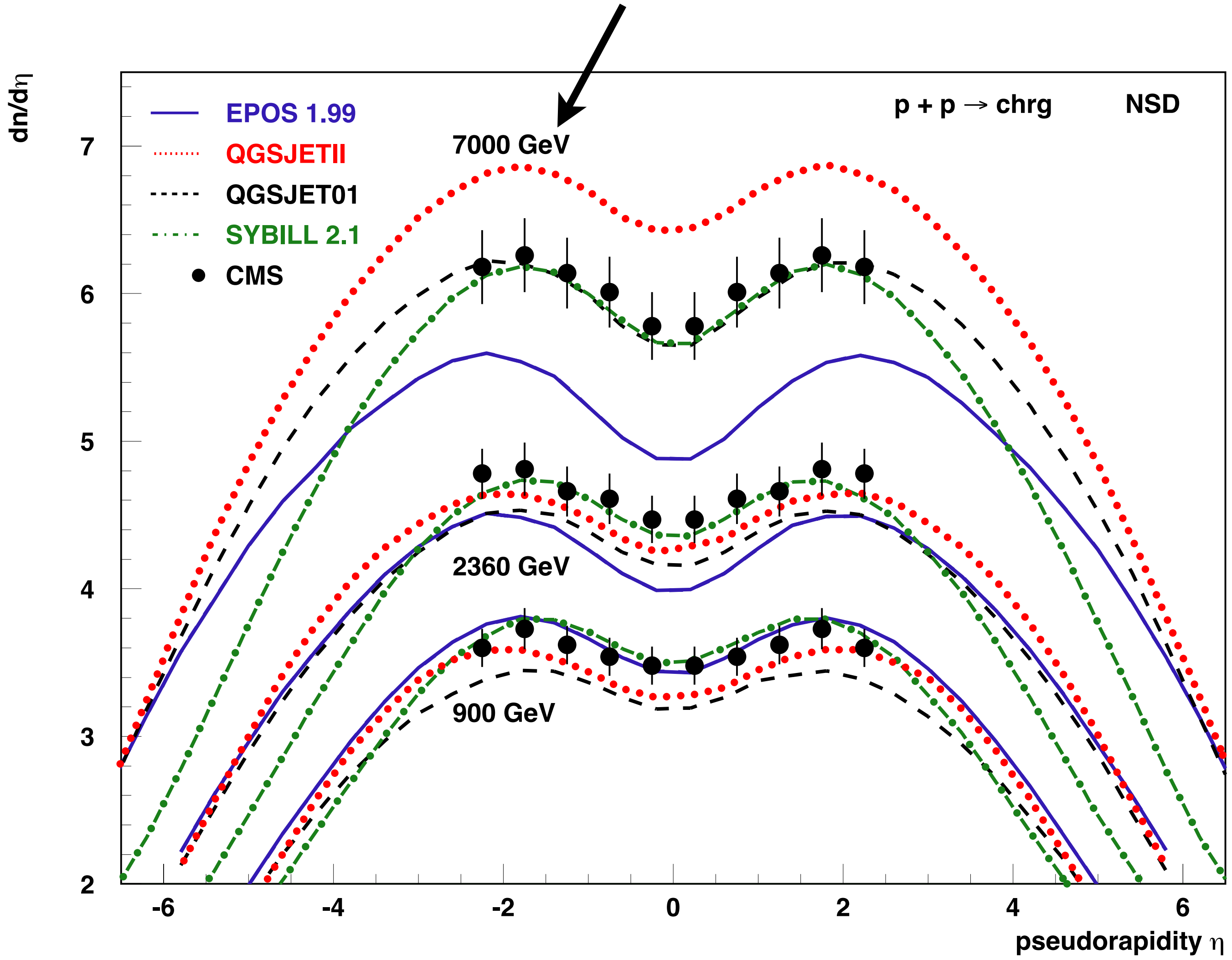

(data from all LHC experiments, CMS shown as example)

Models for air showers typically better in agreement with LHC data

Cross section measurements at LHC

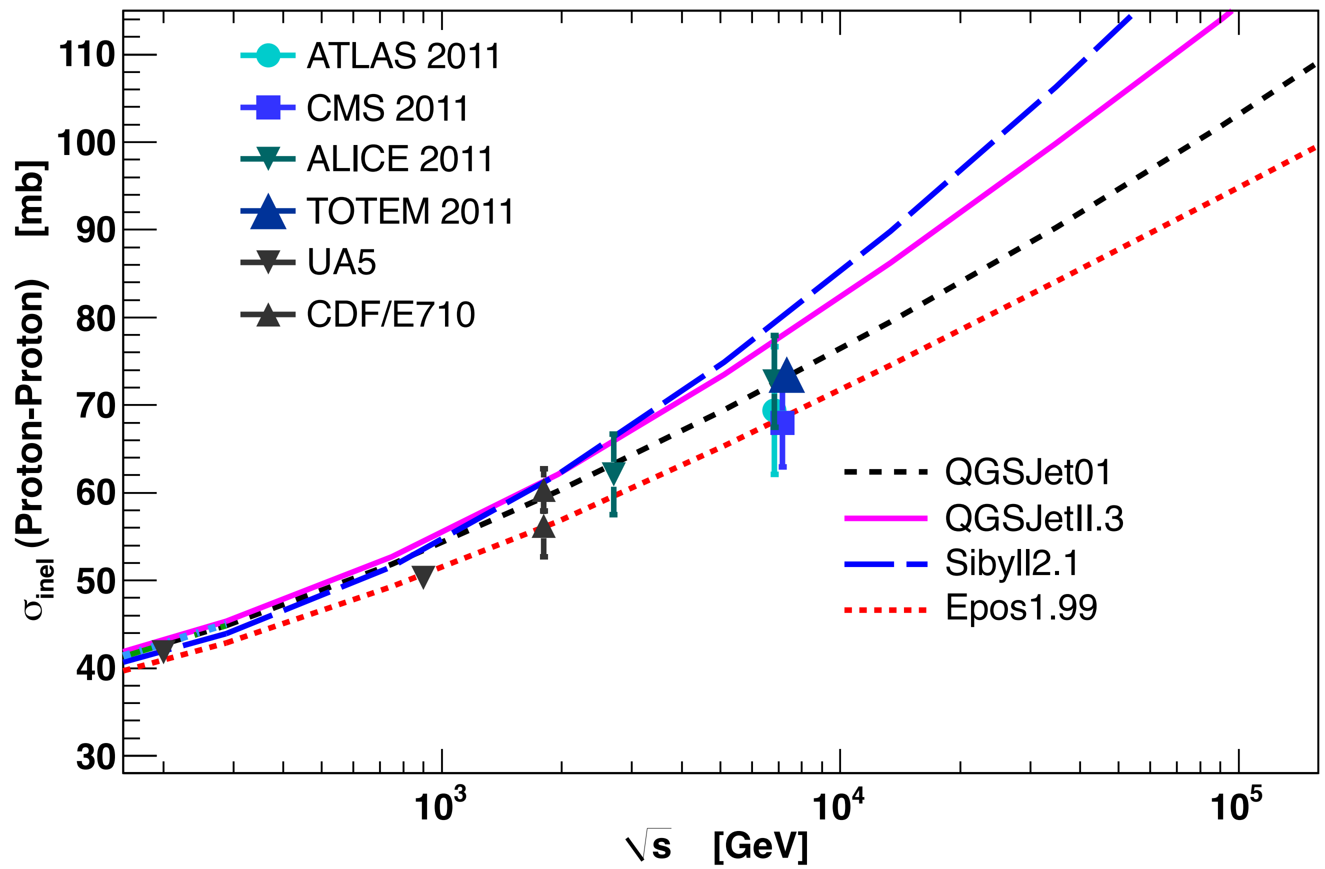

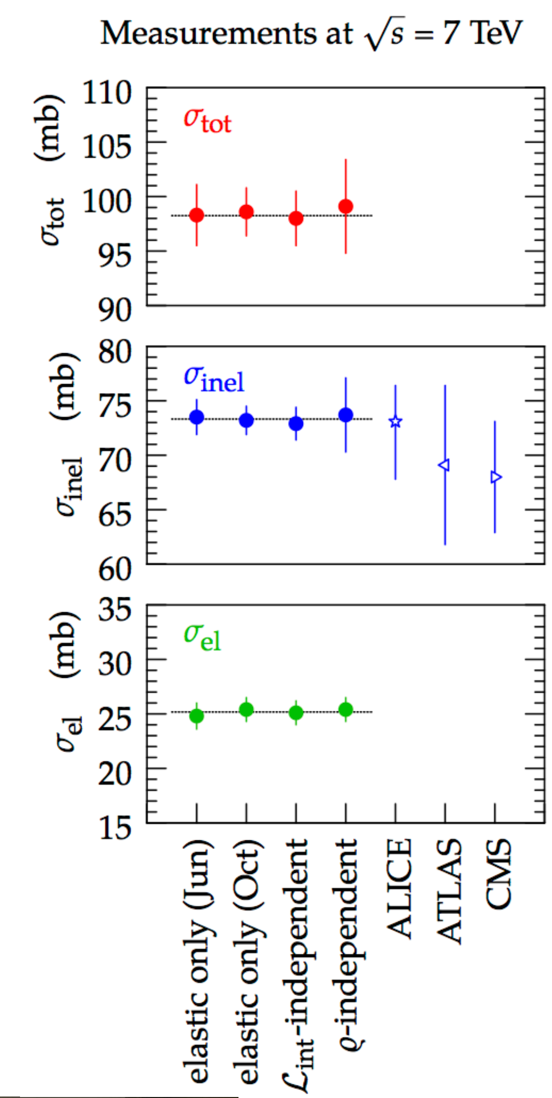

(Cafagna, ICRC 2015)

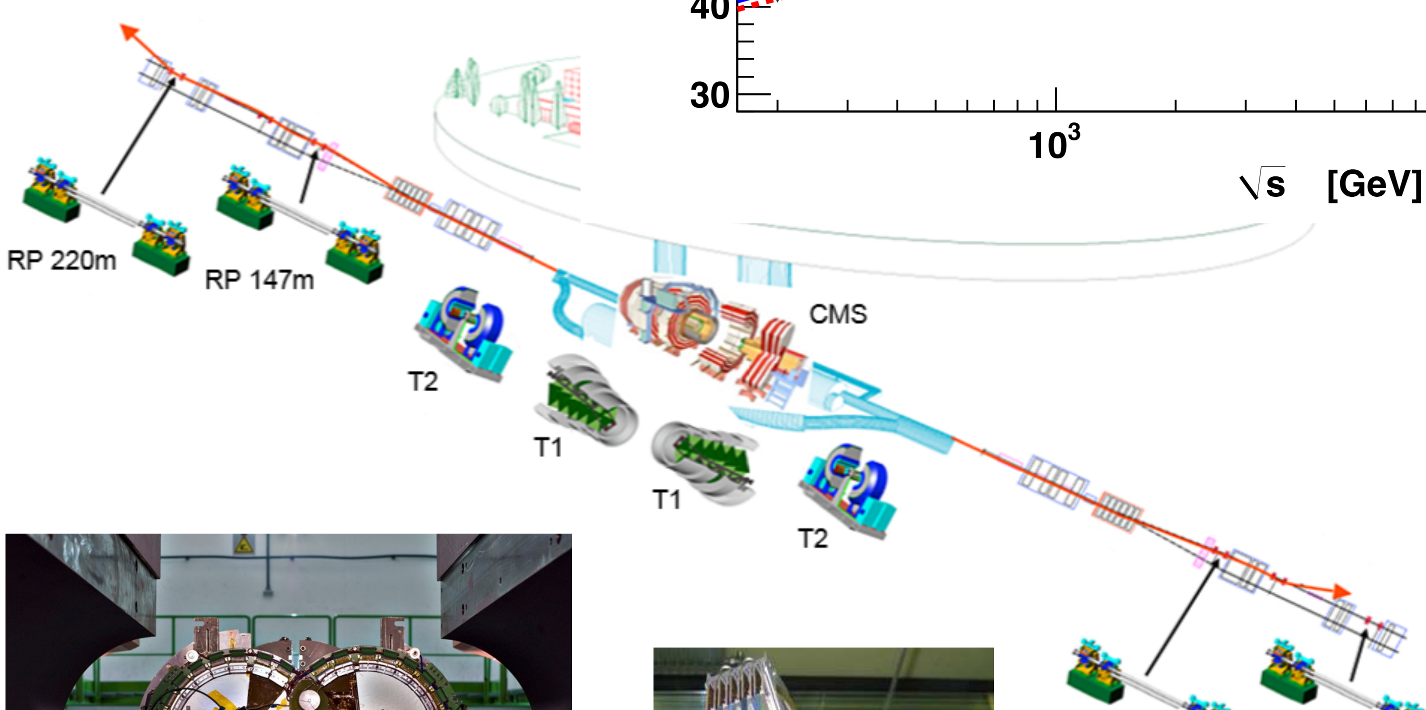

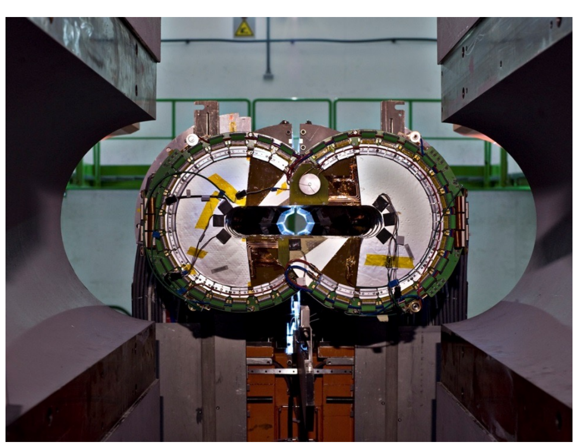

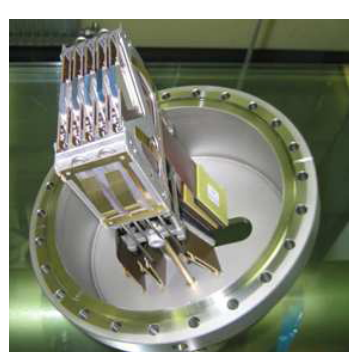

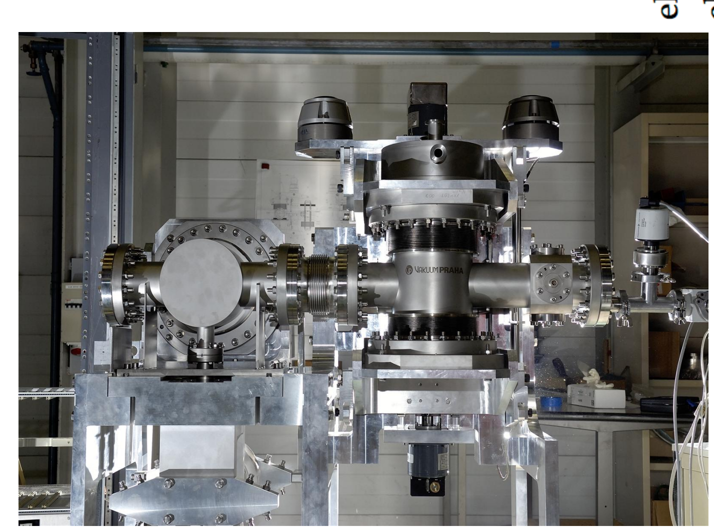

LHCf: very forward photon production at 7 TeV

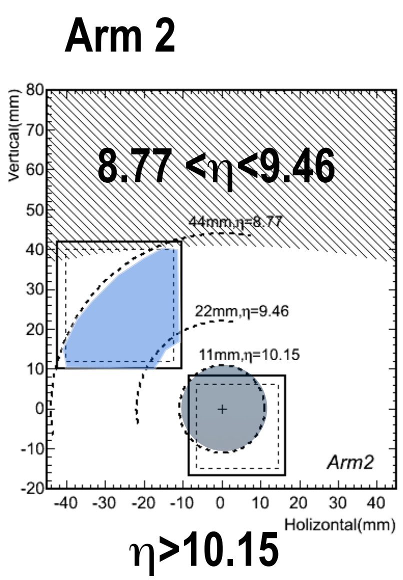

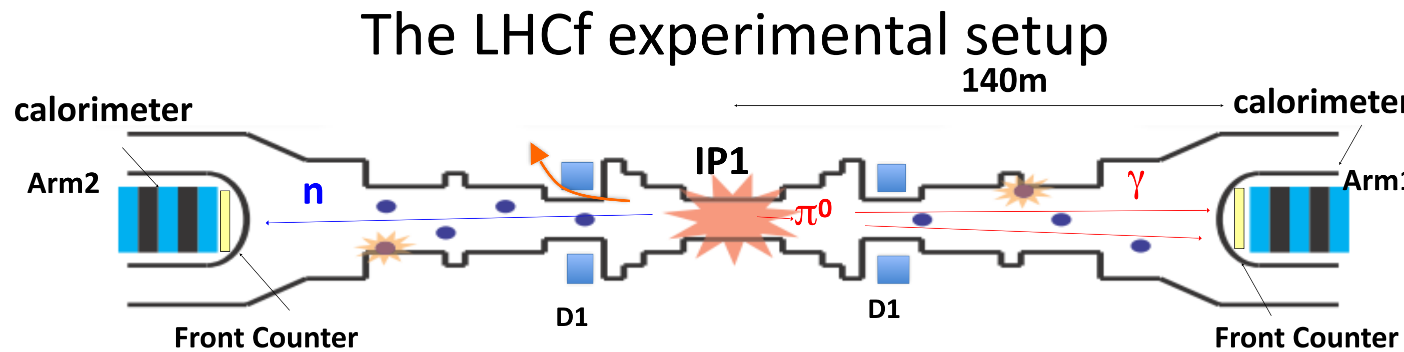

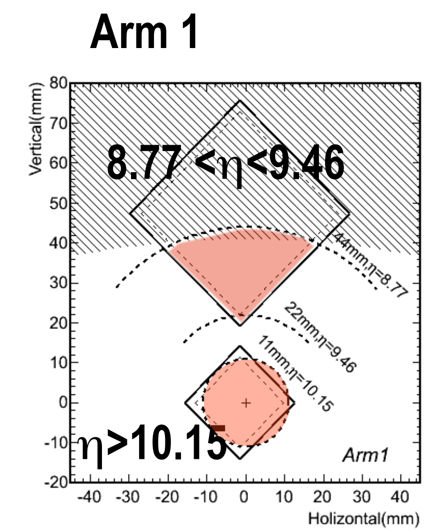

$$pp \to \gamma X$$

(LHCf Collab.)

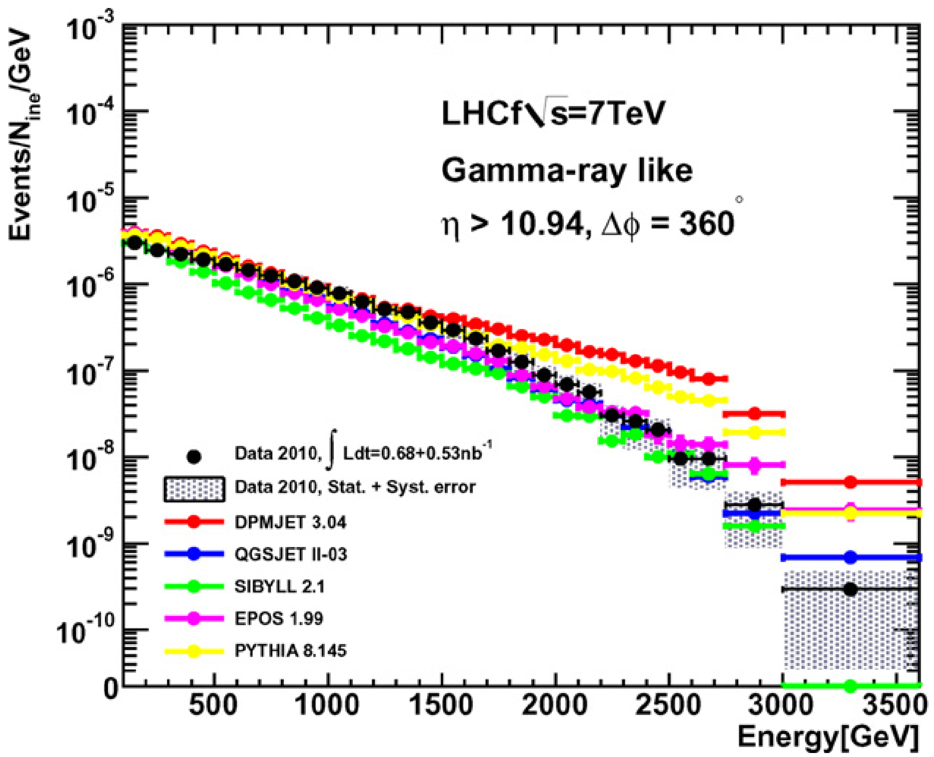

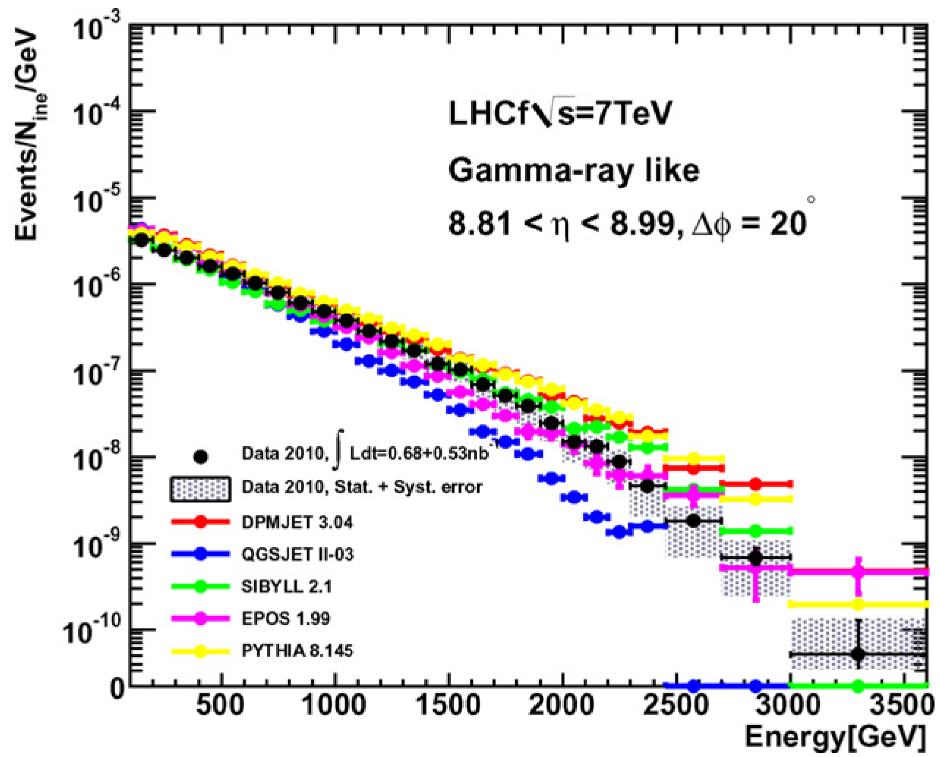

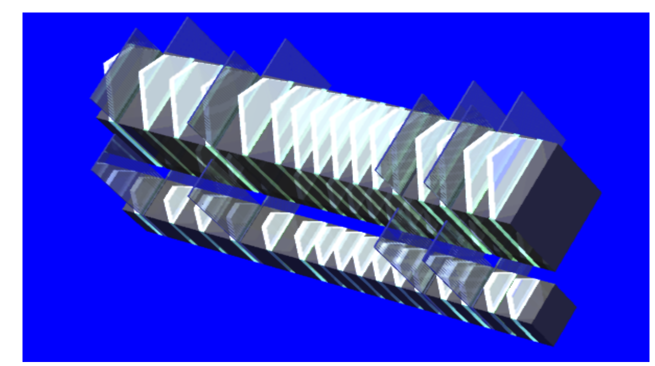

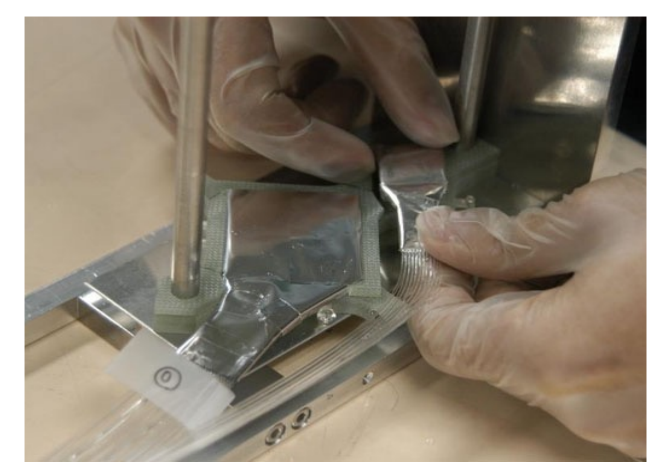

(Itow, ICRC 2015)

Combined CMS and TOTEM measurements

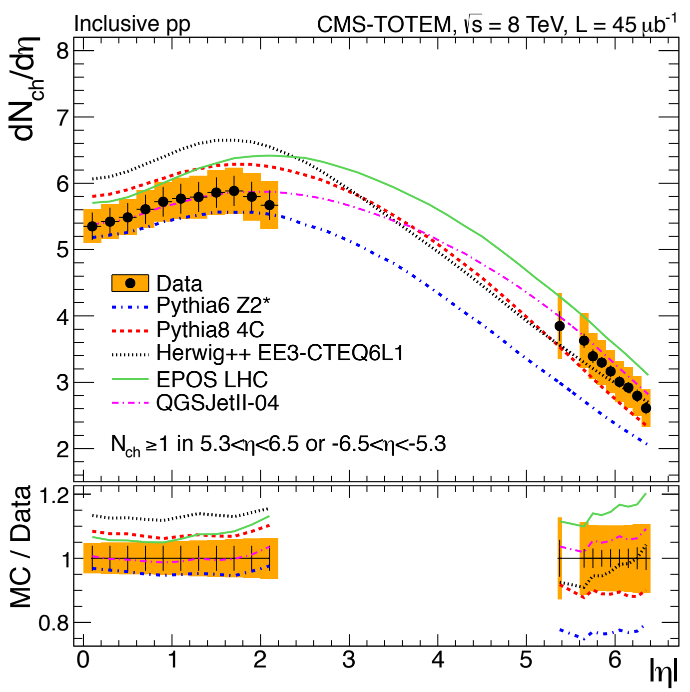

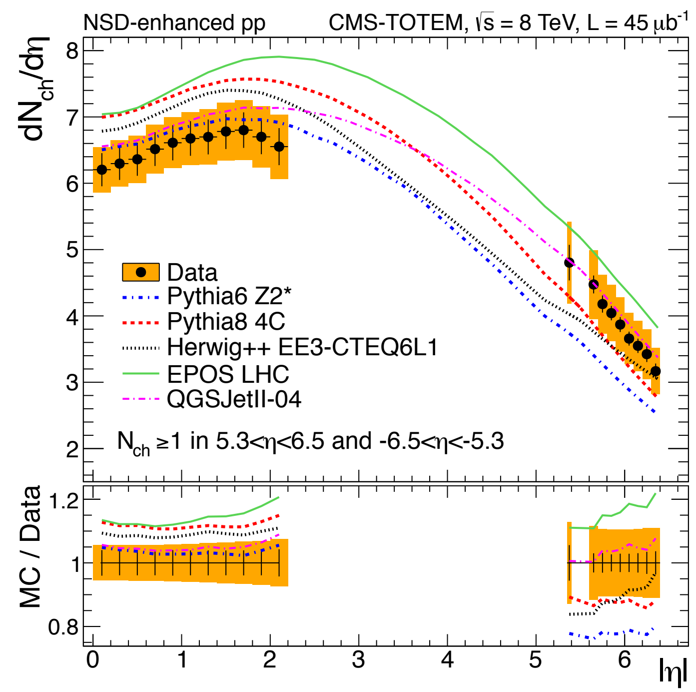

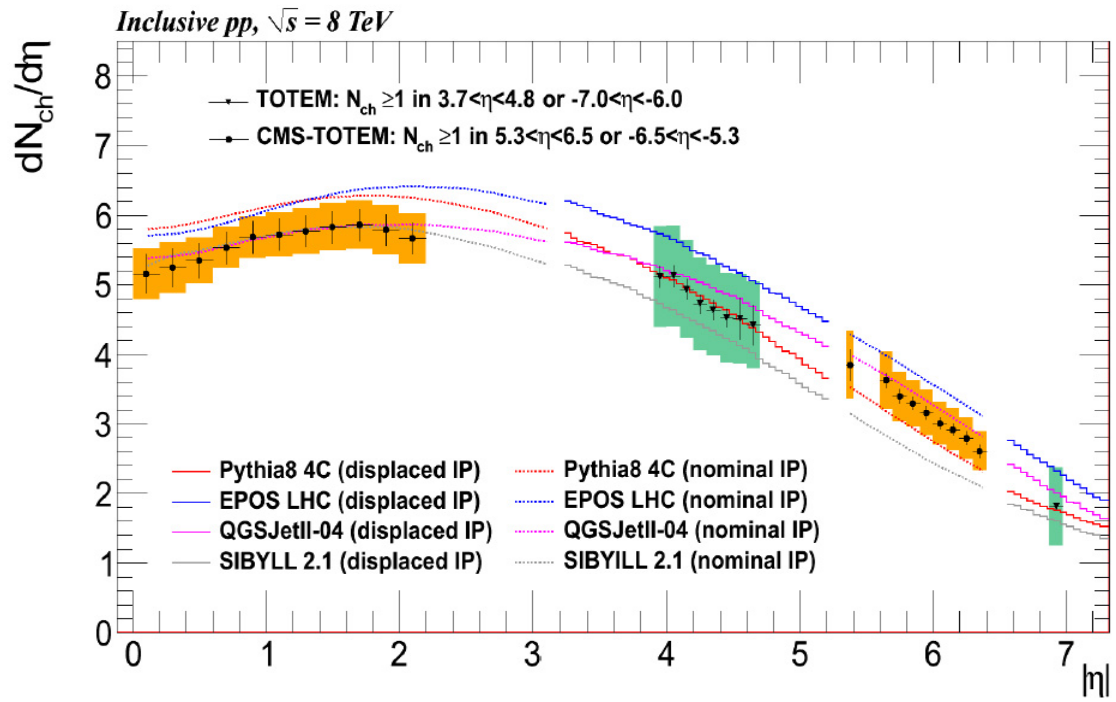

Nominal vertex

Shifted vertex

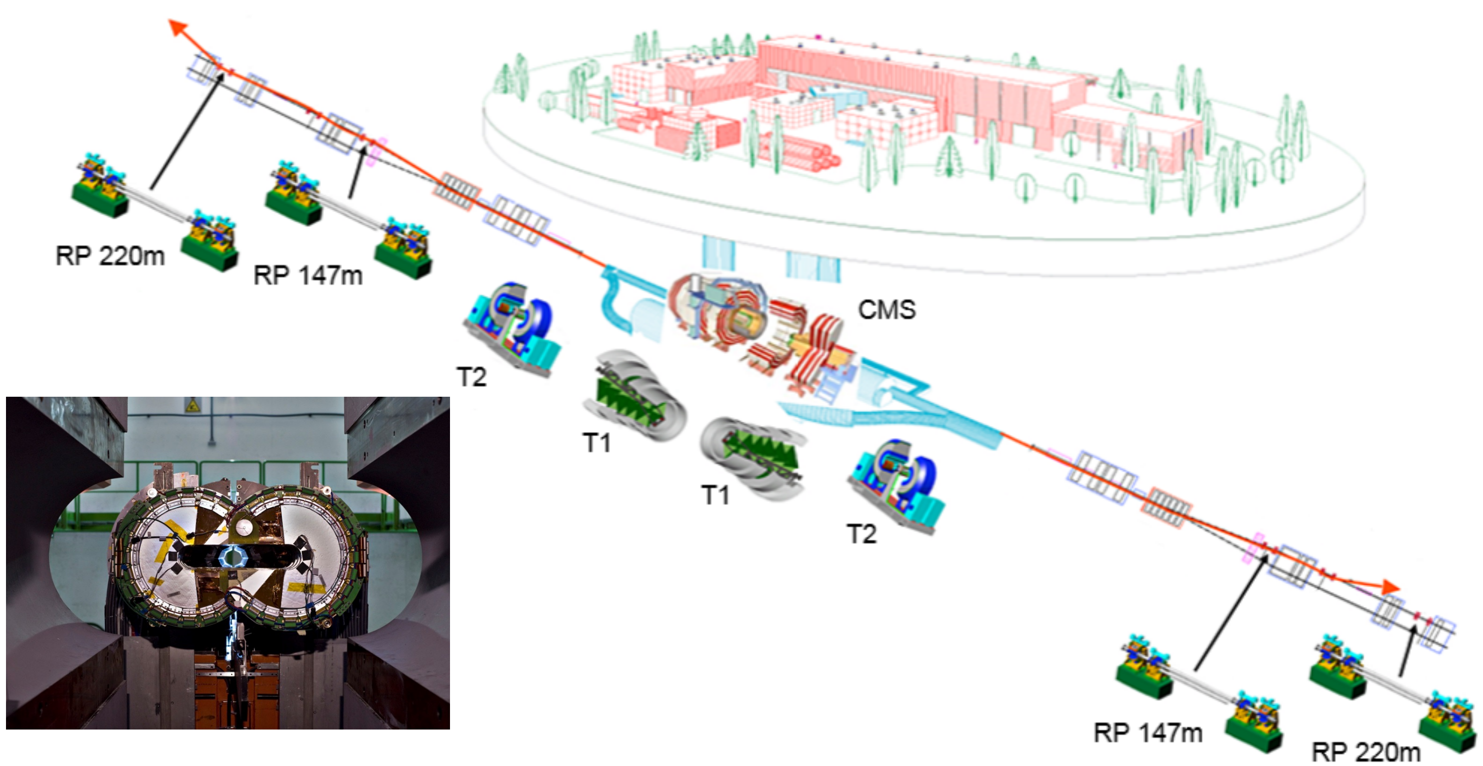

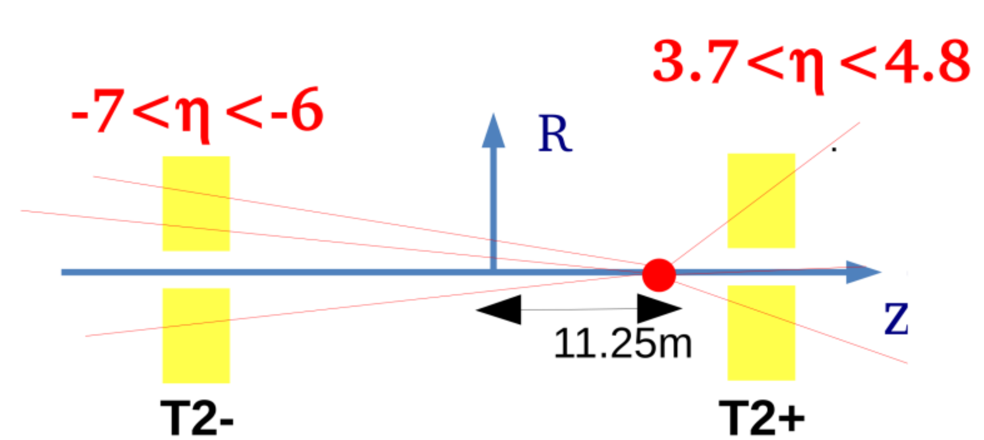

Performance plots of recent model versions

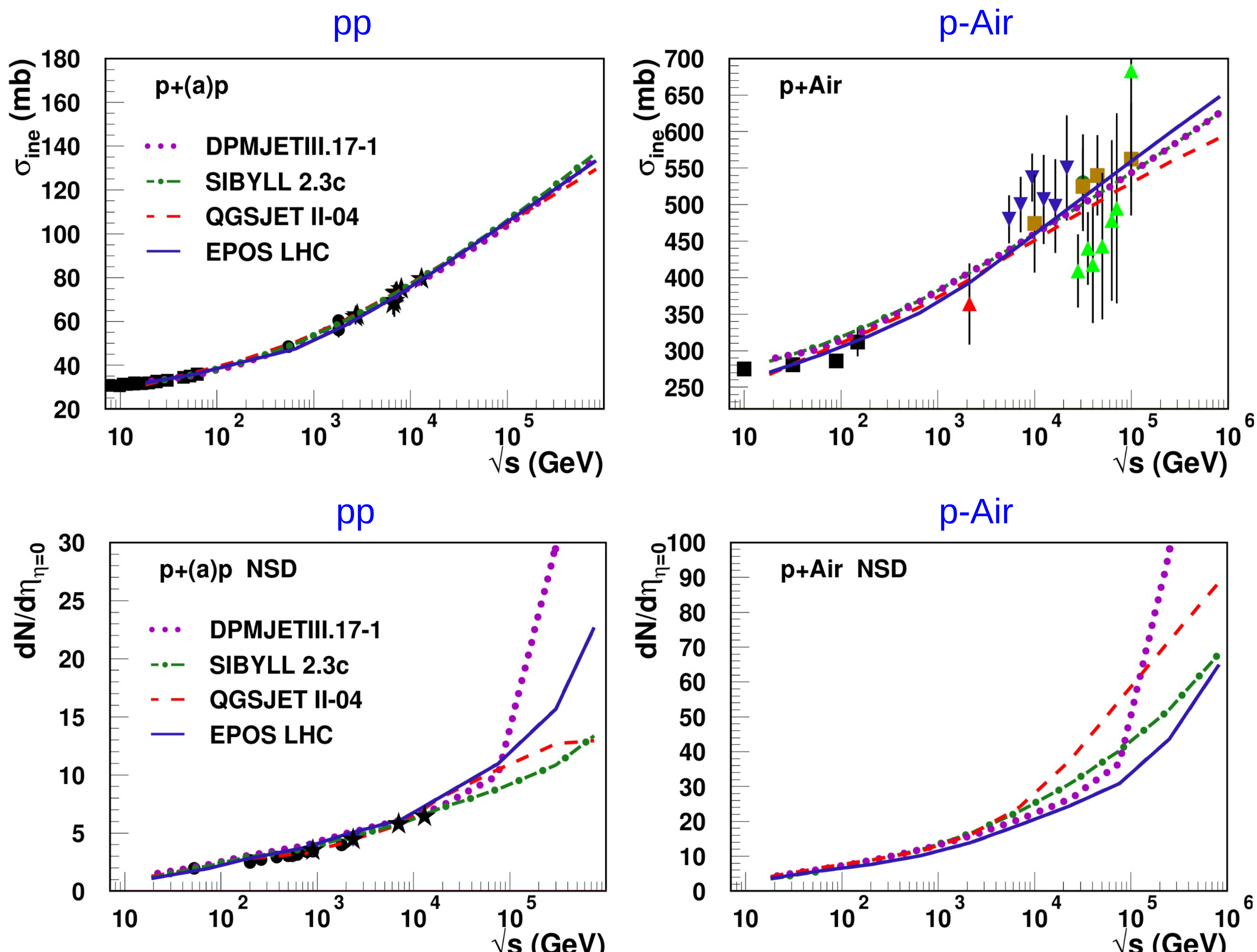

(Pierog ISVHECRI 2018)

Scaling: model predictions (i)

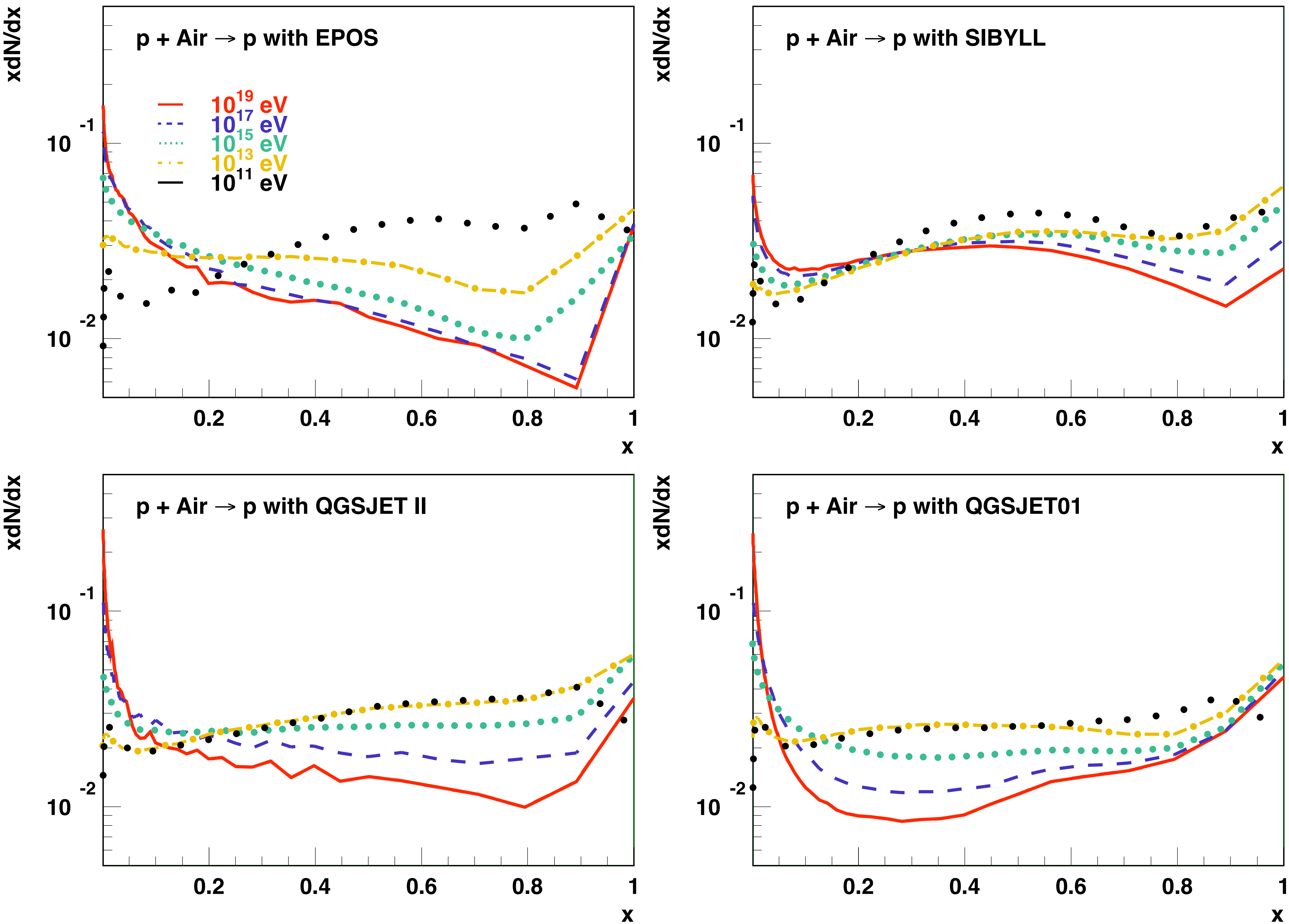

Scaling: model predictions (ii)

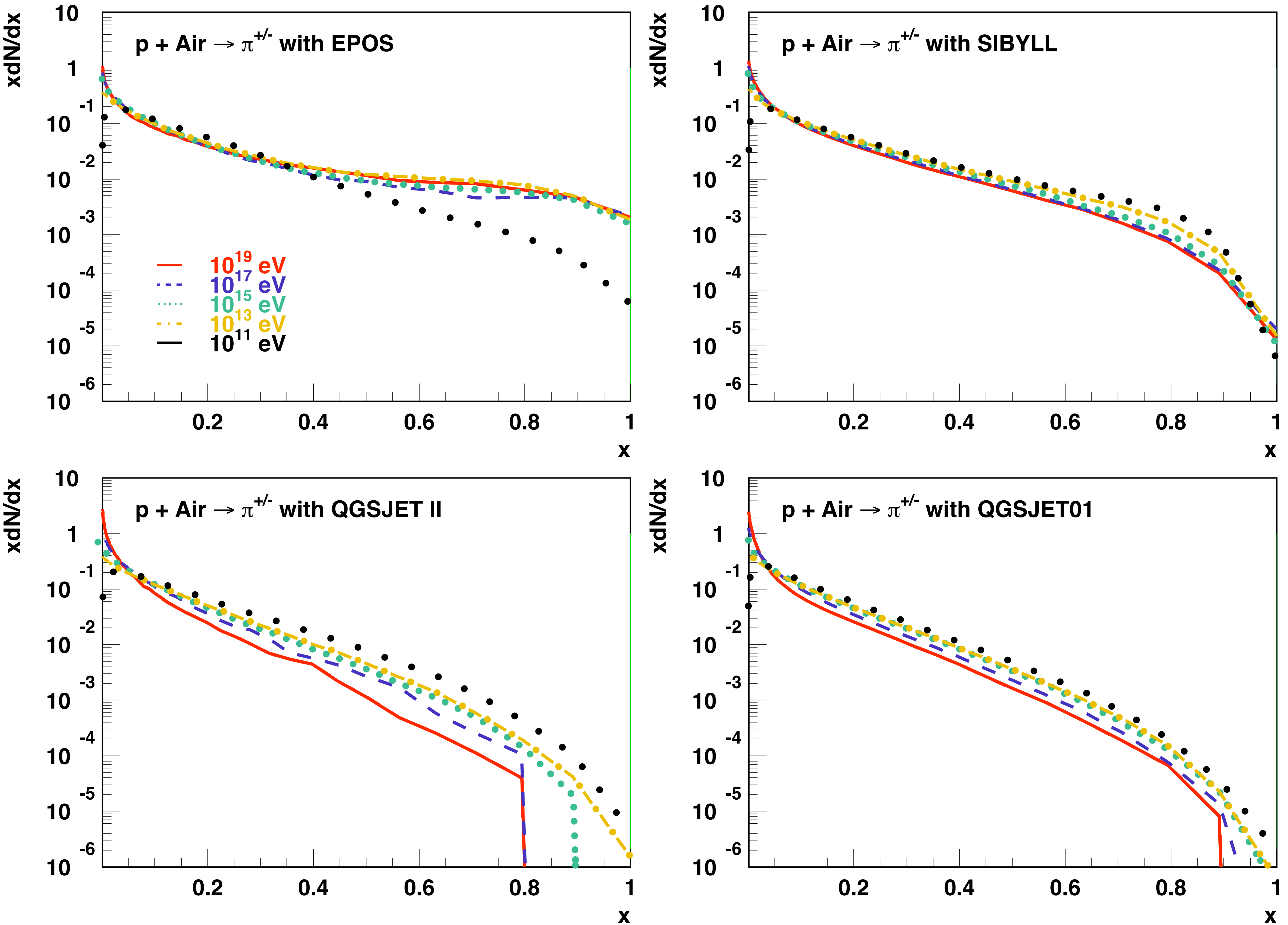

Scaling: model predictions (iii)

Inelasticity: fraction of beam particle energy that is transferred to secondary particles except the leading one

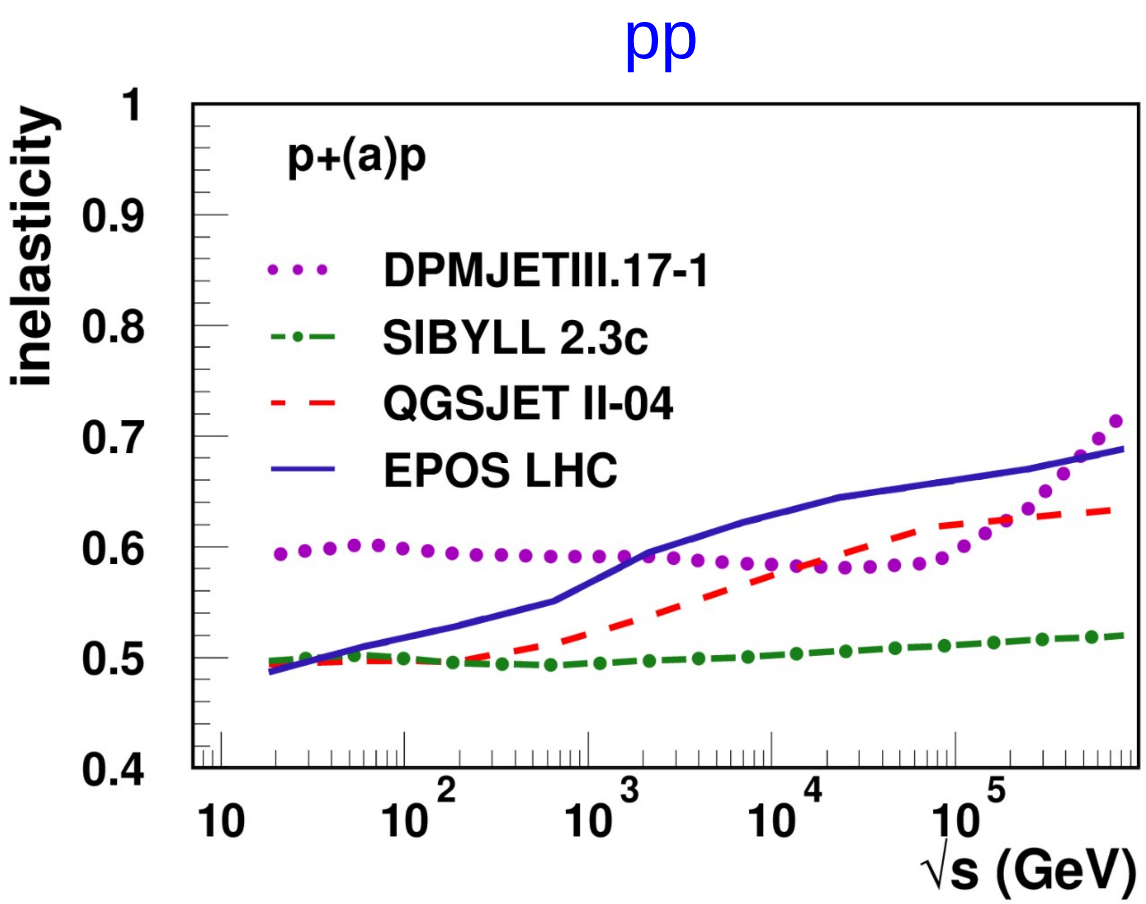

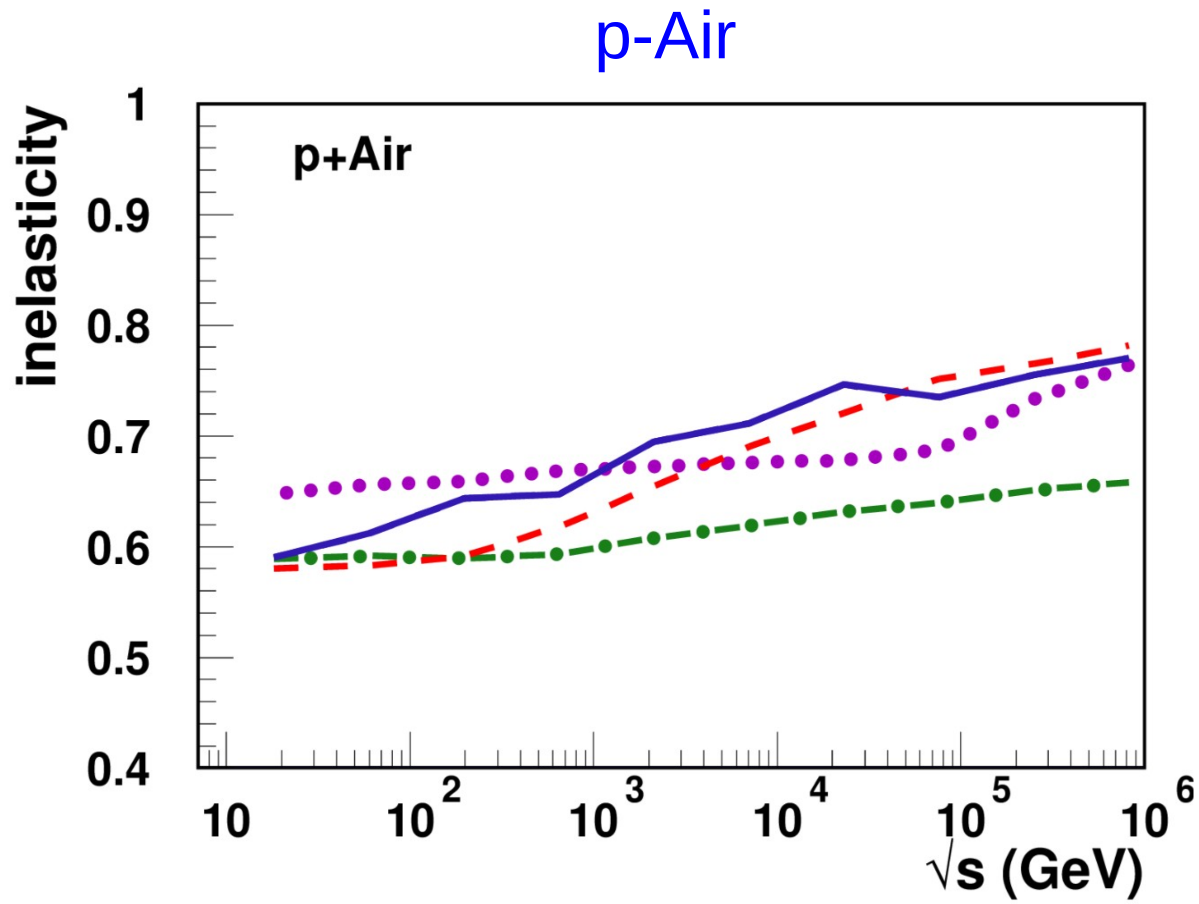

(Pierog ISVHECRI 2018)

Elasticity = 1 - Inelasticity

Collective effects – hydrodynamics and hadronization

Very high energy density
at initial stage of collision:
hydrodynamical state of q and g
(Quark-Gluon Plasma)

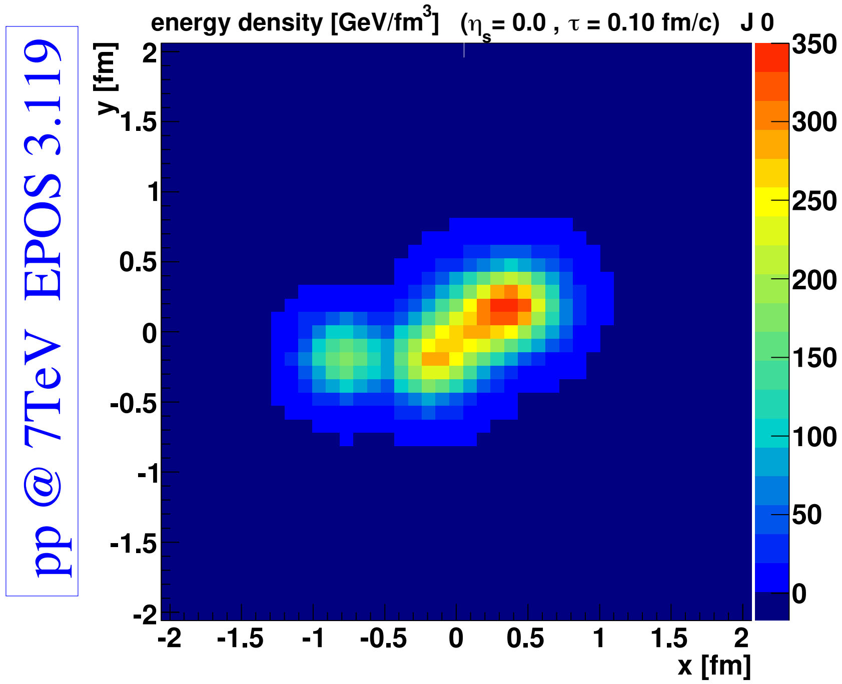

(Werner ISAPP 2018)

Particle spectra affected by radial flow

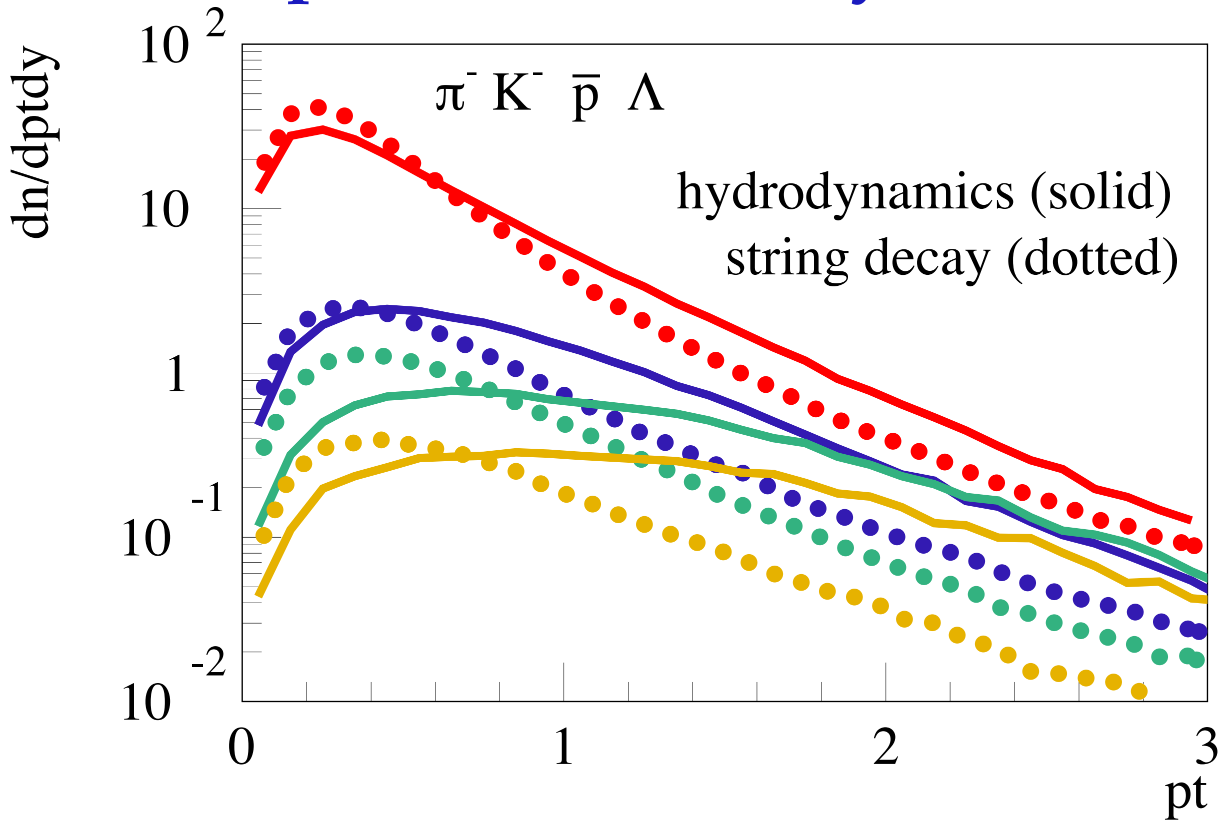

Omega to pion ratio (GC)

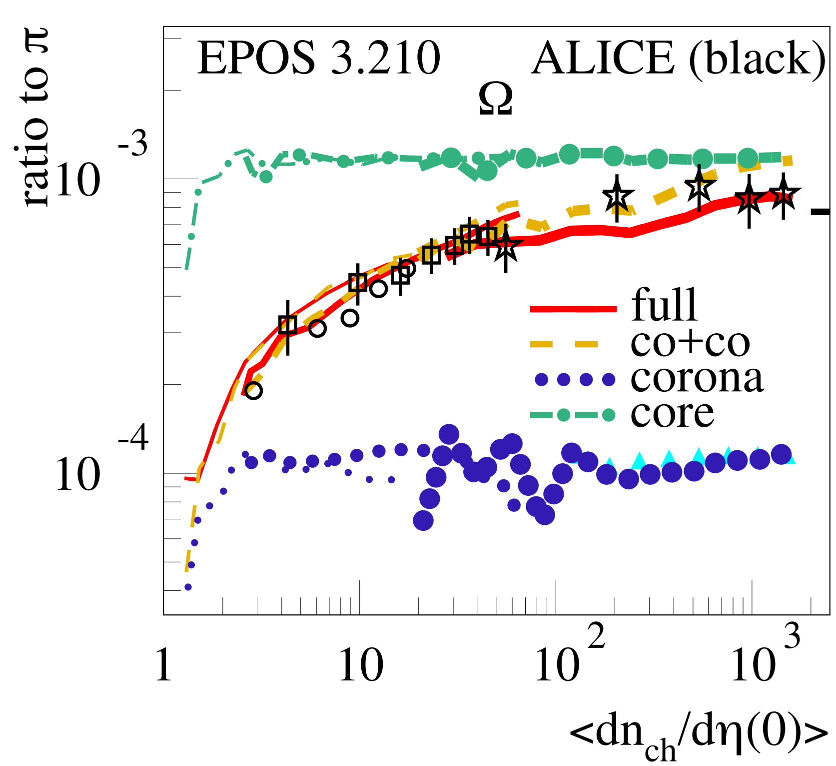

thick lines = pp (7TeV)
thin lines = pPb (5TeV)
circles = pp (7TeV)
squares = pPb (5TeV)
stars = PbPb (2.76TeV)

Effect on cosmic ray observables expected
to be small, but see Baur et al. arXiv:1902.09265

Black disk scenario of high energy scattering ?

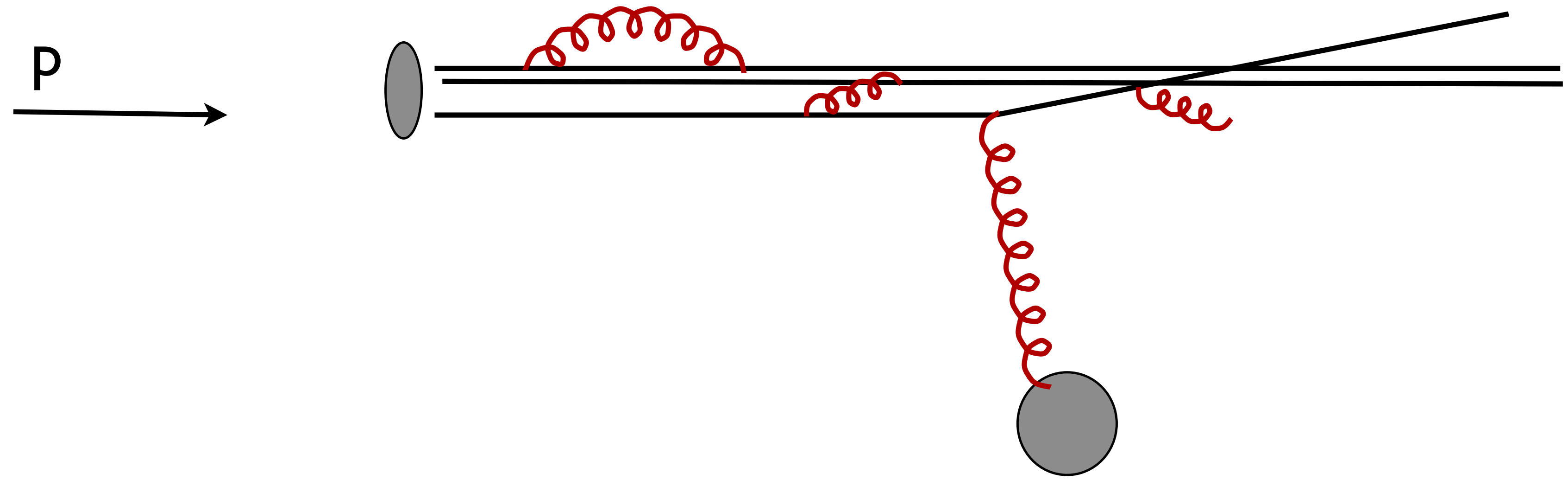

High energy scattering

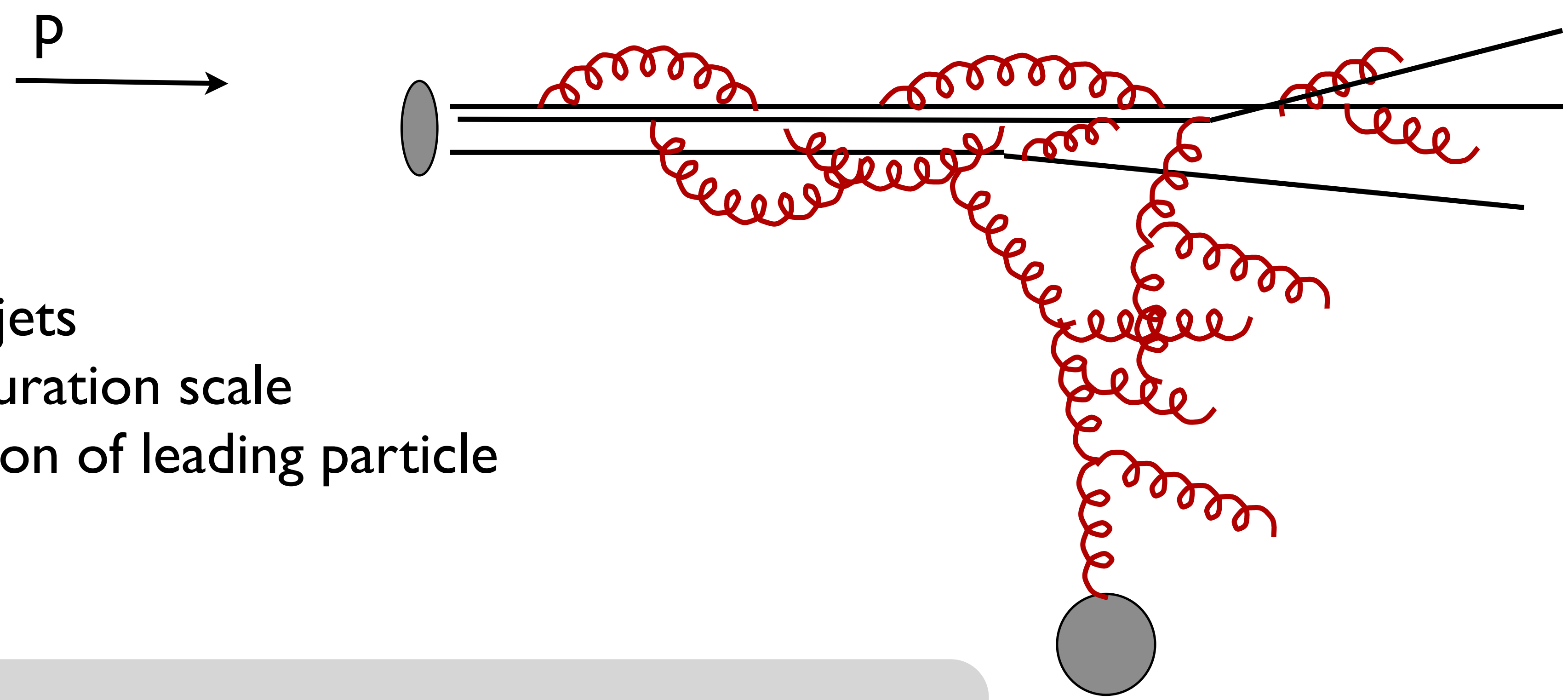

Black Disk Model

- large number of minijets
- high perturbative saturation scale
- complete disintegration of leading particle

Not implemented as dominating process in current models

(Drescher et al. Phys. Rev. Lett. 94, 2005)

Interaction models for high and ultra-high energies

Minijet production changes characteristics of interactions

- Predicted within perturbative QCD
- Natural source of scaling violations
- Parameters for calculation very uncertain
- Saturation effects very important, not really understood
- Collective effects more and more established (Quark-Gluon Plasma?)

Models construction

- Construction elements very similar
- Model philosophies complementary
- Tuned to data from fixed target and collider experiments
- Differences in treatment of key questions for high-energy extrapolation

Difference between models does probably not cover full range of uncertainty

Appendix

QCD color flow and soft interaction topologies

Soft physics: large N_c-N_f expansion of QCD

Problem: no small coupling constant for perturbative expansion in soft physics

´t Hooft, Veneziano, Witten (1974)

$$N_c \to \infty$$

$$N_c/n_f = \text{const}$$

$$\boxed{g^2 N_c \simeq 1}$$

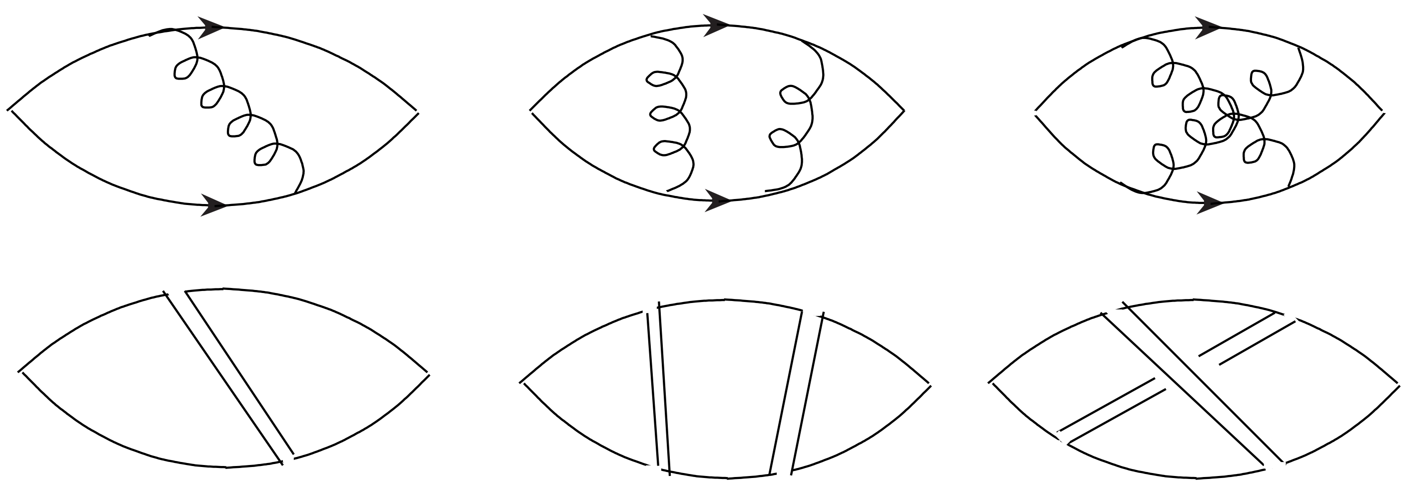

Graphs can be sorted according to number of colors and power of coupling constant

Topology of graph: surface on which it can be drawn without crossing color lines

Planar diagrams preferred: planar diagram theory of QCD

Color flow topologies in large-N_c/n_f QCD (i)

Partons only asymptotically free, work with ´strings´ instead

Example:

meson propagation

time

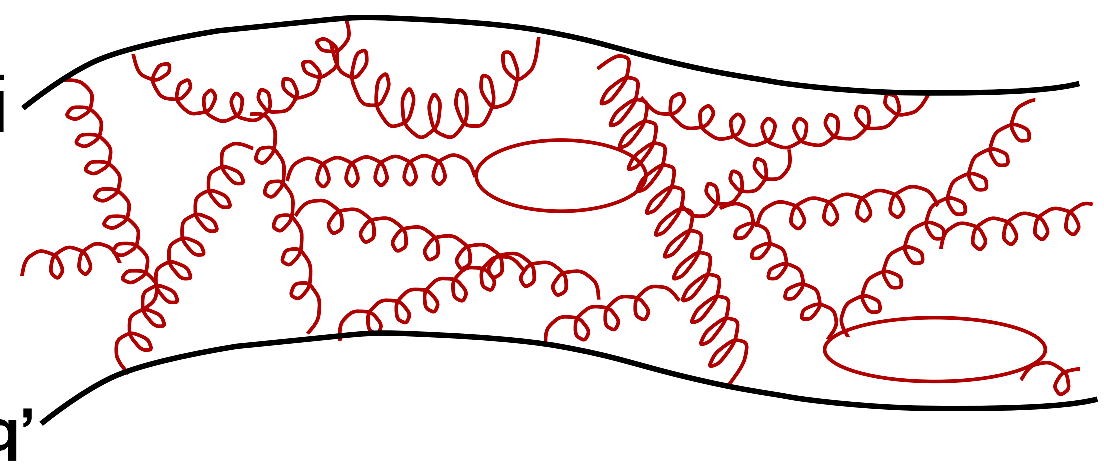

Scattering process:

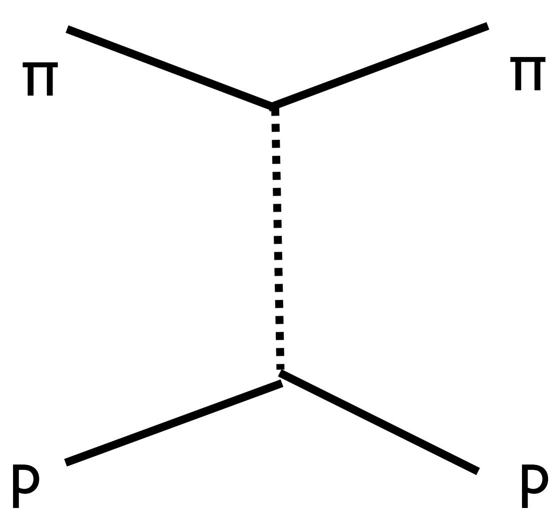

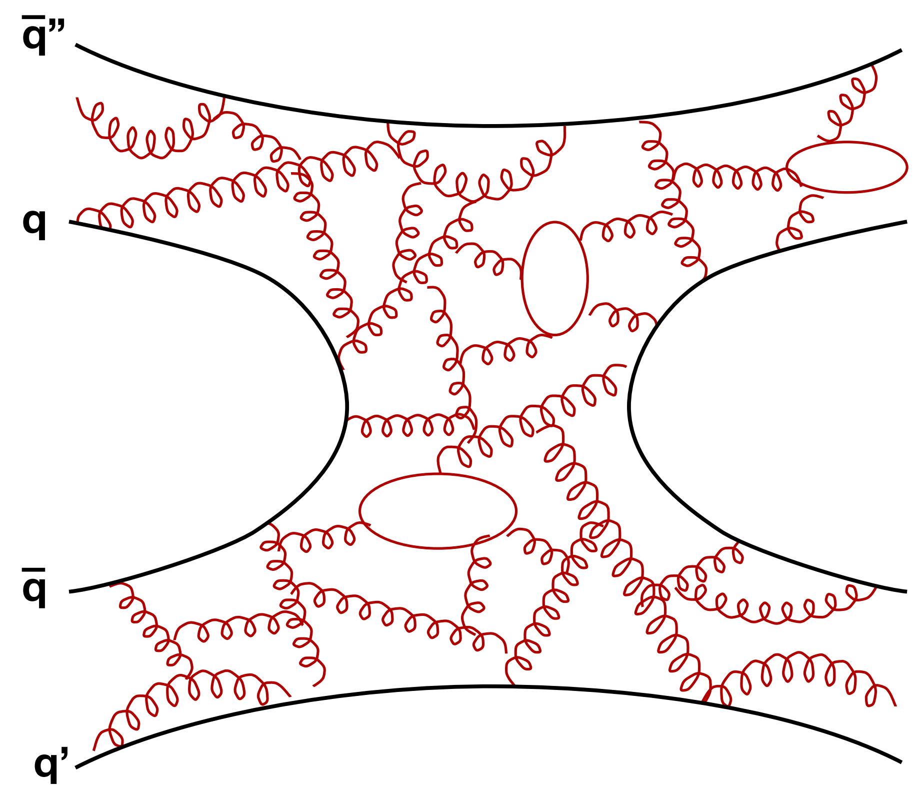

Color flow topologies in large-N_c/n_f QCD (ii)

Reggeon exchange

flat topology (dependence
on valence quark combinatorics)

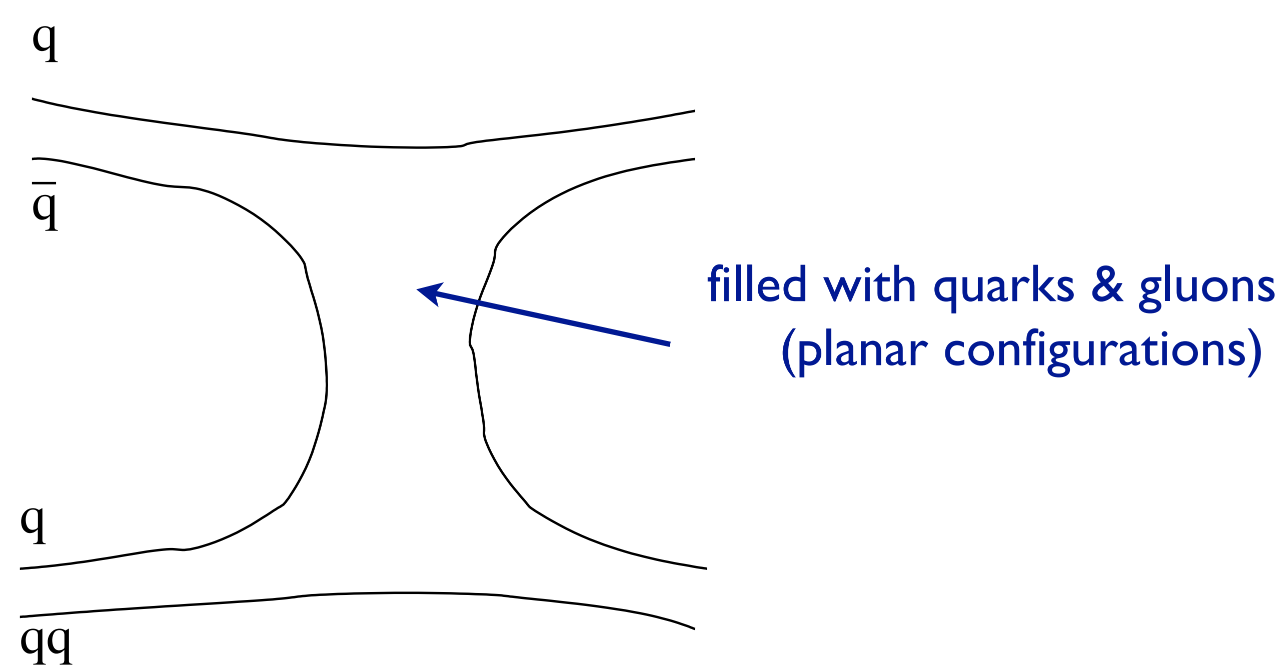

Pomeron exchange

cylinder topology (does not depend
on flavour of scattering particles)

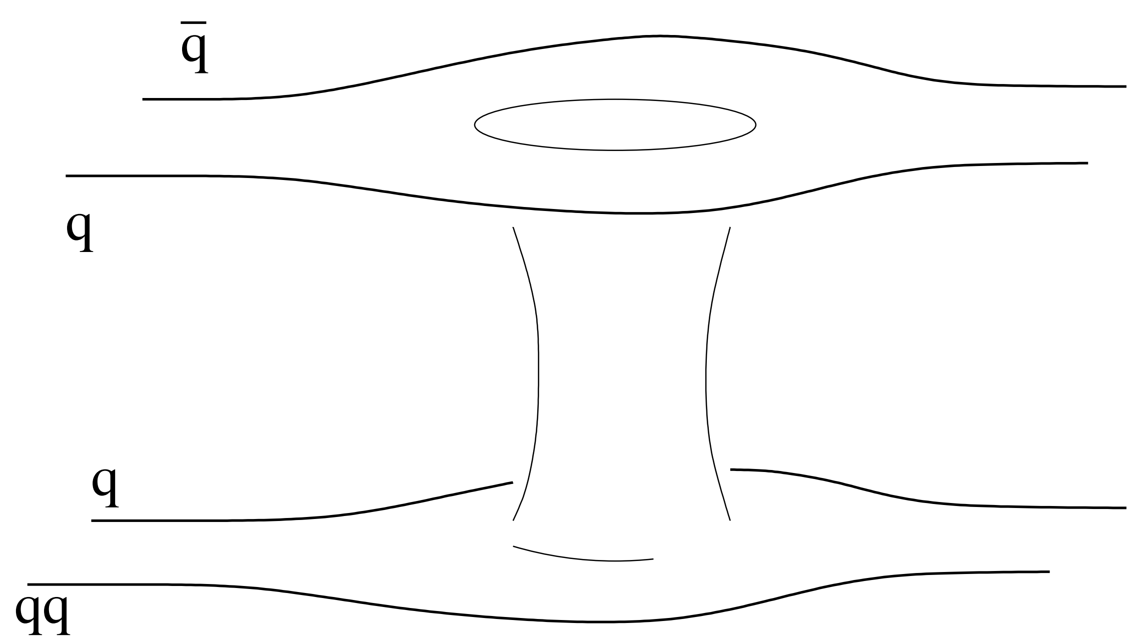

time

Graphical representation of optical theorem (i)

Standard method of calculating cross sections

$$\sigma_{\text{tot}} = \frac{1}{\Phi} \sum_X \int dP_X \, |M_{pp\to X}|^2$$

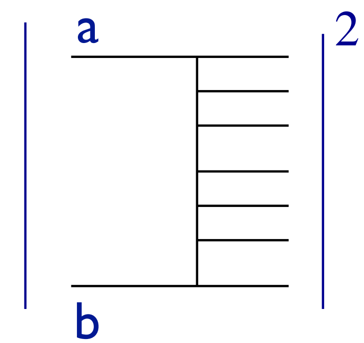

$$dP_X = \prod_j \frac{d^3 k_j}{2E_j}$$

sum over all
final states

integration over phase
space of final state particles

$$= \frac{1}{\Phi} \sum_X \int dP_X \, M^+_{pp\to X} M_{pp\to X}$$

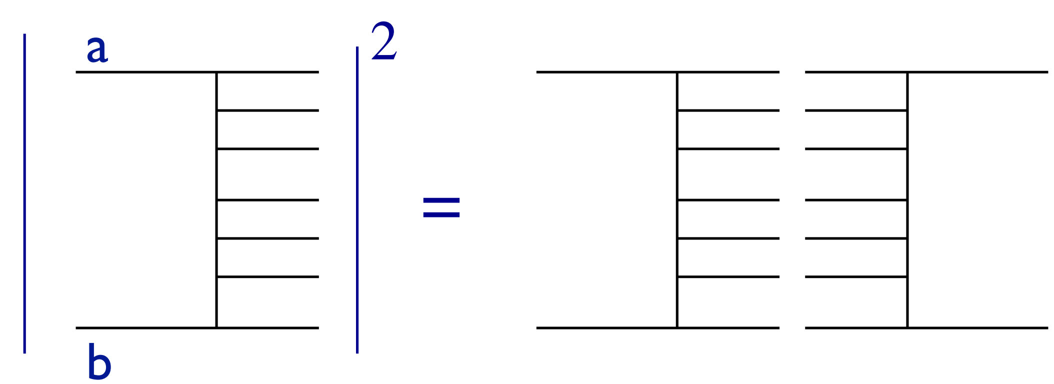

Optical theorem (elastic scattering)

$$= \frac{1}{s} \Im m(A_{\text{ela}}(s, t = 0))$$

$\Im m$

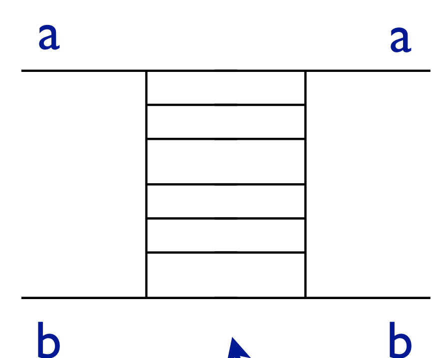

sum over all intermediate states

Graphical representation of optical theorem (ii)

$\Im m$ 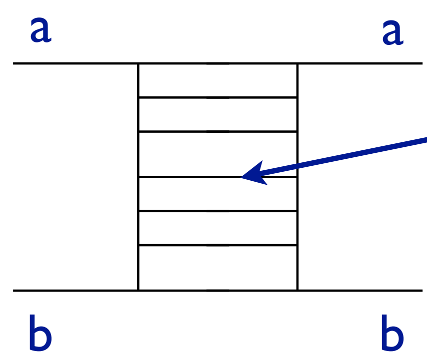

Field theory: particle propagator $\dfrac{d^4k}{k^2 - m^2 + i\varepsilon}$

Imaginary part of particle propagator

particle put on mass shell

$$\Im m\left(\frac{d^4k}{k^2-m^2+i\varepsilon}\right) = \delta(k^2-m^2)\,d^4k = \frac{d^3k}{2E}$$

$\Im m$ 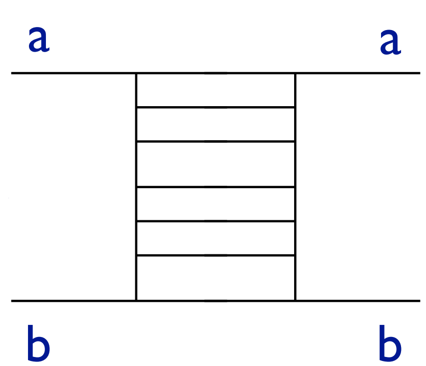

=

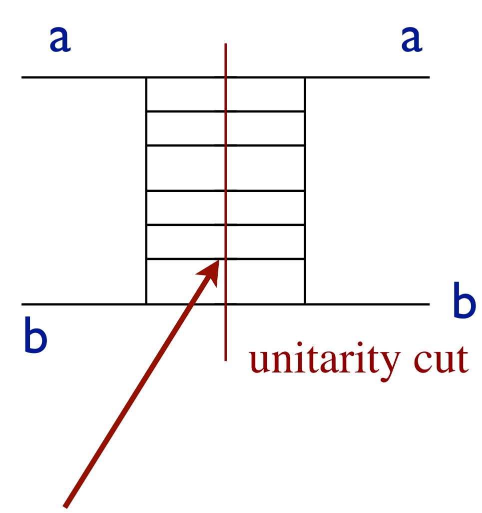

Calculating imaginary part shows particle configurations of final state for total cross section

cut particle lines correspond to particles in final state

Unitarity cuts (optical theorem): final state particles

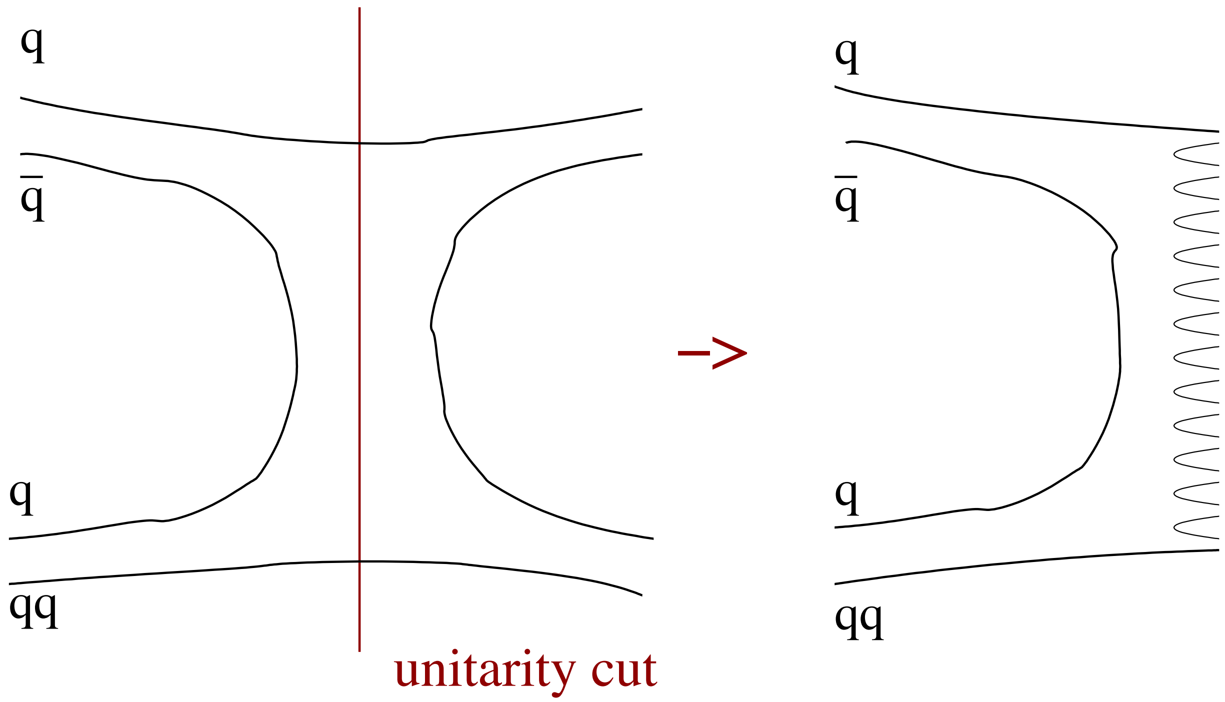

Unitarity cut of Reggeon exchange: chain of hadrons

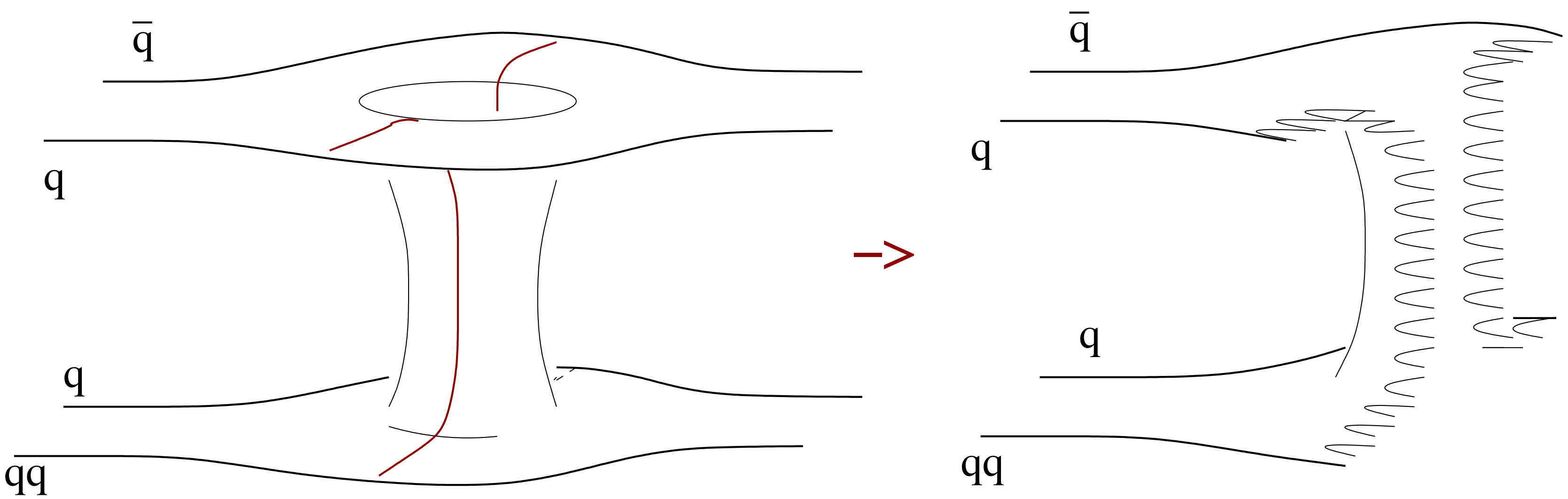

Pomeron exchange: two chains of hadrons

elastic scattering

inelastic scattering

(Capella et al. Phys.Rep. 1994, Kaidalov et al.)

Gluon-gluon scattering and cylinder topology

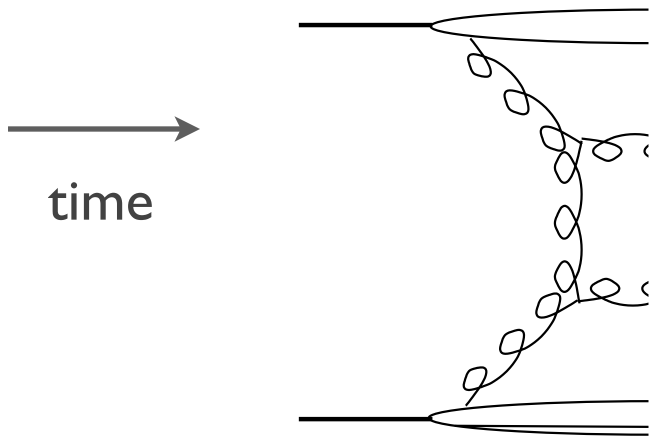

Generic diagram of hard scattering

$$\sigma_{QCD} = \sum_{i,j,k,l} \frac{1}{1+\delta_{kl}} \int dx_1\, dx_2 \int_{p_\perp^{\rm cutoff}} dp_\perp^2\, f_i(x_1,Q^2)\, f_j(x_2,Q^2)\, \frac{d\sigma_{i,j\to k,l}}{dp_\perp}$$

Standard procedure: total gluon-gluon cross section obtained by squaring matrix element

Same calculation using optical theorem: need to cut graph for elastic scattering

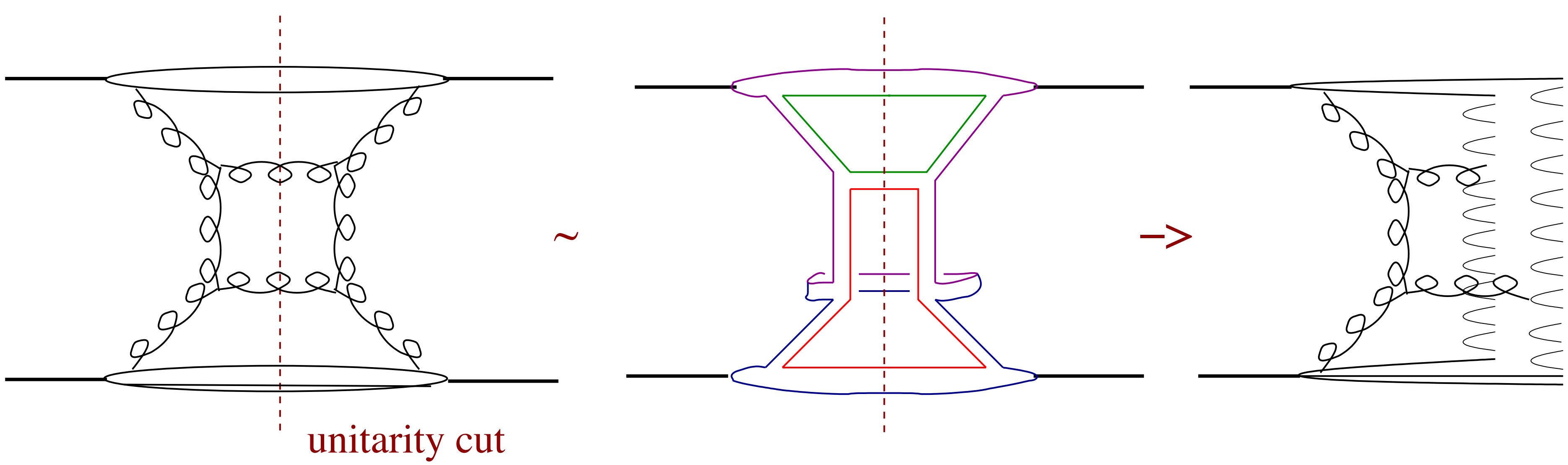

leading contribution: cylinder topology